Distribution Agreement

In presenting this thesis or dissertation as a partial fulfillment of the requirements for an advanced degree from Emory University, I hereby grant to Emory University and its agents the non-exclusive license to archive, make accessible, and display my thesis or dissertation in whole or in part in all forms of media, now or hereafter known, including display on the world wide web. I understand that I may select some access restrictions as part of the online submission of this thesis or dissertation. I retain all ownership rights to the copyright of the thesis or dissertation. I also retain the right to use in future works (such as articles or books) all or part of this thesis or dissertation.

Signature:

_____ _____
                Lei Xing   Date

Localization, Mechanisms and Functions of SMN and hnRNP-Q1

By

Lei Xing
Doctor of Philosophy

Graduate Division of Biological and Biomedical Sciences
Program in Biochemistry, Cell and Developmental Biology

_____
Gary Bassell, Ph.D.
Advisor

_____   _____
Victor Faundez, M.D., Ph.D.   Xiao-Jiang Li, Ph.D.
Committee Member   Committee Member

_____   _____
Yue Feng, Ph.D.   Maureen Powers, Ph.D.
Committee Member   Committee Member

_____
Winfield S. Sale, Ph.D.
Committee Member

Accepted:

_____
Lisa A. Tedesco, Ph.D.
Dean of the James T. Laney School of Graduate Studies

_____
Date

Localization, Mechanisms and Functions of SMN and hnRNP-Q1

By

Lei Xing

B.S., Nankai University, 1999

Advisor: Gary Bassell, Ph.D.

An abstract of

A dissertation submitted to the Faculty of the James T. Laney School of

Graduate Studies of Emory University in partial fulfillment

of the requirements for the degree of

Doctor of Philosophy

Graduate Division of Biological and Biomedical Sciences

Program in Biochemistry, Cell and Developmental Biology

2010

Abstract

Localization, Mechanisms and Functions of SMN and hnRNP-Q1

By   Lei Xing

Diverse types of messenger ribonucleoprotein (mRNP) complexes/granules, exist in the cytoplasm to enable the post-transcriptional regulation of gene expression e.g. mRNA transport granules, stress granule and P-bodies. However, their inter-relationships are unclear. Various mRNA binding proteins have been shown to influence mRNP granule assembly and/or regulate the recruitment and shuttling of target mRNAs. The cellular functions of mRNA binding proteins localized to mRNP granules and mechanisms underlying mRNA regulation are poorly understood. Some components of mRNP granules are affected in genetic diseases, such as the Survival of Motor Neuron protein (SMN), reduced levels of which leads to a motor neuron degenerative disease, Spinal Muscular Atrophy (SMA). The best understood SMN function is to facilitate spliceosome assembly. The overall objectives of my thesis were to characterize components of cytoplasmic RNA granules, assess their dynamic inter-relationships, and elucidate novel cellular functions of component mRNA binding proteins. This thesis research led to the discovery of an SMN-Gemin multiprotein complex within axonal transport granules, which are deficient of spliceosomal proteins. The mRNA binding protein, hnRNP-Q1, which directly interacts with SMN, was shown to be a novel component of SMN transport granules in neuronal processes, further suggesting a non-canonical function of SMN in axonal mRNA regulation. The results further showed that hnRNP-Q1 is a component of multiple RNA granules, and associates with several compartmented mRNAs. We revealed an unexpected role of hnRNP-Q1 to regulate RhoA signaling and found that after hnRNP-Q1 knockdown, hippocampal neurons exhibited a reduced dendritic spine density, and C2C12 cells exhibited enhanced cell spreading and increased focal adhesions and stress fibers. These phenotypes mimic effects observed upon the activation of the RhoA/ROCK signaling cascade and were rescued by a ROCK antagonist. Further studies demonstrated that hnRNP-Q1 associates with RhoA mRNA and negatively regulates its translation. hnRNP-Q1 depletion upregulated both RhoA protein levels and activities of the RhoA/ROCK signaling pathway. Collectively, this dissertation research has uncovered novel functions of mRNA granule components in mRNA regulation and should further motivate studies directed to understand the complex cytoplasmic regulation of mRNA underlying cellular development and diseases.

Localization, Mechanisms and Functions of SMN and hnRNP-Q1

By

Lei Xing

B.S., Nankai University, 1999

Advisor: Gary Bassell, Ph.D.

A dissertation submitted to the Faculty of the James T. Laney School of

Graduate Studies of Emory University in partial fulfillment

of the requirements for the degree of

Doctor of Philosophy

Graduate Division of Biological and Biomedical Sciences

Program in Biochemistry, Cell and Developmental Biology

2010

Acknowledgements

I truly enjoyed my student life in the Bassell lab as well as the Department of Cell Biology and the Biochemistry, Cell and Developmental Biology graduate program. I have been extremely lucky for having so many people helping with my studies in the past a number of years. Without these help, it wouldn't be possible for me to complete this dissertation.

I am particularly grateful for the tremendous mentoring I have received from my advisor, Dr. Gary Bassell. I would like to thank you for taking me as one of your student and directing my studies in the past six years. You have provided the most ideal environment for me to be trained as a scientist. You allowed and always encouraged me to develop my own thoughts and finally transform them into testable ideas. This dissertation is a combined outcome of your continuous inspiration, advice, encouragement and patience along with my studies. You helped me develop such a rich ground where my future scientific successes can be rooted.

I would like to thank all the current and past members of the Bassell lab. They were always available to help me solve any of my questions and technical difficulties. The bassell lab members had always been the first audiences of my works and they provided numerous critics and suggestions which were invaluable for my successful thesis studies. Particularly, Drs. Yukio Sasaki, Wilfried Rossoll and Christina Gross, they were my first resource for answers and discussion before I went to Gary's office. I would like to thank Dr. Honglai Zhang for his help and productive collaboration in the first two years of my studies and his contribution for this dissertation. I am also indebted to Dr. Kristy Welshhans and Xiaodi Yao for sharing their original research data which ensured the integrity of my dissertation, and Andrew Swanson for his help with image processing and analysis. I would also like to thank Drs. Christina Gross, Wilfried Rossoll and Kristy Welshhans, and Sharon Swanger for their critical reading of my dissertation.

To my thesis committee members, Drs. Victor Faundez, Yue Feng, Xiao-Jiang Li, Maureen Powers and Win Sale, I am going to miss all the meetings I had with you. As I said in my committee meeting, I feel very lucky to have such a great committee to

supervise and help with my studies. Your unique insights and advice constituted a very important component and were integrated into my dissertation.

Finally, my family has provided tremendous support for me to pursue my academic goals. My mom and Dad, Shuling Xiang and Jianzhong Xing, raised me through many difficult years for the family. I am extremely grateful for your hard wording in supporting my growing and years of education. I know it had not been easy to raise four children and make us your proud. I know you are always by me side to make me strong to challenge all the coming difficulties. My sincere gratitude also goes to my wife and my dearest friend, Xiaodi Yao. You have been the one who made me a strong mind to pursue my dreams fearlessly. I know that my dreams are always yours and you have sacrificed so much just for that. Being a classmate, friend and colleague of yours had been an extraordinary experience for me. Your loving, caring and supporting make my life an enjoyable and fruitful one. I would also like to thank my brother and sisters and their families for their emotional support and my in-lows for taking me as one of their family members and always being kind and supportive to me. My own contribution in this dissertation is truly dedicated to my parents, Shuling Xiang and Jianzhong Xing, and my wife, Xiaodi Yao.

Table of Contents

Table of Figures

Chapter I

General Introduction

In the early life of an mRNA molecule, the corresponding pre-mRNA transcribed from its DNA template is processed through 5'end capping, splicing and 3'end polyadenylation in a way coupled with transcription. Eventually, mature nuclear mRNAs associated with RNA binding proteins in the form of messenger ribonucleoproteins (mRNPs) are exported into the cytoplasm for translation. In the past several decades, a tremendous amount of studies have focused on the role of transcription in the regulation of gene expression. Yet some recent studies also emphasized the essential role of post-transcriptional regulation of gene expression in multiple cellular activities, such as cell polarity establishment and maintenance, cell motility and neuronal plasticity (Holt and Bullock, 2009; Lin and Holt, 2008; Martin et al., 2000). Post-transcriptional regulation of gene expression allows cells to modulate protein expression on a subcellular level with temporal and spatial resolution via the regulation of mRNA localization, translation and stability (Anderson, 2008; Martin and Ephrussi, 2009; Paquin and Chartrand, 2008). Below, I will introduce three well studied subtypes pf mRNP complexes, termed "granules", "particles" or "bodies", based on their microscopic appearance. These are: transport mRNP granules (or particles), stress granules and processing bodies. The functions of mRNA binding proteins in post-transcriptional regulation of gene expression, such as mRNA transport and localization, mRNA translation and mRNA degradation, with respect to the above mRNP complexes, and their implication in development and human diseases will be discussed.

mRNPs and related granules

Besides actively translated mRNAs in polysomes, translationally silenced mRNAs with their associating RNA binding proteins are assembled into functionally

different mRNP granules, including transport mRNP granules, stress granules and processing bodies **(Figure 1-1)** (Balagopal and Parker, 2009; Kiebler and Bassell, 2006). These mRNP granules are believed to be functionally connected, dynamic subcellular structures which play important roles in posttranscriptional regulation of gene expression **(Figure 1-1)**.

Transport mRNP granules

Asymmetrical subcellular distribution of mRNAs has been observed by *in situ* hybridization studies in multiple cell types. For example, β-actin mRNA was discovered to be highly enriched in the leading lamellea of motile chicken embryonic fibroblast cells and growth cones of cultured primary neurons (Kislauskis et al., 1993; Lawrence and Singer, 1986; Zhang et al., 1999). In budding yeast, Ash1 mRNA is transcribed from the mother nucleus and accumulated in the bud cortex of the daughter cell (Long et al., 1997). In the *Drosophila* oocyte, bicoid mRNA and oskar mRNA were shown to be highly enriched in the anterior and posterior pole, respectively (Berleth et al., 1988; Rongo et al., 1995). The asymmetrical localization of these mRNAs suggests an active mechanism by which cells selectively pack these mRNAs into distinct transport granules and deliver them to the target locations through cytoskeletal structures. As one of the earlier demonstrations of active mRNA transport, Knowles et al. first observed the bidirectional, microtubule-dependent movement of endogenous RNA containing granules in live cells using an RNA-dye, SYTO-14 (Knowles et al., 1996). Recent development of a fluorescent protein-tagged MS2/RNA system further proves the existence of transport mRNP granules. In addition, this technique enabled the visualization and mechanistic studies of transport mRNP granules in multiple cell types (Bertrand et al., 1998;

Dictenberg et al., 2008; Forrest and Gavis, 2003). In this system, the bacteriophage coat protein, MS2, binds to a RNA stem-loop structure in a sequence-specific manner. Co-expression of fluorescent protein-tagged MS2 and mRNAs of interest fused with multiple copies of the MS2-binding sequence leads to the labeling of reporter mRNAs with fluorescent proteins, which enables observations of mRNA particle transport in live cells.

Efforts have been taken to reveal the composition of transport mRNP granules by biochemistry and proteomics analyses. Based on the observation that mRNP transport in neuronal cells is microtubule-dependent, Kanai et al. purified transport mRNP granules from adult rat brain lysate using the cargo-binding domain of a conventional Kinesin (Kif5b) (Kanai et al., 2004). Several dendritic localized mRNAs (e.g. *CamkIIα* and *Arc/Arg3.1* mRNAs) were enriched in this preparation and a large number of RNA-binding proteins were identified, including several proteins which have been shown to be important for mRNA transport, such as FMRP and Staufen (Antar et al., 2004; Dictenberg et al., 2008; Kohrman et al., 1999). Elvira et al. took a centrifugation approach to purify mRNP granules from embryonic rat brain; these mRNP grnualescontained enriched β-actin mRNA (Elvira et al., 2006), an mRNA localized to both developing axons and dendrites (Bassell et al., 1998a; Eom et al., 2003; Zhang et al., 2001). Besides ribosomal components and translation factors identified in these granules, a large number of RNA-binding proteins were characterized, including Zipcode binding protein1 (Zbp1) and HuD (ELVA-like 4) (Elvira et al., 2006). Indeed, a large number of RNA binding proteins are common components identified in these two independent proteomic analyses, such as hnRNP-Q (Syncrip), hnRNP U and several DEAD-Box Helicases (Elvira et al., 2006; Kanai et al., 2004). Disparities in protein and mRNA

composition of the mRNP granules described in these two studies might be due to the different developmental stages of the brain tissue used (adult versus embryonic brain). Results from both groups were validated by overexpression experiments using primary neurons to examine the localization and transport activity of identified mRNA binding proteins. Additionally several RNA binding protein co-immunoprecipitation experiments also revealed that mRNP granules contain many common components but with considerable heterogeneity (Bannai et al., 2004; Jonson et al., 2007; Mallardo et al., 2003). The common components are possibly essential for the assembly of mRNPs whereas the heterogeneous components may mark mRNPs to recruit different mRNAs. Studies have shown that double-strand RNA binding protein Staufen is a common component of both oskar and bicoid mRNPs and required for their localization in the Drosophila oocyte (Berleth et al., 1988; Roegiers and Jan, 2000; Rongo et al., 1995). Yet unique components associated with these mRNPs may distinguish one mRNP from the other and lead to the localization of oskar mRNP to the posterior pole whereas bicoid mRNP to the anterior pole. However, this hypothesis remains to be tested.

mRNAs within transport mRNP granules are generally believed to be translationally silenced, although this notion is hypothetical rather than supported by solid experimental evidence. First, among the mRNP components identified, several of them were well characterized as both mRNA transporters and translational repressors for their binding mRNAs. Several studies have addressed the essential role of Zbp1 in *β-actin* mRNA transport and localization. Decreasing the expression of Zbp1 by morpholino antisense oligos or disrupting the interaction of Zbp1 and β-actin reduced the localization of β-actin mRNA (Eom et al., 2003; Zhang et al., 2001). In a recent study,

Huttelmaier et al. demonstrated the function of Zbp1 as a translational repressor for β-actin mRNA showing that Zbp1 represses β-actin mRNA translation by blocking the recruitment of 60S ribosomal subunits and that depletion of Zbp1 by RNAi leads to enhanced translation of β-actin mRNA (Huttelmaier et al., 2005). Being repressed from translation will ensure the delivery of mRNAs to their target cell compartments and allow the production of protein in proper places where these proteins are needed. In many situations, especially during embryogenesis, ectopic expression and mislocalization of some transcripts can cause developmental abnormalinities, as shown for oskar in *Drosophila* oocytes (Ephrussi and Lehman, 1992; Smith et al., 1992). In addition, translation inhibition of oskar mRNA is required for its efficient localization to the posterior pole of a *Drosophila* oocyte (Nakamura et al., 2004). Overexpression of Zbp1 promoted the asymmetrical distribution of β-actin protein to the leading edge of neuroblastoma cells as a consequence of enhanced β-actin mRNA localization and possibly also by maintaining β-actin mRNA in an untranslated complex during transport. As β-actin mRNA localized to the leading edge of this type of cells, Zbp1 is locally phosphorylated by Src to release β-actin mRNA for translation (Huttelmaier et al., 2005).

<u>Stress granules</u>

Stress granules are a type of mRNP granule induced by stress, such as UV-irradiation, heat-shock and oxidative stress, and generally are not observed in cells growing in normal conditions. Stress granules are identified as TIA-1/R-enriched large aggregates containing GTPase-activating protein, SH3 domain binding protein 1(G3BP1), cytoplasmic poly(A) binding protein 1 (PABPC1) and poly(A) mRNAs (Kedersha and Anderson, 2002). TIA1/R is an RNA binding protein containing a Prion-

like domain which facilitates the formation of TIA1/R aggregates (Gilks et al., 2004). TIA1/R is predominantly localized to the nucleus under normal conditions. In response to environmental stress, TIA1/R is translocated to the cytoplasm and forms aggregates (Gilks et al., 2004). Stress granule formation is initiated with stress-induced phosphorylation of eukaryotic initiation factor 2α (eIF2α) which interferes with translation initiation by blocking pre-initiation complex formation and, together with cytoplasmic TIA1/R, leads to translation arrest and release of mRNAs from polysomes (Kedersha et al., 2002). TIA1/R aggregates further recruit mRNAs and their associated proteins to form large mRNP granules. Besides being detected in the peri-nuclear area, stress granules are also detected in distal dendrites in mature neurons (Vessey et al., 2006). Studies have shown that some components of transport mRNP granules are also found in stress granules, such as CPEB, Staufen, FMRP and Zbp1 (Mazroui et al., 2002; Stohr et al., 2006; Wilczynska et al., 2005). FRAP analyses indicated that RNA binding proteins in stress granules are dynamic components exhibiting constant exchange with their soluble pools (Kedersha et al., 2005). The dynamics of the RNA binding proteins may represent the dynamic exchange of RNAs between stress granules and other types of mRNP granules **(Figure 1-1)**. In fact, mRNAs appear to be constantly exchanged between stress granules and polysomes, as arresting mRNAs in polysomes by treating cells with cycloheximide impairs stress granule formation and diminishes pre-existing stress granules (Mollet et al., 2008). Similar to transport mRNP granules, mRNAs in stress granules are translationally silenced.

Stress granules provide transient subcellular mRNA-containing compartments which are proposed to be a self-defense mechanism for cells to sequester and protect

mRNAs from further damage during stress. Subsequent to the release of stresses, mRNAs in stress granules will be recycled for translation. If stress persists, certain mRNAs may also be processed for degradation. Additionally, the recruitment of mRNAs to stress granules is highly selective, further indicating that the formation of stress granules is an active defensive process. Examples of mRNAs that escape recruitment into stress granules are mRNAs encoding heat-shock proteins (HSPs), including HSP70 and HSP90; these mRNAs are not or only weakly detected in stress granules after oxidative stress (Kedersha and Anderson, 2002; Stohr et al., 2006). Heat shock proteins are protein chaperones preventing the formation of protein aggregates. The exclusion of HSP mRNAs from stress granules allows their efficient translation under harmful conditions, and potentially serves as a feedback protective mechanism in response to stress, which is supported by the observation that HSP70 overexpression diminishes arsenite-induced stress granules (Gilks et al., 2004).

Processing bodies

Processing bodies (P-bodies) are granule-like structures containing enzymatic and structural proteins specialized in mRNA degradation, such as Dcp1 and 2, Lsm1-7 and a 5'- to 3'- exoribonuclease, Xrn1 (Balagopal and Parker, 2009; Franks and Lykke-Andersen, 2008). In addition, machineries involved in siRNA and miRNA-mediated mRNA degradation and/or translational repression are also highly enriched in these cytoplasmic foci (Eystathioy et al., 2003; Meister et al., 2005). P-bodies were first identified as Xrn1-enriched granules following the discovery of this enzyme with exoribonuclease activity (Bashkirov et al., 1997). P-bodies essentially exist in all cell types. The enrichment of mRNA degradation enzymatic complexes and miRNA

processing machineries suggest potential functions of P-bodies in mRNA decay and miRNA-mediated translational repression. P-body formation is possibly a reflection of the existence of non-translating mRNAs since cycloheximide treatment which arrests translation elongation and depletes non-translating mRNAs eliminate P-bodies; further addition of non-translating mRNA leads to the reappearance of P-bodies even in the presence of cycloheximide (Cougot et al., 2004; Franks and Lykke-Andersen, 2007). Besides the induction of stress granules, oxidative stress dramatically increases the number of P-bodies which are closely associated with stress granules (Cougot et al., 2004). This increased assembly of P-bodies has been thought to be caused by the increase in non-translating mRNAs during cellular stress.

P-bodies share many common components with transport mRNP granules and stress granules, especially RNA binding proteins. For example, FMRP and CPEB which are components of transport granules and stress granules are also localized to P-bodies (Cougot et al., 2008; Wilczynska et al., 2005). As proposed for stress granules, the co-existence of certain RNA-binding proteins suggests that RNA binding proteins may be dynamic components shuttling between P-bodies and other mRNP granules (Figure 1-2). RNA binding proteins serve as a link between P-bodies and other mRNP granules and regulate mRNA degradation and/or translation through P-body components. Evidence for this is derived from the studies of TTP and BRF, two members of AU-Rich Element (ARE)-binding proteins promoting mRNA decay. The localization of TTP and BRF to P-bodies delivers their bound mRNAs to P-bodies and incurs rapid mRNA degradation (Franks and Lykke-Andersen, 2007).

Although strong evidence suggests a function of P-bodies in mRNA degradation and miRNA-mediated translational regulation, whether the formation of P-bodies is essential for efficient mRNA decay is still unclear. In yeast, the disruption of P-bodies by co-deletion of Edc3 and the LSm4 C-terminus, the interaction of which facilitates P-body assembly, has no effect on mRNA decay (Decker et al., 2007; Reijns et al., 2008). In mammalian cells, knockdown of GW182 leads to impaired P-body assembly yet did not interfere with ARE-mediated mRNA decay (Eulalio et al., 2008). In addition, the function of GW182 in miRNA-mediated translation repression is independent of both its localization to P-bodies and its association with P-body component, AGO1 (Eulalio et al., 2009). Similar to stress granules, there is no clearly established biological function of P-bodies in mRNA regulation, yet they do provide compartments to store and sequester mRNA, which could have indirect effects on mRNA availability for translation.

mRNA localization in polarized cells provides mechanism for protein sorting

Asymmetrical localization of mRNA is a conserved cellular activity observed in multiple cell types and organisms. In budding yeast *Saccharomyces cerevisiae*, *Ash1* mRNA is localized to the bud cortex of daughter cells during late anaphase (Long et al., 1997). The local translation of Ash1 mRNA restricts the expression of Ash1p in daughter cells, which controls mating type switching. It is well established that mRNA localization in oocytes and embryos is necessary for protein sorting, the establishment of morphogenic gradients, cell type specification and patterning during development (Johnstone and Lasko, 2001; Zhou and King, 2004). In the *Drosophila* oocyte, *bicoid* mRNA is localized to the anterior pole, whereas oskar and nanos mRNAs are localized to the posterior pole, as reviewed in (Kugler and Lasko, 2009). A similar phenomenon is

also observed in *Xenopus* oocytes, in which Vg1 mRNA is localized to the vegetal pole (Deshler et al., 1997; Yisraeli and Melton, 1988). In addition, mRNA localization is a prevailing phenomenon for multiple mRNAs in various types of cells. A recent examination of 3370 transcripts in *Drosophila* embryos by high throughput *in situ* hybridization revealed that 71% of them exhibited a distinct non-uniform distribution (Lecuyer et al., 2007). *In situ* hybridization analysis of individual mRNAs revealed that a large number of mRNAs are also asymmetrically localized in neuronal cells. A recent microarray analysis identified several hundred transcripts in axonal fractions purified from cortical neurons (Taylor et al., 2009); in addition, the pools of mRNAs purified from normal and injured axons exhibit differential compositions (Taylor et al., 2009; Willis et al., 2007; Yoo et al., 2009). Proteins encoded by these axonally localized mRNAs play various roles, such as in translational regulation, active transport, cytoskeleton dynamics and signal transduction (Taylor et al., 2009; Willis et al., 2007; Yoo et al., 2009). In addition, localized mRNAs in neurons seem to be always targeted to the location where their protein products are needed; axonal protein, Gap43 and Tau encoding mRNAs are selectively localized to axons (Litman et al., 1993; Paradies and Steward, 1997) and mRNAs encoding the dendritically localized protein Map2 and PSD95 are targeted to dendrites (Garner et al., 1988; Muddashetty et al., 2007). In oligodendrocytes, myelin basic protein (MBP) mRNA is localized to myelinating compartments (Hoek et al., 1998).

mRNA localization provides a mechanism for efficient protein localization. Translation of localized mRNAs enables massive protein production in restricted locations which allows cells or organisms to generate timely responses to external stimuli

or internal developmental codes. During *Drosophila* oogenesis, for example, local translation of anterior localized bicoid mRNA and posterior localized oskar and nanos mRNAs generate a great amount of proteins in the anterior and posterior poles, respectively (Kugler and Lasko, 2009). Diffusion of these proteins results in protein gradients which are essential for the establishment of the anteroposterior body axis of the *Drosophila* embryo. Since translation of these mRNAs will not be activated until they are properly localized, the deleterious effect of ectopic expression of these proteins is avoided.

The role of mRNA localization and local translation was also investigated in polarized mamallian cells, such as migrating fibroblast cells and primary neurons. β-actin mRNA is one of the best studied asymmetrically localized mRNAs in both type of cells. In primary chicken fibroblast cells, β-actin mRNA is localized to the leading lamellipodia (Kislauskis et al., 1993) where the local translation of β-actin mRNA is essential for the directional cell migration (Shestakova et al., 2001). In cultured primary neurons, β-actin mRNA is localized to both developing axonal growth cones (Zhang et al., 1999) and dendrites (Eom et al., 2003); whereas its homolog γ-actin mRNA is restrained to the neuronal cell body (Bassell et al., 1998b; Eom et al., 2003). In the central nervous system, axons guidance is an essential targeting process for the formation of functional neuronal circuits. This steering phenomenon is a consequence of axon responsiveness to both chemoattractant and chemorepulsive guidance cues. A recent study shows that localization of β-actin mRNA and its local translation are an important mediator for BDNF induced growth cone turning, an effect that was abolished by disrupting the active transport of β-actin mRNA with an antisense oligonucleotide to its localization elements

(Yao et al., 2006). In addition, the growth cone localization of β-actin mRNA is essential for neutrophin induced axon growth (Zhang et al., 2001). Other studies also showed that localization and local translation of RhoA mRNA and Par6 mRNA play a role in Semaphorin3A-induced growth cone collapse and growth factor induced axon elongation, respectively (Hengst et al., 2009; Wu et al., 2005). Moreover, accumulated evidence indicates that local translation of certain mRNAs also plays role in post-synaptic neuronal plasticity, which further demonstrates the importance of mRNA localization and local translation along with the entire developmental process (Bramham, 2008; Martin et al., 2000).

Molecular mechanisms of mRNA localization: interactions between cis-acting elements and mRNA binding proteins

The specific subcellular localization of an mRNA is determined by its intrinsic cis-acting elements and their association with trans-acting RNA binding proteins. Conserved cis-acting localization elements, also known as zipcode sequences, are frequently located within the 3' untranslated region (UTR) of a localized mRNA and occasionally in the coding region or 5' UTR. The specific interaction of cis-acting localization elements and RNA binding proteins leads to the formation of mRNP granules which will be recruited onto transport machineries and delivered to specific subcellular compartments (Bullock, 2007; Martin and Ephrussi, 2009).

Multiple cis-acting elements are always present in a localized mRNA and possibly play their function in a synergistic way. Yeast Ash1 mRNA is one of the best characterized localized transcripts. Within the coding region and the 3'UTR of Ash1 mRNA, four cis-acting elements, E1, E2A, E2B and E3, were identified by their ability to

localize Ash1 reporter transcripts (Chartrand et al., 1999). E1, E2A and E2B are within the coding regions and E3 encompasses part of the coding region and 3' UTR (Chartrand et al., 1999). Although each element alone is sufficient to localize Ash1 reporter transcripts, the presence of four elements dramatically increases the efficiency of localization. For nanos mRNA, four cis-acting elements were identified, but each individual element possesses only weak mRNA localization ability (Gavis et al., 1996). Similar to yeast Ash1 transcripts, the existence of four localization elements provides enhanced localization strength. Two zipcode sequences were identified within the 3'UTR of β-actin transcripts: a 54nt zipcode sequence and a 43nt zipcode sequence (Kislauskis et al., 1994). The 54nt zipcode sequence is proximal to the stop codon and plays a major role in β-actin mRNA localization which is mediated by the specific interaction of its conserved sequence ACACCC with Zbp1 (Ross et al., 1997). In contrast, the 43nt zipcode exhibits only weak capability to localize β-actin mRNA when examined with an mRNA localization assay. A recent study showed that both zipcodes and the sequence in between were required for the Zbp1-mediated translational repression which has been proposed as an important process in the efficient localization of β-actin mRNA (Huttelmaier et al., 2005). Although not experimentally tested, it would still be plausible to propose that the presence of multiple cis-acting elements within one mRNA may act as a backup mechanism for mRNA localization or provide additional information which enables fine modulation of protein expression for cells to generate precise responses to various stimuli or environmental changes.

Besides conserved sequences, secondary structures may also be required for the function of a cis-acting localization element. In *Drosophila* oocytes, the anterior pole

localization of bicoid mRNA is determined by several bicoid localization elements (BLEs) within a 625nt long region of the 3 'UTR which forms 5' stem-loop structures (Macdonald et al., 1993; Macdonald and Struhl, 1988). Stem-loop IV and V are essential for bicoid mRNA localization at early oocyte developmental stage and only a 50nt region (BLE1) is required at later stage. Bicoid mRNAs carrying mutations of the primary sequence of BLEs which do not affect stem-loop structures are properly localized (Ferrandon et al., 1997). Ferrandon et al. proposed that the dimerization of bicoid mRNA through stem-loop structures is required for its localization. The stems or dimerized structures recruit a double-strand RNA binding protein, Staufen, which has been demonstrated to be important for the posterior localization of bicoid mRNA (Ferrandon et al., 1997). Functional analysis of Fragile X Mental Retardation Protein (FMRP) in mRNA localization provides an indirect support for the role of secondary structure in mRNA localization. One model proposed for the interaction of FMRP and its binding mRNAs is that FMRP binds to its target mRNAs through G-quartet structures formed by G-rich sequences (Darnell et al., 2001). A recent study showed that FMRP plays an essential role in dendritic localization of its binding mRNAs in response to DHPG stimulation; in neurons cultured from *Fmr1* knockout mice, DHPG induced dendritic mRNA localization is diminished (Dictenberg et al., 2008). Further evidence in support of this hypothesis could be obtained by experiments testing the effect of mutations in the G-quartet structure of a specific mRNA on its localization.

mRNA localization is a transport activity mediated by molecular motors. However, no RNA binding activity for molecular motors has been reported up to date. RNA binding proteins may serve as adaptors for localized mRNAs by anchoring mRNAs

to the respective molecular motors. A protein complex known as "locasome" was identified for the localization of Ash1 transcript, including She1p/Myo4p, She2p and She3p (Long et al., 2000). She2p is an RNA binding protein shuttling between the nucleus and the cytoplasm, which forms mRNP granules with Ash1 mRNA by direct interaction with its cis-acting elements; She1p/Myo4p is a type V Myosin which exerts actin filament-mediated transport; She3p acts as an adaptor mediating the association of She2p/Ash1 mRNA complexes with She1p/Myo4p. As mentioned previously, β-actin mRNA localization is mediated through its direct interaction with Zbp1 through the 54nt zipcode sequence and a number of mRNAs are targeted to dendrites through their interacting with FMRP. Similar to the function of She2p/(She1p/Myo4p) complex in Ash1 mRNA localization, RNA binding proteins like FMRP and Zbp1 may bridge the association of mRNAs with molecular motors. This postulation is strongly supported by the observation that the association of FMRP-binding mRNAs with conventional Kinesin heavy chain was dramatically reduced following depletion of FMRP (Dictenberg et al., 2008). In addition, Zbp1 has been observed to interact with a Kinesin light chain protein, Pat1, through which Zbp1 couples its binding mRNAs to microtubules and exerts its function in mRNA transport and localization (unpublished data, Dictenberg and Bassell).

RNA-binding proteins in mechanisms of translational regulation

Translational repression and mRNA transport are thought to be coupled processes. Recent studies indicate that transport mRNAs are likely translationally quiescent and RNA binding proteins required for mRNA transport also function as translation repressors (Deng et al., 2008; Hachet and Ephrussi, 2004; Huttelmaier et al., 2005; Lasko, 2003). Zbp1 is one of such example whereby the localization and

translational regulation of β-actin mRNA in neuroblastoma cells are coupled, as discussed above (Huttelmaier et al., 2005). The binding of Zbp1 to the β-actin zipcode sequence blocks the recruitment of 60s ribosome subunit and the formation of translation initiation complexes (Huttelmaier et al., 2005). However, this study also showed that a large fragment of β-actin mRNA 3'UTR, including both 54nt and 43nt zipcode and the sequence in between, is required for the function of Zbp1 as a translation repressor (Huttelmaier et al., 2005). It is very likely that additional trans-acting factors possibly binding to this larger RNA fragment are involved. For certain localized mRNAs, additional transacting factors may be required to silence translation. Following the nuclear-cytoplasmic export of Ash1 mRNA, besides Ash2p which is directly involved in Ash1 mRNA localization, two RNA binding proteins, Khd1p and Puf6p, are loaded to repress its translation by blocking the recruitment of 40s or 60s ribosome subunits (Deng et al., 2008; Paquin et al., 2007). After the delivery of Ash1 mRNPs to the bud cortex, Khd1p and Puf6p are phosphorylated by two membrane localized protein kinases, Yck1p and Ck1p, respectively, which leads to release of Khd1p and Puf6p, followed by Ash1 translation. For β-actin mRNA, when it is localized to the leading lamellae of fibroblast cells and growth cones of neurons, Zbp1 is phosphorylated by Src to release its binding and translation repression (Huttelmaier et al., 2005).

Similar to Zbp1 and Khd1p/Puf6p, the majority of studies are mainly focused on the function of RNA binding proteins in translational initiation, although translation may also be arrested at elongation stages. One established model for translational repression is that RNA binding proteins recruit specific eIF4E-BPs which can block the interaction of eIF4E and eIF4G, which is a prerequisite for recruiting 60S ribosomal subunit to form

80S ribosome for Cap-dependent translation initiation. In Drosophila oocyte, RNA binding proteins Bruno and Smaug negatively regulate the translation of oskar and nanos mRNAs during localization, respectively (Nakamura et al., 2004; Nelson et al., 2004). Bruno and Smaug recruit CUP, an eIF4E-BP, onto their targeting mRNAs and thus block the binding site of eIF4E for eIF4G. A similar observation was made in mammalian cells. CYFIP1, an eIF4E-BP was shown to directly interact with FMRP and thereby mediate the function of FMRP as a translation repressor (Napoli et al., 2008). Blockage of translation initiation can also be accomplished by modulating the length of the poly(A) tail. In Xenopus eggs, maternal mRNAs containing only short poly(A) tails are translationally quiescent. The short poly(A) tail of cytoplasmic polyadenylation element (CPE)-containing mRNAs is achieved by recruiting poly(A) nuclease through CPEB and Maskin protein complex (Cao and Richter, 2002). CPEB directly interacts with CPE and Maskin interacts with eIF4E and blocks its interaction with eIF4G. Progesterone-treatment triggers CPEB phosphorylation which further recruits the protein xGLD2 to CPE-containing mRNAs. xGLD2 is a poly(A) polymerase which catalyzes poly(A) tail elongation (Barnard et al., 2004). Binding of PABP to the long poly(A) tail thereby facilitates the eIF4E-eIF4G complex formation and translation initiation by disrupting eIF4E-Maskin interaction. A similar mechanism may also be involved in the translational regulation of CPE-containing mRNAs in the central nervous system (Huang et al., 2002).

Non-coding mRNAs may also be components for RNA binding protein-mediated translational repression. BC1 is a non-coding small RNA localized to neuronal dendrites (Tiedge et al., 1991). The direct interaction of BC1 RNA with eIF4A inhibits eIF4A helicase activity and blocks translation initiation of BC1 associated mRNAs (Lin et al.,

2008). Another study also showed that BC1 RNA interacts with FMRP and possibly acts as a functional component for FMRP-mediated translation repression (Zalfa et al., 2003). miRNAs constitute a large fraction of non-coding RNAs involved in mRNA translation silencing. A recent study investigated a potential function of miRNA in RNA binding protein-mediated translation repression. Kim et al. uncovered that HuR recruited Let-7 miRNA and the RISC complex to negatively regulate c-Myc mRNA translation. HuR and Let-7 miRNA are interdependent in their function to repress c-Myc expression since both depletion of HuR and blockage of Let-7 miRNA result in reduced association of c-Myc mRNA with RISC complex (Kim et al., 2009).

Apart from their frequently studied function as translation repressors, RNA binding proteins also play a role in translation activation. In *Fmr-/-* cells, protein levels of Superoxide Dismutase-1 and Achaete-scute Homologue-1 are reduced (Bechara et al., 2009; Fahling et al., 2009). Further studies showed that FMRP activates the translation of their corresponding mRNAs by interacting with the 5'UTRs (Bechara et al., 2009; Fahling et al., 2009). The differential effects of FMRP on translation are possibly related to the location of its binding sites on mRNAs. When binding to 3'UTRs, FMRP represses translation; similar phenomena were reported for several other RNA binding proteins, such as Zbp1for β-actin mRNA (Huttelmaier et al., 2005), Khd1p and Puf6p for yeast Ash1 mRNA (Deng et al., 2008; Paquin et al., 2007) and Bruno and Smaug for oskar and nanos mRNA, respectively (Nakamura et al., 2004; Nelson et al., 2004). In contrast when binding to 5'UTRs, FMRP acts as a translation activator. Besides the conventional cap-dependent mechanism, translation can be initiated through internal ribosomal entry sites (IRESes). Several RNA binding proteins, including La autoantigen, hnRNP D and

hnRNP-Q, can bind to various IRES elements and enhances IRES-mediated translation (Cho et al., 2007; Kim et al., 2001; Paek et al., 2008). For example hnRNP-Q activates BiP mRNA IRES function and increases BiP expression in response to heat stimulation (Cho et al., 2007). In addition, the function hnRNP-Q in IRES-mediated translation plays an important role in circadian rhythm control by activating serotonin N-acetyltransferase protein expression (Kim et al., 2007).

RNA-binding proteins regulating mRNA degradation

Gene expression can also be regulated through mRNA degradation, a process likewise regulated by RNA binding proteins. mRNA degradation is an essential mechanism for cells to eliminate aberrant transcripts containing premature stop codons or introns and to avoid the production of truncated or abnormal proteins. mRNAs in cells exhibit variant half-lives indicating the possible role of mRNA degradation in gene expression regulation. For example, ARE-containing mRNAs usually have short half-lives. AREs were initially identified within the 3'UTRs of many transcripts encoding cytokines and transcription factors, the expression of which are under tight control since many of them are involved in cell proliferation. A systematic genome-wide analysis estimated that 5 to 8% human transcripts contain AREs (Bakheet et al., 2003, 2006). A large number of RNA binding proteins have been shown to interact with AREs in a sequence-dependent manner, such as HuR, HuD, AUF1, KSRP, TTP and BRF (Barreau et al., 2005); and the list of ARE binding proteins is still being extended. The function of ARE binding proteins have been analyzed by the consequence of protein depletion or overexpression. Based on the effect of these proteins on mRNA stability, ARE binding proteins can be generally devided into two classes, stabilizing factors and destabilizing

factors. HuR is one of the well characterized stabilizing factors. For example, knockdown of HuR dramatically reduced the half life of its associating mRNAs, such as TNF-α (Dean et al., 2001). Although the precise molecular mechanism by which HuR stabilizes its associated mRNAs remains unknown, it is well believed that the effect of HuR on mRNA stability is regulated through its cytoplasm localization and association with its targeting mRNAs. However, binding of another class of ARE binding proteins, such as KSRP, TTP and BRF1, leads to reduced mRNA stability (Chou et al., 2006; Gherzi et al., 2004; Gherzi et al., 2006). Mechanistic studies revealed for example that KSRP promotes mRNA degradation by recruiting mRNA degradation machineries, including poly(A) ribonuclease (PARN) and exosomes (Gherzi et al., 2004). Following the elimination of poly(A) tail by PARN, exosome complexes degradate mRNAs from the 3' end. In addition, poly(A) tail shortening triggers exoribonuclease-mediated mRNA decay through the 5' end following the removal of cap structures by decapping enzyme complexes (Tharun and Parker, 2001). TTP and BRF1 were shown to promote the degradation of ARE containing mRNA by delivering them to P-bodies (Franks and Lykke-Andersen, 2007). This was supported by the observation that both overexpression of TTP or BRF and knockdown of decapping enzymes leads to an enhanced accumulation of ARE-containing mRNA in P-bodies (Franks and Lykke-Andersen, 2007). Since both stabilizing and destabilizing factors can bind to AREs, it is very likely that the half-life of an ARE-containing mRNA will be determined by the relative abundance of these two classes of trans-acting factors. This may also provide a plausible mechanism for the function of cytoplasmic localization of HuR on ARE mRNA stabilization.

Coding region determinants (CRDs) are another family of RNA cis-acting elements regulating mRNA instability. CRD is located within the coding region of an mRNA. The discovery of CRD mediated mRNA decay provided a direct link of mRNA translation and mRNA degradation. Earlier studies revealed that CRD mediated mRNA decay is translation-dependent; impeding translation of CRD-containing mRNAs by translation inhibitors or introducing a stable stem-loop structure upstream of the translation initiation codon led to mRNA stabilization (Schiavi et al., 1994). c-myc and c-fos mRNAs are the two best studied CRD-containing transcripts: Zbp1 is a CRD binding protein for c-myc mRNA and Unr, PAIP-1, hnRNP-D and hnRNP-Q associate with the CRD of c-fos mRNA, overexpression of these proteins stabilizes c-myc and c-fos mRNA stability, respectively (Bernstein et al., 1992; Grosset et al., 2000). A study of c-myc mRNA showed that the CRD contains two rare codons in its 3' end, the presence of which leads to translation pauses and thereby exposes the CRD to a polysome-associated endoribonuclease which cleaves the c-myc CRD sequence. Binding of Zbp1, also known as CRD-BP, to the CRD of c-myc mRNA restrains the accessibility of this endoribonuclease and consequently stabilizes c-myc mRNA (Lemm and Ross, 2002; Sparanese and Lee, 2007). A later study also showed that hnRNP-Q1 is also involved in c-myc mRNA stability control possibly in a similar way to Zbp1 (Weidensdorfer et al., 2009). However, this model cannot explain the observation that treatment with a polysome stabilizing translation inhibitor, cycloheximide, which arrests translation elongation, protected c-fos mRNA from CRD-mediated decay. To explain this phenomenon, one alternative model would be that CRD binding proteins stabilize mRNA partially by inhibiting translation initiation. Supportive evidence can be derived from a

Zbp1 knockdown analysis, in which Weidensdorfer et al. found that, in addition to reduced c-myc mRNA stability, knockdown of Zbp1 increased the ratio of translating (present in polysomes) and nontranslating (present in mRNP) c-myc mRNA (Weidensdorfer et al., 2009).

Besides CRD-mediated mRNA decay, the coupling of mRNA degradation with translation may act as a general mechanism for cells to eliminate translated mRNAs, especially mRNAs with long half-lives. This hypothetical model is supported by some recent progress in the study of the involvement of translation termination factors in poly(A) tail shortening and mRNA degradation (Funakoshi et al., 2007; Hosoda et al., 2003). mRNA poly(A) tail in complexes with PABPC1 is required for both efficient Cap-dependent translation initiation and mRNA stability by preventing the attack of exoribonucleases. The shortening of poly(A) tails has been thought to be a speed-limiting step for general mRNA degradation. In eukaryotic cells, translation termination and the release of freshly synthesized peptides are facilitated by the recruitment of eRF1-eRF3 releasing factor complex to the ribosomal A site (Zhouravleva et al., 1995). eRF1 recognizes all three stop codons and eRF3 is a small GTPase interacting with eRF1 in a GTP binding dependent manner (Kobayashi et al., 2004; Zhouravleva et al., 1995). eRF3 consists of two functional domains, a C-terminal domain which contains full functions for translation termination (Eurwilaichitr et al., 1999) and a N-terminal domain which is important for translation-coupled events (Hosoda et al., 2003). Yeast cells expressing eRF3 with N-terminus deletion (*eRF3ΔN*) on an *eRF3-null* background exhibit normal translation termination but with elongated mRNA half-lives associated with longer poly(A) tails (Hosoda et al., 2003), suggesting that mRNA poly(A) tail shortening and

translation termination are tightly coupled. Additional biochemical studies revealed that both eRF3 and deadenylase complexes, Pan2-Pan3 and Caf1-Ccr4, directly interact with the C-terminal domain of PABPC1 (Funakoshi et al., 2007). The interaction with PABPC1 is essential for the catalytic activity of Pan2-Pan3 (Uchida et al., 2004). The binding of N-terminal domain of eRF3 to PABPC1 prevents the latter from interacting with deadenylases complexes. When translating polysomes proceed to a stop codon, eRF1 recruits GTP-bound eRF3 and possibly disrupts the interaction between eRF3 and PABPC1. Consequently, PABPC1 recruits and activates Pan2-Pan3 and/or Caf1-Ccr4 which catalyze deadenylation reactions resulting in mRNA poly(A) tail shortening and subsequent mRNA degradation. Although some refinement may be needed, this model seems to be an appealing mechanism for cells to control protein expression level by selectively degrading translating mRNAs.

RNA-binding proteins and diseases

Posttranscriptional regulation of gene expression plays a major role in multiple cellular events during development, such as embryogenesis, cell migration and neuronal plasticity. Aberrant expression of RNA binding proteins functioning in this regulatory pathway has been shown to be associated with human diseases. Upregulation of the RNA stabilizing protein, HuR, has been found in multiple forms of human tumors. HuR promotes tumor cell proliferation by enhancing the stability of mRNAs encoding oncogenes, growth factors, cytokines and cell cycle regulators (Nabors et al., 2001; Nabors et al., 2003; Ortega et al., 2008; Suswam et al., 2005). The expression of Zbp1 is developmentally regulated with high expression level at embryonic stages and low level or no expression after adulthood. Re-expression of ZBP1 was observed in certain primary

human tumors, such as breast cancer, colon and lung tumors (Ioannidis et al., 2003a, b; Ioannidis et al., 2001; Ross et al., 2001). Transgenic overexpression of Zbp1 in mammary epithelial cells induced mammary tumors, in part by stabilizing *Igf2* mRNA stability and enhancing Igf2 protein expression (Tessier et al., 2004). In colorectal carcinomas, the expression level of Zbp1 positively correlates with the potency of tumor cell metastasis (Vainer et al., 2008). Fragile X mental retardation is caused by FMRP inactivation by CGG trinucleotide expansion in the promoter region (Pietrobono et al., 2005). FMRP acts as a translation repressor in regulation of dendritic local protein synthesis, possibly in post-synaptic compartments (Bassell and Warren, 2008; Feng et al., 1997; Li et al., 2001). Loss of FMRP leads to enhanced neuronal activity, particularly mGluR-mediated long-term depression, a major process associated with learning ability and memory formation (Huber et al., 2002). Spinal Muscular Atrophy (SMA) may be another human inherited disease associated with defects of posttranscriptional regulatory events. SMA and the role of several different mRNA binding proteins for the pathogenesis of this disease will be discussed in detail below.

Spinal Muscular Atrophy (SMA) and Survival of Motor Neuron protein

SMA is a recessive neurodegenerative disease characterized by the loss of motor neurons and muscle weakness. In SMA patients, motor neurons in the lower spinal cord are primarily affected. SMA is the most common inherited cause of infant death diagnosed in one of every 6000 infants and is caused by low levels of the Survival of Motor Neuron protein (SMN) or mutations affecting its function. SMN is ubiquitously expressed in all cells and all tissues (Lefebvre et al., 1995), with high expression levels in the nervous system, especially the spinal cord. SMN is an essential protein for general

cell growth and survival; in mice, knockout of SMN gene causes massive cell death and subsequent embryonic lethality at early developmental stages (Schrank et al., 1997). Unlike other species (i.e. mice) that have only one copy of the *SMN* gene, human SMN is encoded by two *SMN* genes on chromosome 5q13 with one telomeric copy, *SMN1* and one centromeric copy, *SMN2*. Only homozygous deletion or mutations of SMN1 leads to SMA; whereas the loss of SMN2 has no consequence, although it contains similar transcription regulatory elements and is transcribed at similar strength as SMN1 (Figure 1-2) (Echaniz-Laguna et al., 1999). In human cells, 90% of the protein product of *SMN1* is full-length SMN and the other 10% is encoded by *SMN2*. The low productivity of *SMN2* is caused by a C-T nucleotide transition in the exon7 which leads to a less efficient incorporation of exon7 into the mature mRNA (Lorson and Androphy, 2000; Lorson et al., 1999); its protein product lacking the carboxyl-terminal exon-7 (SMNΔ7) is unstable and rapidly degraded (**Figure 1-2**) (Lorson and Androphy, 2000). *SMN2* is an essential modifier for SMA; especially in the circumstance of *SMN1* deletion or mutation, the small amount of full-length SMN produced by *SMN2* is sufficient to rescue embryonic lethality but leads to a motor neuron specific degeneration (Figure 1-2) (Monani et al., 2000b). By introducing the human *SMN2* gene into mice with Smn-/- background, a SMA mouse model was generated; these animals exhibit a similar motor neuron phenotype and muscle weakness as seen in SMA patients. In addition, SMA patients with high copy numbers of *SMN2* have less severe symptoms, which could also be observed in SMA mouse models (Monani et al., 2000a).

SMN can be detected in both the cytoplasm and the nucleus in forms of punctae. By immunofluorescence staining, SMN is detected as small granules in the cytoplasm; in

the nucleus, SMN protein was highly enriched in several dot-like structures termed Gems (Liu and Dreyfuss, 1996; Zhang et al., 2003) and Cajal bodies (Carvalho et al., 1999; Young et al., 2000). A similar pattern of subcellular localization of SMN can also be recapitulated by over-expressing fluorescent protein-tagged protein (Dundr et al., 2004; Zhang et al., 2003). The granular distribution of SMN indicates that SMN plays a role in the assembly of large protein complexes with other proteins. Although Smn has only weak RNA binding activity on its own, it does play a role in assembling diverse ribonucleoprotein complexes. Indeed, SMN has been found in complexes with many ribonucleoproteins and RNA binding proteins by direct or indirect interactions, such as Gemin2-8, Unrip, Profilin, Sm and Sm-like proteins, hnRNP-Qs/R, KSRP and FMRP (Burghes and Beattie, 2009). Several domains have been identified in SMN as functional motifs including Gemin2 binding domain (exon 2b), Tudor domain (exon3) for the interaction with Sm and other RNA binding proteins, profilin binding domain (exon5) and a self-association (exon6) domain (Briese et al., 2005; Monani, 2005). In addition, a cytoplasmic targeting sequence (QNQKE) was identified in exon7, the lack of which leads to nuclear accumulation of over-expressed protein (Zhang et al., 2003). The majority of disease-causing point mutations are found in the Tudor domain and the self-association domain, indicating that the interaction of SMN with RNA binding proteins as well as its self-oligomerization are essential for normal SMN functions (Burghes and Beattie, 2009).

One well-characterized SMN containing complex is the SMN-Gemin protein complex composed of SMN, Gemin2-8 and UNR-interacting protein (Unrip), in which SMN forms a core structure possibly by its oligomerization and further recruitment of

other proteins. SMN-Gemin protein complex plays an essential role in the assembly of the splicing machinery - so called spliceosomes which catalyze the removal of introns from pre-mRNAs (Kolb et al., 2007; Pellizzoni, 2007). Spliceosomes are a family of small nuclear RNP complexes (snRNPs), each composed of a uridine-rich small nuclear RNA (snRNA, including U1, U2, U3, U4, U5, U11, U12 etc) and a heptameric ring structure of Sm and/or Lsm proteins. Although these snRNPs can be self-assembled at low efficiency *in vitro*, the presence of SMN-Gemin protein complex greatly facilitates this process (Pellizzoni et al., 2002). Mechanistic studies revealed that the SMN-Gemin complex acts as a platform for snRNP assembly, in which SMN recruits Sm proteins by direct interaction with the methylated RGG domains of Sm proteins through its Tudor domain and Gemin5 recognizes snRNAs (Battle et al., 2006b; Friesen and Dreyfuss, 2000). The simultaneous loading of Sm proteins and snRNAs onto SMN-Gemin complex brings them to a close distance and facilitates their association. Together with the SMN-Gemin protein complex, snRNPs are translocated into the nucleus for further maturation (Pellizzoni, 2007).

Based on the function of SMN on spliceosome assembly, a snRNP assembly model has been proposed for the pathogenesis of SMA, especially motor neuron degeneration. Studies using a SMA mouse model suggest that the levels of endogenous snRNPs are universally reduced in the spinal cord of SMA mice, particularly U11 and U12-containing minor snRNPs, the levels of which were also reduced in the brain (Gabanella et al., 2007; Zhang et al., 2008). The reduced formation of snRNPs is correlated with the severity of SMA (Gabanella et al., 2007; Zhang et al., 2008). A later genome-wide analysis demonstrated a widespread deregulation of splicing in multiple

tissues of postnatal day 11 SMA mice, and mRNAs containing a large number of introns seem to be primarily affected (Zhang et al., 2008).

However, these observations cannot provide a plausible explanation for the motor neuron specific phonotype of SMA, indicating the loss of additional functions of SMN may be involved, such as mRNP assembly and mRNA localization. Evidence for these novel functions SMN has been accumulated in the recent several years. Besides localization to the perinuclear cytoplasm and the nucleus, SMN protein is also detected in distal axons and growth cones (Zhang et al., 2003). The overexpressed fluorescent protein-tagged SMN forms granules in neuronal axons and exhibits bidirectional movement in a cytoskeleton-dependent manner (Zhang et al., 2003). In addition, endogenous SMN colocalizes with ribosomal RNAs in axons, suggesting a possible function of SMN in mRNA metabolism, possibly mRNA transport and/or local translation in axons. A study using motor neurons cultured from SMA mice showed that both protein and mRNA level of β-actin were greatly reduced in growth cones, indicating a requirement of SMN for the axonal transport of β-actin mRNA which is impaired in the absence of SMN (Rossoll et al., 2003). As a consequence, these cells exhibit reduced axon length and growth cone size. A similar axonal phenotype was also observed in *Zebrafish* and *Xenopus* embryos following SMN depletion (McWhorter et al., 2003; Ymlahi-Ouazzani et al., 2009). These observations suggest that SMN has functions beyond splicing, and point studies of SMA pathogenesis towards a new direction, i.e. the function of SMN in axonal mRNA transport and related regulation.

In addition, SMN has been reported to directly or indirectly interact with mRNA binding proteins in RNP complexes, such as KSRP, FMRP, and hnRNP-Qs/R

(Mourelatos et al., 2001; Piazzon et al., 2008; Rossoll et al., 2002; Tadesse et al., 2008). Our unpublished data showing the interaction of SMN with Zbp1 and HuD further extend this list. All these RNA binding proteins are localized to neuronal processes and play essential roles in mRNA transport or other aspects of posttranslational regulation (Bannai et al., 2004; Dictenberg et al., 2008; Gu et al., 2002; Smith et al., 2004; Zhang et al., 2001; Zhang et al., 1999). In all these cases, SMN protein, either endogenous or overexpressed, is partially colocalized with the RNA binding protein within axons. In the study of SMN and KSRP interaction, Tadesse et al. reported that SMN possibly acts as a molecular chaperone which regulates KSRP methylation (Tadesse et al., 2008). The loss of SMN leads to KSRP destabilization and further alters KSRP-mediated mRNA degradation. Rossoll et al. suggested that SMN plays a role in β-actin mRNA transport through its interaction with hnRNP-R which associates with β-actin 3'UTR (Rossoll et al., 2003; Rossoll et al., 2002). A study using a *zebrafish* SMA model further enhances this hypothesis. In this study, the authors demonstrated that defective axon growth in SMN-depleted *zebrafish* is snRNP assembly-independent, since these defects can be fully rescued by a synthetic SMN mutant which does not function in snRNP assembly (Carrel et al., 2006).

So far, the exact role of SMN in posttranscriptional regulation remains largely as an open question. One postulated mechanism is that SMN plays its role in mRNP assembly in a similar fashion as snRNP assembly and the loss of SMN may cause defective posttranscriptional regulation of gene expression which leads to motor neuron developmental abnormalities (Burghes and Beattie, 2009). The SMN-Gemin protein complex may be the functional unit in this process, as shown by Piazzon et al. that SMN

interacts with FMRP in the form of an SMN-Gemin complex and FMRP co-precipitates Gemin proteins in a SMN-dependent manner (Piazzon et al., 2008); however, other SMN-containing complexes may exist. A biochemical identification of these SMN-containing complexes and the functional demonstration will be of great importance to address questions related to this potential novel function of SMN and its implication to the pathogenesis of SMA.

Outline of this dissertation

The overall objective of my thesis research is to elucidate potential functions and mechanisms of components of cytoplasmic RNA granules, particularly SMN and hnRNP-Q1, in mRNA regulation. We hypothesized that SMN, in a complex with its interacting mRNA binding proteins, e.g hnRNP-Q1, plays a role in the post-transcriptional regulation of gene expression. In this dissertaion, we examined the axonal localization and composition of SMN granules (**Chapter II**), investigated the function of hnRNP-Q1 in the translational regulation of RhoA mRNA and the subsequent effects of hnRNP-Q1 depletion (**Chapter III**) and further assessed the distribution of hnRNP-Q1 and SMN in various forms of mRNP granules (**Chapter IV**). Our findings suggest novel functions of SMN and hnRNP-Q1 in mRNA regulation, and bring forth a new direction for studies regarding mechanisms underlying the pathogenesis of SMA. Finally, several future studies which may further test our main hypothesis are discussed (**Chapter V**).

Processing Body
(translational repression; mRNA degradation; RISC, Dcp1a, LSm1)

Stress Granule
(storage of translationally repressed mRNAs; SMN, FMRP and ZBP1; TIA-R/1, PABP, G3BP)

Transport mRNP
(transport of translationally repressed mRNAs; Zbp1, FMRP and Staufen)

Polyribosome
(actively translated mRNAs; Ribosomal proteins, PABP and FMRP)
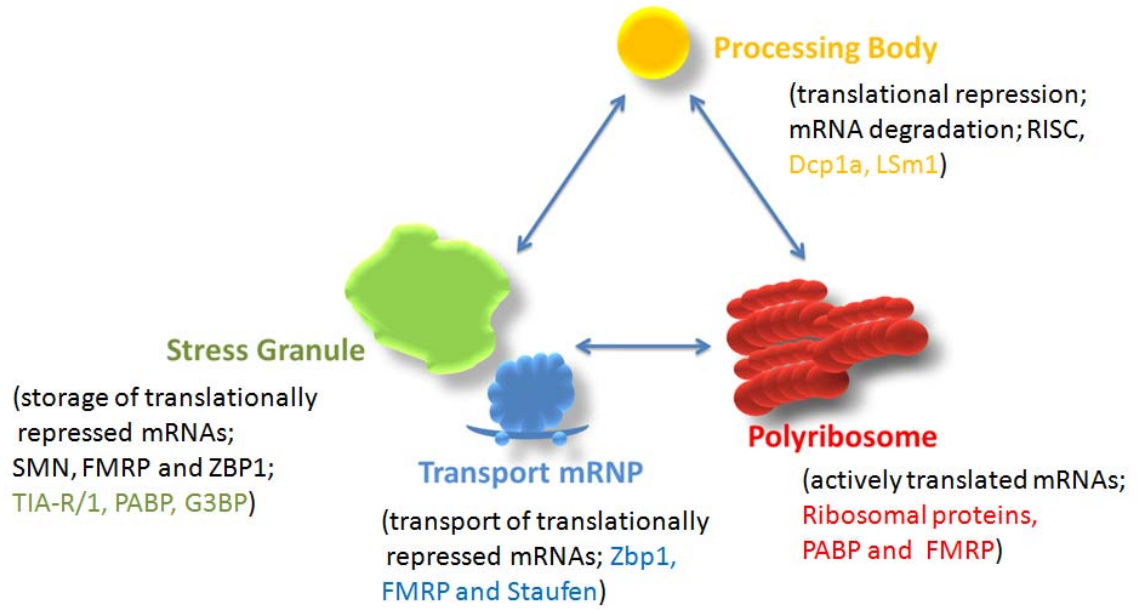
Figure 1-1. Proposed dynamic interaction of mRNA-containing granules and polyribosomes (for reviews, see Balagopal and Parker, 2009; Kiebler and Bassell, 2006). Specific mRNA binding proteins appear to play key roles in each mRNP complex are shown. TIAR/1, poly(A)-binding protein (PABP) and GTPase-activating protein, SH3 domain binding protein (G3BP) are markers of stress granules. RNA-binding proteins such as FMRP and zipcode-binding protein 1 (ZBP1), and RNA-binding protein-associated factors such as the survival of motor neuron protein (SMN) were also detected in stress granules. ZBP1, FMRP and Staufen were identified as components of transport mRNP granules. Both stress granules and transport mRNP granules contain translationally scilenced mRNAs. Decapping proteins such as Dcp1a and exosome protein Sm-like protein 1 (LSm1) are enrighed in P-bodies and used as markers for this type of mRNP granule. In addition, conponents of RNA-induced scilencing complex (RISC) are also localized to P-bodies. P-bodies are proposed as sites for both mRNA degradation and translational scilencing. Both PABP and FMRP associate with active polyribosomes (polysomes). As resolved by a linear sucrose gradient, the enrichment of PABP and FMRP in polysome fractions were observed.

Normal

	SMN1	SMN2

DNA: Ex1-6 — C/G Ex7 — Ex8 3'UTR

DNA: Ex1-6 — T/A Ex7 — Ex8 3'UTR

10% / 90%

mRNA: Ex1-6 Ex7* Ex8 3'UTR

mRNA: Ex1-6 Ex7* Ex8 3'UTR | Ex1-6 *Ex8 3'UTR

Protein: functional SMN

Protein: functional SMN | unstable SMNΔ7

Rapidly degraded

* : translation stop codon

SMA

	SMN1	SMN2

DNA: Ex1-6 — C/G Ex7 — Ex8 3'UTR

DNA: Ex1-6 — T/A Ex7 — Ex8 3'UTR

10% / 90%

mRNA: Ex1-6 Ex7* Ex8 3'UTR

mRNA: Ex1-6 Ex7* Ex8 3'UTR | Ex1-6 *Ex8 3'UTR

Protein: functional SMN

Protein: functional SMN | unstable SMNΔ7

Rapidly degraded

Figure 1-2. Loss of human *SMN1* leads to SMA. Human SMN is encoded by two SMN genes, *SMN1* and *SMN2*, which differ in only one nucleotide in their coding regions, with C in *SMN1* and T in *SMN2* (Lorson and Androphy, 2000; Lorson et al., 1999). Such nucleotide transition does not alter the encoded amino acid, yet leads to a less efficent incprporation of exon7 into mature *SMN2* mRNAs. Thus 90% of proteins encoded by *SMN2* are in a truncated form named SMNΔ7, which is unstable campared with full-length SMN and rapidly degradted (Lorson and Androphy, 2000). (A) In normal cells, full-length functional SMN is translated from *SMN1* mRNA and a small fraction of *SMN2* mRNA containing exon7. (B) Deletions or mutations of human *SMN1* leads to SMA (Lefebvre et al., 1995), yet the loss of *SMN2* has no effect when *SMN1* is functional. *SMN2* is an essential modifier for the functions of *SMN1*. In species with only one *SMN* gene, such as mice, the loss function of SMN leads to embryonic lethality (Schrank et al., 1997). The tranagene of *SMN2* into the mouse genome rescues the embryonic lethality caused by the loss of *SMN1*, but leads to SMA with motor neuron degeneration and muscle weakness (Monani et al., 2000a).

Chapter II

Multiprotein Complexes of the Survival of Motor Neuron Protein SMN with Gemins Traffic to Neuronal Processes and Growth Cones of Motor Neurons

Honglai Zhang,[2][*] Lei Xing,[1][*] Wilfried Rossoll,[1] Hynek Wichterle,[3] Robert H. Singer,[2] and Gary J. Bassell[1]

[*]These authors contributed equally to this work

[1]Department of Cell Biology and Center for Neurodegenerative Disease, Emory University, Atlanta, Georgia 30322, [2]Department of Anatomy and Structural Biology, Albert Einstein College of Medicine, Bronx, New York 10461, and [3]Department of Pathology, Columbia University College of Medicine, New York, New York 10032

Abstract

Spinal Muscular Atrophy (SMA), a progressive neurodegenerative disease affecting motor neurons, is caused by mutations or deletions of the *SMN1* gene encoding the Survival of Motor Neuron (SMN) protein. In immortalized non-neuronal cell lines, SMN has been shown to form a ribonucleoprotein complex with Gemin proteins which is essential for the assembly of snRNPs. An additional function of SMN in neurons has been hypothesized to facilitate assembly of localized mRNP complexes. We have shown that SMN is localized in granules that are actively transported into neuronal processes and growth cones. In cultured motor neurons, SMN granules colocalized with ribonucleoprotein Gemin proteins, but not spliceosomal Sm proteins needed for snRNP assembly. Quantitative analysis of endogenous protein colocalization in growth cones following 3D reconstructions revealed a statistically non-random association of SMN with Gemin2 (40%) and Gemin3 (48%). SMN and Gemin containing granules distributed to both axons and dendrites of differentiated motor neurons. A direct interaction between SMN and Gemin2 within single granules was indicated by FRET analysis of fluorescently tagged and overexpressed proteins. High speed dual channel imaging of live neurons depicted the rapid and bi-directional transport of the SMN-Gemin complex. The amino-terminus of SMN was required for the recruitment of Gemin2 into cytoplasmic granules and enhanced Gemin2 stability. In addition, SMN partially colocalized with hnRNP-Qs/R and fluorescent protein-tagged SMN and hnRNP-Q1 were co-transported in neuronal processes. These findings provide new insight into the molecular composition of distinct SMN multi-protein complexes in neurons and motivation to investigate deficiencies of localized RNPs in SMA.

<u>Introduction</u>

Spinal muscular atrophy (SMA) is a common inherited disease, characterized by neurodegeneration of α-motor neurons (Frugier et al., 2002). SMA is caused by mutation and/or deletion of the *SMN1* gene that encodes the Survival of Motor Neuron protein (SMN) (Frugier et al., 2002). SMN localizes to both the cytoplasm and the nucleus; in the nucleus it is found in gems (Liu and Dreyfuss, 1996) that often colocalize with coiled (Cajal) bodies (Carvalho et al., 1999; Young et al., 2000). Based on biochemistry studies of non-neuronal cell lines, several SMN-associated proteins, named Gemins, have been identified as integral components of the SMN ribonucleoprotein complex (Gubitz et al., 2004; Yong et al., 2004). While it is clear that a critical function for the SMN-Gemin complex is to act as an assembly machine to facilitate spliceosomal snRNP assembly (Paushkin et al., 2002) it is unclear why motor neurons are more vulnerable to loss of SMN. One hypothesis is that reduction of SMN levels in neurons (particularly motor neurons) may compromise splicing machinery more seriously (Gubitz et al., 2004). So far there is no evidence for mRNA splicing defects in SMA patients or SMA models.

An alternative view is that the SMN complex is used for an additional function in neurons, such as assembly and regulation of localized mRNP complexes (reviewed in: (Briese et al., 2005; Monani, 2005). Previous immunocytochemical studies have detected SMN in both dendrites and axons *in vivo* (Bechade et al., 1999; Pagliardini et al., 2000). Using immuno-fluorescence on cultured primary neurons, endogenous SMN was localized in granules that extend throughout processes and into growth cones (Zhang et al., 2003). Live cell imaging has revealed rapid and cytoskeletal-dependent movements of EGFP-SMN granules (Zhang et al., 2003). SMN was shown to bind hnRNP-R (Rossoll et

al., 2002), an mRNA binding protein that can associate with β-actin mRNA *in vitro* (Rossoll et al., 2002). While the precise role of hnRNP-R in the mechanism of β-actin mRNA localization is unknown, deficiency of SMN, in a mouse transgenic model of SMA (Monani et al., 2000b), results in reduced localization of β-actin mRNA in cultured motor neurons (Rossoll et al., 2003). This study suggests some role of SMN in the assembly and/or localization of β-actin mRNP complexes. Since previous studies have identified an important function for β-actin mRNA localization (Zhang et al., 2001) and local protein synthesis (Campbell and Holt, 2001) in mediating growth cone motility and chemotropic responses, the hypothesis that SMN participates in some aspect of cytoplasmic-directed RNA localization and/or translation in growth cones is very appealing.

In order to understand how SMN may be involved in the assembly and/or localization of ribonucleoprotein complexes in neurons, it is first necessary to identify the protein components of SMN granules and elucidate their molecular interactions with SMN. Past studies have been inconclusive on whether Gemin proteins are present as particles within neuronal processes and whether they colocalize with SMN. In one report, SMN was distributed in a particulate pattern in processes of cultured motor neurons, yet Sip1 (Gemin2) was uniformly distributed and showed little colocalization (Jablonka et al., 2001). More recently, SMN and several of the Gemin proteins were shown by double label IF to be co-enriched in neuritic protrusions of PC12 cells (Sharma et al., 2005), however, this study did not utilize methods to permit assessment of whether SMN and Gemins colocalize within individual particles or granules. In this study, we have employed fluorescence microscopy, digital imaging and quantitative analyses of live and

fixed neurons to demonstrate the formation of an SMN-Gemin complex in neuritic granules, yet our data also suggest the presence of SMN granules lacking Gemins. In addition, we show that molecular interactions between SMN and Gemin proteins can affect the assembly and localization of this complex. We then assessed whether some SMN granules in neuronal processes colocalized with hnRNP-Qs, a family of RNA binding proteins which have been shown to directly interact with SMN and are implicated in mRNA transport. We observed that SMN and hnRNP-Qs/R were partially colocalized in granules in processes of primary hippocampal neurons and overexpressed mRFP-SMN and EGFP-hnRNP-Q1 formed granules, in which these proteins were colocalized and actively transported along neuronal processes.

Materials and Methods

Chick forebrain and rat and mouse hippocampal cultures

Chick forebrain neurons were cultured as described previously (Zhang et al., 2001; Zhang et al., 2003). Briefly, chick forebrains (E8) were dissected, trypsinized (0.15% in HBSS) at $37^{o}C$ for 7 minutes, and plated on poly-L-lysine (0.4mg/ml) and laminin (0.02mg/ml) -coated coverslips. Cells were inverted onto a monolayer of astrocytes in N_3-conditioned medium with 2% FBS, and cultured for 4 days at 37ºC in 5% CO_2. N_3-conditioned medium containing minimum essential medium eagle (MEM) supplemented with transferrin (0.2%), ovalbumin (0.1%), insulin (10 μg/ml), putrescine (32 μg/ml), sodium selenite (26 ng/ml), progesterone (12.5 ng/ml), hydrocortisone (9.1 ng/ml), T3 (3, $3^{'}$, $5^{'}$-triiodo-L-thyronine, sodium salt, 20ng/ml) and BSA (10 μg/ml). Rat

(embryonic day 18) or mouse (embryonic day 16) hippocampi were cultured for four days as described (Antar et al., 2004).

<u>Primary and ES-cell derived motor neuron cultures</u>

Primary mouse motor neuron cultures were prepared from E13.5 mouse spinal cords essentially as described previously (Arce et al., 1999) but the magnetic column step was omitted, and metrizamide was replaced by Optiprep (10%; Nycomed Pharma, Oslo, Norway) for gradient centrifugation. Cells in the motor neuron-enriched fraction were plated on 15-mm glass coverslips coated with poly-ornithine/ laminin. Motor neurons were identified by morphological criteria and by immunofluorescence staining of choline acetyltransferase (ChAT) with rabbit anti-ChAT (Chemicon International Inc.). More than 90% of the purified cells were positive for ChAT (data not shown). Culture medium was Neurobasal (Invitrogen) supplemented with B27 (Invitrogen), horse serum (2% v/v; Sigma), Glutamax-1 (0.5 mM; Invitrogen), 2-mercaptoethanol (25μM), BDNF and CNTF (10ng/ml; Peprotech).

Mouse HB9::eGFP embryonic stem cells (HBG3 cells) were cultured and differentiated into motor neurons as previously described (Wichterle et al., 2002) with the following minor modifications. ES cells were plated at 10^5 cells per ml in DFNK medium (DMEM:F12:Neurobasal in 1:1:2 ratio supplemented with 10% Knockout SR, 0.1 mM 2-mercaptoethanol (Sigma), 200 mM L-Glutamine and 1x Penicillin/Streptomycin (Invitrogen, wherever not specified)). Two day old embryoid bodies were induced with 1μM retinoic acid (Sigma) and 1μM HhAg1.3 (Frank-Kamenetsky et al., 2002). Four days after induction motor neurons were dissociated using the papain dissociation system

(Worthington) and plated on poly-D-lysine and laminin (20µg/ml) coated coverslips, cultured for three days and fixed.

Immunofluorescence

All cells were fixed in paraformaldehyde (4% in 1x PBS) for 20 minutes at room temperature and washed in 1x PBS with 5mM $MgCl_2$ three times.

Monoclonal antibodies to SMN (BD Biosciences; 1:1000), Gemin3 (Abcam Limited, Cambridge, UK; 1:1000), and a rabbit antibody to Gemin2 (provided by Utz Fischer; 1:1000) (Jablonka et al., 2001), were used for detection of the endogenous proteins in cultured chick forebrain and ES-cell derived motor neurons. To analyze the distribution of snRNPs with respect to SMN, primary cultures of motor neurons were double stained with a monoclonal antibody (Y12) to Sm proteins (provided by Utz Fischer; 1:2000) and a rabbit polyclonal antibody to SMN (Santa Cruz Biotech., Inc; 1:500); the specificity of which was tested by western blot. Primary antibodies were detected by affinity-purified donkey antibodies to mouse or rabbit IgG conjugated to fluorochromes, Cy3 or Cy5 (Jackson ImmunoResearch Lab., Inc). A polycolonal antibody recognizing all hnRNP-Q isoforms and hnRNP-R (rabbit anti-Syncrip, 1:5000, provided by Dr. Mikoshiba) were used for the colocalization study of hnRNP-Qs/R and SMN. For quantitative colocalization analysis, mouse anti-SMN was conjugated with Alexa Fluro 647 and mouse anti-Gemin2, Gemin3 and Synaptophysin (Sigma, Saint Louis) were conjugated with Alexa Fluro 568 using Zenon mouse IgG1 labeling kits (Invitrogen) according to manufacturer instructions. Alexa fluorochrome-conjugated antibodies were used at 1:600 for mouse anti-SMN, Gemin2 and Gemin3 antibodies, and 1:200 for mouse anti-synaptophysin. Alexa fluorochrome-conjugated mouse antibodies to

SMN and Gemin2 were also used to detect SMN-Gemin complex in primary cultures of rat hippocampal neurons and mouse motor neurons. Axons and dendrites were discriminated by IF with rabbit anti-tau (Sigma, Saint Louis; 1:2000) or rabbit anti-MAP2 (Sigma, Saint Louis; 1:1500) and visualized with Cy2 conjugated secondary antibody (Jackson ImmunoResearch Lab., Inc). Antibody incubations were for 1 hour at room temperature in Tris-Buffered Saline (TBS) with BSA (2%) and triton X-100 (0.1%). Coverslips were mounted in a mount medium, as described previously (Zhang et al., 2001) .

Fluorescence protein-reporter constructs

Full-length cDNA of the human *SMN1* was subcloned into pEGFP-C1 (EGFP-SMN) as previously described (Zhang et al., 2003). In the present study, full-length cDNA of *SMN1* was inserted into pEYFP-C1 (BD Biosciences Clontech, Palo Alto, CA) and pmRFP-C1 using HindIII and EcoRI sites (YFP-SMN). Full-length cDNAs of human Gemin2, Gemin3 and hnRNP-Q1 were obtained by RT-PCR from total RNA extracts of HEK293 cells. Gemin2 was inserted into pEGFP-C1 or pECFP-C1 (BD Biosciences Clontech, Palo Alto, CA) using BglII and EcoRI sites (EGFP-Gemin2 or ECFP-Gemin2); Gemin3 was inserted into pEGFP-C1 or pECFP-C1 using BglII site (EGFP-Gemin3 or ECFP-Gemin3); hnRNP-Q1 was inserted into pEGFP-C1 using Xho1 site (EGFP-hnRNP-Q1). To determine domain-dependent interaction of SMN with Gemin2, a human SMN cDNA with deletions of exon-1 and 2a (the first 53 amino acids), which includes the 39 amino acids (encoded by chick SMN cDNA) that contains the Gemin2 binding site (Wang and Dreyfuss, 2001b), was generated using PCR primers and then subcloned into pEYFP-C1 (EYFP-SMNΔN53). For Co-IP experiments, YFP sequence was substituted

with a Flag-tag (MDYKDDDDK) in the above SMN constructs using AgeI and HindIII sites (Flag-SMN, Flag-SMNΔ7, and Flag-SMNΔN53). All of the constructs were purified (Qiagen) and sequenced to ensure that no frame shift had occurred.

Transfection

Chicken forebrain neuron transfections were performed using DOTAP liposomal reagent (Roche), as described previously (Zhang et al., 2001; Zhang et al., 2003). In co-transfection experiments, two DNA constructs were mixed equivalently (2-3μg in total) and diluted to 100μl with transfection buffer (20mM HEPES, 150mM NaCl, pH 7.4) and then incubated with DOTAP (5μl), as described above. Rat hippocampal neurons were transfected with Amaxa nucleofector (Lonza) according to the manufacturer's protocol.

HEK293 cells were transfected with Flag- and EGFP-tagged constructs. HEK 293 cells were cultured in DMEM containing 10% FBS (Sigma). Cells were briefly washed with pre-warmed medium before transfection. Equivalent amount of Flag- and EGFP-tagged constructs (2-3μg in total) were diluted to 100μl in the transfection buffer and then incubated with 5μl of FuGENE 6 transfection reagent (Roche) for 15 minutes at room temperature. After incubation with the DNA mixtures for one hour, the cells were cultured in DMEM containing 10% FBS for 24 hours. Protein lysates were prepared as described below.

Fluorescence microscopy and digital imaging

Fixed neurons were visualized using a Nikon Eclipse inverted microscope equipped with a 60x Plan-Neofluar objective, phase optics, 100W mercury arc lamp and

HiQ bandpass filters (Chroma Tech). Images were captured with a cooled CCD camera (Quantix, Photometrics) using a 35 mm shutter and processed using IP Lab Spectrum (Scanalytics). Fluorescence images were acquired with specific filters, including Cy2, Cy3 or Cy5. In the transfected neurons, specific signals of EGFP, ECFP and EYFP were observed using narrow band-pass filters. Exposure time was kept constant and below gray scale saturation.

Live neurons that co-expressed ECFP-Gemin2 or ECFP-Gemin3 with EYFP-SMN were imaged in a sealed environmental chamber (Bioptechs Focht Chamber) using a TILL Photonics Imaging System. ECFP and EYFP images were alternately acquired by a CCD camera (Imago QE, TILL-Photonics, Germany) and synchronized with a monochromator with millisecond response time that was switching between 442 nm (ECFP) and 510 nm (EYFP) excitation (Polychrome II, TILL-Photonics, Germany). Images were captured at an exposure rate of 0.5 second for each frame, with a total of 200 frames. Images representing the cotransport of mRFP-SMN and EGFP-hnRNP-Q1 were acquired at an exposure rate of half second per frame with a Nikon TE2000 microscope equipped with a RFP/GFP duel-view system which allows the simultaneous acquisition of EGFP and mRFP signals.

Colocalization analysis

To quantify the colocalization of SMN and Gemin proteins, rat hippocampal neurons were double stained with Alexa 647 conjugated mouse anti-SMN and Alexa 568 conjugated mouse anti-Gemin2, Gemin3 respectively or to anti-synaptophysin, as a negative control. Growth cones were imaged in each channel along the z axis (11 sections at 0.1μm each) and five in-focus sections from each z-stack were deconvolved using a 3D

blind algorithm (Autoquant X, Bitplane) and analyzed for colocalization (see below). Images were registered using fiduciary beads (conjugated with multiple fluorochromes) present in mounting medium.

Colocalization was measured using ImarisColoc (Imaris 4.5.2, BitPlane). The threshold of each channel used to quantify colocalization was determined by creating IsoSurface (Imaris 4.5.2, BitPlane), which represents the signal range of a dataset. Colocalization was defined as the overlap of two channels in 3-dimensions and calculated by the program automatically. The degree of colocalization was represented by percentage of voxels of each channel above the threshold colocalized. Ten datasets from each sample were analyzed with an unpaired Student's t test.

Fluorescence Resonance Energy Transfer (FRET)

To evaluate whether SMN interacts with Gemin proteins within granules, Fluorescence Resonance Energy Transfer (FRET) was performed on neurons that co-expressed EYFP-SMN and either ECFP-Gemin2 or ECFP-Gemin3. ECFP as a donor and EYFP as an acceptor is a preferred pair for FRET analysis because the emission spectrum of ECFP significantly overlaps the excitation spectrum of EYFP. The resulting energy from donor ECFP may directly excite the acceptor EYFP when the distance of two fluors is less than 10 nm (Gordon et al., 1998). FRET measurements were performed by acceptor-bleaching with a confocal laser scanning microscope (LEICA TCS SP2 AOBS, Leica, Mannheim, Germany), equipped with a 63x/1.3 NA oil immersion objective. Fluorescence for ECFP and EYFP were imaged at emission 460-490nm (laser: 458nm) and emission 520-620nm (laser: 514nm), respectively. In all cases the ECFP signal was below saturation. EYFP was photobleached in the selected region of interest (ROI 1). In

total, ten neurons (74 neuritic granules) were traced and subjected to FRET measurements between EYFP-SMN and ECFP-Gemin2. Six neurons co-expressing EYFP-SMN and ECFP-Gemin3 were also imaged and 36 granules in the photobleaching area were selected for FRET measurements. ECFP fluorescence intensities within each ROI were compared between pre- and post-photobleaching. To show that FRET occurred specifically between SMN and Gemins, a small region that was outside the neurite, but within the bleached ROI, was also circled for measurements of changes in ECFP fluorescence, and used as a background correction. As controls, granules were also selected from neurites that were not photobleached. FRET efficiency ($FRET_{Eff}$) was calculated for each pixel from the increase of the donor fluorescence according to $FRET_{Eff} = 1 - ECFP_{Pre}/ECFP_{Post}$. Percentage of the granules that showed increase of ECFP fluorescence at post-bleaching was defined as FRET frequency. FRET average was the mean increase of ECFP fluorescence intensities in the granules showing FRET.

To ensure that there was no bleed-through between ECFP and EYFP, control transfections were done with either EYFP-SMN or ECFP-Gemin2 alone, and then fluorescence intensities in the other channel was examined. In these single transfections, the ECFP or EYFP signals could only be observed and detected with their own emission.

Co-Immunoprecipitation and Western Blot

To show interactions of SMN with Gemin2 and hnRNP-Q1, co-immunoprecipitation experiments were performed on transfected HEK293 cells. One day after transfection with EGFP- and Flag-tagged constructs, HEK293 cells were lysed using an ice-cold buffer (50mM Tris-HCl, 150mM NaCl, 0.1% NP-40 and 0.1% sodium deoxycholate, pH 7.4). The total protein solution was incubated with a rabbit anti-Flag

antibody (2μl) (Sigma) and protein-A agarose (60μl) (Roche) or a mouse anti-GFP antibody (5μl) (JL-8, Clontech) at 4°C overnight with rotation. After washing with a high-salt buffer (50mM Tris-HCl, 300mM NaCl, 0.1% NP-40), the agarose pellets were re-suspended in SDS-PAGE loading buffer (60μl) and heated at 100°C for 5 minutes. 20μl of the proteins from the agarose pellets was loaded onto 12% SDS-PAGE gel. The protein supernatant (20μl) from each transfection was also run onto the gel. Fractionated proteins were transferred to Hybond ECL nitrocellulose membranes (Amersham Biosciences) or PVDF membranes (Bio-Rad) at 4°C overnight. Endogenous Gemin2, Gemin3 or SMN was detected with monoclonal antibodies (1: 2000 diluted in TBS buffer), as used for immunofluorescence staining. Monoclonal antibodies (1:4000 diluted in TBS buffer) to Flag (Sigma) or EGFP (BD Biosciences) were used for detection of the transfected fusion proteins. The membrane was washed and incubated with peroxidase-conjugated donkey anti-mouse IgG (Jackson Immunoresearch). The signal was developed using ECL detection reagents (Amersham Biosciences).

Results

Non-random localization of the SMN-Gemin complex in granules within neurites and growth cones

Previous biochemical studies in non-neuronal cell lines have isolated an SMN complex with Gemin proteins and shown its function in snRNP assembly (Gubitz et al., 2004). Here we have used high resolution fluorescence imaging methods to demonstrate the formation and trafficking of SMN-Gemin multiprotein complexes in neurites and growth cones of cultured neurons. These studies were done in different types of cultured neurons: embryonic sources of primary forebrain, hippocampal and motor neurons and

ES-cell derived motor neurons. There are several past demonstrated advantages of primary forebrain and hippocampal neurons for the study mRNA granule trafficking. These include polarization of axons and dendrites, the presence of large and flat growth cones amenable to quantitative analysis of colocalization, optimization of transfection methods to preserve growth cone morphology and optimization of conditions for live cell imaging (Tiruchinapalli et al., 2003; Zhang et al., 2001). Here we also report use primary embryonic and ES-cell derived motor neurons for immunofluorescence studies.

Double label immunofluorescence on cultured forebrain neurons (4DIV) detected endogenous Gemin2 protein within granules that co-distributed with SMN throughout neurites and into the growth cone **(Figure 2-1A)**. Higher magnification analysis revealed substantial colocalization of SMN (red) and Gemin2 (green) in growth cones **(inset 1, arrows)** and neurites **(inset 2, arrows)**. A similar pattern of localization was observed in neurites of cultured motor neurons, derived from ES cells **(Figure 2-1B)**. SMN granules were frequently colocalized with Gemin2 **(Figure 2-1B, inset, arrows)** in axons of motor neurons. These ES-cell derived motor neurons were obtained from transgenic mice that express EGFP using an HB9 promoter, specific for motor neurons (see Methods). The expression of EGFP in the same cell is shown in **Figure 2-1C**. Detection of Gemin3 by immunofluorescence (red) also revealed granules that extended into the axons and growth cones of EGFP-marked motor neurons **(Figure 2-1D)**.

Primary embryonic mouse motor neurons were purified by Optiprep gradient centrifugation and cultured for seven days. Immunofluorescence detection of choline acetyltransferase (ChAT) revealed positivity for this motor neuron marker in over 90% of the neurons (data not shown; see Methods). Triple label IF detection of SMN, Gemin2

and either tau or MAP2, as axonal and dendritic markers respectively, demonstrated the presence of SMN and Gemin in both axons **(Figure 2-2E, F)** and dendrites **(Figure 2-2G, H)**. SMN colocalization with Gemin2 was noted in many granules (arrows), yet there was also large population of SMN and Gemin2 granules which did not colocalize. Comparable results were also observed for SMN and Gemin localization to axons **(Figure 2-2A, B)** and dendrites **(Figure 2-2C, D)** of hippocampal neurons cultured for one week.

We used primary hippocampal neurons for quantitative analysis of SMN and Gemin protein colocalization in growth cones. Hippocampal neurons, cultured on poly-l-lysine, often display large and flat growth cones, which were ideally suited to analyze for the possible non-random distribution and colocalization of SMN with Gemin proteins. Three immunofluorescence color-pairs were analyzed for colocalization in individual growth cones following 3D reconstruction of deconvolved optical sections. Only primary antibodies were used which were directly conjugated with fluorochromes (see methods). The experimental group was double label immunofluorescence for either SMN-Gemin2 or SMN-Gemin3. Using 3D colocalization anlysis software (Imaris), the voxel overlap in these two data sets were compared statistically to the negative control pair (SMN-synaptophysin). A representative example is shown for SMN-synaptophysin **(Figure 2-3C)**, SMN-Gemin2 **(Figure 2-3D)** and SMN-Gemin3 **(Figure 2-3E)**. 3D reconstructions were done on ten growth cones from each color pair. Quantiative analyses of these 3D data sets demonstrated a statistically non-random colocalization of SMN with Gemins **(Figure 2-3A)** or Gemins with SMN **(Figure 2-3B)**. These values ranged from a low of 33% (Gemin2 with SMN) to a high of 47% (SMN with Gemin3). In contrast, the

colocalization of SMN and Gemins with synaptophysin, an equally abundant protein, only revealed at most 15% overlap. These data indicate the presence of SMN-Gemin containing granules in growth cones, yet also indicate that not all SMN is in a complex with Gemins and vice versa. In addition, we also noted from the growth cone analysis, that SMN-Gemin granules frequently were present in filopodial protrusions **(Figure 2-3D, E; boxed regions)**.

In non-neuronal cells, the SMN-Gemin complex has been shown to interact with spliceosomal Sm proteins to promote the cytoplasmic assembly of small nuclear ribonucleoproteins (snRNPs), which function in pre-mRNA splicing (Fischer et al., 1997; Yong et al., 2004). An important question addressed here is whether the SMN-Gemin granules in neurites were associated with spliceosomal Sm proteins. We hypothesized that the SMN-Gemin complex in neurites is novel and spatially distinct from those involved in snRNP assembly. Using immunofluorescence staining of primary motor neurons with a monoclonal antibody (Y12) to Sm proteins, the major component of snRNPs, we observed that Sm proteins were highly enriched in the nucleus and also showed significant staining in the perinuclear cytoplasm **(Figure 2-4B, red)**, where there was colocalization with SMN (green) **(Figure 2-4C, inset a)**. SMN was also abundant in the nucleus and cytoplasm **(Figure 2-4A)**, yet in contrast to Sm proteins, SMN was prevalent throughout the neurite length **(Figure 2-4C, insets b and c)**. The density of Sm proteins decreased markedly with distance from the soma, where its levels in distal neurites were very low **(Figure 2-4C, inset c)**. These results indicate that the vast majority of SMN granules in neurites lack Sm proteins, yet also indicate that Sm proteins may be present at very low levels.

Analysis of SMN-Gemin interactions using fluorescently tagged proteins

Since SMN is known to bind Gemin2 directly *in vitro* (Liu et al., 1997), we used FRET analysis of fluorescently tagged and overexpressed proteins to assess direct physical interactions of SMN with Gemins in neuritic granules. This interaction and others were examined in detail using a co-transfection approach between SMN and specific Gemin proteins, using both wild type and mutant forms tagged with different fluorescent proteins. Cultured forebrain neurons were first co-transfected with EYFP-SMN and ECFP-Gemin2. All constructs were human forms of these proteins (see Methods). We first verified that the overexpressed fluorescent proteins colocalized with endogenous Gemins. Endogenous Gemin3 was present in granules that co-localized with co-expressed EYFP-SMN and ECFP-Gemin2 **(Figure 2-5A-E)**. Eight discrete granules (arrows) are depicted in two neurites showing presence of EYFP-SMN **(Figure 2-5A)**, ECFP-Gemin2 **(Figure 2-5B)** and endogenous Gemin3 **(Figure 2-5C)** at the same locations (merge of all three is shown in **Figure 2-5D)**.

Live neurons expressing EYFP-SMN and ECFP-Gemin2 were also analyzed by high-speed dual channel imaging (see methods). The co-transport of SMN and Gemin2 was evident within single granules that could be tracked together for several microns **(Figure 2-5F, see white arrows in inset)**. Both anterograde and retrograde (not shown) trajectories were noted.

Fluorescence Resonance Energy Transfer (FRET) has been used to localize protein-protein interactions within cells (Jobin et al., 2003). FRET was used to quantify molecular interactions in transfected neurons expressing EYFP-SMN and ECFP-Gemin2. The results from one neuron are depicted in Figure 2-6. Briefly, a region of interest (RO1)

was photobleached in the EYFP (acceptor) channel **(Figure 2-6B, D)** and then any increased fluorescence was measured in the ECFP (donor) channel. One region of interest (ROI 1) containing two neurites is shown and was analyzed pre- and post-photobleaching **(Figure 2-6A-D)**. The fluorescence intensities within fourteen encircled granules (ROI 2-15) were measured. As controls, fluorescence intensities were also examined in bleached regions outside the cell (ROI 16) and within non-bleached regions of other neurites (ROI 17-19). In total, we examined for possible FRET interactions in 74 granules from ten transfected neurons. A high frequency (77%) of Gemin2 granules showed increased ECFP fluorescence intensities post-photobleaching, when compared to pre-photobleaching **(Figure 2-6E)**. The average increase in ECFP fluorescence intensity (19.8%) indicated a close interaction between EYFP-SMN and ECFP-Gemin2 in single granules. In contrast, granules from non-photobleached neurites did not show increased ECFP fluorescence nor did we observe changes in ECFP fluorescence in photobleached regions outside the cell. Similar FRET experiments also suggested an interaction between EYFP-SMN and ECFP-Gemin3 **(Figure 2-6E)**. The observed frequency of FRET interactions between SMN-Gemin3 was significantly lower than observed with SMN-Gemin2.

<u>Recruitment of Gemin2 into complex and granules is dependent on interactions SMN</u>

We hypothesized that Gemin proteins can be recruited into SMN granules when present at stoichiometric levels and that this interaction is dependent on specific domain(s) of SMN. Following EGFP-Gemin2 overexpression (green) by itself, neurons were fixed for IF analysis of endogenous SMN (red) and the nucleus was stained with DAPI (blue). The EGFP-Gemin2 fluorescence was diffuse and filled nucleus, cytoplasm and processes

(Figure 2-7A). This finding suggests that the endogenous SMN within neuritic granules is in a complex with the endogenous Gemins or other proteins and is unavailable to bind to the overexpressed Gemin2. Consistent with this idea, when EGFP-Gemin2 was co-transfected with Flag-SMN (red), the EGFP-Gemin2 signal was now granular and colocalized with SMN (red); both proteins were often co-enriched in neuritic filopodia and growth cones **(Figure 2-7B, inset arrows)**.

We then investigated if deletion of SMN amino-terminus, which contains the Gemin2 binding site (Liu et al., 1997; Wang et al., 2004), was required for the recruitment of Gemin2 into granules by SMN following their co-transfection. First, we show here that single expression of ECFP-Gemin2 **(Figure 2-8A)** or ECFP-Gemin3 **(Figure 2-8D)** was diffuse and non-granular, whereas co-expression of ECFP-Gemin2 or ECFP-Gemin3 with EYFP-SMN showed their colocalization in granules **(Figure 2-8B, E; arrows)**. An amino-terminal deletion mutant of SMN (EYFP-SMNΔN53) was unable to recruit the over-expressed ECFP-Gemin2 into granules **(Figure 2-8C)**; while EYFP-SMNΔN53 was still able to form neuritic granules **(Figure 2-8C, arrows)**, ECFP-Gemin2 (green) was diffuse through the cytoplasm and nucleus. Deletion of the amino-terminus of EYFP-SMN did not affect colocalization with ECFP-Gemin3 in neuritic granules **(Figure 2-8F, arrows)**. These data show that the co-localization of SMN and Gemin2 within neuritic granules is dependent on their levels in the cell and known molecular interactions. In addition, these results show that the amino-terminus of SMN is not necessary for granule formation or interactions with Gemin3.

Co-immunoprecipitation (Co-IP) and Western Blot experiments in transfected HEK293 cells were used to show that Gemin2 was stabilized by its interaction with SMN.

First, we show that Gemin2 could be co-precipitated with both Flag-SMN and Flag-SMNΔ7 (**Figure 2-8G, lanes 1, 5**), but not with Flag-SMNΔN53 (**Figure 2-8G, lane 3**), which lacks the Gemin2 binding site. EGFP-Gemin2 was also only weakly apparent in the protein supernatant from cells expressing Flag-SMNΔN53 (**Figure 2-8G, lane 4**). These low levels of EGFP-Gemin2 in both pellets and supernatants from cells expressing Flag-SMNΔN53 compared to cells expressing Flag-SMN and Flag-SMNΔ7 suggested that EGFP-Gemin2 could be stabilized by interactions with the amino-terminus of SMN. This idea was further supported by Western Blot analysis. EGFP-Gemin2 levels were very low when it was expressed by itself (**Figure 2-8H, lanes 1, 2, 3**), when compared to co-transfection with full-length SMN (**Figure 2-8H, lanes 4, 5, 6**). For example, at the 12 hour time point, EGFP-Gemin2 is barely apparent on the gel (**Figure 2-8H, lane 1**), whereas a distinct band is noted when co-expressed with full-length SMN (**Figure 2-8H, lane 4**). EGFP-Gemin2 and Flag-SMN levels were both substantially increased over the 48 hour time course. In contrast, EGFP-Gemin2 levels were consistently lower in cells co-transfected with Flag-SMNΔN53 (**Figure 2-8H, lane 7, 8, 9**). These results are consistent with previous *in vitro* observations that Gemin2 is unstable when not bound with SMN (Wang and Dreyfuss, 2001b). Collectively, our findings suggest that a stable SMN-Gemin complex exists in granules in neuronal processes and that the molecular interactions between SMN and Gemins are required for maintaining Gemin proteins in this stable complex.

Association of SMN and hnRNP-Q1 in neuronal processes

The axonal localization and active transport of SMN and its association with ribosomal RNA (Zhang et al., 2003) and poly(A) mRNA (Zhang et al., 2007) suggest a

potential function of SMN in axonal mRNA transport and/or local translational regulation. SMN possibly exerts these functions through the interaction with mRNA binding proteins since no RNA binding domain has been identified within SMN protein sequence. hnRNP-Qs/R are candidate SMN interacting RNA binding proteins in neurons due to their direct interaction with SMN in vitro (Mourelatos et al., 2001; Rossoll et al., 2002). Moreover, hnRNP-Qs have been isolated from RNA transport granules using biochemical and proteomics methods (Bannai et al., 2004; Kanai et al., 2004). Consistent with previous studies (Mourelatos et al., 2001; Rossoll et al., 2002), our co-immunoprecipitation results showed that overexpressed Flag-SMN pulled down EGFP-hnRNP-Q1 in 293 cells and vice versa **(Figure 2-9B)**. In addition, endogenous Gemin3 was also co-precipitated with EGFP-hnRNP-Q1 **(Figure 2-9B)**. Although both SMN and hnRNP-Qs have been detected in neuronal processes, however, whether they associate with each other in this compartment has not been studied. To test this hypothesis, we performed fluorescent immunostaining experiments to examine the colocalization of endogenous SMN and hnRNP-Qs in hippocampal neurons. hnRNP-Qs were detected with an polycolonal antibody recognizing all hnRNP-Q isoforms and hnRNP-R (Bannai et al., 2004). In neurites of hippocampal neurons, colocalized SMN and hnRNP-Qs/R signals were frequently observed in granules **(Figure 2-9A)**.

The association of SMN and hnRNP-Q1 in real time was analyzed in rat hippocampal cotransfected with plasmids expressing mRNP-SMN and EGFP-hnRNP-Q1 **(Figure 2-10)**. The co-movement of mRFP-SMN and EGFP-hnRNP-Q1 was examined with dual channel time-lapse imaging. In these cells, we found that overexpressed mRFP-SMN and EGFP-hnRNP-Q1 were well colocalized in neuritic granules. The continuous

movement of an mRFP-SMN/EGFP-hnRNP-Q1 granule was tracked for 115 seconds until it moved out of the field. This observation suggests that hnRNP-Q1 is a functional component of SMN transport granules and suggests a possible role of SMN in mRNA transport and/or translational regulation.

Discussions

Localization of an SMN-Gemin complex in axons and dendrites that is deficient of spliceosomal Sm proteins

Previous immunocytochemical studies have documented the localization of the Survival of Motor Neuron (SMN) protein to axons and dendrites of spinal cord neurons *in vivo* (Battaglia et al., 1997; Bechade et al., 1999; Pagliardini et al., 2000). In cultured forebrain neurons, we have previously shown that SMN is localized in granules that are actively transported into developing neurites and growth cones (Zhang et al., 2003). In an effort toward understanding the function of SMN in neuronal processes and how loss of SMN leads to SMA, it is essential to identify proteins that associate with SMN in neuronal processes. Ideally, these studies should be conducted in motor neurons.

Since previous biochemistry studies in immortalized non-neuronal cells have shown that SMN is present in a tight complex with several Gemin proteins (Paushkin et al., 2002), it is critical to know whether the SMN-Gemin complex is present in neuronal processes and growth cones. Previous studies have had conflicting results on whether these proteins colocalize in neuronal processes (Jablonka et al., 2001; Sharma et al., 2005). One confounding factor is that only conventional immunofluorescence analysis was performed in these previous studies. While this method may be useful to show that both proteins are both present in a neurite or growth cone, it is not possible to know if

they associate together in single particles or granules. This type of analysis necessitated use of higher resolution imaging methods. In this study, we demonstrate, for the first time, the colocalization of SMN and Gemin2 and Gemin3 in granules that distribute to neuronal processes and growth cones of primary hippocampal and motor neurons, and ES-cell derived motor neurons. Quantitative analyses of 3D reconstructed growth cones indicate a statistically non-random association of SMN with Gemin2 (40%) and Gemin3 (48%). In addition, we used fluorescently tagged and overexpressed SMN and Gemin proteins to demonstrate a FRET interaction and co-transport of complex. Our data also suggest the presence of SMN and Gemin particles that do not colocalize. These results suggest the presence of diverse SMN-containing multiprotein complexes in neuronal processes. Our observations for the lack of spliceosomal Sm proteins in processes and the colocalization and co-transport of SMN and hnRNP-Q1 further suggest an additional function for SMN complexes that are localized to neuronal processes. We speculate that the SMN-Gemin complex may play a role in some aspect of mRNP assembly, as it has been shown for snRNP assembly (Briese et al., 2005; Monani, 2005).

Possible functions for SMN multiprotein complexes in neurons

One possible function for the SMN-Gemin complex may be the assembly of a localized β-actin mRNP complex. A seminal report by Rossoll et al. has shown that motor neurons cultured from an SMA transgenic mouse model, having low SMN levels, showed reduced localization of β-actin mRNA and protein in axonal growth cones (Rossoll et al., 2003). Axons were also shorter in length and their growth cones were smaller in size; there was no evidence for dendritic impairments (Rossoll et al., 2003). These findings provide evidence of a role for SMN in some aspect of the well studied

molecular mechanism of β-actin mRNA localization and its function in β-actin protein sorting and axon growth cone motility (Zhang et al., 2001; Zhang et al., 1999). Since the assembly of a β-actin mRNA localization complex appears to involve the coordinated binding of two mRNA binding proteins, ZBP1 and ZBP2, to a stem-loop structure within a 54 nt zipcode sequence within the 3'UTR (Gu et al., 2002; Ross et al., 1997), we speculate that the SMN-Gemin complex might facilitate these molecular interactions. In addition, it has been shown that SMN interacts with the mRNA binding protein, hnRNP-R, which colocalized with SMN in processes of motor neurons (Rossoll et al., 2002). Moreover, hnRNP-R associates with β-actin mRNA *in vitro* and enhances its localization in neurites when overexpressed in PC12 cells (Rossoll et al., 2003). In this study, we found that SMN and hnRNP-Q1 are colocalized and co-transported in neuronal processes. hnRNP-Qs and hnRNP-R share over 80% protein sequence similarity and contains essentially identical RNA binding domains (three RRM domains and one RGG domain), suggesting a possible functional similarity. Thus, it is likely hnRNP-Q1 also associates with β-actin mRNA and mediates the SMN function in β-actin mRNA localization. It will be of interest to know whether ZBP1 interacts with hnRNP-Qs/R and if the SMN-Gemin complex may facilitate these interactions to affect assembly of a β-actin mRNP complex that is then localized.

Since mRNA localization and translation in growth cones have been linked to growth cone motility and axon guidance (Martin, 2004), it will be interesting to also assess a possible function for the SMN-Gemin complex in translational regulation during axonal pathfinding. Our data indicate that the SMN-Gemin complex is frequently present within lamellar and filopodial protrusions from axonal growth cones. An exciting report

has shown that knockdown of SMN in zebrafish resulted in axon-specific pathfinding defects in motor neurons, which were partially rescued by full length human SMN, but not by SMNΔ7 (McWhorter et al., 2003). Recent data also indicate a role for β-actin mRNA localization and its local translation in axon guidance of Xenopus spinal neurons (Yao et al., 2006), and so it will be important to examine how an SMN complex may be involved in this process.

As SMN is also localized to dendrites of adult motor neurons *in vivo* (Bechade et al., 1999), and in developing dendrites in culture at 7DIV (**Figure 2-2**), further work is needed to assess a possible functional role for SMN in dendrites. While the study by Rossoll et al., (2003) did not observe gross defects in dendritic development or branching in cultured SMA motor neurons, it is possible that SMN may play a role in dendrites at the synapse. In addition to β-actin mRNA localization to the developing axon (Zhang et al., 2001), we later showed that it is also localized to developing dendrites (Eom et al., 2003). ZBP1 mediated localization of β-actin mRNA was shown to be necessary for the formation of filopodia and filopodial-synapses in developing dendrites in response to BDNF stimulation (Eom et al., 2003). Perhaps SMN may interact with this dendritic ZBP1-β-actin mRNP complex. Another possible dendritic interacting protein for SMN is hnRNP-Q1 (Rossoll et al., 2002) which is colocalized in dendritic RNA granules with the inositol triphosphate receptor (IP3R) mRNAs (Bannai et al., 2004).

SMN may also function in other less well-defined aspects of ribonucleoprotein regulation in the cytoplasm. An interesting report has shown that SMN colocalized with markers for stress granules (SG) i.e. TIA-1/R and G3BP and could induce their formation upon overexpression (Hua and Zhou, 2004). Stress granules serve as depots to recruit

poly (A) mRNA, poly (A)-binding protein, ribosomes and translational components in response to environmental stresses, such as heat shock and oxidative stress (Kedersha et al., 1999). mRNAs within SG are translationally repressed, and following recovery from the stress response, they are released from SG and translated. A role for SMN in SG formation may have important implications for understanding the molecular basis for axon degeneration in SMA.

<u>Molecular interactions for assembly and localization of SMN-Gemin complexes</u>

An amino-terminal deletion of SMN (SMNΔ53), which cannot bind Gemin2 (Wang and Dreyfuss, 2001a), was able to form granules and be transported into processes. Gemin2 was not recruited into SMNΔ53 granules and was diffusely distributed. These data show that molecular interactions known to be involved in SMN binding to Gemin2 are necessary for the recruitment of Gemin2 into SMN granules. However, SMN can indeed form granules and be transported in the absence of interactions with Gemin2. We also show that overexpression of either Gemin2 or Gemin3 individually (without SMN) was diffuse and non-granular, likely because their levels were in excess of the endogenous SMN and insufficient to be recruited into granules. These findings indicate that the stoichiometry between SMN and Gemin proteins are important factors that influence assembly of proteins into granules.

The association of Gemin2 with SMN was also shown to stabilize Gemin2. Western Blot analysis of cells co-transfected with Gemin2 and SMN led to increased Gemin2 levels over time following transfection. Collectively, our results suggest that the binding of Gemin2 to the amino-terminus of SMN is required for Gemin2 to form granules, and this biochemical association within granules has a stabilizing effect on

Gemin2. Previous biochemical studies have also provided evidence for the stabilization of Gemin2 by SMN (Jablonka et al., 2001; Wang and Dreyfuss, 2001a). There has been genetic evidence suggesting a functional interaction between SMN and Gemin2. Gemin2/Smn double heterozygous deficient mice showed motor neuron degeneration which was significantly higher than in Smn heterozygous mice (Jablonka et al., 2002).

Acknowledgement

Figures and Legends

A (SMN & Gemin2)

5 µm

1

1.25 µm

2

B (SMN & Gemin2)

5µm

C

1 µm

D (Gemin3 and GFP)

5 µm
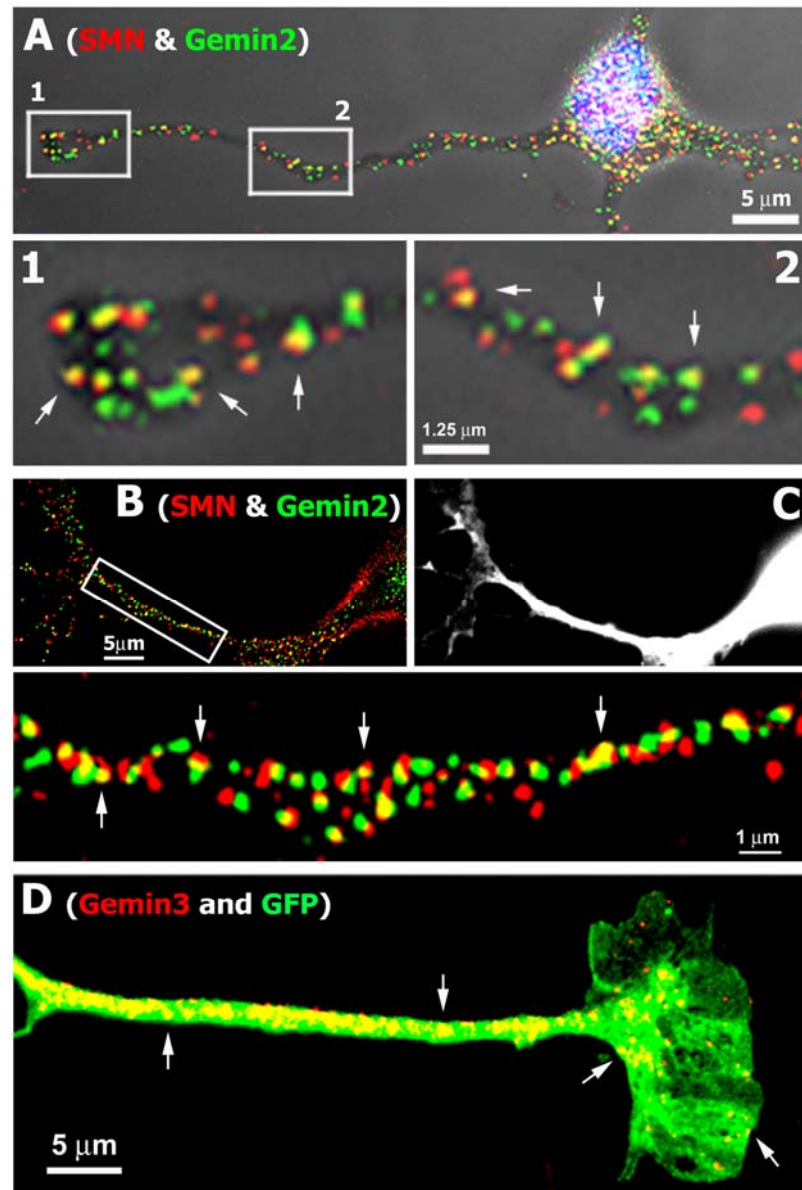
Figure 2-1. Colocalization of endogenous SMN and Gemin proteins in neurites and growth cones in primary forebrain culture and ES-cell derived motor neurons

(A) SMN (red) and Gemin2 (green) in cultured forebrain neurons (3DIV) were detected by double-label immunofluorescence using a monoclonal antibody to SMN and polyclonal antibody to Gemin2. The nucleus was stained with DAPI (blue). Higher magnification of two regions (insets 1, 2 from upper panel are enlarged in lower panel) depicts the frequent co-localization between SMN and Gemin2 within granules in the growth cone (1, arrows) and neurite (2, arrows). **(B)** Double label IF showing colocalization of SMN (red) and Gemin2 (Cy5 antibody displayed in green) in neurites of ES-cell derived differentiated motoneuron. Higher magnification of a boxed region depicts numerous granules with colocalization between SMN and Gemin2 (lower panel, arrows). **(C)** These cells express EGFP from a motor neuron specific promoter. **(D)** IF detection of Gemin3 with a monoclonal antibody depicts many granules localized to the EGFP-positive axon and growth cone of the motor neuron (arrows). (Panel A contributed by Dr. Honglai Zhang)
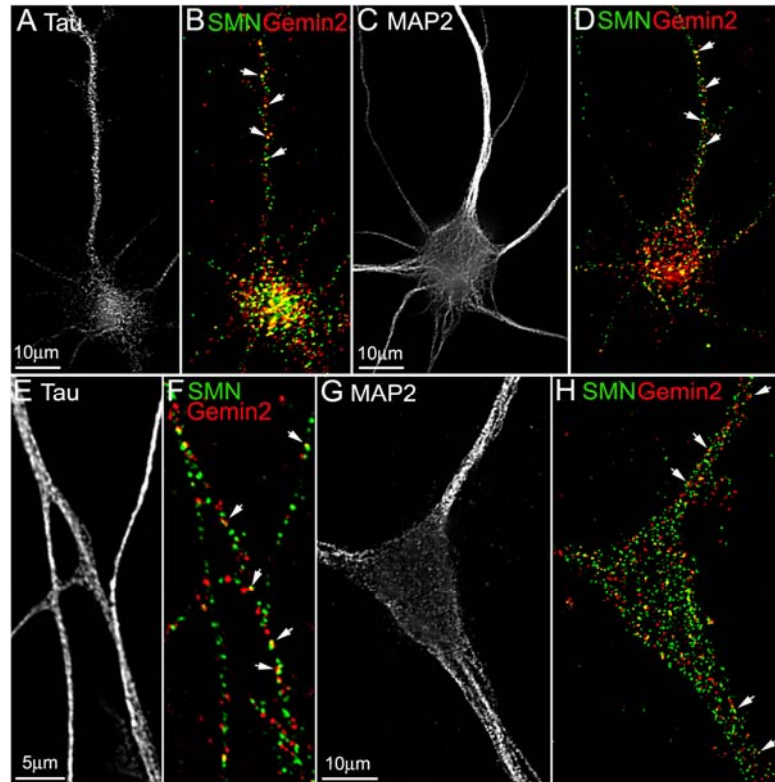
Figure 2-2. Colocalization of endogenous SMN and Gemin2 in axons and dendrites of differentiated cultures of primary hippocampal and motor neurons

Primary cultures of rat hippocampal neurons **(A, B, C, D)** and embryonic mouse motor neurons **(E, F, G, H)** were fixed with 4% PFA at 7DIV and processed for triple label IF to detect the colocalization of endogenous SMN and Gemin2 in both axons and dendrites. Monoclonal antibodies to SMN and Gemin2 were directly conjugated with Alexa647 and Alexa568 respectively (see methods). Axons and dendrites were discriminated by IF staining with a polyclonal antibody to tau **(A, E)** or MAP2 **(C, G)** and Cy2-conjugated secondary antibody. The colocalization (indicated by arrows) of SMN (green) and Gemin2 (red) in both axons **(B, F)** and dendrites **(D, H)** of hippocampal neurons and mouse motor neurons was observed.
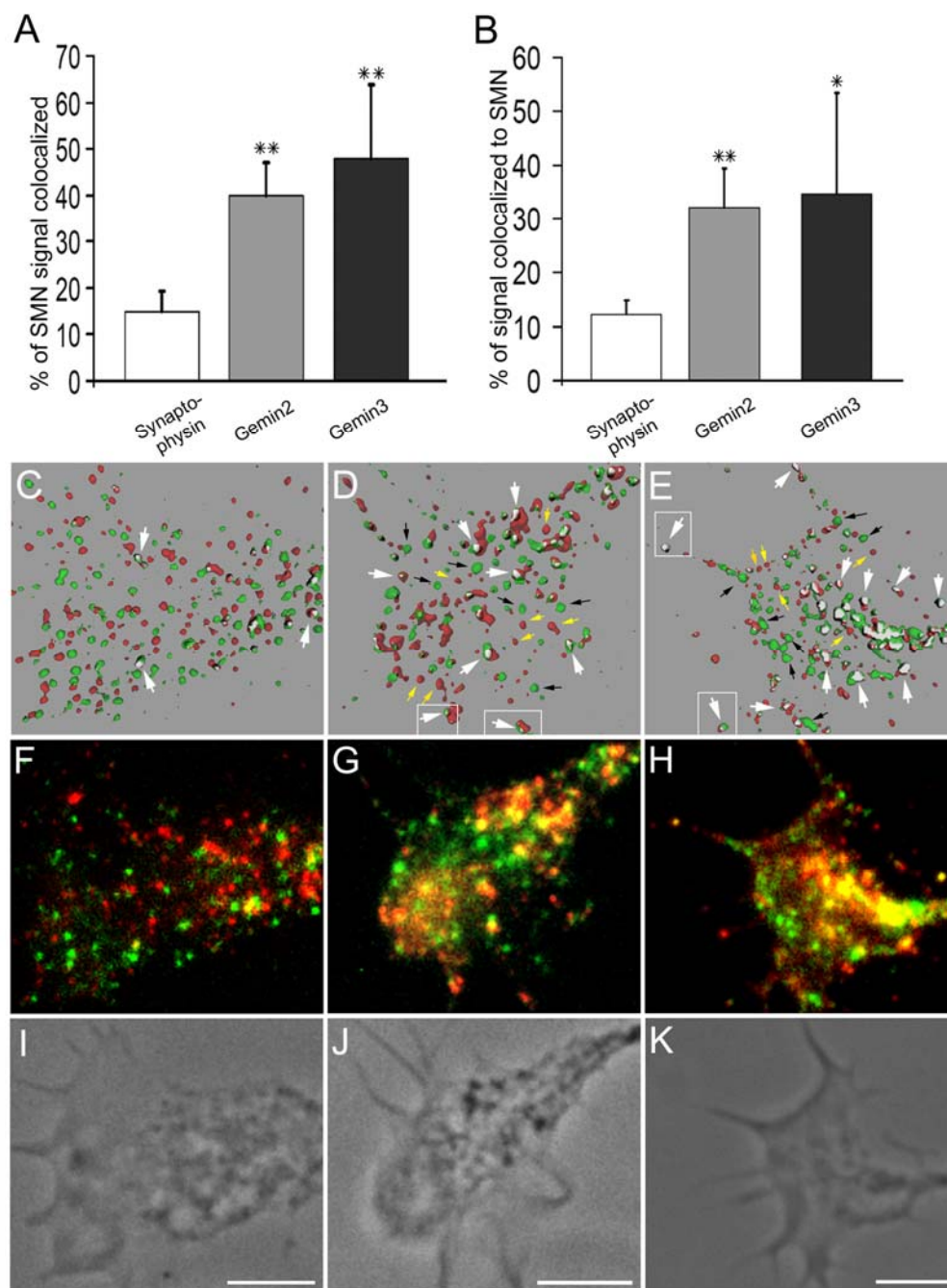
Figure 2-3. Quantitative analysis of SMN-Gemin colocalization in growth cones following 3D reconstruction

Hippocampal neurons were cultured for 4DIV, processed for double label immunofluorescence using directly conjugated monoclonal antibodies. Growth cones (n=10, per color pair) were imaged in 3D, deconvolved, thresholded and statistically analyzed for percent of voxels with colocalized signals above threshold (Imaris). **(A)** The SMN signal colocalized to Gemin2 ($40.0\pm7.0\%$) and Gemin3 ($47.8\pm15.8\%$) was 1.7 and 2.2 times higher than the signal of SMN colocalized to synaptophysin ($15.0\pm4.5\%$), which was equally abundant within growth cones. **(B)** The Gemin2 signal ($32.3\pm7.2\%$) was 1.6 times higher than the synaptophysin signal ($12.3\pm2.6\%$) colocalized to SMN; and Gemin3 signal ($34.7\pm18.8\%$) colocalized to SMN was 1.8 times higher than synaptophysin ($12.3\pm2.6\%$). (**$p<0.001$; *$p<0.01$). Colocalization of SMN (green) and synaptophysin, Gemin2 or Gemin3 (red) were represented by deconvolved and reconstructed images shown in panels **C**, **D** and **E**, respectively. Colocalized voxels (white) are indicated by white arrows. Noncolocalized signals are indicated by black arrows (SMN) or yellow arrows (Gemin2 and Gemin3). The raw unprocessed data for these three growth cones is shown in **F**, **G** and **H**. Corresponding phase images are shown in **I**, **J** and **K**. The presence of SMN-Gemin granules in filopodial protrusions from the growth cone is noted in boxed regions in panels **D**, **E**. Scale bar is equal to 5 m.
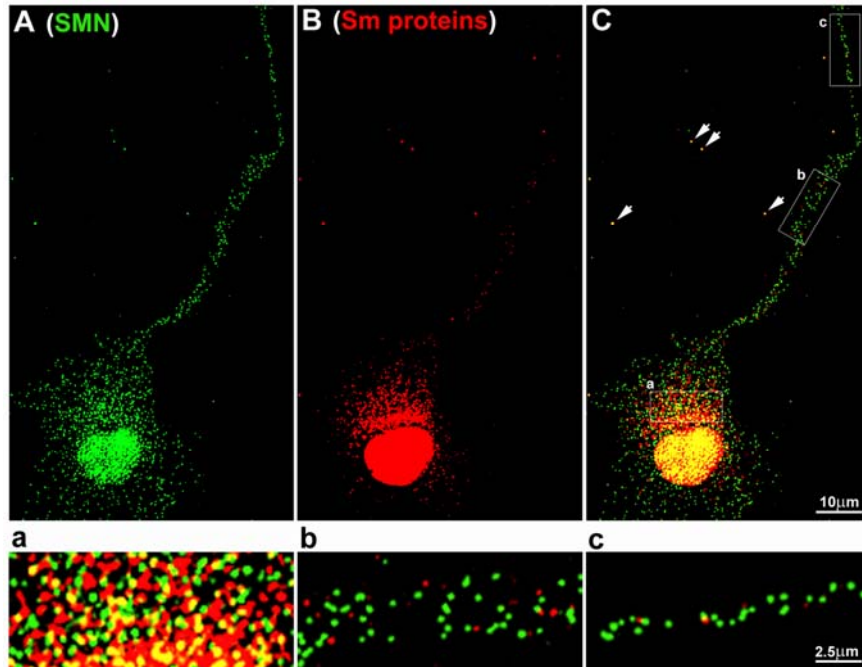
Figure 2-4. SMN granules within neurites are deficient of Sm proteins in motor neurons

Primary cultured mouse motor neurons were double immunostained for SMN (**A,** in green) and Sm proteins (**B,** in red), a major component of snRNPs. Images were deconvolved, superimposed and registered using fiduciary beads (arrows) in the mounting medium. (**A**) SMN was prevalent in the nucleus, and was distributed throughout the cytoplasm and neurites within granules. (**B**) Sm proteins were highly enriched in the nucleus and showed significant staining only within the perinuclear cytoplasm, where there was colocalization with SMN (**C**, merged colors, inset "a" enlarged in bottom row). (**C**) In the neurite, a very low frequency of colocalized signal (in yellow) appeared. Sm protein levels in the middle neurite segment (see enlarged inset "b" in bottom row) were markedly reduced compared to SMN. In the distal neurite segment, the amount of Sm proteins was extremely low with respect to SMN (enlarged inset "c").
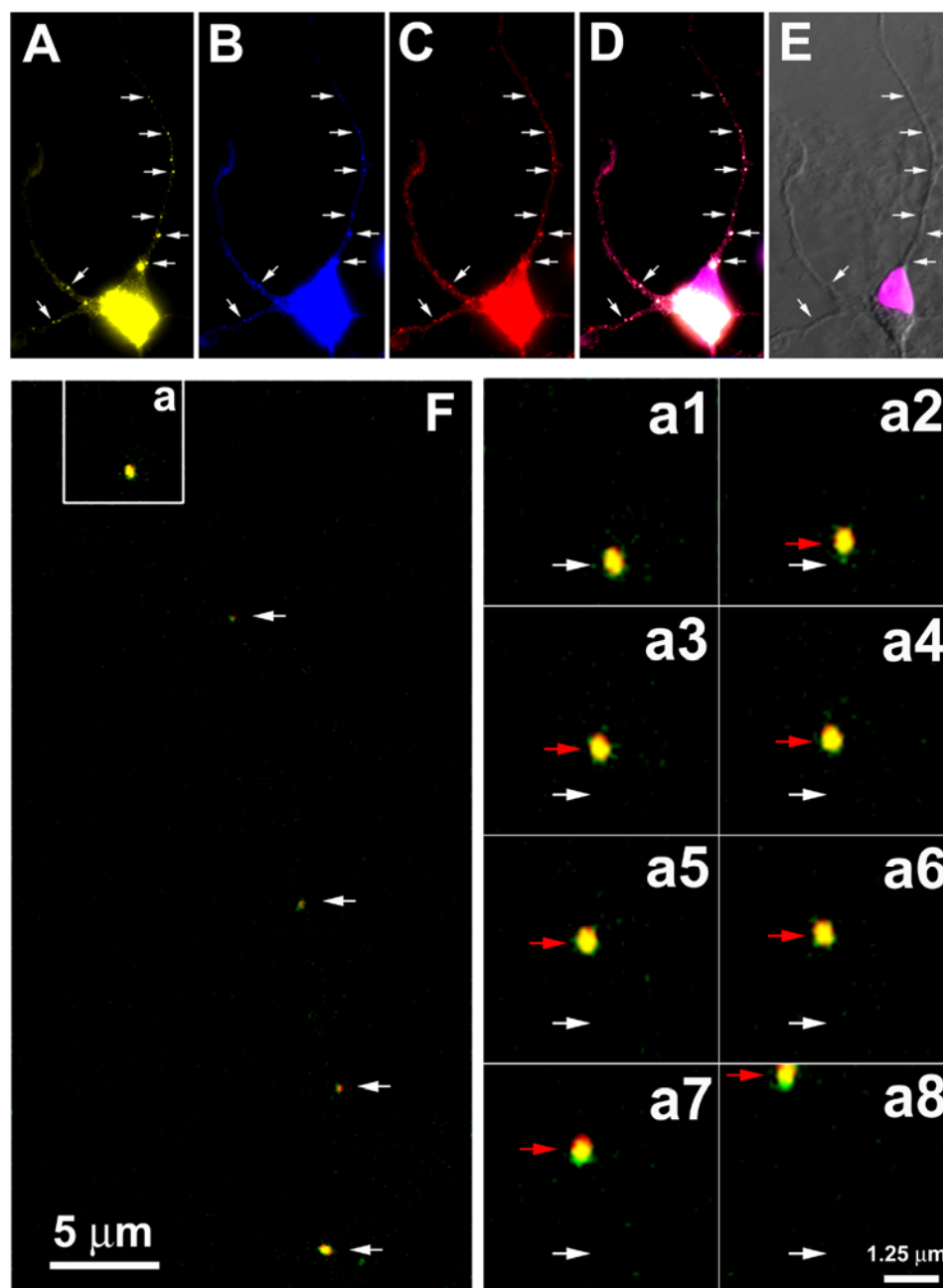
Figure 2-5. Colocalization and co-transport of fluorescently tagged and overexpressed SMN and Gemin2 Cultured forebrain neurons were co-transfected with EYFP-SMN **(A,** yellow**)** and ECFP-Gemin2 **(B,** blue**)** and then fixed for immunofluorescence detection of endogenous Gemin3 **(C,** red**)** using a monoclonal antibody. Co-localization of EYFP-SMN, ECFP-Gemin2 and Gemin3 within eight discrete granules is shown in neurites **(D,** arrows, merged signals**)**. **(E)** The nucleus was stained with DAPI (pink) and overlaid with DIC optics. **(F)** In another experiment, neurons were co-transfected with EYFP-SMN (red) and ECFP-Gemin2 (green) and imaged in live cells using high speed, dual-channel imaging. Five granules, containing both molecules, are depicted along the length of a neurite (arrows). One of these granules (a) is tracked for eight frames and displays an anterograde trajectory (white arrow denotes starting point, red arrows show position during subsequent frames, a1-a8). (Contributed by Dr. Honglai Zhang)
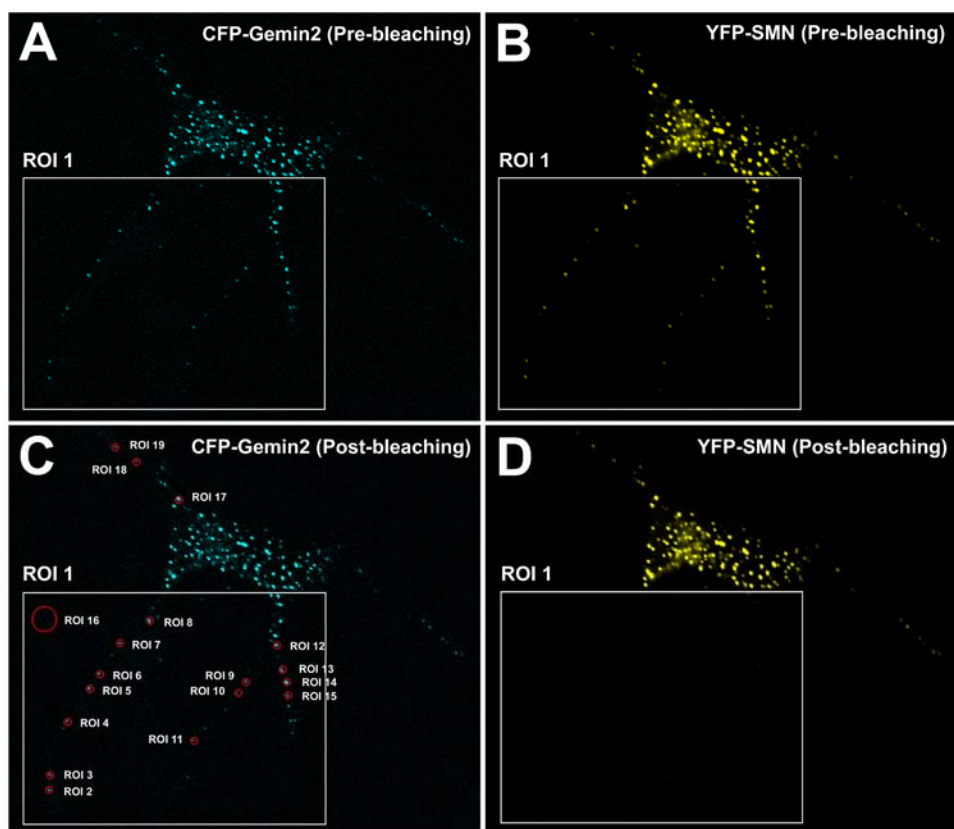
E		FRET experimental			FRET control		
	Cells	Granules	FRET frequency	FRET average	Granules	FRET frequency	FRET average
CFP-Gemin2	10	74	77%	19.8%	23	13%	1.7%
CFP-Gemin3	6	36	56%	19.6%	6	17%	3.0%

Figure 2-6. FRET analysis depicts interaction between EYFP-SMN and ECFP-Gemin2 or ECFP-Gemin3 in neurites

Fluorescence Resonance Energy Transfer (FRET) was used to detect protein-protein interactions between SMN and Gemins in neurites. Cultured forebrain neurons were transfected with ECFP-Gemin2 or ECFP-Gemin3, as the donor, and EYFP-SMN, as the acceptor fluorophore, for FRET analysis. Fluorescence was imaged using a confocal microscope (see methods). One neuron is shown here as an example. **(A, B)** ECFP-Gemin2 granules **(A,** blue**)** and EYFP-SMN granules **(B,** yellow**)** prior to photobleaching of EYFP. **(C)** ECFP-Gemin2 fluorescence post-photobleaching of boxed region (ROI 1). Each granule within RO1 1 was outlined in red and indicated as ROIs 2-15. An area (ROI 16) outside the neurite was also circled within ROI 1 as a control for measurement of increased fluorescence in ECFP channel after photobleaching of EYFP. Three granules, labeled as ROI 17-19, in another neurite that was not photobleached, were used as additional controls for FRET measurements. **(D)** Fluorescence signals of EYFP-SMN granules were eliminated by photobleaching with a laser in the selected area (ROI 1). **(E)** FRET measurements are indicated in the table. FRET frequency indicates the percentage of granules showing increased ECFP fluorescence post-photobleaching of EYFP. FRET average indicates the percent increase in ECFP fluorescence after EYFP-photobleaching. (Contributed by Dr. Honglai Zhang)
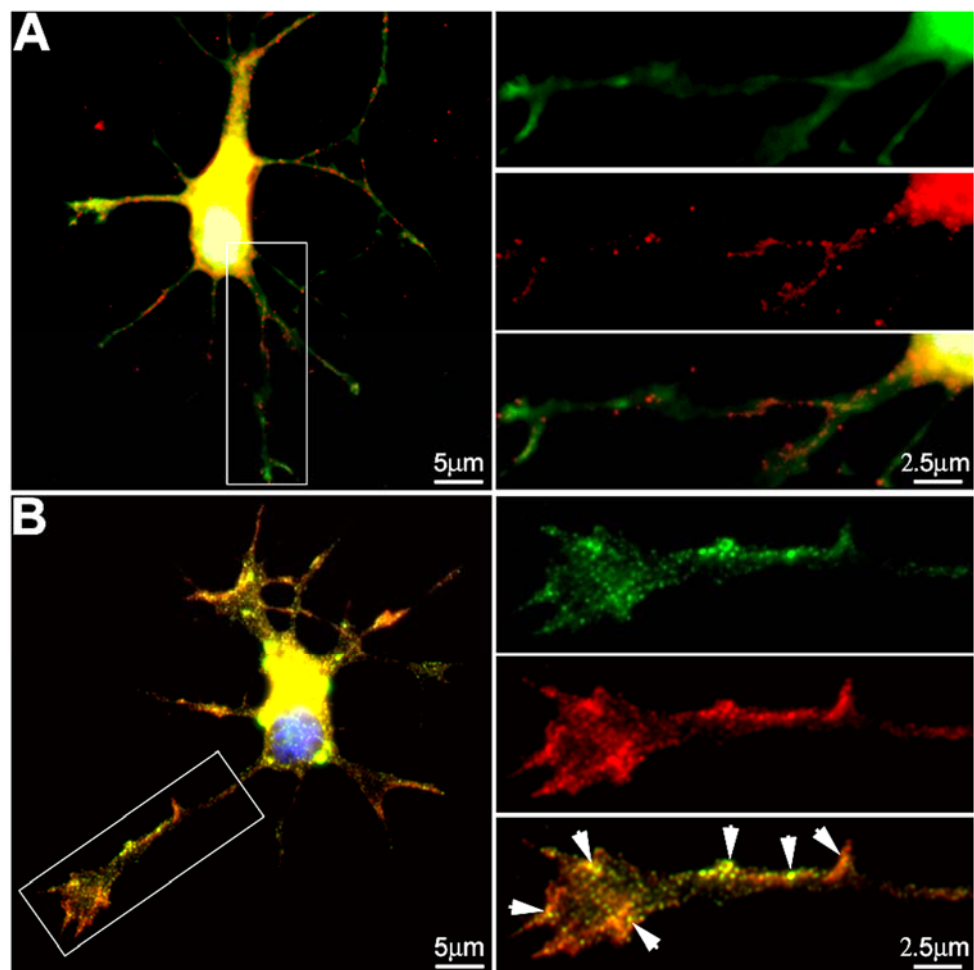
Figure 2-7. Gemin2 is recruited by SMN into granules within neurites and growth cones

(A) Following transfection of EGFP-Gemin2 (green), cultured forebrain neurons (4DIV) were fixed for IF analysis of endogenous SMN (red) and the nucleus was stained with DAPI (blue). The EGFP-Gemin2 fluorescence was mostly diffuse and filled all cellular regions including cytoplasmic processes and the nucleus. Note the blue stain of the nucleus was not visible in the merged overlay due to the strong EGFP signal. The distribution of SMN (red) was highly granular or punctate as described previously (Zhang et al., 2003). One neurite from the boxed inset is enlarged at right to show EGFP-Gemin2 (top), SMN (middle) and overlay (bottom). **(B)** In contrast, when EGFP-Gemin2 was co-transfected with Flag-SMN (red), the EGFP-Gemin2 signal is now granular and frequently colocalized with SMN (red) in neurites, growth cones and filopodia (arrows). One neurite (boxed inset) is enlarged to the right and shows EGFP-Gemin2 (top), Flag-SMN (middle) and overlay (bottom). Note also that the DAPI-stained nucleus (blue) is now visible, as the EGFP-Gemin2 signal is observed in puncta (likely gems) in contrast to filling the entire nucleus as in **(A)**.

5 μm
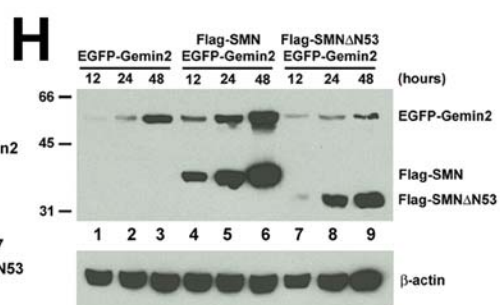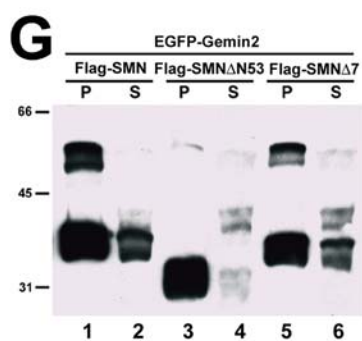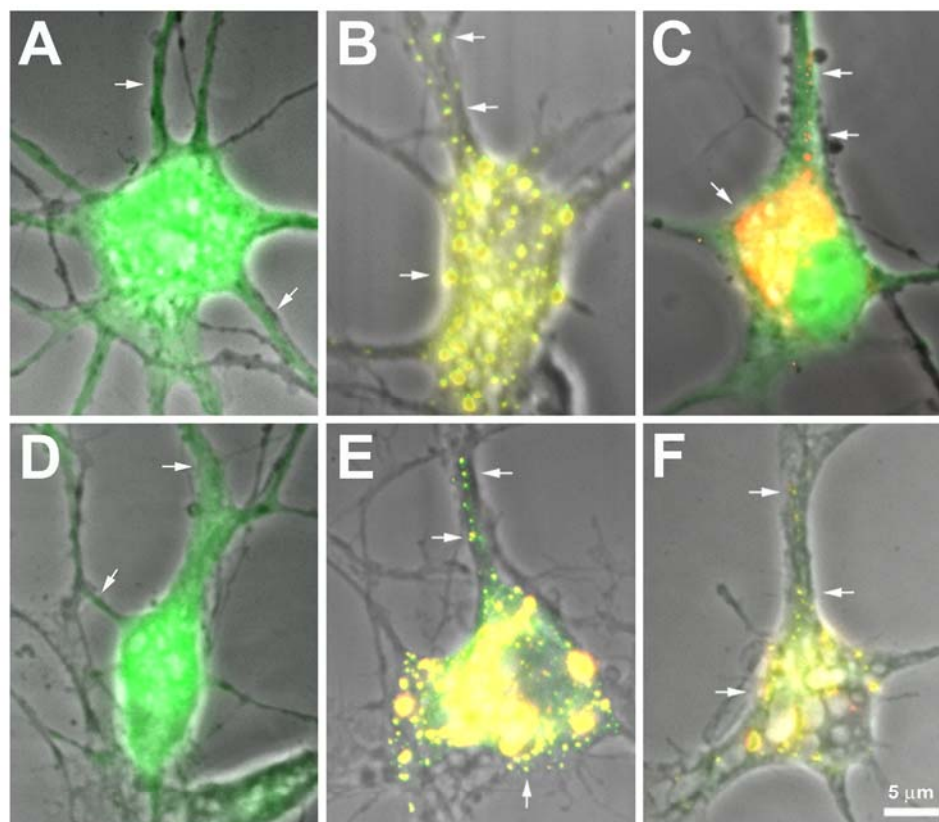
Figure 2-8. Interactions between Gemin2 with SMN necessary for recruitment into granules and stabilize Gemin2

(A, D) Overexpression of ECFP-Gemin2 **(A)** or ECFP-Gemin3 **(D)** by themselves in cultured forebrain neurons (4DIV) showed diffuse and uniform fluorescence, with no evidence for discrete granules (green, arrows). **(B, E)** In contrast, when ECFP-Gemin2 **(B,** green**)** or ECFP-Gemin3 **(E,** green**)** was co-transfected with EYFP-SMN (red), the recruitment of Gemins into SMN granules was observed **(B, E**: merged images, arrows). **(C)** In contrast, co-expression of the amino-terminal deletion mutant of SMN (EYFP-SMNΔN53), which lacks the known binding site for Gemin2, was not able to recruit Gemin2 into granules. EYFP-SMNΔN53 (red) showed a granular pattern in neurites **(C,** arrows), yet ECFP-Gemin2 **(C,** green**)** remained in a diffuse pattern. The red and green signal in the neurite showed little colocalization. **(F)** ECFP-Gemin3 (green) was recruited into granules by co-transfection with EYFP-SMNΔN53 (red) as evident by colocalization of the merged images (yellow, arrows). **(G)** Gemin2 stabilization by interactions with SMN. HEK293 cells were co-transfected with EGFP-Gemin2 and Flag-tagged SMN constructs. Cells were lysed, immunoprecipitated with anti-Flag antibodies and analyzed for EGFP and Flag expression by Western Blot. EGFP-Gemin2 was co-IP IP with Flag-SMN (lane 1) or Flag-SMNΔ7 (lane 5), but not Flag-SMNΔN53 (lane 3), which lacks the known Gemin2 binding domain. **(H)** Western Blot analysis at 12, 24, and 48 hours expression showed that EGFP-Gemin2 was present at higher levels over time when co-expressed with Flag-SMN (lane 4, 5, 6), compared to when Gemin2 was expressed by itself (lane 1, 2, 3) or co-expressed with Flag-SMNΔN53 (Lane 7, 8, 9). Flag- and EGFP-

tagged proteins were detected with monoclonal antibodies. β-actin was detected with a monoclonal antibody as loading control. (Contributed by Dr. Honglai Zhang)

A SMN hnRNP-Q1 Merge

10μm

Immunoprecipitation

B

	No antibody			Rabbit anti-Flag			Mouse anti-GFP			Western Blot
	Input	Supernate	Pellet	Input	Supernate	Pellet	Input	Supernate	Pellet	
Gemin3										Mouse anti-Gemin3
GFP-hnRNPQ1										Mouse anti-GFP
Flag-SMN										Mouse anti-Flag
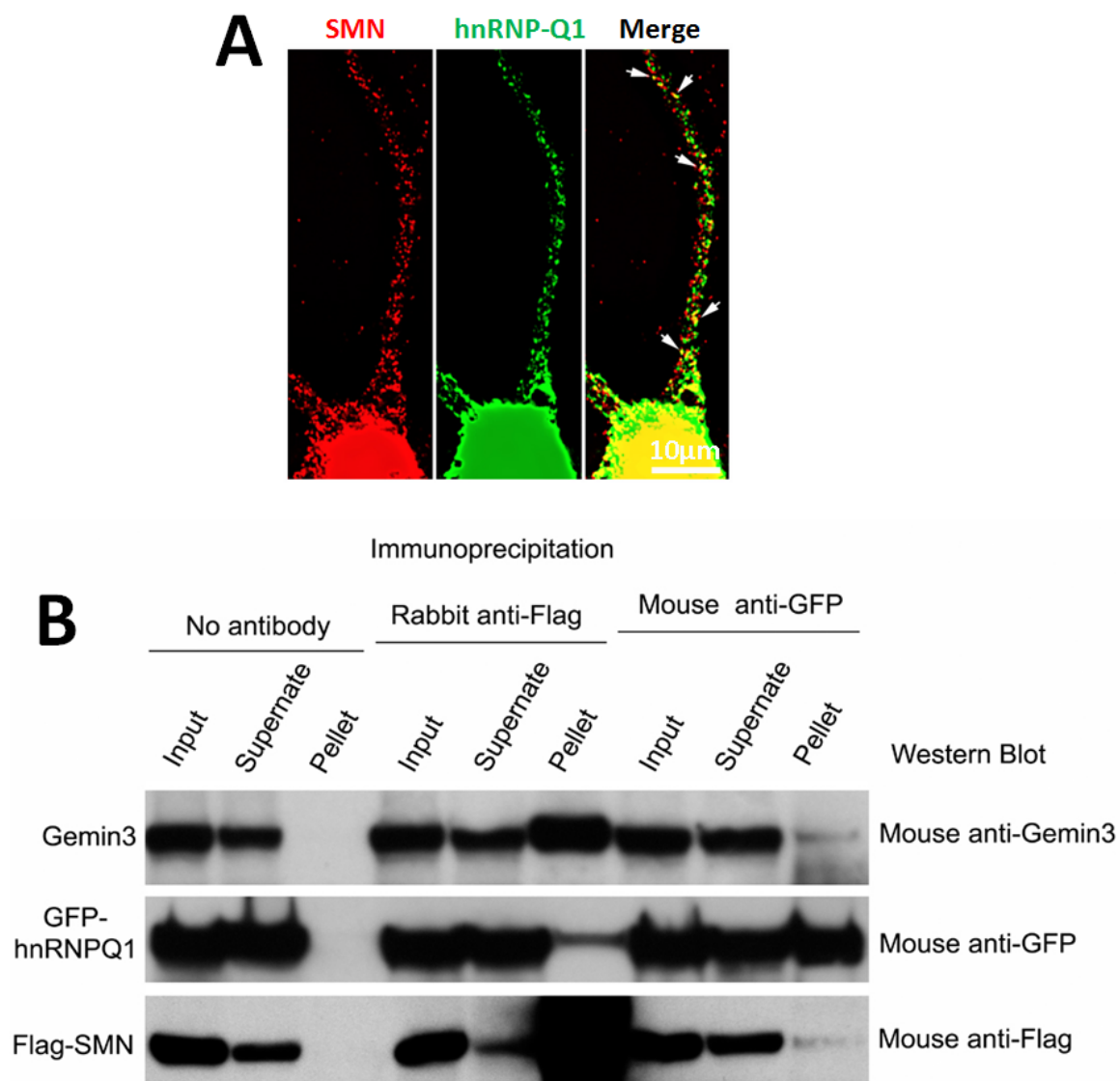
Figure 2-9. Association of SMN and hnRNP-Q1 in 293 cells and hippocampal neurons

(A) Fluorescent immunostaining of endogenous SMN and hnRNP-Q1 in hippocampal neurons. A frequent colocalization of SMN (red) and hnRNP-Q1 (green) were observed in neurites and examples of colocalized SMN and hnRNP-Q1 granules were indicated by arrows. **(B)** Co-immunoprecipitation analysis of Flag-SMN and EGFP-hnRNP-Q1 expressed in 293 cells. Flag-SMN and EGFP-hnRNP-Q1 were expressed in 293 cells for over 16 hours before lysed in immunoprecipitation buffer. Flag-SMN and EGFP-hnRNP-Q1 were immunoprecipitated with a rabbit anti-Flag and mouse anti-GFP antibody, respectively. For western blot, mouse antibodies for Flag, GFP or Gemin3 were used.
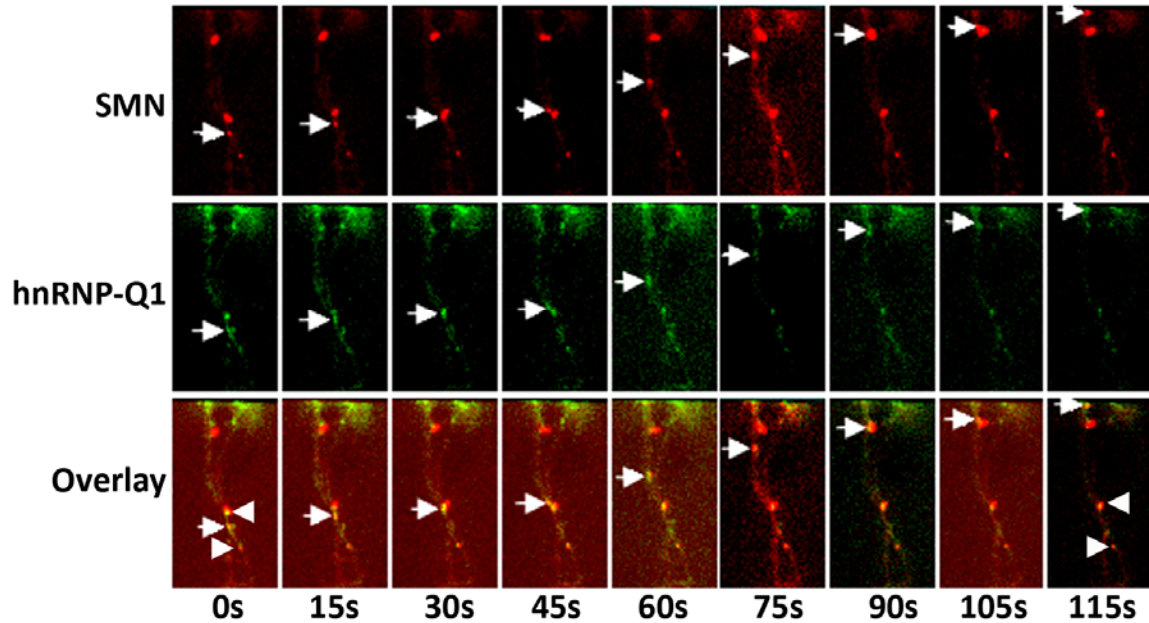
Figure 2-10. Co-transport and colocalization of mRFP-SMN and EGFP-hnRNP-Q1 in live rat hippocampal neurons

Rat embryonic hippocampal neurons cotransfected with mRFP-SMN and EGFP-hnRNP-Q1 were imaged with Nikon TE2000 microscope equipped with a GFP/RFP dual view system. Time-lapse images were captured at 0.5 second/frame without interval. An example of moving granules (indicated by arrows) was tracked within a period of 115 second and shown frame by frame with 15 second intervals except 10 seconds for the last one. An oscillatory granule was marked by arrowheads. (Contributed by Dr. Kristy Welshhans)

Chapter III

hnRNP-Q1 regulates cellular morphogenesis by inhibiting RhoA mRNA translation

Introduction

hnRNP-Qs are a family of hnRNPs that directly interact with the Survival of Motor Neuron protein (SMN) (Mourelatos et al., 2001; Rossoll et al., 2002). This interaction has been implicated in the pathogenesis of Spinal Muscular Atrophy (SMA), a recessive inherited motor neuron degenerative disease caused by the reduced expression of SMN (Lefebvre et al., 1995). The human hnRNP-Qs are composed of three isoforms including hnRNP-Q1, Q2 and Q3, which exist due to alternative splicing of human *hnRNP-Q* transcripts (Mourelatos et al., 2001). hnRNP-Q3 is also known as Glycine-Arginine-Tyrosine-rich RNA-binding protein (GRY-RBP) (Blanc et al., 2001). hnRNP-Q1 is known as NS1-associating protein-1 (NSAP) and Synaptotagmin-binding, cytoplasmic RNA-interacting protein (SYNCRIP), due to its structural features, association with murine viral protein-NS1 (Harris et al., 1999) and multiple isoforms of Synaptotagmin (Mizutani et al., 2000), respectively. In mouse cells, only hnRNP-Q1 and Q3 have been identified.

Recent studies suggest that hnRNP-Qs are multifunctional proteins that play roles in pre-mRNA splicing, RNA editing, cytoplasmic mRNA transport, translational regulation and mRNA degradation (Bannai et al., 2004; Blanc et al., 2001; Chen et al., 2008; Grosset et al., 2000; Kanai et al., 2004; Mourelatos et al., 2001; Weidensdorfer et al., 2009). hnRNP-Qs are believed to be components of spliceosomes due to their interaction with SMN and the observation that depletion of hnRNP-Qs leads to inefficient splicing of pre-mRNAs (Mourelatos et al., 2001). hnRNP-Q3 interacts with APOBEC1, which catalyzes a C to U ribonucleotide transition found in Apolipoprotein B mRNA through an mRNA editing process (Blanc et al., 2001). hnRNP-Qs were also identified as

components of transport mRNP granules in the central nervous system, as they were co-purified with the KIF5 kinesin cargo binding domain (Kanai et al., 2004). In neuronal dendrites, hnRNP-Q1 has been shown to be associated with Staufen, a double-strand RNA binding protein, in transport mRNP granules and colocalized with *inositol 1,4,5-trisphosphate receptor type 1* (*IP₃R1*) mRNA (Bannai et al., 2004). Moreover, hnRNP-Q1 plays an essential role in coding region instability determinant (CRD)-mediated and AU-rich element (ARE)-mediated mRNA degradation (Grosset et al., 2000; Weidensdorfer et al., 2009). However, none of these functions have been well studied.

In this study, we characterized the subcellular localization of hnRNP-Qs and their homolog, hnRNP-R, and found that hnRNP-Q1 is the isoform localized to distal axons and dendrites. In addition, we identified hnRNP-Q1 as a trans-acting factor for RhoA mRNA. Importantly, RhoA mRNA is localized to the growth cone and its local translation is involved in Semaphorin-induced growth cone collapse (Wu et al., 2005). We further demonstrated that hnRNP-Q1 negatively regulates the incorporation of RhoA mRNA into polysomes. Through this study, we provide the first evidence for the function of hnRNP-Q1 in regulating cell morphology and motility. Our results show that knockdown of hnRNP-Q1 leads to defective spine morphogenesis in mature neurons. In C2C12 cells, hnRNP-Q1 knockdown results in enhanced cell spreading and reduced cell motility accompanied with increased focal adhesions and stress fibers. These findings suggest that hnRNP-Q1 negatively regulates RhoA mRNA translation, and thereby modulates actin dynamics during cellular morphogenesis.

Materials and Methods

Cell cultures

Neuro2a and C2C12 myoblastoma (ATCC) cells were maintained in DMEM (Sigma) with 10% FBS (Sigma), 100U/ml penicillin and 100mg/ml of streptomycin (Invitrogen) at 5% CO_2 and 37ºC according to general cell culture procedure. For treatment with lysophosphatidic acid (LPA), C2C12 cells were starved in serum-free DMEM for 2 hours. 5mM of LPA (Sigma-Aldrich) was added to each well with an additional incubation for 30 minutes.

Primary mouse hippocampal neurons were cultured from E16 mouse embryos as described previously (Antar et al., 2006). In brief, dissected hippocampi were trypsinized with 0.25% trypsin for 10 minutes and triturated in MEM with 10% FBS. Dissociated neurons were plated on poly-L-lysine (Sigma) coated coverslips and incubated for 2 hours. After that, neurons were co-cultured with glial cells in Neurobasal (Invitrogen) supplemented with 2% B27 (Invitrogen) and 1X Glutamax (Invitrogen).

Preparation for Axonal and synaptosome fractions

For axon purification, cortical neurons harvested from E16 embryonic mouse brains were suspended in Neurobasal medium supplemented with B27, Glutamax and 10% horse serum. Neurons were cultured in hang-drops with 10 thousand neurons in each drop for 2 to 3 days to allow the formation of aggregates. The neuronal aggregates were collected and washed with culture medium to remove single neurons and small aggregates. Individual aggregates were plated on cell culture dishes pre-treated with poly-L-Lysine at low density and cultured in Neurobasal medium supplemented with B27, Glutamax and 2% horse serum. 24 hour post plating, neuronal aggregates were treated with 3μM cytosine arabinofuranoside (Ara-C) for additional 24 hours to eliminate glial cells. Then the Ara-C-containing culture medium was replaced with fresh medium and

aggregates were cultured for 3 to 5 day to allow axon outgrowth. To collect distal axons, neuronal aggregates were washed with ice-cold PBS and bodies of neuronal aggregates were removed with 200μl pipette tips. After the removal of PBS, remaining cellular compartments containing distal axons were collected into cell lysis buffer. The purity of axonal fractions was tested by the presence of Tau and the lack of dendritic protein Map2.

Synaptosomes were prepared as described previously (Muddashetty et al., 2007). Briefly, cortex from 21 day old mice was dissected and homogenized at 4°C in 10 volumes of homogenization buffer (pH 7.4) containing 118mM NaCl, 4.7mM KCl, 1.2mM $MgSO_4$, 2.5mM $CaCl_2$, 1.53mM KH_2PO_4, 212.7mM glucose, 1mM DTT, protease inhibitors (Roche) and RNase inhibitor (Applied Biosystem). Samples were passed through two 100 μm nylon mesh filters, followed by one 10 μm MLCWP 047 filter (Millipore) and centrifuged at 1000 x g for 15 min. The pellets containing synaptosomes were resuspended in homogenization buffer. Protein concentrations were estimated using BCA protein assay (Thermo Scientific).

hnRNP-Q1 antibody production

An hnRNP-Q1 specific antibody was produced by immunizing rabbits with a keyhole limpet hemocyanin-conjugated synthetic peptide corresponding to the C-terminal sequence of hnRNP-Q1 (KGVEAGPDLLQ, through Sigma-Genosys). The hnRNP-Q1 antibody (anti-hnRNP-Q1) was purified using an affinity column covalently coupled with the peptide used for animal immunization. Specificity of anti-hnRNP-Q1 was tested by western blot against 293 cell lysate with or without overexpressed EGFP-hnRNP-Q1.

Plasmid and siRNA transfection

Full-length cDNA of human hnRNP-Q1 was obtained by RT-PCR from total RNA extracted from HEK 293 cells, and inserted into pEGFP-C1 vector by the XhoI site. The EGFP-hnRNP-Q1 was confirmed by DNA sequencing. To achieve hnRNP-Q1 knockdown, hnRNP-Q1 siRNA (sense: GAUGCAGUUUCAGGUGUAAUCAUCA and antisense: UGAUGAUUACACCUGAAACUGCAUC) and control siRNA with the same nucleotide composition (sense: GAUUUGAGACUUGUGCUAAACGUCA and antisense: UGACGUUUAGCACAAGUCUCAAAUC) were purchased from Invitrogen.

Mouse hippocampal neurons cultured on coverslips were transfected with NeuroMag transfection reagent (OZ Biosciences) in a 6-well plate. Before transfection, coverslips were transferred to a new well with 1.5ml of B27-free Neurobasal medium with 1X Glutamax. For transfection in one well, 200pmol of siRNA or 100pmol of siRNA with 1μg of pEGFPC1 were mixed with 3μl of transfection reagent in 200μl of Neurobasal medium with 1X Glutamax and incubated for 15 minutes at room temperature. Such mixtures were added to cell cultures and incubated on a magnetic place for 15 minutes followed by an additional incubation for 45 minutes without the magnetic plate. After transfection, coverslips were transferred back to the original glial cell plates.

Lipofectamine 2000 (Invitrogen) transfection reagent was used for C2C12 and Neuro2a cell transfection. Plasmid transfections were performed according to the manufacturer's suggested protocol, except that only half the amount of plasmid and transfection reagent recommended was used. To deliver siRNA duplex into C2C12 and fibroblast cells in one well of a 6-well plate, 100pmol of siRNA was diluted in 250 μl of Opti-MEM and mixed with 250μl of Opti-MEM pre-mixed with 5 μl of Lipofectamine

2000 and incubated for 30 minutes at room temperature. Before transfection, C2C12 or primary fibroblast cells were trypsinized and suspended in DMEM with 10% FBS. 1.5ml of cells were mixed with siRNA-Lipofectamine 2000 mixture and incubated at 37 ℃ for 30 minutes. Cells were plated into cell culture plates and cultured for 72 hours for biochemical analysis, or trypsinized and replated onto coverslips at 48 hours with additional 24 hours culture for immunofluorescence staining and microscopy studies. For rescue experiment, C2C12 cells were transfected with plasmids expressing EGFP, or EGFP-hnRNP-Q1 24 hours post siRNA transfection and cultured for an additional 48 hours.

Antibodies and Immunofluorescence staining

Immunofluorescence staining was performed as described previously (Zhang et al, 2006). In brief, all cells were fixed with 4% paraformaldehyde in PBS containing 5mM $MgCl_2$ for 18 min at room temperature and then washed with PBS/ $MgCl_2$ three times. Cells were permeabilized with PBS/0.3% Triton X-100 for 5 minutes followed by 30 minutes of incubation with blocking buffer containing 5% BSA in PBS/0.1% Triton X-100 (PBST). Primary and secondary antibodies were diluted in blocking buffer. Cells were incubated with primary antibodies for 1 hour at room temperature or overnight at 4 ℃ and incubated in secondary antibody for 1 hour at room temperature, followed by three washes with PBST. Coverslips were mounted in mounting medium.

The following antibodies were used in this study. Rabbit anti-Syncrip (1:10000, kindly provided by Dr. Katsuhiko Mikoshiba) (Mizutani et al., 2000), rabbit anti-hnRNP-Q1 (1:500, generated in this study), mouse anti-Tau (1:1500, Sigma-Aldrich); mouse anti-Map2 (1:1500, Sigma-Aldrich); mouse anti-GFAP (1:3000, Sigma-Aldrich); mouse

anti-α-tubulin (1:40000, Sigma-Aldrich); mouse anti-Paxillin (1:150, BD Biosciences); mouse anti-RhoA (1:200, Cytoskeleton Inc.); rabbit anti-Phospho-Cofilin (1:5000, Cell signaling) and rabbit anti-Cofilin (1:10000, Sigma-Aldrich). Secondary antibodies conjugated with Cy2 (1:500), Cy3 (1:1000) or Cy5 (1:500) were purchased from Jackson ImmunoResearch Inc.

Fluorescence microscopy and digital imaging

Fixed cells were visualized using a Nikon Eclipse inverted microscope (TE300) equipped with a 60x Plan-Neofluar objective, phase optics, 100W mercury arc lamp and HiQ bandpass filters (Chroma Tech). Images were captured with a cooled CCD camera (Quantix, Photometrics) using a 35 mm shutter and processed using IP Lab Spectrum (Scanalytics). Fluorescence images were acquired with specific filters, including Cy2, Cy3 or Cy5. For quantitative analysis, exposure time was kept constant and below gray scale saturation. Images were deconvolved by AutoQuantX2 software to minimize background.

For morphological analysis of dendritic spines, dendrites of EGFP-positive neurons were imaged along the z axis for a total of 6μm with 0.2μm intervals. After deconvolution, three-dimensional images were reconstructed with Imaris computer software (Version 6.2, Bitplane). Dendrite length and numbers of dendritic spines were quantified manually using Imaris. Both filopodia and mushroom-like protrusions were classified as dendritic spines in this study.

Transwell migration experiment

Transwell cell migration assay was performed using 8μm-pore PET track-etched membrane cell culture inserts (Becton Dickinsin Labware). 72 hours after siRNA transfection, C2C12 cells were trypsinized and plated onto inserts coated with Fibronectin on the bottom surface. Cells were fixed with 4% paraformaldehyde eight hours after plating and stained with DAPI. Ten random optical fields from each insert were imaged with a 4x objective and the average number of DAPI granules was quantified as the total number of cells. After quantifying the total number of cells, the top layer (non-migrating) cells were removed with a swab, followed by washes with PBS to remove residual cell debris. Remaining cells representing migrating cells were counted. Efficiency of cell migration was measured as the ratio of migrating cells to total cells.

Immunoprecipitation and Quantitative RT-PCR (qRT-PCR) analysis

Neuro2a cell lysates were prepared with cell lysis buffer (50mM Tris-HCl, 150mM NaCl, 5mM $MgCl_2$, 1mM DTT, and 1% NP-40, pH7.5) supplemented with complete protease inhibitors (Roche), and RNase inhibitor (SUPERNASin, Ambion). Cells were lysed by further incubation on ice for 10 minutes and cleared by centrifugation at 20,000g for 15 minutes at 4 ℃. Supernatant was incubated with anti-Flag agarose beads for 2 hours at 4 ℃ with rotation. Beads were pelleted by a brief spin at 4 ℃ and washed extensively with cell lysis buffer. After the final wash, immuprecipitation pellets were resuspended in Trizol reagent (Invitrogen) for RNA extraction.

Total RNAs were reverse transcribed with Transcriptor First Strand cDNA Synthesis Kit (Roche) according to the suggested protocol. Real-time PCR and analysis was performed in a LightCycler real-time PCR system with LightCycler SYBR Green I reagent (Roche). Gene specific primers were used as listed below. CTAGCAGTGG

GCAGTACATT and TCTGTGCATACTGTAGAATG for Creb; AAGAAGCTGACAGGAATCAA and TGGCTCACAAAGGCTTGC for Cofilin; TATGATGAAAAGGTGGACGT and TTGAGGCCAAAGTCCATAGT for Lim Kinase1; CATTGACAGCCCTGATAGTT and TCGTCATTCCGAAGGTCCTT for RhoA; ACAAGATGGTGTCAAGCC and CATCGGTAGTAGCAGAGC for Gap43; CTGGTGGATCTCTGTGAGCAC and AAACGTTCCCAACTCAAGGC for γ-actin; AGCAGTTGGTTGGAGCAAACATCC and GGTGAGGGACTTCCTGTAACCACTTA for β-actin.

Western blot analysis

Protein samples were resolved by sodium dodecyl sulfate polyacrylamide gel electrophoresis (SDS-PAGE) and transferred onto PVDF membranes. For protein detection, PVDF membrane was incubated with blocking solution (5% fat-free milk in PBST) for 30 minutes at room temperature and further probed with primary antibodies diluted in blocking solution for 1 hour at room temperature or overnight at 4ºC. After three washes with PBST, PVDF membrane was incubated with HRP-conjugated donkey anti-mouse or rabbit secondary antibodies (1:3000, Amersham Biosciences) in blocking solution for 1 hour at room temperature. After washing with PBST, the signal was detected using ECL chemiluminescence reagents (Amersham Biosciences) and exposed to films. To detect phospho-protein, TBST (50mM Tris-HCl, 150 mM NaCl, and 0.1% Triton X-100, pH 7.5) were used and 5% BSA in TBST as blocking solution.

mRNA stability assay

C2C12 cells transfected with hnRNP-Q1 siRNA or control siRNA were treated with 5μg/ml Actinomycin D (Sigma) for transcription blockage. Total RNA was extracted from C2C12 cells with Trizol reagent at 0, 4.5 and 9 hours after Actinomycin D treatment. cDNAs were reverse transcribed from 1μg of total RNA, and then each sample was diluted and used for qRT-PCR analysis. Remaining mRNA normalized to 0 hour was quantified as $2^{-(Ct-Ct0)}$. To examine the effect of translation on mRNA degradation, cells were treated with 20 μg/ml anisomycin (Sigma) together with Actinomycin D.

Polysome fractionation

A 10cm plate of C2C12 cells transfected with hnRNP-Q1 siRNA or control siRNA were pretreated with 100μg/ml of cycloheximide for 10 minutes. After a brief wash with ice-cold HBSS with 20mg/ml of cycloheximide (Sigma), cells were harvested into 1ml of cell lysis buffer (50mM Tris-HCl, 150mM NaCl, 5mM $MgCl_2$, 1mM DTT, and 1% NP-40, pH7.5) supplemented with 100 mg/ml of cycloheximide, complete protease inhibitors (Roche), and RNase inhibitor (SUPERase-In, Ambion). Cells were homogenized with 5 strokes and cleared by centrifugation at 20,000g for 30 minutes at 4 ºC. 500μl of supernatant was loaded on a 15 to 45% linear sucrose gradient (in 20 mM Tris-HCl, 100 mM KCl, 5 mM $MgCl_2$, pH7.5) supplemented with 20mg/ml of cycloheximide and spun at 38,000 rpm for 90 min in an SW41 rotor (Stefani et al., 2004). Sucrose gradient was collected as 11 fractions at 1ml/each with absorbance of 254nm recorded to monitor polysome profiles. Total RNA was extracted from each fraction with Trizol LS reagent (Invitrogen) according to the manufacturer's suggested protocol. The same volume of RNA from each fraction was reverse transcribed and mRNAs of interest were analyzed by qRT-PCR.

Results

Subcellular distribution of hnRNP-Q1 and its association with axonal mRNAs

Previously, hnRNP-Qs had been identified as components of transport mRNP granules, suggesting a role for hnRNP-Qs in mRNA transport and translational regulation in neurons (Bannai et al., 2004; Elvira et al., 2006; Kanai et al., 2004). Thus, we analyzed the presence of endogenous hnRNP-Qs in axonal and synaptic fractions by western blot with an antibody recognizing all isoforms of hnRNP-Qs and hnRNP-R. Axonal fractions were purified from *in vitro* cultured mouse cortical neuronal aggregates, the purity of which was confirmed by the presence of axon-enriched Tau protein and the lack of dendrite-localized protein Map2. As shown in **Figure 3-1A**, a substantial amount of hnRNP-Q1 and a much lower proportion of hnRNP-Q3 and its homolog, hnRNP-R, were detected in the axonal fraction. A similar result was obtained with synaptosome fractions purified from mouse brains **(Figure 3-1B)**, which represents enriched synaptic compartments with limited glial cell and cytoplasmic contamination, as demonstrated by enriched postsynaptic density protein-95 (PSD-95) and reduced glial fibrillary acidic protein (GFAP)**.** The presence of hnRNP-Q1 in axonal and synaptic fractions suggests that hnRNP-Q1 is the major isoform for the functions of hnRNP-Qs in cytoplasmic mRNA regulation, such as mRNA transport, stability control and translation.

To enable analysis of endogenous hnRNP-Q1 localization, an hnRNP-Q1-specific antibody targeting to the C-terminal sequence of hnRNP-Q1 was generated **(Figure 3-2A)**. The specificity of this antibody was confirmed by western blot analysis against both endogenous hnRNP-Q1 and over-expressed EGFP-tagged hnRNP-Q1. This antibody only detects endogenous and overexpressed hnRNP-Q1 **(Figure 3-2B)** with no cross-

reaction with overexpressed EGFP-hnRNP-Q3 and EGFP-hnRNP-R **(Supplemental Figure 3-1)**. Indirect immunofluorescence staining with this antibody showed that hnRNP-Q1 was mainly distributed in the cytoplasm of cultured primary hippocampal neurons. hnRNP-Q1 granules were detected in both dendrites **(Figure 3-2C)** and axons **(Figure 3-2D)** which were identified by Map2 and Tau specific staining, respectively. A substantial amount of hnRNP-Q1 granules were observed overlapping with microtubules in growth cones and distal axons **(Figure 3-2E)**.

Based on the observation that hnRNP-Qs are components of transport mRNP granules (Bannai et al., 2004; Elvira et al., 2006; Kanai et al., 2004), we investigated the association of hnRNP-Q1 with mRNAs in Neuro2a cells. Flag-mCherry-hnRNP-Q1 and Flag-mCherry were overexpressed in Neuro2a cells and immunoprecipitated. Several endogenous mRNAs co-immunoprecipitated with Flag-mCherry-hnRNP-Q1 were examined by qRT-PCR with gene specific primers. We found that hnRNP-Q1 exhibited high selectivity to its associated mRNAs; particularly several mRNAs, including Creb (Cox et al., 2008), Gap-43 (Smith et al., 2004) and RhoA mRNA (Vogelaar et al., 2009; Wu et al., 2005), which have been shown to be localized to axons and growth cones, were highly enriched in Flag-mCherry-hnRNP-Q1 pellets **(Figure 3-3)**. These observations are consistent with a previous report that hnRNP-Q1 is a component of transport mRNP granules, a complex actively transported along microtubules through molecular motors (Singer, 2008).

Knockdown of hnRNP-Q1 reduces the density of dendritic spines

To investigate the function of hnRNP-Q1 in neuronal development, we analyzed the effect of hnRNP-Q1 knockdown on mature neurons. In particular, we looked for

possible defects in dendritic spine morphology, because their development and maintenance are highly sensitive to environmental changes and cellular activities (Calabrese et al., 2006; Yoshihara et al., 2009). An hnRNP-Q1-specific siRNA was synthesized by targeting to the unique 3'UTR of mouse hnRNP-Q1 transcript; this ensured specific knockdown of hnRNP-Q1 without affecting hnRNP-Q3 and hnRNP-R. A scrambled siRNA with the same nucleotide composition was used as a negative control. High density cultured hippocampal neurons were transfected with siRNA at day 9 in vitro (DIV9) followed by a second round of siRNA transfection at DIV12, along with an EGFP expressing plasmid to highlight neuronal morphology. Neurons were fixed at DIV13 and examined for possible developmental defects of fine dendritic structures. hnRNP-Q1 siRNA transfection leads to an efficient reduction of hnRNP-Q1 protein **(Supplemental Figure 3-2B)** compared with neurons transfected with control siRNA **(Supplemental Figure 3-2A)**. A quantitative analysis revealed that the dendritic spine density of neurons transfected with hnRNP-Q1 siRNA **(Figure 3-4C, C' and E)** was reduced by over 30% with 3.3 spines per 10μm, compared with 4.8 spines per 10μm for neurons transfected with control siRNA **(Figure 3-4A, A' and E)**. The reduced spine density of mature neurons is reminiscent of the effect observed upon the activation of small GTPase RhoA/ROCK sigmaling pathway (Elia et al., 2006; Govek et al., 2005; Tashiro and Yuste, 2008; Zhang and Macara, 2008). Studies have shown that in mature neurons, excessive RhoA activation by depletion of RhoA inhibitors or overexpression of a constitutively active form of RhoA alters dendritic spine morphogenesis, including a reduced number of spines (Elia et al., 2006; Tashiro and Yuste, 2008; Zhang and Macara, 2008). Therefore, we hypothesize that the effect of hnRNP-Q1 knockdown on spine

morphogenesis may be mediated by an upregulation of the RhoA/ROCK signaling pathway. To test this hypothesis, we treated neurons with the ROCK inhibitor Y-27632 (20μM) for 5 hours and examined its effects on spine densities. We found that after Y-27632 treatment, the dendritic spine density of hnRNP-Q1 siRNA transfected neurons was recovered to a similar level of non-treated control cells with 4.7 spines per 10μm **(Figure 3-4D, D'** and **E)**. Treatment with Y-27632 on control siRNA transfected cells has no significant effect **(Figure 3-4B, B'** and **E)**. These results indicate that the RhoA/ROCK signaling pathway contributes to the morphological change induced by hnRNP-Q1 knockdown in mature neurons.

Knockdown of hnRNP-Q1 enhances cell spreading and reduces motility of C2C12 cells in association with enhanced focal adhesion formation

To test whether the function of hnRNP-Q1 in cellular morphogenesis is conserved in other cell types, we examined the effect of hnRNP-Q1 knockdown in C2C12 mouse myoblast cells. Immunoblot analysis showed that 72 hours post siRNA transfection, the protein level of hnRNP-Q1 was obviously reduced **(Figure 3-5A)**. Most C2C12 cells treated with hnRNP-Q1 siRNA exhibited a flattened cell shape, whereas cells transfected with control siRNA were spindle-like **(Figure 3-5B, b'** and **b'')**. We quantified the average cell area and found that knockdown of hnRNP-Q1 led to about a 70% increase in cell area **(Figure 3-5C)**. Importantly, expression of siRNA-insensitive EGFP-tagged hnRNP-Q1, containing only the coding region, into siRNA-treated C2C12 cells successfully abolished the effect of hnRNP-Q1 siRNA **(Figure 3-5D)**, indicating that the cell spreading phenotype of C2C12 cells was specific to hnRNP-Q1 knockdown. In addition, hnRNP-Q1 siRNA treated cells exhibited reduced motility as tested with a

trans-well cell migration assay performed in normal culture medium (as described in methods; **Figure 3-5E**). Moreover, hnRNP-Q1 knockdown enhanced spreading of newly plated C2C12 cells **(Figure 3-6A and B)**. Treatment with Y-27632 induced dramatic morphological changes on both control siRNA and hnRNP-Q1 siRNA transfected C2C12 cells; these cells exhibited an elongated cell shape with tail-like structures **(Figure 3-7)**.

To further characterize the effects of hnRNP-Q1 knockdown on C2C12 cells, we surveyed possible alterations in actin and microtubule filaments, and focal adhesions by Phalloidin or immunofluorescence staining of α-tubulin and Paxillin proteins, respectively. Compared to control siRNA treated cells, hnRNP-Q1 siRNA treated C2C12 cells exhibited a 38% increase of focal adhesions accompanied by enhanced stress fiber formation **(Figure 3-8A** and **B, Supplemental Figure 3-3C** and **D)**; whereas no obvious microtubule disorganization was observed **(Supplemental Figure 3-3A and B)**. Collectively, these observations suggest a function of hnRNP-Q1 in regulating cellular morphogenesis, in which the RhoA/ROCK signaling pathway is downstream to hnRNP-Q1 and possibly mediating the function of hnRNP-Q1 to regulate actin filament dynamics. These observations thus led us to assess the functional connection between hnRNP-Q1 and RhoA/ROCK signaling pathway.

<u>hnRNP-Q1 knockdown leads to unregulated RhoA protein expression</u>

Studies have shown that activation of RhoA triggers focal adhesion and stress fiber formation in multiple cell types (Besson et al., 2004; Mohseni and Chishti, 2008; Nobes and Hall, 1995; Ozawa et al., 2005; Ridley and Hall, 1992). In certain cell types, over-activation of the RhoA pathway leads to reduced cell motility (Besson et al., 2004; Ozawa et al., 2005; Mohseni and Chishti, 2008). Collectively, with the selective

association of hnRNP-Q1 with RhoA mRNA, we hypothesize that the effects of hnRNP-Q1 knockdown on cellular morphogenesis is mediated through the deregulation of RhoA protein expression. Thus, we first examined the protein levels of RhoA. Three days after siRNA transfection, C2C12 cells were denatured with protein sample buffer and used for western blot analysis. RhoA protein and hnRNP-Q1 were detected with specific antibodies and α-tubulin was used as an internal loading control. By densitometric analysis, we found a 50% increase in RhoA protein in C2C12 cells transfected with hnRNP-Q1 siRNA, as compared to control siRNA transfected cells **(Figure 3-9A** and **B)**. The effect of hnRNP-Q1 knockdown of RhoA expression was also examined in primary mouse embryonic fibroblast cells, where a similar increase (about 50%) of RhoA protein level was observed **(Supplemental Figure 3-4A)**. In addition, hnRNP-Q1 siRNA transfected primary fibroblast cells exhibit a flattened cell morphology and enhanced cell spreading, as compared to control siRNA treated cells, just as we observed in C2C12 cells **(Supplemental Figure 3-4B)**.

The function of RhoA on actin filament dynamics is mediated through the RhoA-ROCK-LIM kinase signaling pathway (Amano et al., 2001; Leung et al., 1996; Maekawa et al., 1999; Sumi et al., 2001a). Activation of LIM Kinase by ROCK following RhoA activation leads to Cofilin phosphorylation at the S3 site, which inactivates its function as an actin filament destabilizer (Sumi et al., 2001b; Sumi et al., 1999). Thus, we accessed the effect of hnRNP-Q1 knockdown on Cofilin phosphorylation. We predicted that hnRNP-Q1 knockdown-induced RhoA upregulation would enhance Cofilin phosphorylation and such effect would be exaggerated by additional RhoA activation. 72 hours post siRNA transfection, C2C12 cells were first starved in serum-free medium for

2 hours to eliminate the interference of serum components, and then further incubated for 30 minutes with 10μM LPA to activate RhoA. Phospho-Cofilin was probed by immunoblot analysis with phospho-Cofilin (S3)-specific antibodies and total Cofilin was blotted as the internal control. We found that following hnRNP-Q1 knockdown, levels of phospho-Cofilin were increased by more than 40% over control siRNA transfected cells and over 130% when treated with LPA **(Figure 3-9C and D)**.

hnRNP-Q1 negatively regulates RhoA mRNA translation

To have a further understanding of how the knockdown of hnRNP-Q1 leads to upregulated RhoA protein expression, we first examined RhoA mRNA levels. Several studies have shown that downregulation of some RNA binding proteins, especially those functioning as mRNA destabilizers, results in mRNA accumulation and increased protein expression (Gherzi et al., 2004; Gherzi et al., 2006; Lykke-Andersen and Wagner, 2005). We expected that the increased RhoA protein level was a consequence of upregulated RhoA mRNA level due to enhanced transcription or increased RhoA mRNA stability. However, we constantly observed a slight reduction (about 10%) of RhoA mRNA level in C2C12 cells transfected with hnRNP-Q1 siRNA; whereas the level of γ-actin mRNA, a less enriched mRNA with hnRNP-Q1 immunoprecipitation, was not affected **(Figure 3-10A)**. We further examined the stability of RhoA mRNA in hnRNP-Q1 and control siRNAs-transfected cells. C2C12 Cells were treated with 5μM actinimycin D to block transcription and total mRNA was collected after 0, 4.5 and 9 hours of actinomycin D incubation. The mRNA level of RhoA and γ-actin were measured by qRT-PCR. The remaining mRNA levels were normalized to the level at 0 hour and calculated as $2^{-\Delta Ct}$. Consistent with the decreased RhoA mRNA level in hnRNP-Q1 siRNA transfected cells,

the rate of RhoA mRNA degradation was enhanced **(Figure 3-10D)**, indicating reduced RhoA mRNA stability; yet the decay rate for γ-actin mRNA from the same experimental conditions remained unchanged **(Figure 3-10B)**.

The unexpected changes of RhoA mRNA level and stability failed to provide a rationale for the increased RhoA protein level after hnRNP-Q1 knockdown. We speculate that the inverted RhoA protein and mRNA level change is caused by enhanced RhoA mRNA translation following hnRNP-Q1 knockdown; in such a case, RhoA mRNA would be degraded in a translation termination-coupled mRNA decay pathway as described recently (Funakoshi et al., 2007), and increased translation would lead to enhanced mRNA degradation, suggesting a use-dependent decay mechanism. To test the effect of hnRNP-Q1 on RhoA mRNA translation, we analyzed the polysome profiles of RhoA and γ-actin mRNA in C2C12 cells treated with hnRNP-Q1 or control siRNA **(Figure 3-11A and B)**. Cell lysates from both conditions were prepared from cells pre-treated with cycloheximide to block translation elongation and preserve polysomes. Cell lysates were pre-cleared by centrifugation and resolved in a 15-45% linear sucrose gradient. Eleven gradient fractions were collected and absorbance at 254nm was monitored as an indicator of ribosomal profile **(Supplemental Figure 3-5A and B)**. Western blot analysis of ribosomal P0 protein shows that hnRNP-Q1 knockdown has no effect for the overall profile of polysomes **(Supplemental Figure 3-5C and D)**, indicating that hnRNP-Q1 knockdown does not interfere with general translation. RhoA and γ-actin mRNAs in each fraction were quantified by qRT-PCR. We found that RhoA mRNA was mainly distributed through fractions 5-8 representing mRNAs associated with 3 to 8 ribosomes **(Supplemental Figure 3-5B)**. The peak of RhoA mRNA in hnRNP-Q1 siRNA

transfected cell was observed in the fraction 7; whereas in control siRNA transfected cells, the RhoA mRNA peak was in the fraction 6 **(Figure 3-11A)**. The right shift of the RhoA mRNA peak into heavier sucrose fractions suggests more ribosomes associated with RhoA mRNAs in cells with hnRNP-Q1 knockdown, indicating increased translation efficiency. In the same condition, the distribution of γ-actin mRNA was not affected **(Figure 3-11B)**.

Knockdown of hnRNP-Q1 induces RhoA mRNA decay coupled with translation

We then tested the effect of translation blockage on RhoA mRNA stability. If the reduced RhoA mRNA stability observed in hnRNP-Q1 knockdown cells was indeed caused by enhanced translation, the blockage of translation would abolish this phenomenon. In addition to actinomycin D, we treated cells with a translation inhibitor, anisomycin, at the same time. In contrast to the results from experiments using actinomycin D only **(Figure 3-10D)**, the levels of remaining RhoA mRNA in hnRNP-Q1 knockdown cells remained similar to cells transfected with control siRNA when treated with anisomycin **(Figure 3-10E)**. Together with the shift of RhoA mRNA in polysome profile mentioned above, these observations suggest that hnRNP-Q1 is a trans-acting factor which negatively regulates RhoA mRNA translation.

Discussion

hnRNP-Q1, Q2 and Q3 are a family of ubiquitously expressed RNA binding proteins which have been implicated in multiple aspects of mRNA regulation in both the nucleus and the cytoplasm as well as the pathogenesis of SMA (Bannai et al., 2004; Blanc et al., 2001; Chen et al., 2008; Grosset et al., 2000; Kanai et al., 2004; Mourelatos et al., 2001; Weidensdorfer et al., 2009). In this study, we found that hnRNP-Q1 is

localized to both axons and dendrites, suggesting a role for hnRNP-Q1 in cytoplasmic mRNA regulation. Therefore, we focused on the functional analysis of hnRNP-Q1. Through this study, we uncovered a novel regulatory mechanism for the function of the small GTPase RhoA, showing that hnRNP-Q1 negatively regulates RhoA mRNA translation and thus affects RhoA protein level and downstream actin filament dynamics.

hnRNP-Q1 negatively regulates the function of RhoA

Rho GTPases, particularly RhoA, Rac1 and Cdc42, are important regulators of actin filament dynamics (Nobes and Hall, 1995; Ridley and Hall, 1992). In fibroblast cells, RhoA activation triggers stress fiber and focal adhesion formation; Rac1 activation leads to disassembly of stress fibers and focal adhesions and their subsequent rearrangement into meshwork structures such as lamellipodia and membrane ruffles; Cdc42 activation promotes the formation of spike-like filopodia (Nobes and Hall, 1995; Ridley and Hall, 1992). Current studies have revealed a regulatory mechanism for the function of Rho GTPases on the protein level, by which the activity of Rho GTPase is tightly controlled by the relative amount of the active GTP-bound form to inactive GDP-bound form (Sinha and Yang, 2008). The switch from GTP to GDP-bound form is regulated by GTPase activating proteins (GAPs) which directly interact with Rho GTPases and promotes GTP hydrolysis through the intrinsic GTPase activity of Rho GTPases; whereas a reverse switch is promoted by the binding of guanine nucleotide exchange factors (GEFs) which enhance the exchange of GDP for GTP, and binding of the latter leads to Rho GTPase activation (Sinha and Yang, 2008). For RhoA regulation, p190RhoGAP (Arthur and Burridge, 2001) and p200RhoGAP (Moon et al., 2003) are GAPs inhibiting RhoA activity, whereas GEF-H1 (Ren et al., 1998) and Tech (Marx et

al., 2005) are examples of exchange factors activating RhoA. In addition, RhoA binding proteins, including Oligophrenin-1 (Billuart et al., 1998; Govek et al., 2004), p27^{Kip1} (Besson et al., 2004) and p120 catenin (Anastasiadis et al., 2000; Elia et al., 2006), repress RhoA activities by disrupting the interaction of RhoA and exchange factors. Loss of function or overexpression of these RhoA interacting proteins leads to aberrant activation or inactivation of RhoA (Billuart et al., 1998; Castano et al., 2007; Govek et al., 2004). For example, loss of p190RhoGAP or overexpression of a dominant negative form of this protein promotes stress fiber formation and reduced cell motility of fibroblast cells due to RhoA activation; while overexpression of p190RhoGAP enhances cell migration and diminishes stress fibers and focal adhesions (Arthur and Burridge, 2001). A similar phenomenon was seen in cells lacking p27^{Kip1} (Besson et al., 2004). In neuronal cells, loss of RhoA inhibitors, such as p190RhoGAP, p120 catenin and Oligophrenin-1, incurs defective development of dendrites exhibiting reduced spine density (Elia et al., 2006; Govek et al., 2004; Zhang and Macara, 2008).

Our results support hnRNP-Q1 as a novel inhibitory factor for the function of RhoA. Knockdown of hnRNP-Q1 in C2C12 cells led to enhanced stress fiber and focal adhesion formation and reduced motility. In mature mouse hippocampal neurons, depletion of hnRNP-Q1by RNAi caused a reduction of spine density, as seen in studies of other RhoA inhibitory factors (Elia et al., 2006; Govek et al., 2004; Zhang and Macara, 2008). The phenotype observed in cells with hnRNP-Q1 knockdown phenocopied the effect of enhanced RhoA activation. Two sets of experiments were performed to validate that RhoA is a downstream effecter of hnRNP-Q1. Firstly, we treated cells with the ROCK inhibitor Y-27632 to block the downstream signaling of RhoA and examined

subsequent effects. In mature neurons, treatment with Y-27632 reversed the effect of hnRNP-Q1 knockdown on dendritic spine morphogenesis. Results from C2C12 cell show that the application of Y-27362 on control siRNA treated cells had a dramatic impact on cell spreading and contraction, as the cells had an elongated cell morphology with tail-like structures. A similar effect of Y-27632 was also observed on cells with hnRNP-Q1 knockdown. Secondly, we tested the effect of hnRNP-Q1 knockdown on a downstream effector Cofilin, the phosphorylation of which can be induced by RhoA activation through ROCK and the downstream kinase, LIM Kinase (Sumi et al., 2001b; Sumi et al., 1999). Thus, treatment with RhoA activator would have an augmented effect on Cofilin phosphorylation. For this purpose, we treated cells with LPA which has been widely used for RhoA activation. As shown in **Figure 3-9C** and **D**, a 40% increase of phospho-Cofilin was observed in cells with hnRNP-Q1 depletion knockdown (normalized to control cells under starved condition), however, the increase was augmented to 130% when treated with LPA. These results confirmed that RhoA was a mediator for the function of hnRNP-Q1 in regulating actin filament dynamics.

hnRNP-Q1 acts as a trans-acting factor in regulating RhoA mRNA translation

Recent studies have shown that the expression and function of RhoA are also regulated at the mRNA level (Wu et al., 2005). Posttranscriptional modulation of gene expression is an essential mechanism for the proper functions of many proteins. For instance, the expression level of a protein can be regulated by the efficiency of mRNA incorporation into polysomes (Deng et al., 2008; Huttelmaier et al., 2005; Kim et al., 2009) and the level of mRNA through selective stabilization or destabilization (Ruggiero et al., 2007; Wang et al., 2000). In addition, spatial and temporal expression of certain

proteins can be regulated by asymmetrical distribution of their corresponding transcripts and the subsequent local translation (Martin and Ephrussi, 2009). In developing neurons, certain mRNAs encoding proteins enriched or functioning in growth cones are selectively localized and locally translated in this compartment (Taylor et al., 2009; Vogelaar et al., 2009; Willis et al., 2007). RhoA mRNA is one such mRNA (Vogelaar et al., 2009; Wu et al., 2005). Stimulating neurons with Semaphorin triggers the local translation of RhoA mRNA in growth cones, which mediates Semaphorin-induced growth cone collapse (Wu et al., 2005). Asymmetrical mRNA localization is a result of recruitment of mRNAs and their associating RNA binding proteins into transport mRNP granules, in which mRNAs are translationally dormant (Kiebler and Bassell, 2006; Martin and Ephrussi, 2009). Yet, RNA binding proteins in association with RhoA mRNA that might regulate its localization and translation have been unexplored. In this study, we found that RhoA mRNA was selectively enriched in hnRNP-Q1 immunoprecipitation pellets. Our results show that knockdown of hnRNP-Q1 in C2C12 cells and primary fibroblast cells results in an upregulation of RhoA protein. The effect is unlikely to be a consequence of enhanced transcription, since we did not observe an increase in RhoA mRNA level in these cells. Instead, the level of RhoA mRNA was reduced in cells transfected with hnRNP-Q1 siRNA. We hypothesized that hnRNP-Q1 negatively regulates RhoA mRNA translation and the loss of hnRNP-Q1 would lead to enhanced translation. As demonstrated by polysome profiling experiments, we found that RhoA mRNA was shifted into heavier polysome fractions in cells with hnRNP-Q1 knockdown, whereas the distribution of γ-actin mRNA was not affected. These results suggest that hnRNP-Q1 is a translational repressor for RhoA mRNA. The increased RhoA protein expression following hnRNP-

Q1 knockdown may cause enhanced RhoA activation, possibly by disrupting the balance between RhoA and inhibitory RhoA binding proteins. A similar effect was observed in smooth muscle cells, in which a moderate increase of RhoA protein leads to a dramatic increase of GTP-bound RhoA (Sawada et al., 2009).

The function of RNA binding proteins in translation repression has been reported previously (Deng et al., 2008; Huttelmaier et al., 2005; Li et al., 2001). For example, Zipcode binding protein 1 (Zbp1) has been demonstrated to be a translational repressor for β-actin mRNA (Huttelmaier et al., 2005). Zbp1 also mediates the localization of β-actin mRNA in neurons and fibroblasts (Eom et al., 2003; Ross et al., 1997; Zhang et al., 2001). The loss of ZBP1 results in impaired growth cone motility (Zhang et al, 2001) and dendrite spine formation (Eom et al, 2003). FMRP inhibits the translation of its associated mRNAs, such as PSD-95 and Map1b (Li et al., 2001; Muddashetty et al., 2007). Besides its function in translation, FMRP also mediate the transport and localization of their associated mRNAs (Dictenberg et al., 2008). The loss of FMRP results in an excess of spine-like protrusion along dendrites (Antar et al., 2006). In the current study, we focused on the novel role of hnRNP-Q1 in regulation of RhoA expression and cell morphology, but did not investigate its possible function in mRNA localization. However, such a function of hnRNP-Q1 has been suggested by previous studies. Kanai et al. identified hnRNP-Q1 as a component of transport mRNP granules in the central nervous system (Kanai et al., 2004) and hnRNP-Q1 was shown to be actively transported in neuronal processes (Bannai et al., 2004). Here we report the discovery of hnRNP-Q1 as a trans-acting factor of RhoA protein expression and signaling; further

work is needed to assess whether hnRNP-Q1 is also necessary for RhoA mRNA localization.

In this study, we reported that RhoA mRNA stability was reduced following hnRNP-Q1 knockdown. We reason that this effect is a consequence of enhanced RhoA mRNA translation, because reduced RhoA mRNA stability was abolished by treating cells with a translation inhibitor. The coupling of mRNA degradation with translation has been reported in two scenarios (Funakoshi et al., 2007; Grosset et al., 2000; Schiavi et al., 1994). In the first scenario, translation-coupled mRNA degradation is mediated through a RNA destabilizing element within the coding region, termed coding region instability determinant (CRD) (Grosset et al., 2000; Schiavi et al., 1994). CRD-containing mRNAs exhibit short half-lives and are rapidly degraded. c-fos and c-myc are two examples of mRNAs that exhibit CRD-mediated mRNA degradation (Bernstein et al., 1992; Grosset et al., 2000; Schiavi et al., 1994). In both cases, hnRNP-Q1 was identified as a functional factor in stabilizing these CRD-containing mRNAs (Grosset et al., 2000; Weidensdorfer et al., 2009). However, this is unlikely to be the mechanism for translation-coupled degradation of RhoA mRNA, because this mRNA is relatively stable although it associates with hnRNP-Q1. We think that the degradation of RhoA mRNA may fall into the second scenario, in which mRNA degradation is coupled to translation through translation releasing factors (eRF1 and eRF3) which link poly(A) tail shortening to translation termination (Funakoshi et al., 2007). Besides the function in releasing newly synthesized peptides, protein eRF3 directly associates with cytoplasmic poly(A) binding protein (PABPC1), which binds to the poly(A) tail of mRNAs (Cosson et al., 2002; Kononenko et al., 2009; Uchida et al., 2002). As demonstrated in a recent study, when a

ribosome reaches a stop codon, eRF1 is firstly recruited to the ribosomal A site, and subsequently GTP-bound eRF3, to accomplish their function in peptide releasing (Kononenko et al., 2008; Merkulova et al., 1999). In the mean time, the binding of eRF1 to GTP-eRF3 disrupts the interaction of eRF3 and PABPC1; consequently, PABPC1 recruits and activates Pan2-Pan3 poly(A) specific ribonuclease complex which catalyzes mRNA poly(A) tail shortening, an earlier step for mRNA degradation (Funakoshi et al., 2007). Our observation of the linkage of facilitated RhoA mRNA degradation and its enhanced translation provides a possible example for this mRNA degradation pathway, which may serves as a feedback mechanism for cells to restrict excessive protein production. In addition, the enhanced RhoA mRNA degradation in cells with hnRNP-Q1knockdown provides indirect evidence for the function of hnRNP-Q1 as a translation repressor for RhoA mRNA.

Our novel finding that hnRNP-Q1 regulates RhoA expression and cellular morphogenesis provides further motivation to study the underlying molecular mechanism. In addition, this work should motivate inquiry into the possible role of hnRNP-Q1 in other aspects of neuronal morphogenesis known to dependent on RhoA signaling, such as axon guidance and nerve regeneration (Gross et al., 2007; Li et al., 2004; Wu et al., 2005). Since hnRNP-Q1 directly interacts with SMN, it will be interesting to know whether aspects of hnRNP-Q1 function are altered in the condiction of deficiency of SMN which leads to spinal muscular atrophy. In fact, Bowerman et al. demonstrated that knockdown of SMN in PC12 cells upregulated RhoA protein expression and incurred defective cytoskeletal structures and neuritogenesis (Bowerman et al., 2007). Recently the same research group showed that blockage of the RhoA/ROCK

signaling pathway in a type of SMA mice by administrating the ROCK inhibitor, Y-27632, partially rescued developmental defects of neuromuscular junctions and effectively promoted the survival rate of this type of SMA mice (Bowerman et al., 2010). Such obversations encourage a further investivation for the functional link of SMN and RhoA regulation. A likely underlying mechanism could be that SMN may play a role in regulating RhoA expression through its interaction with hnRNP-Q1. Lastly, we anticipate that the development of mice deficient for hnRNP-Q1 would have a number of impairments in mRNA regulation needed for neuronal development, plasticity and repair.

Figures and Legends
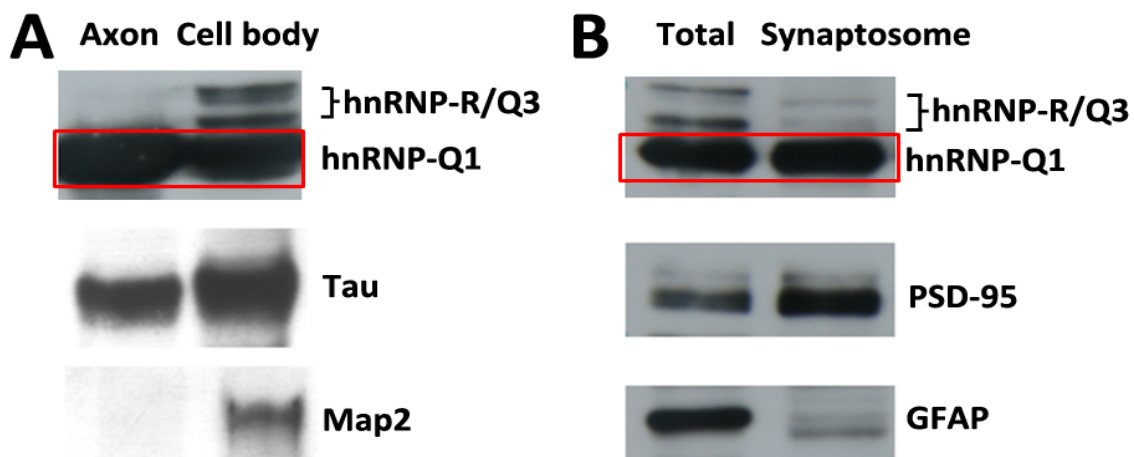
Figure 3-1. Western blot analysis of axonal fractions purified from cultured cortical neurons and synaptic fractions from brain. **(A)** Axonal fractions and **(B)** synaptosome fractions reacted with a pan-hnRNP-Qs/R antibody; boxed areas indicate hnRNP-Q1 specific signal. The purity of axonal fraction was tested by the presence of Tau but lack of Map2 signal; the enrichment of synaptic compartments was tested by the enrichment of PSD-95 and the limited contamination of glial cell protein, GFAP.

A

```
hnRNP-Q1  P-GSARGVRGARGG-AQQQRGRGVKGVEAG----------------PDLLQ--------  561
hnRNP-Q3  P-GSARGVRGARGG-AQQQRGRGVRGARGGRGGNVGGKRKADGYNQPDSKRRQTNNQ-NW  585
hnRNP-Q2  P-GSARGVRGARGG-AQQQRGRGVRGARGGRGGNVGGKRKADGYNQPDSKRRQTNNQ-NW  550
hnRNP-R   PLGPPRGSRGGRGGPAQQQRGRGSRGSRGNRGGNVGGKRKADGYNQPDSKRRQTNNQQNW  597
          * *..** **.*** ******** :* ...                    **  :

hnRNP-Q1  ------------------------------------------
hnRNP-Q3  GSQPIAQQPLQ-GGDHSGNYGYKSENQEFYQDTFGQQWK  623
hnRNP-Q2  GSQPIAQQPLQ-GGDHSGNYGYKSENQEFYQDTFGQQWK  588
hnRNP-R   GSQPIAQQPLQQGGDYSGNYGYNNDNQEFYQDTYGQQWK  636
```

B

EGFP-hnRNP-Q1

hnRNP-Q1

C

hnRNP-Q1   Map2   Phase DAPI

D

hnRNP-Q1   Tau   Phase DAPI

E

hnRNP-Q1
α-Tubulin
F-actin

a

Figure 3-2. Localization of hnRNP-Q1 granules in neuronal processes and growth cones.

(A) An hnRNP-Q1-specific antibody to the C-terminal sequence (underlined in red) was generated. **(B)** Anti-hnRNP-Q1 antibody specifically recognizes both endogenous and over-expressed hnRNP-Q1. **(C, D)** Immunofluorescence staining of cultured mouse hippocampal neurons shows that hnRNP-Q1 protein exists in granules localized in both dendrites **(C)** and axons **(D)**, as identified by staining with Map2 and Tau-specific antibodies, respectively. Nuclei were highlighted by DAPI staining. **(E)** hnRNP-Q1 granules were detected in growth cones of primary cultured mouse hippocampal neurons. Enlarged boxed area **(a)** shows the microtubule association of hnRNP-Q1 granules. Scale bar, 10µm.
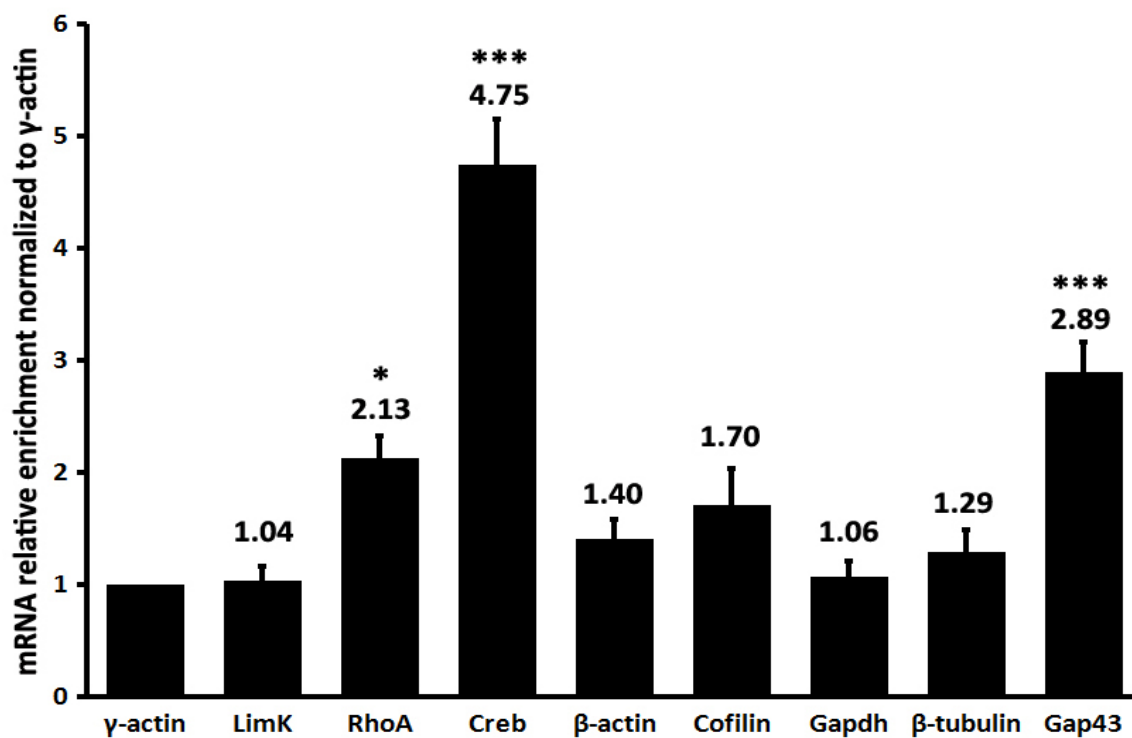
Figure 3-3. Selective enrichment of mRNAs in immunoprecipitated Flag-mCherry-hnRNP-Q1 containing complexes. Flag-mCherry-hnRNP-Q1 and Flag-mCherry were overexpressed in Neuro2a cells and immunoprecipitated with agarose beads conjugated with mouse anti-Flag antibodies. Levels of indicated mRNAs were quantified by qRT-PCR and normalized to input. All mRNAs were enriched in Flag-mCherry-hnRNP-Q1 pellets compared with Flag-mCherry. To assess whether some mRNAs were selectively enriched, levels of each mRNA was normalized to γ-actin mRNA. As shown in this figure, RhoA, Creb, and Gap43 mRNA were enriched in Flag-mCherry-hnRNP-Q1 at a higher extent with statistical significance (One-way ANOVA followed by Tukey HSD, three experiments, $*p<0.05$, $***p<0.001$); these mRNA have been reported as being localized to the neuronal growth cone.

control siRNA

control siRNA + Y-27632

hnRNP-Q1 siRNA

hnRNP-Q1 siRNA + Y-27632
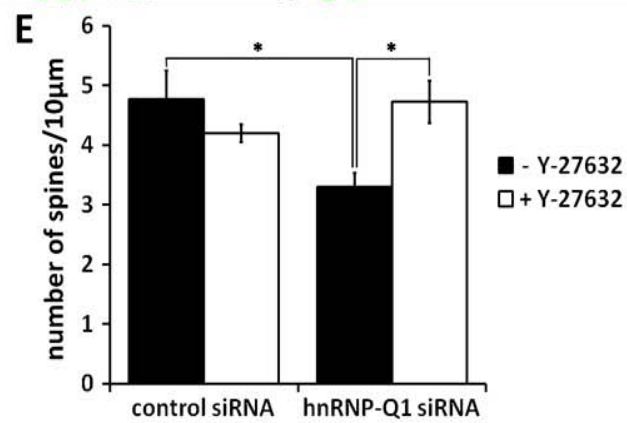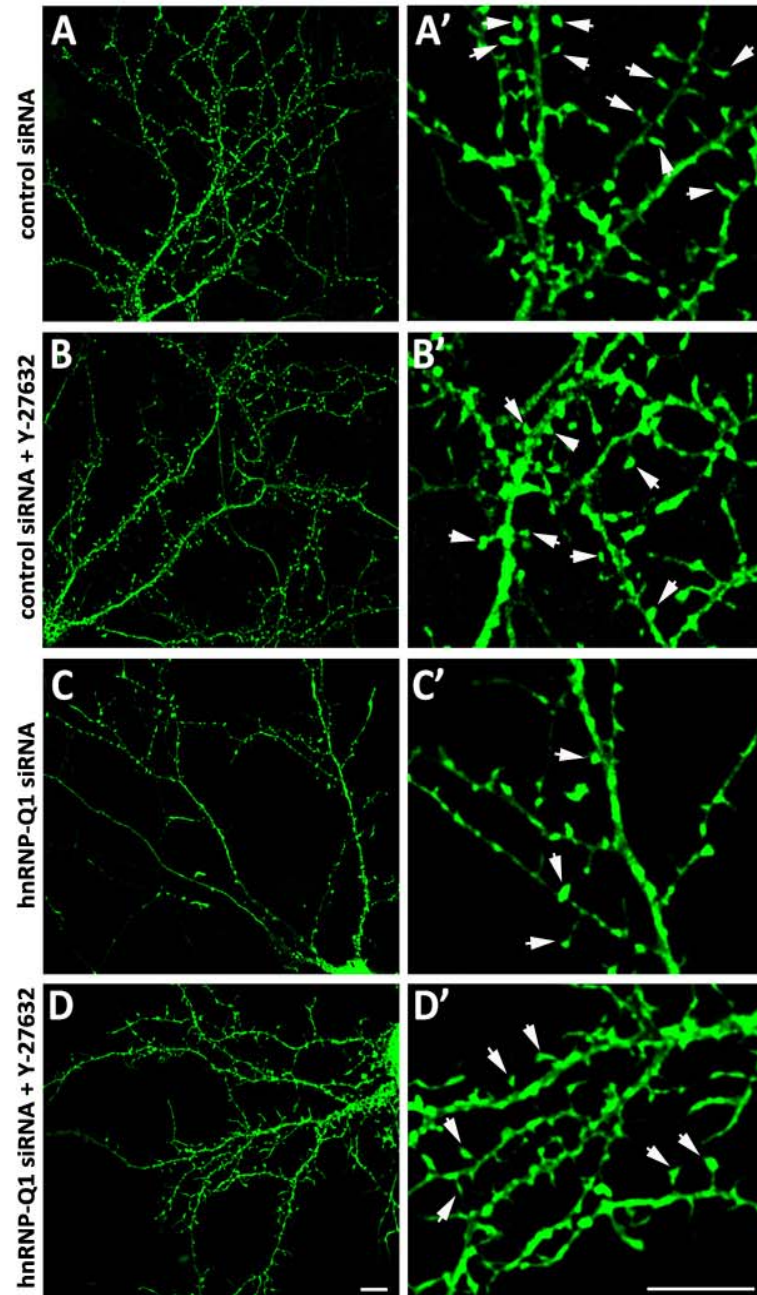
Figure 3-3. hnRNP-Q1 knockdown leads to reduced spine density of mature mouse hippocampal neurons. To knockdown hnRNP-Q1, high density hippocampal neurons were transfected with siRNA at DIV9 and DIV12 for a two round siRNA delivery. In the second round of transfection, an EGFP expressing plasmid was co-transfected to mark fine structures of individual neurons. Representative examples show control siRNA **(A and B)** and hnRNP-Q1 siRNA **(C and D)** transfected EGFP-positive neurons. The corresponding higher magnification images are shown in **(A'-D')**. Images of panel **(B and B')** and **(D and D')** represent Y-27632 treated neurons transfected with control siRNA and hnRNP-Q1 siRNA, respectively. **(E)** Quantitative analysis of dendritic spine density of control and hnRNP-Q1 siRNA transfected neurons treated with or without Y-27632. Neurons transfected with control siRNA transfected had an average spine density of 4.8 spines/10µm (33 neurons, 3 experiments). Neurons transfected with hnRNP-Q1 siRNA exhibit reduced spine density with 3.3 spines/10µm (28 neurons, three experiments). Such reduction is recovered by Y-27632 treatment to the level of control cells with 4.7 spines/10µm (18 neurons, three experiments). The spine density of control neurons is slightly reduced to 4.2 spines/10µm (33 neurons, three experiments), which is not statistically significant to non-treated cells (p=0.26). Statistical analysis, one-way ANOVA followed by Tukey HSD, *p<0.05. Scale bar, 10µm. (Contributed by Xiaodi Yao)
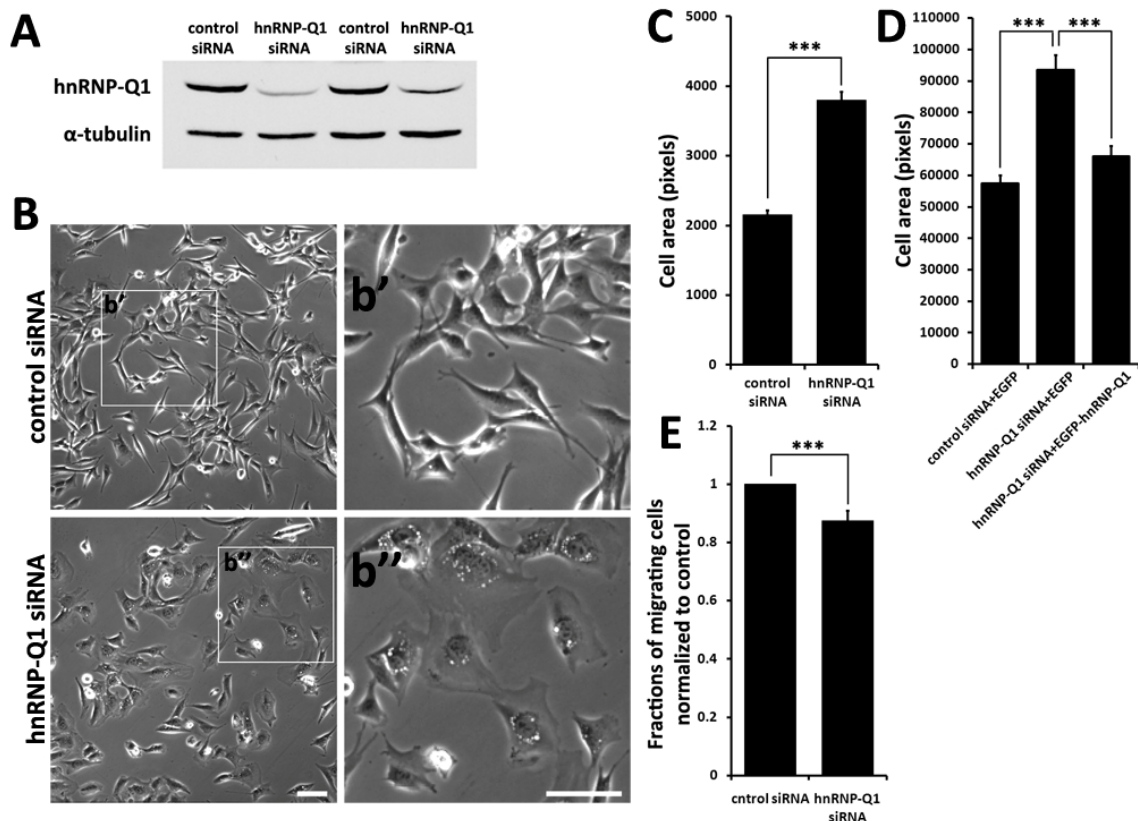
Figure 3-5. Knockdown of hnRNP-Q1 in C2C12 cells by RNAi leads to enhanced cell spreading and reduced motility. **(A)** Western blot analysis of C2C12 cell lysate 72 hours post siRNA transfection showing efficient hnRNP-Q1 knockdown. **(B)** Knockdown of hnRNP-Q1 enhances C2C12 cell spreading. Enlarged boxed areas are shown in **(b' and b'')**. **(C)** Quantification of cell area 72 hours post siRNA transfection (230 to 250 cells total from 3 experiments for each condition; student t-test, *** $p<0.005$). Images were acquired with a 10X objective. **(D)** Re-expression of EGFP-hnRNP-Q1 in hnRNP-Q1 siRNA transfected cells rescues cell area changes (One-way ANOVA followed by Tukey HSD, ***$p<0.001$). Images were acquired with a 60X objective to enable the detection of EGFP signals. **(E)** Trans-well migration assay demonstrated reduced motility of C2C12 cells after hnRNP-Q1 knockdown (4 experiments; student t-test, ***$p<0.005$). Scale bar, 50μm.
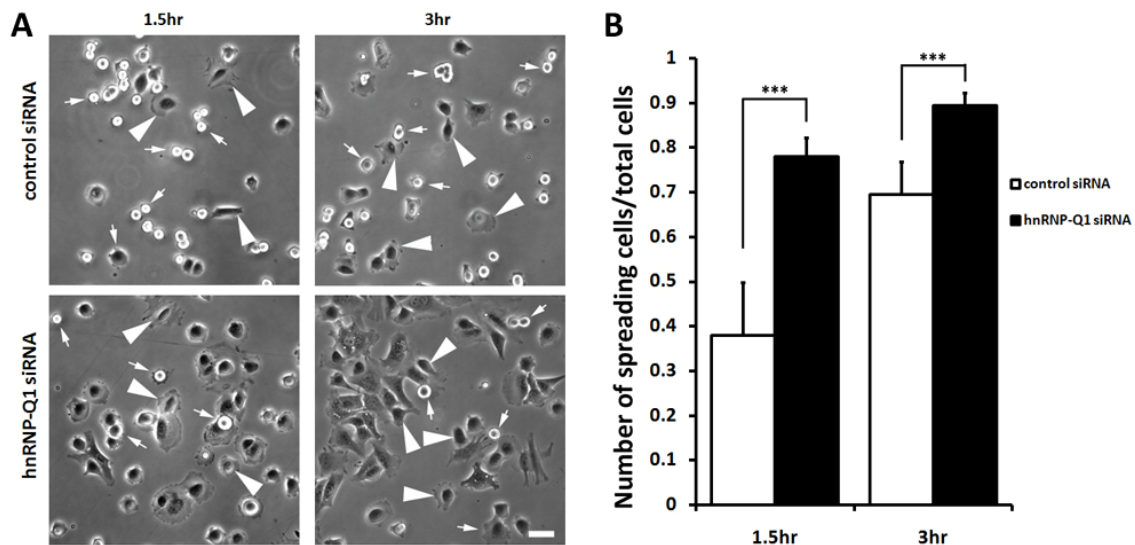
Figure 3-6. hnRNP-Q1 knockdown leads to enhanced spreading of newly plated C2C12 cells. C2C12 cells transfected with hnRNP-Q1 or control siRNAs for 72 hours were trypsinized and replated onto coverslips. Cells were imaged at 1.5 or 3 hours after plating. Ten random fields were imaged at each time point for each condition. Spreading cells were characterized by the presence of lamella over one cell body size. Total number of cells and spreading cells in each image were counted. **(A)** Representative images for each condition and time point. Examples of non-spreading cells and spreading cells were indicated by arrows and arrowheads, respectively. Scale bar, 50μm. **(B)** Quantification of spreading C2C12 cells. Numbers represent ratios of spreading cells to total number of cells (Student t-test, ***$p < 0.001$, three experiments). Scale bar. 50μm.
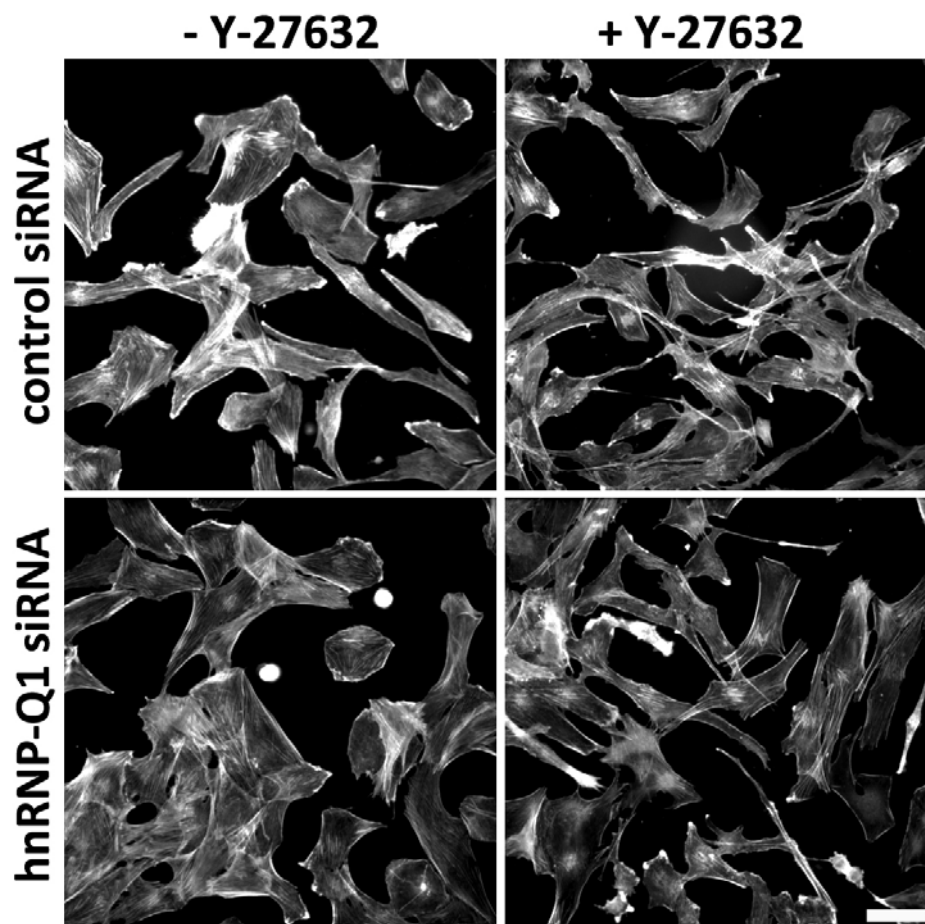
Figure 3-7. Effects of ROCK inhibitor Y-27632 on the morphology of C2C12 cells transfected with control and hnRNP-Q1 siRNA. Three days after siRNA transfection, cells were treated with 10μM ROCK inhibitor Y-27632 for 16 hours and fixed for phalloidin staining to highlight cell morphology. Treatment with Y-27632 induces similar cell morphology changes on both control siRNA and hnRNP-Q1 siRNA transfected cells; these cells exhibit an elongated cell shape and tail-like processes. Scale bar, 50μm.
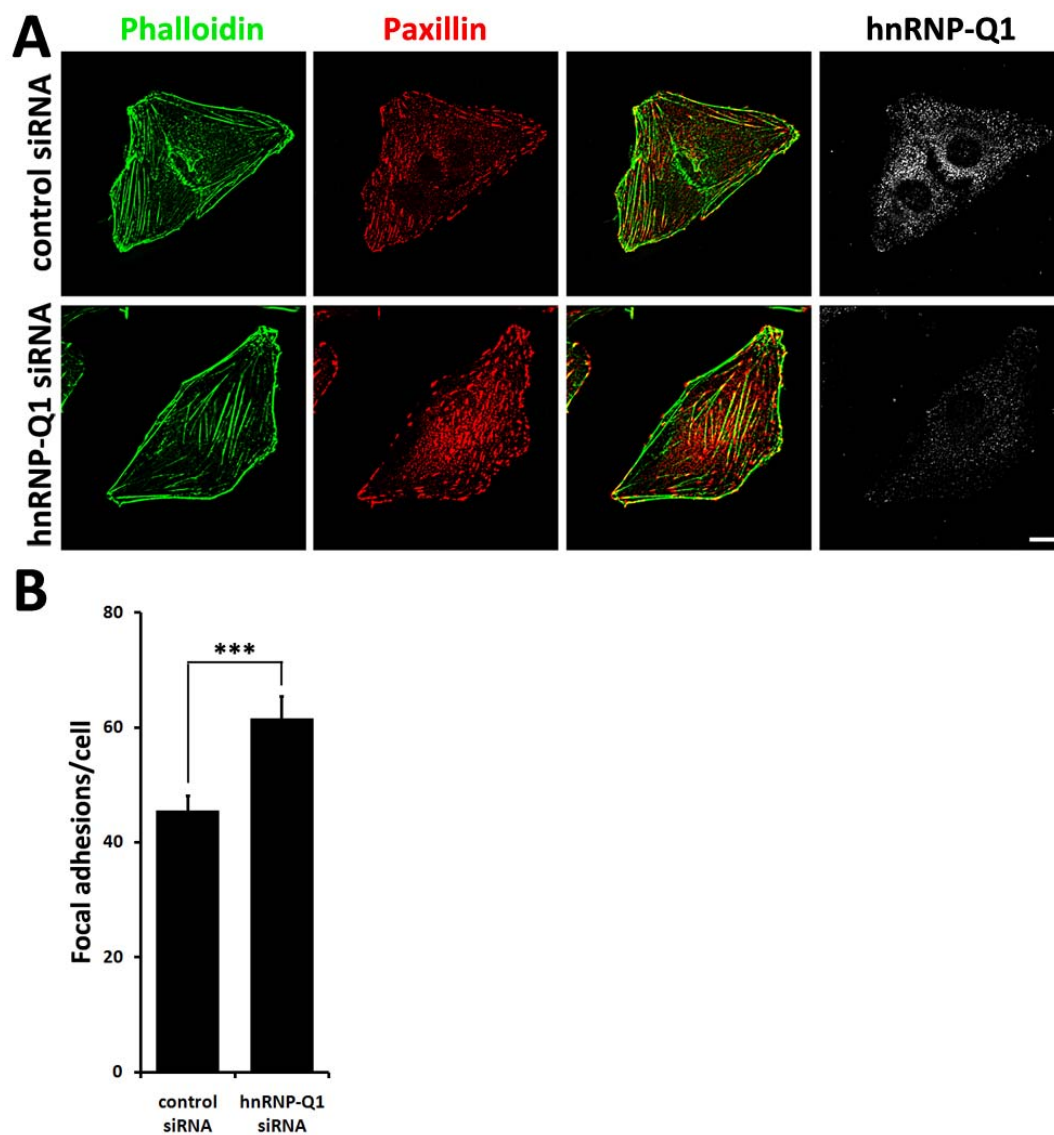
Figure 3-8. hnRNP-Q1 knockdown leads to enhanced focal adhesion and stress fiber formation. **(A)** Representative images of Paxillin immunofluorescence staining for focal adhesions and Phalloidin staining for actin filaments in C2C12 cells treated with control or hnRNP-Q1 siRNA. Scale bar, 10μm. **(B)** Quantification of number of focal adhesions in C2C12 cells transfected with control and hnRNP-Q1 siRNA (3 experiments, 80 to 90 cells total for both conditions; student t-test, ***p<0.005).
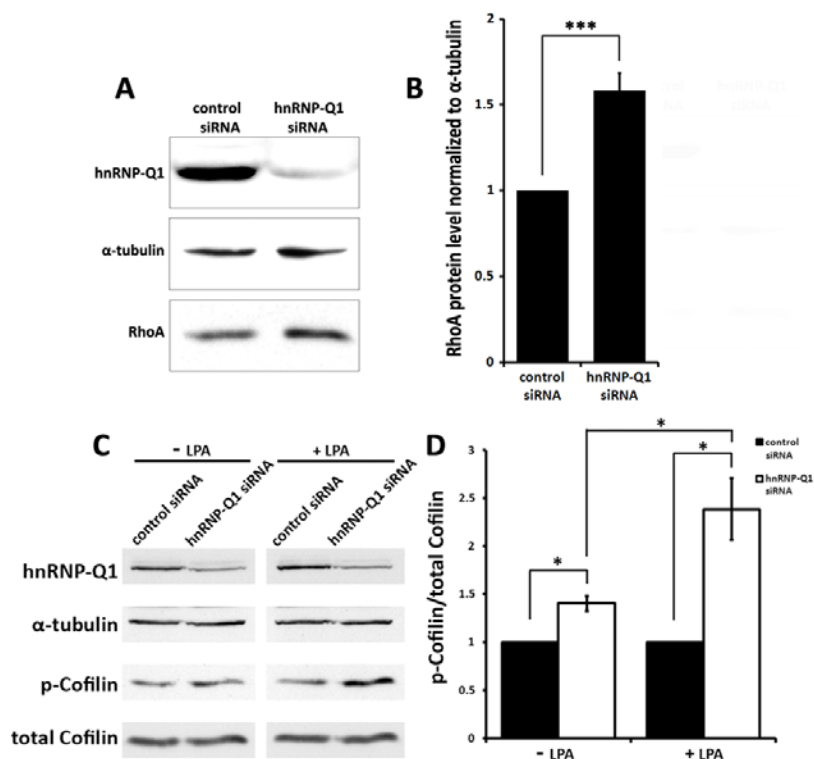
Figure 3-9. hnRNP-Q1 knockdown upregulates RhoA protein expression and Cofilin phosphorylation. **(A, B)** Knockdown of hnRNP-Q1 led to upregulated RhoA protein expression in C2C12 cells. RhoA protein levels were quantified by densitometric analysis and normalized to α-tubulin. A 50% increase of RhoA protein was observed after a 72 hour treatment with hnRNP-Q1 siRNA (5 experiments, *** $p<0.005$). Representative western blot is shown as **(A)**. **(C, D)** Western blot analysis of Cofilin phosphorylation in hnRNP-Q1 siRNA and control siRNA transfected cells treated with or without the RhoA activator, LPA. **(D)** Quantitative analysis of the levels of phospho-Cofilin by normalizing to total Cofilin. Without LPA treatment, a 40% of increase of phospho-Cofilin was obtained in cells transfected with hnRNP-Q1 siRNA. LPA treatment had a stronger effect on hnRNP-Q1 siRNA transfected cells with 130% more phospho-Cofilin than control cells (3 experiments; one-way ANOVA followed by Tukey HSD, *$p<0.05$).
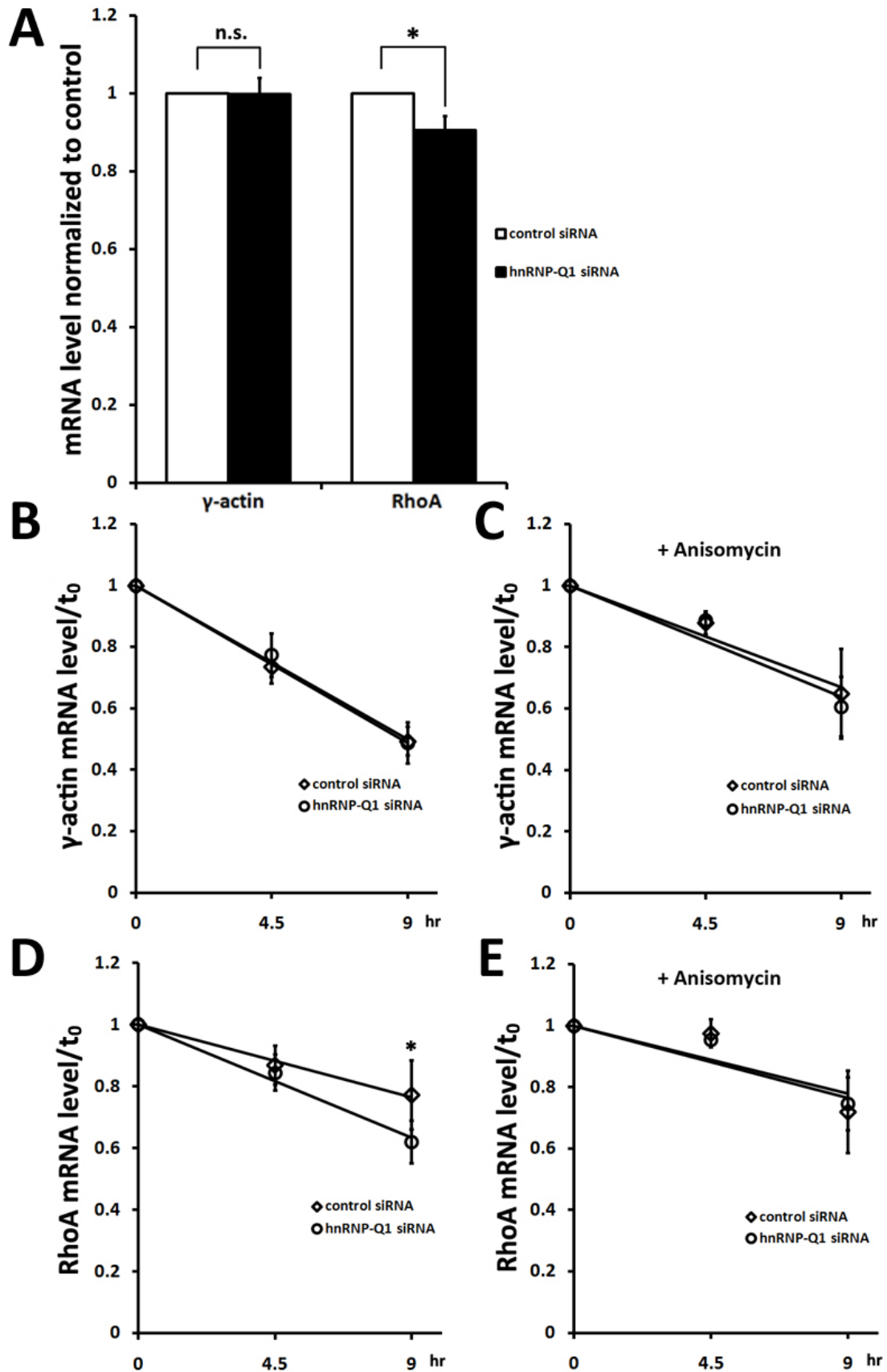
Figure 3-10. Knockdown of hnRNP-Q1 leads to exaggerated RhoA mRNA degradation.

(A) Reduced RhoA mRNA level in hnRNP-Q1 knockdown cells (10 experiments; student t-test, *p<0.05). **(B-E)** γ-actin and RhoA mRNA decay in C2C12 cells transfected with control or hnRNP-Q1 siRNA. Total RNA was collected at 0 hr, 4.5 hr and 9hr after Actinomycin-D treatment to block transcription. mRNA levels were measured by qRT-PCR with gene-specific primers. The mRNA levels remaining at 4.5 hour and 9 hour were normalized to the level at 0 hour and calculated as $2^{-\Delta Ct}$. Neither hnRNP-Q1 knockdown **(B)** nor treatment with anisomycin **(C)** has an effect on γ-actin mRNA degradation. **(D)** hnRNP-Q1 knockdown incurs facilitated RhoA mRNA decay (3 experiments; paired student t-test, *p<0.05). **(E)** Treatment of cells with anisomycin (translational inhibitor) eliminated the change of mRNA stability caused by hnRNP-Q1 knockdown. (3 experiments, not statistically significant).
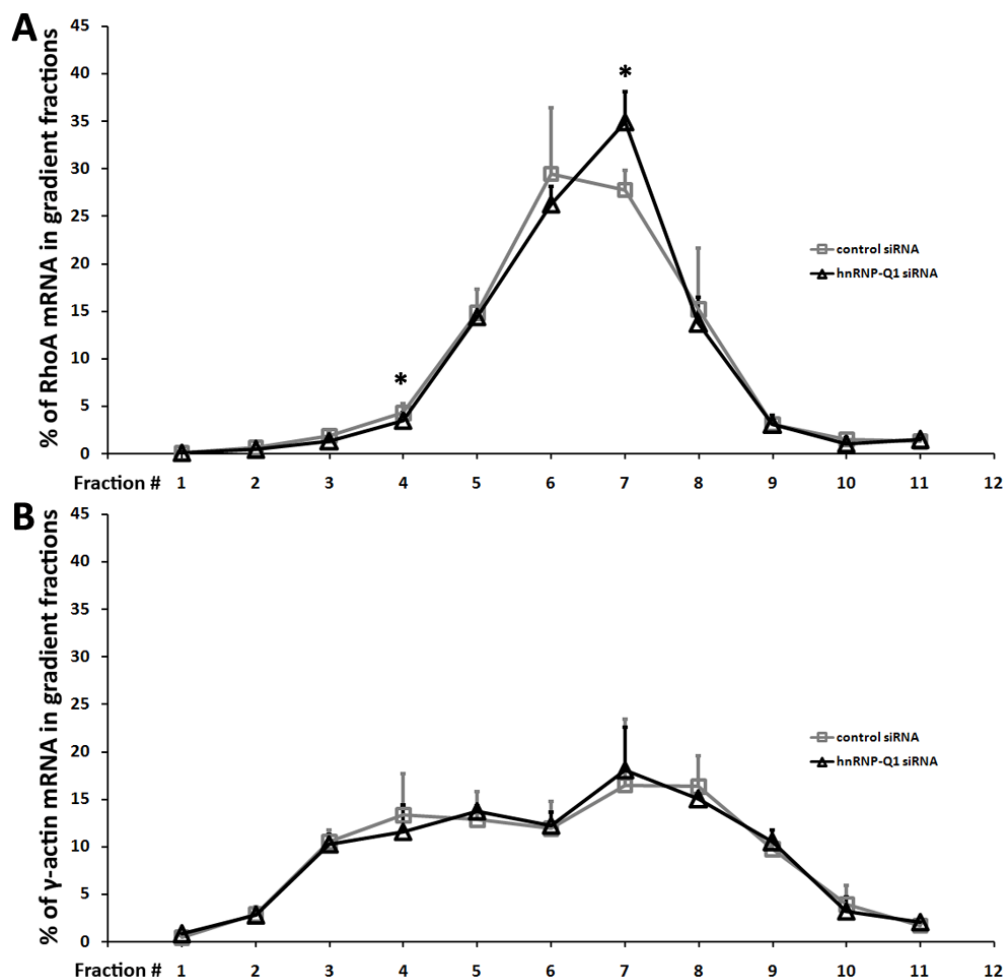
Figure 3-11. Distribution of RhoA and γ-actin mRNAs in linear sucrose gradients. Polysome profiles were resolved in a 15-45% linear sucrose gradient with ultracentrifugation. Each gradient was collected as 11 factions with 1ml/each. mRNA level in each fraction was measure by qRT-PCR. A one fraction shift of RhoA mRNA peak into heavier polysomes was observed in C2C12 cells with hnRNP-Q1 knockdown **(A)** (3 experiments, $*p<0.05$, paired student t-test). The distribution of γ-actin mRNA from the same experimental condition was not changed **(B)**.

Supplemental Figures
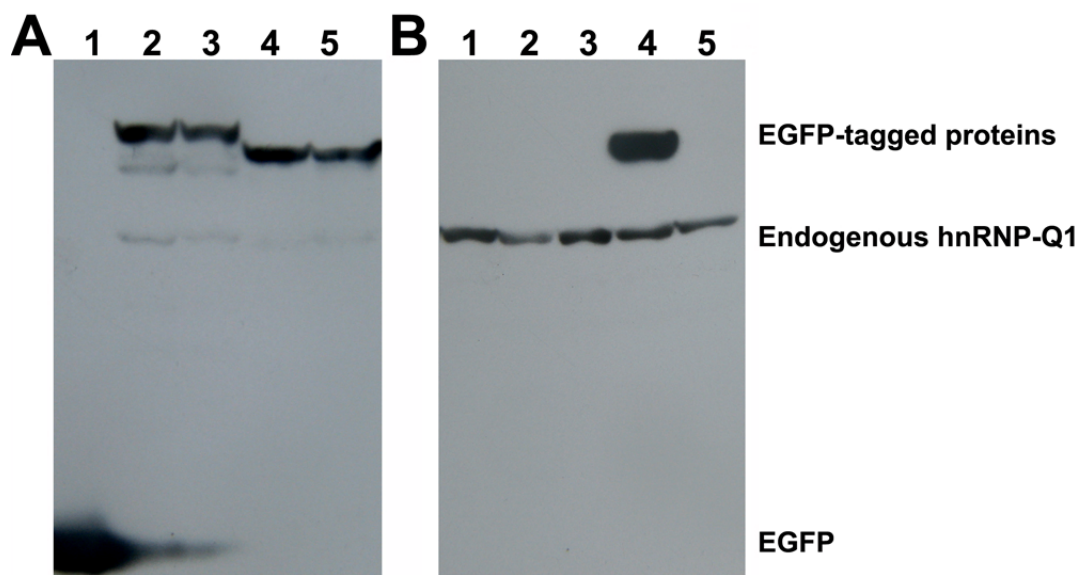
Supplemental Figure 3-1. Western blot analysis of overexpressed EGFP-tagged hnRNP-R, hnRNP-Q3, hnRNP-Q1 and hnRNP-Q1 with C-terminus deletion with hnRNP-Q1 specific antibodies. 293 cell lysate containing overexpressed EGFP (lane1), EGFP-hnRNP-R (lane2), EGFP-hnRNP-Q3 (lane3), EGFP-hnRNP-Q1 (lane4) and EGFP-hnRNP-Q1 C (lane5) were resolved by SDS-PAGE and probed with mouse anti-GFP **(A)** or rabbit anti-hnRNP-Q1 **(B)** antibodies. The hnRNP-Q1 antibody does not show cross-reaction to hnRNP-R and hnRNP-Q3 and the epitope is specific to the C-terminal sequence of hnRNP-Q1.
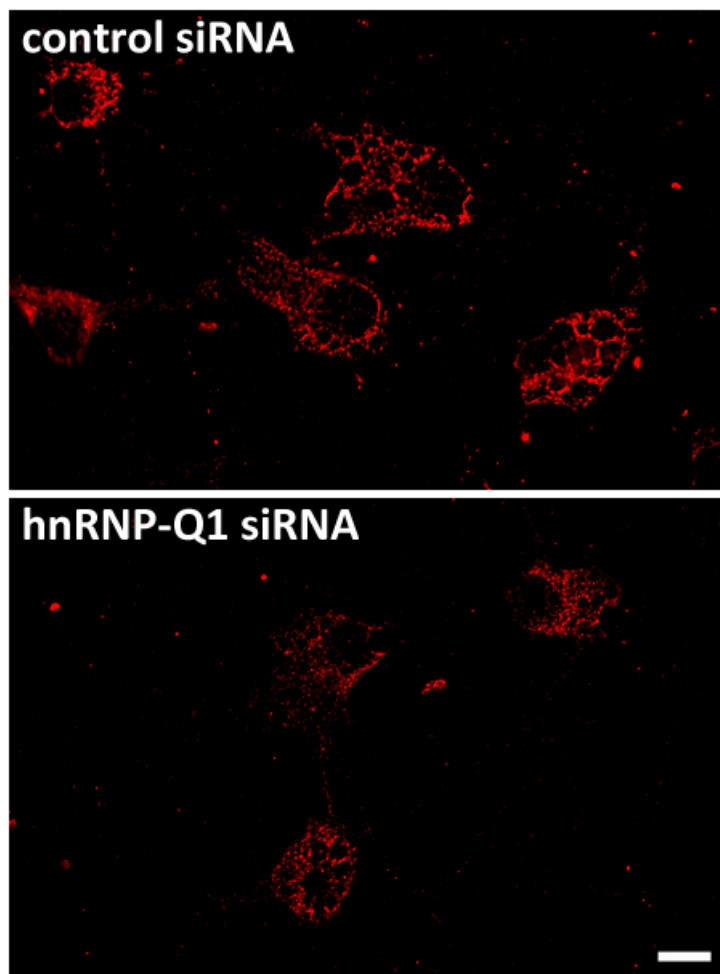
Supplemental Figure 3-2. Efficient knockdown of hnRNP-Q1 in mature mouse hippocampal neurons by RNAi. Four days after siRNA transfection, neurons were fixed and stained with rabbit anti-hnRNP-Q1 antibodies. Majority of neurons transfected with hnRNP-Q1 siRNA **(B)** exhibit reduced hnRNP-Q1 fluorescent signal compared with control siRNA transfected neurons **(A)**. Scale bar, 10μm.
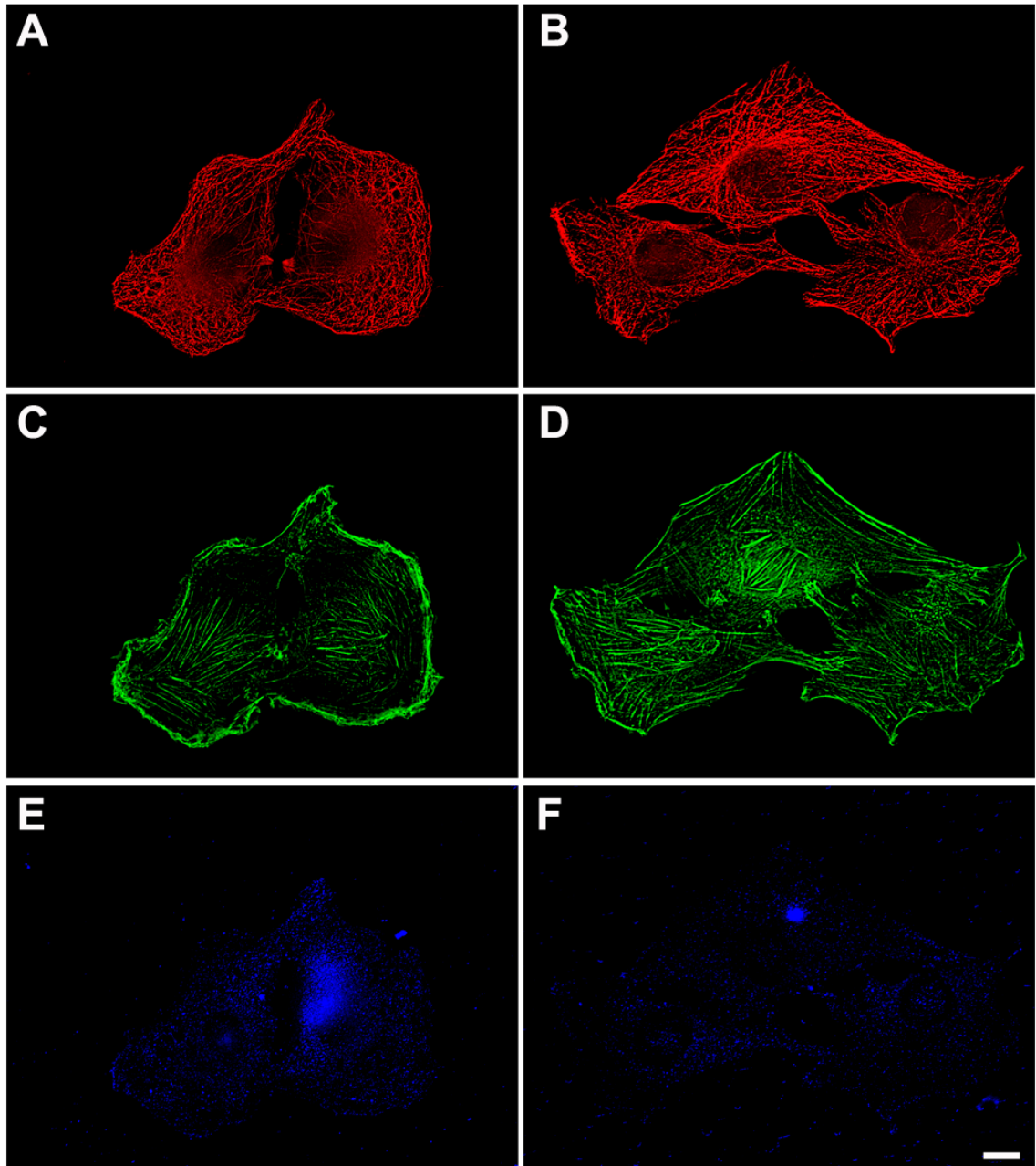
Supplemental Figure 3-3. Knockdown of hnRNP-Q1 in C2C12 cells has no obvious effect on microtubules. C2C12 cells transfected with control siRNA **(A, C and E)** and hnRNP-Q1 siRNA **(B, D and F)** were stained with anti-tubulin antibodies **(A and B)**, Phalloidin **(C and D)** and anti-hnRNP-Q1 antibodies **(E and F)** to visualize microtubules, F-actin filaments, and hnRNP-Q1. Scale bar, 10µm.
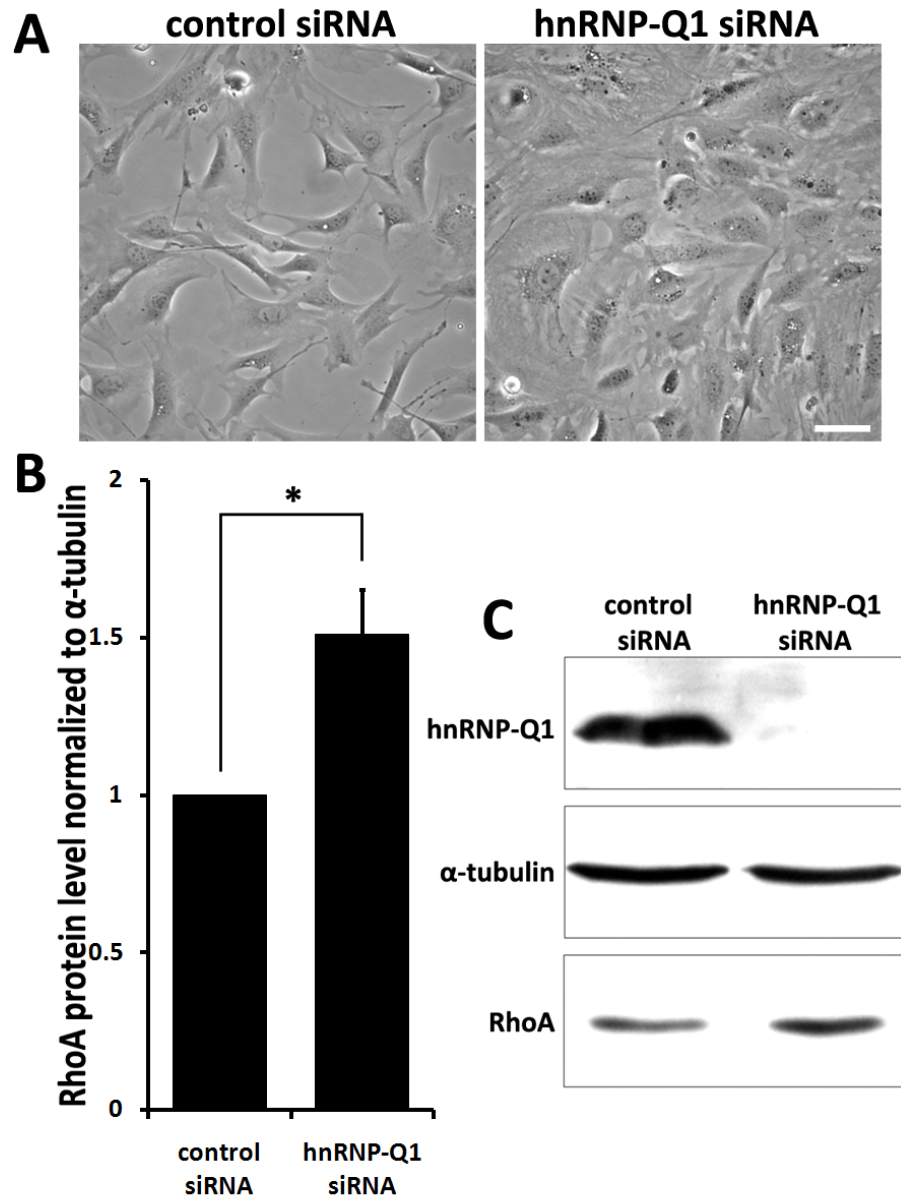
Supplemental Figure 3-4. Enhanced cell spreading **(A)** and upregulated RhoA expression **(B, C)** in primary mouse embryonic fibroblasts with hnRNP-Q1 knockdown. (3 experiments; student t-test, *p<0.05). Scale bar, 50μm.
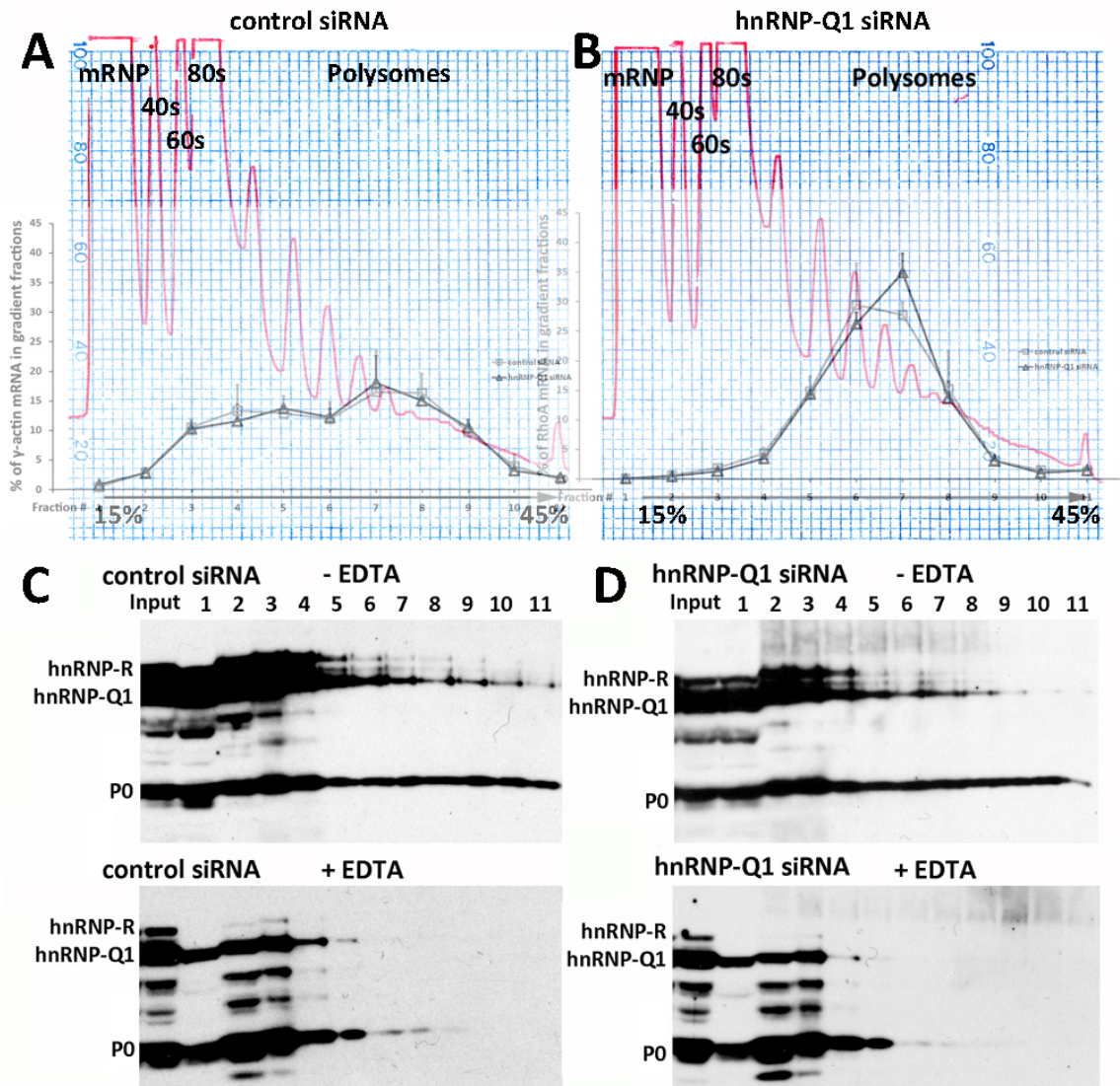
Supplemental Figure 3-5. hnRNP-Q1 knockdown did not affect overall polysome profiles. **(A, B)** Representative 254nm absorbances of a 15 to 45% linear sucrose gradient loaded with cell lysate prepared from C2C12 cells transfected with control or hnRNP-Q1 siRNAs. **(C, D)** Western blot analysis of the distribution of ribosomal P0 protein and hnRNP-Qs/R in fractionated sucrose gradients shows that knockdown of hnRNP-Q1 has no effect on overall polysome formation. EDTA treatment eliminated polysome localization of P0 protein in both conditions, as shown in the lower panels.

Chapter IV

Microscopic analysis and biochemical characterization of hnRNP-Q1-containing mRNP granules

Introduction

The specific association of mRNA with RNA binding proteins and their dynamic exchange between different mRNP granules are important factors for precise mRNA regulation, such as mRNA localization, mRNA translation and degradation (Anderson and Kedersha, 2008; Balagopal and Parker, 2009; Besse and Ephrussi, 2008; Kiebler and Bassell, 2006; Martin and Ephrussi, 2009). In eukaryotic cells, apart from being actively translated in polysomes, translationally silenced mRNAs and their associated RNA binding proteins are present in functionally distinct granules, including mRNP granules, stress granules and processing bodies (P-bodies) **(Chapter I, Figure 1-1)** (Balagopal and Parker, 2009; Kiebler and Bassell, 2006). Particularly in polarized cells such as migrating primary fibroblast cells and neurons, certain mRNP granules are actively transported leading to asymmetrical distribution of mRNAs (Besse and Ephrussi, 2008; Martin and Ephrussi, 2009). These granules are termed transport mRNP granules, in which RNA binding proteins mediate the association of localized mRNAs with molecular motors (Singer, 2008). Stress stimuli such as oxidative stress induce individual mRNP granules to fuse into large mRNP aggregates named stress granules, which are postulated as sites for mRNP storage and remodeling or sorting (Balagopal and Parker, 2009). The functions of P-bodies have been linked to mRNA degradation and miRNA-mediated translation repression. Enzymatic and structural proteins functioning in mRNA degradation, such as decapping proteins Dcp1a and Dcp2, Xrn1 exoribonuclease, Sm protein-like protein (LSm) 1-7 and proteins involved in miRNA-mediated mRNA degradation and translational repression, such as GW182 and Agronate2, are enriched in P-bodies (Franks and Lykke-Andersen, 2008; Parker and Sheth, 2007).

hnRNP-Qs and hnRNP-R compose a family of RNA-binding proteins which share more than 80% similarity of amino acid sequences (Mourelatos et al., 2001; Rossoll et al., 2002). The human *hnrnp-q* gene encodes three hnRNP-Q isoforms, including hnRNP-Q1, Q2 and Q3, due to alternative splicing; whereas only hnRNP-Q1 and Q3 were identified in mouse cells. All hnRNP-Q isoforms and hnRNP-R contain three RNA-recognition-motifs (RRMs) and one arginine-glycine rich (RGG) domain for RNA binding and/or protein-protein interaction **(Supplemental Figure 4-1)**.

Recent overexpression studies show that hnRNP-Q1 is localized to the cytoplasm, whereas hnRNP-Q2 and Q3 are mainly localized to the nucleus (Chen et al., 2008). Their differential subcellular distribution suggests that some functions of each protein may be different. By yeast-two hybridization and co-immunoprecipitation analyses, hnRNP-Qs and R have been shown to directly interact with Survival of Motor Neuron protein (SMN) (Mourelatos et al., 2001; Rossoll et al., 2002). The reduced expression or loss of function of SMN causes Spinal Muscular Atrophy (SMA), a recessive inherited motor neuron degenerative disease (Burghes and Beattie, 2009). SMN forms protein complexes with Gemin proteins (Gemin 2-8) and Unrip, such protein complexes facilitate the assembly of spliceosomes, a family of small nuclear RNPs (snRNPs) composed of uridine-rich small RNAs and Sm proteins (Battle et al., 2006a; Burghes and Beattie, 2009; Kolb et al., 2007). hnRNP-Qs and R are believed to be spliceosome-associated proteins due to their interaction with SMN and their direct involvement in pre-mRNA splicing (Chen et al., 2008; Mourelatos et al., 2001); the immunodepletion of hnRNP-Qs and R leads to less efficient pre-mRNA splicing (Mourelatos et al., 2001). However, the role of different hnRNP-Q isoforms in splicing may be different. In fact, one study shows that the

inclusion of exon7 in the mature transcript of *SMN2* gene is differentially regulated by hnRNP-Q1 and hnRNP-Q3 (Chen et al., 2008). In addition, studies shows that hnRNP-Q3 interacts with APOBEC1 and plays a role in RNA editing in the nucleus (Blanc et al., 2001), whereas the functions of hnRNP-Q1 is connected to mRNA transport (Bannai et al., 2004; Kanai et al., 2004) and regulation of mRNA stability in the cytoplasm (Grosset et al., 2000; Weidensdorfer et al., 2009). Our results show that hnRNP-Q1 is localized to both axons and dendrites and negatively regulates RhoA mRNA translation **(Chapter III, Figure 3-1. 3-2, 3-9 and 3-11)**. Moreover, hnRNP-Q1 is also involved in internal ribosomal entry site (IRES) mediated translation initiation (Cho et al., 2007; Kim et al., 2007). These observations for hnRNP-Q1 suggest that hnRNP-Q1 may be localized to different mRNP granules whereby it fulfills its diverse functions in mRNA regulation.

In this study, we analyzed the subcellular distribution of endogenous hnRNP-Qs and R and confirmed that in contrast to hnRNP-Q3 and R, hnRNP-Q1 was mainly localized to the cytoplasm. We further characterized the nature of hnRNP-Q1-containing mRNP-granules and found that hnRNP-Q1was localized to transport mRNP granules, stress granules and P-bodies. Besides, we found that hnRNP-Q1 interacting protein SMN was localized to stress granules as described previously (Hua and Zhou, 2004) but not P-bodies. We then determined the RGG domain of hnRNP-Q1 was necessary and sufficient for its interaction with Dcp1a and all three RRM domains and the RGG domain were required for its RNA binding ability. Besides, we also examined the P-body localization of several other RNA binding proteins which are components of mRNP granules, including Zbp1, HuD, FMRP, Pumilio2 and PABPC1. We uncovered an RNA-independent interaction of these RNA binding proteins and P-body proteins, Dcp1a and

LSm1. Our results suggest that interaction of hnRNP-Q1 and Dcp1a and LSm1 may play an essential role for the functions of hnRNP-Q1 in mRNA regulation in the cytoplasm.

Materials and Methods

Cell culture and treatments

293T, Neuro2a neuroblastoma and COS7 were maintained in DMEM with 10% FBS, 100U/ml penicillin and 100mg/ml of streptomycin at 5% CO_2 and 37ºC according to general cell culture procedures. To induce stress granules, 293T and COS7 were treated with 5mM sodium arsenate for 30 minutes before fixation for immunofluorescence staining.

Primary mouse hippocampal neurons were cultured as described previously (Antar et al., 2006). Embryonic hippocampi were dissected from E16 mouse embryos and trypsinized with 0.25% trypsin for 10 minutes. Cells were triturated in MEM with 10% FBS and plated on nitric acid-treated coverslips coated with poly-L-lysine. Two hours after plating, cell culture medium was changed to Neurobasal (Invitrogen) supplemented with B27 and Glutamax (Invitrogen).

Fluorescent protein reporter constructs and plasmid transfection

Full-length cDNAs of human hnRNP-R, PABP, Dcp1a and LSm1 were obtained by RT-PCR from total RNA extracts of HEK 293 cells, and inserted into pEGFP-C1 vector or other fluorescent protein (mRFP and 3XFlag-mCherry) vectors. All constructs were confirmed by DNA sequencing. Pumilio2 construct was provided by Dr. Michael Kiebler (Vessey et al., 2006) and hnRNP-Q3 was provided by Dr .Wilfried Rossoll

(Rossoll et al., 2002). Truncated hnRNP-Q1 constructs were generated by PCR from EGFP-hnRNP-Q1 plasmid (**Chapter II**).

Cells were transfected with Lipofectamine 2000 (Invitrogen) according to the manufacturer's protocol using half of the recommended amount of plasmid and transfection reagent.

<u>Antibodies and indirect immunofluorescence staining</u>

The following antibodies were used for immunofluorescence staining or western blot analysis in this study. Rabbit anti-Zbp1 (1:2000, provided by Dr. Robert Singer); rabbit anti-PABP (1:200, provided by Dr. Jurgen Brosius); mouse anti-FMRP (1:500, provided by Dr. Jennifer Dranell); rabbit anti-DDX6 (1:1000, provided by Dr. Wayne Sossin); mouse anti-Flag (M2, 1:3000, Sigma-Aldrich); mouse anti-Myc (9E10, 1:3000, Sigma-Aldrich); mouse anti-GFP (Jl-8, 1:3000, Clontech); moust anti-eIF4E (1:300, Santa Cruz Biotechnology); mouse anti-SMN (clone 8, 1:800 for immunostaining or 1:3000 for western blot, BD biosciences); goat anti-TIA-1 (1:100, Santa Cruz Biotechnology); rabbit anti-Dcp1a (1:500, provided by Dr. Jens Lykke-Anderson); rabbit anti-Syncrip (pan-hnRNP-Qs/R antibody, 1:10000, provided by Dr. Katsuhiko Mikoshiba), huaman anti ribosomal P0 antibody (1:500, provide by Dr. Morris Reichlin) and rabbit anti-hnRNP-Q1 (1:500, as described in Chapter II). Cy2 (1:500), Cy3 (1:1000) or Cy5 (1:500) conjugated donkey anti-mouse/rabbit/goat antibodies were purchased from Jackson ImmunoResearch Inc.

Immunofluorescence staining was performed as described previously (Zhang et al, 2006). In brief, cells were fixed with 4% paraformaldehyde in PBS containing 5mM $MgCl_2$ for 18 min at room temperature and washed with PBS/ $MgCl_2$ three times. Cells

were permeabilized with PBS/0.3% Triton X-100 for 5 minutes followed by 30 minutes of incubation with blocking buffer containing 5% BSA in PBS/0.1% Triton X-100 (PBST). Primary and secondary antibodies were diluted in blocking buffer. Cells were incubated with primary antibodies for 1 hour at room temperature or over night at 4 ºC and secondary antibody for 1 hour at room temperature followed by three washes with PBST. Coverslips were mounted in a mount medium as described previously (Zhang et al, 2006).

Fluorescence microscopy and digital imaging

Fixed cells were visualized using a Nikon Eclipse inverted microscope (TE300) equipped with a 60x Plan-Neofluar objective, phase optics, 100W mercury arc lamp and HiQ bandpass filters (Chroma Tech). Images were captured with a cooled CCD camera (Quantix, Photometrics) using a 35 mm shutter and processed using IP Lab Spectrum (Scanalytics). Fluorescence images were acquired with specific filters, including Cy2, Cy3 or Cy5.

For living cell imaging, primary hippocampal neurons cultured in MedTek dishes for 3 days were transfected with plasmid expressing EGFP-hnRNP-Q1 using Lipofectamine 2000. For one plate of cells, 1.5µg of plasmid encoding EGFP-hnRNP-Q1 was used with a plasmid/transfection reagent ratio at 1:1. Cells were imaged 16 hours post transfection. Images were acquired at 170ms per frame with a Swept Field Confocal Microscope (Nikon) equipped with a humid chamber.

Immunoprecipitation

293T or Neuro2a cell lysate were prepared with cell lysis buffer (50mM Tris-HCl, 150mM NaCl, 5mM MgCl$_2$, 1mM DTT, and 1% NP-40, pH7.5) supplemented with complete protease inhibitors (Roche), and RNase inhibitor (SUPERase-In, Ambion). Cells were extracted by further incubation on ice for 10 minutes and cleared by centrifugation at 20,000g for 15 minutes at 4 ºC. Supernatant was incubated with mouse anti-Flag (Sigma) or rabbit anti-Myc (Sigma) antibodies conjugated agarose beads for 2 hours to overnight at 4 ºC with rotating. Beads were pelleted by brief centrifugation at 4 ºC and washed extensively with lysis buffer. After final wash, immuprecipitates were denatured with protein sample buffer at 95 ºC for western blot analysis or suspended in Trizol reagent (Invitrogen) for RNA extraction and qRT-PCR analysis.

To determine RNA-dependent protein-protein association, RNase inhibitor was omitted from cell lysis buffer. Cleared cell lysate was supplemented with 1mM CaCl2 and treated with or without 200U/ml S7 nuclease (Roche) at 37 ºC for 1 hour. To inactivated S7 nuclease if necessary, 5mM EDTA were added to cell lysates which were further incubated at 37ºC for 10 minutes.

Neuro2a cell fractionation

Subconfluent Neuro2a cells in a 6cm cell culture dish washed with ice-cold PBS were scraped into 5ml PBS and pelleted by centrifugation at 100g for 5 minutes at 4ºC. Cell pellets were suspended in 1ml nuclei extraction buffer (10mM HEPES, 10mM KCl, 1.5mM MgCl2 and 0.5mM DTT, pH7.4) and incubated on ice for 10 minutes. Insoluble fractions containing nuclei were precipitated by centrifugation at 100g for 5 minutes at 4ºC. Supernatant was collected as cytoplasmic fractions and pellets were washed twice

and suspended in 1ml nuclei extraction buffer as nuclear fractions. Equal volume of cytoplasm and nuclear extracts was used for western blot analysis.

<u>Western blot analysis</u>

Protein samples were resolved by sodium dodecyl sulfate polyacrylamide gel electrophoresis (SDS-PAGE) and transferred onto PVDF membranes. For protein detection, PVDF membranes were incubated with blocking solution (5% fat-free milk in PBST) for 30 minutes at room temperature and further probed with primary antibodies diluted in blocking solution for 1 hour at room temperature or over night at 4 ºC. After three washes with PBST, PVDF membranes were incubated with HRP-conjugated donkey anti-mouse or rabbit secondary antibodies (1:3000, Amersham Biosciences) in blocking solution for 1 hour at room temperature. After washing with PBST, the signal was detected using ECL chemiluminescence reagents (Amersham Biosciences) and exposed to films. For immunoprecipitated protein samples, TrueBlot HRP-conjugated anti-rabbit or mouse secondary antibodies (1:2000, eBioscience) were used to minimize the interference of IgG bands.

<u>Quantitative RT-PCR analysis</u>

Total RNAs were reverse transcribed with Transcriptor First Strand cDNA Synthesis Kit (Roche) according to the manufacturer's protocol. Real-time PCR and analysis were performed in a LightCycler real-time PCR system (Roche) with LightCycler SYBR Green I Master mix (Roche). Gene specific primers were used as described in the previous chapter.

<u>Results</u>

Differential subcellular localization of hnRNP-Q1, Q3 and R

Previously, hnRNP-Q isoforms have been shown to localize to separated subcellular compartments (Chen et al., 2008) and we observed that only hnRNP-Q1, but not hnRNP-Q3 and hnRNP-R, was detected in axonal and synaptosome fractions (**Figure 3-1**). To further characterize the subcellular distribution of these proteins, we first examined endogenous proteins by western blot analysis of purified cytoplasmic and nuclear fractions of Neuro2a cells. As shown in **Figure 4-1A**, endogenous hnRNP-Q1 and SMN were detected in both cytoplasmic and nuclear fractions, whereas hnRNP-Q3 and hnRNP-R were highly enriched in nuclear fractions. To validate this result, we then examined the localization of fluorescent protein-tagged protein. Since SMN directly interacts with hnRNP-Qs/R and has been suggested to be important for the cytoplasmic localization of hnRNP-R (Rossoll et al., 2003; Rossoll et al., 2002), we co-expressed mRFP-tagged SMN with EGFP-tagged proteins in Neuro2a cells. We found that overexpressed EGFP-hnRNP-Q3 and R were predominantly confined to the nucleus and EGFP-hnRNP-Q1 was mainly retained in the cytoplasm (**Figure 4-1B**). Consistent with the distribution of endogenous SMN (Liu and Dreyfuss, 1996), mRFP-SMN was observed in both the cytoplasm and nucleus. In the cytoplasm, both EGFP-hnRNP-Q1 and mRFP-SMN form punctuated granules and exhibit a similar pattern of distribution; whereas in the nucleus, mRFP-SMN was enriched in several foci, previously described as Gems (Liu and Dreyfuss, 1996), where EGFP-hnRNP-Q1 signal was not detected (**Figure 4-1B**). In contrast to the previous report that SMN may be required for the cytoplasmic localization of hnRNP-R in PC12 cells (Rossoll et al., 2003), here we found

that overexpression of mRFP-SMN did not promote the cytoplasmic localization of hnRNP-Q3 nor hnRNP-R in Neuro2a cells.

<u>hnRNP-Q1 is an mRNP component</u>

Recent studies demonstrate that hnRNP-Qs associate with ribosomal proteins and other RNA binding proteins involved in RNA transport and translational regulation (Bannai et al., 2004). To further characterize these interactions and the nature of hnRNP-Q1 granules, we performed co-immunoprecipitation experiments with cell lysates treated with micrococcal (S7) nuclease to eliminate endogenous RNAs **(Supplemental Figure 4-2A)** or without nuclease to test the interaction for dependence on RNA. Flag-tagged mCherry and flag-tagged mCherry-hnRNP-Q1 were transiently expressed in 293T cells and immunoprecipitated with anti-Flag antibody-conjugated agarose beads. Co-immunoprecipitated proteins were detected by western blot as indicated. Similar to a previous report (Bannai et al., 2004), ZBP1, PABP, FMRP, DDX6 and ribosomal P0 protein were co-precipitated with Flag-mCherry-hnRNP-Q1 **(Figure 4-2A)**. However, the co-immunoprecipitation of these proteins was abolished by S7 nuclease treatment, indicating that the interaction of hnRNP-Q1 with these proteins is RNA-dependent and hnRNP-Q1 containing granules are mRNP granules. We then determined the essential hnRNP-Q1 domain(s) which may mediate its association with mRNAs. Different hnRNP-Q1 deletion constructs, including Q1(1-161) containing the N-terminal acidic domain, Q1(1-443) containing the acidic domain and three RRMs, Q1(131-443) containing only three RRMs, Q1(131-561) containing three RRM and the RGG domain and Q1(406-561) containing the RGG domain and the following C-terminal sequence, were generated by PCR and inserted into a mammalian expression vector with a Myc-tag

at the N-terminus for immunoprecipitation **(Figure 4-2C)**. In the previous study, we observed that several axonally localized mRNAs including RhoA and Creb, were selectively enriched in immunoprecipitated hnRNP-Q1 mRNP complexes compared with γ-actin mRNA **(Chapter III, Figure 3-3)**. Thus we examined the levels of γ-actin, β-actin, RhoA and Creb mRNA in immunoprecipitates of the hnRNP-Q1 deletion constructs by qRT-PCR. Levels of immunoprecipitated mRNAs were firstly normalized to the Myc-Q1(1-161) sample since this region contains no classical RNA binding motifs. Our results show that all mRNAs examined are enriched in Myc-Q1(131-561) and Myc-hnRNP-Q1 (full-length) pellets **(Supplemental Figure 4-4)**, both containing all three RRM domains and the RGG domain, whereas mRNAs were only weakly enriched in Myc-Q1(1-443) pellets and not enriched in Myc-Q1(131-443) and Myc-Q1(406-561) pellets. Western blot analysis confirmed that roughly equal amount of proteins was immunoprecipitated **(Supplemental Figure 4-3)**. To examine the selective enrichment of RhoA and Creb mRNA, we then normalized the levels of these two mRNAs and also β-actin mRNA to γ-actin. The selective enrichment of these mRNAs was only observed in Q1(131-561) and full-length hnRNP-Q1 pellets. Collectively, these results suggest that both three RRM and the RGG domains are required for the recruitment of hnRNP-Q1 into mRNP granules and its mRNA binding specificity **(Figure 4-2B)**. Thus we tested these truncated forms of hnRNP-Q1 for their localization to mRNP granules. Since we have shown that hnRNP-Q1 is a component of mRNP granules, EGFP-hnRNP-Q1 was used as bait for co-immunoprecipitation analyses. Myc-tagged proteins and EGFP-hnRNP-Q1 were co-expressed in 293T cells to assess possible self-association which is common for mRNA binding proteins that assemble into RNA granules (Nielsen et al.,

2004; Niessing et al., 2004; Wu et al., 1998). Immunoprecipitation was performed with rabbit anti-Myc antibodies and proteins were detected with mouse anti-GFP and anti-Myc antibodies. As shown in **Figure 4-2D**, only Myc-Q1(131-561) and full-length hnRNP-Q1 efficiently pulled down EGFP-hnRNP-Q1, further suggesting the essential role of RRM and RGG domains for the recruitment of hnRNP-Q1 into mRNP granules.

Active transport of EGFP-hnRNP-Q1 mRNP granules

hnRNP-Q1 has been previously identified as a component of transport mRNP granules purified from rat brains with a conventional kinesin (KIF5) cargo binding domain (Kanai et al., 2004). We performed live cell imaging experiments to test in cultured neurons whether hnRNP-Q1 granules are actively transported along neuronal processes. Plasmids encoding EGFP-hnRNP-Q1 were transfected into primary mouse hippocampal neurons and expressed for 16 hour before imaging. As shown in **Figure 4-3A**, EGFP-hnRNP-Q1 granules were localized in neuronal processes. Kymograph analyses **(Figure 4-3A, a** and **b)** revealed that a number of EGFP-hnRNP-Q1 granules exhibited fast, trajectory movement in this process, in either retrograde or anterograde direction, although the majority of EGFP-hnRNP-Q1 granules were stationary and exhibited only oscillatory movements. Examples for both retrograde and anterograde moving granules were analyzed frame by frame; as shown in **Figure 4-3B and C**, these granules were transported at a average rate of 1-2 μm/sec which is consistent with the velocity of microtubule-dependent transport (Kohrmann et al., 1999).

hnRNP-Q1 is localized to stress-granules and P-bodies

Besides transport mRNP granules, also stress granules and P-bodies are found in multiple cell types. mRNAs and RNA binding proteins in stress granules and P-bodies

are dynamic components shuttling between these granules (Anderson and Kedersha, 2008, 2009a). To investigate whether hnRNP-Q1 shuttles between different granules, we examined the localization of hnRNP-Q1 in these two mRNP granules. Stress granules were induced by treating 293T cell with 5mM sodium arsenite for 30 minutes. TIA1 was detected by immunofluorescence staining and used as a marker for stress granules (Gilks et al., 2004). We found that after arsenite treatment endogenous hnRNP-Q1 aggregated into large TIA1-positive granules; whereas these granules were not observed in non-treated cells **(Figure 4-4)**. Consistent with a previous report (Hua and Zhou, 2004), SMN was also detected in stress granules. Moreover, experiments with overexpressed EGFP-hnRNP-Q1 supported our findings for endogenous hnRNP-Q1; when treated with arsenite, EGFP-hnRNP-Q1 was recruited into stress granules **(Figure 4-6A, lower panel)**.

P-bodies are cytoplasmic sites which have been suggested to play roles in mRNA degradation and miRNA-mediated translational regulation (Franks and Lykke-Andersen, 2008; Jakymiw et al., 2007; Lian et al., 2006). P-bodies bodies contain components of the mRNA degradation machinery, such as decapping proteins Dcp1a and the LSm1-7 ring complex (Franks and Lykke-Andersen, 2008). During stress stimuli, P-bodies closely associate with stress granules (Kedersha et al., 2005). A number of RNA binding proteins, such as CPEB and FMRP, both of which regulate mRNA transport and translation, are localized to both stress granules and P-bodies (Cougot et al., 2008; Mazroui et al., 2002; Wilczynska et al., 2005). In addition, hnRNP-Qs when detected using pan-hnRNP-Q antibodies were shown partially colocalized with GW182 granules in U-87 glioblastoma cells (Moser et al., 2007). These GW182 granules are partially

colocalized with P-body protein Xrn1 and LSm4, indicating that hnRNP-Qs are possibly components of P-bodies (Moser et al., 2007). We then examined the localization of hnRNP-Q1 in P-bodies. 293T cells were transiently transfected with mRFP-Dcp1a and EGFP-LSm1 as markers for P-bodies and endogenous hnRNP-Q1 was detected by immunofluorescence staining. As shown in **Figure 4-5A**, hnRNP-Q1 colocalized with EGFP-LSm1 and mRFP-Dcp1a in several cytoplasmic foci. Likewise, EGFP-hnRNP-Q1 could be detected in these foci; however, in these granules, SMN was not detected, indicating that SMN is not a component of P-bodies **(Figure 4-5C)**.

To further characterize the P-body localization of hnRNP-Q1, we used hnRNP-Q1 deletion constructs to identify domains or motifs of hnRNP-Q1 mediating its association with P-body protein Dcp1a. EGFP-tagged full-length or truncated proteins were co-expressed in 293T cells with Dcp1a tagged with the Flag epitope. Flag-Dcp1a was immunoprecipitated and EGFP-tagged proteins were detected by western blot with GFP-specific antibodies. As shown in **Figure 4-5B**, only RGG domain-containing EGFP-tagged proteins were co-precipitated with Flag-Dcp1a, including Q1(131-561), Q1(406-561) and full-length hnRNP-Q1(1-561), indicating that the RGG domain is sufficient and necessary for the binding of hnRNP-Q1 to Dcp1a; such binding might be needed for the localization of hnRNP-Q1 to P-bodies..

The localization of hnRNP-Q1 and several other RNA binding proteins to stress granules and P-bodies were also examined in COS7 cells, since this type of cells have larger cell areas which provide better spatial resolution. Our results showed that overexpressed EGFP-tagged Zbp1 **(Figure 4-6C)**, HuD **(Figure 4-6D)**, FMRP **(Figure 4-6E)** and Pumilio2 **(Figure 4-6F)** were all colocalized with mRFP-Dcp1a granules; after

arsenite treatment, these proteins were recruited into large aggregates which have been identified as stress granules (Burry and Smith, 2006; Mazroui et al., 2002; Stohr et al., 2006; Vessey et al., 2006). Although mainly localized to the nucleus, EGFP-hnRNP-R **(Figure 4-6B)** was also observed in both P-bodies and stress granules. In contrast, EGFP-PABPC1 **(Figure 4-6G)** was recruited into stress granules as observed previously (Kedersha et al., 2005) but excluded from P-bodies. Interestingly, arsenite treatment abolished the P-body localization of EGFP-FMRP and Pumilio2, but not EGFP-hnRNP-Q1, hnRNP-R, Zbp1 and HuD, suggesting a potential functional difference of these proteins in mRNA regulation in response to stress.

The association of RNA binding proteins with Dcp1a and LSm1 is RNA-independent

P-bodies have been characterized as mRNA-containing granules (Brengues et al., 2005; Liu et al., 2005; Sheth and Parker, 2006; Teixeira et al., 2005). mRNA accumulation in P-bodies has been observed in certain circumstances, such as knockdown of mRNA degradation machineries or overexpression of mRNA destabilizing factors (Cougot et al., 2004; Franks and Lykke-Andersen, 2007). We therefore investigated whether the association of the above analyzed RNA binding proteins with P-bodies is RNA dependent, since RNAs have been involved in the association of hnRNP-Q1 with several RNA binding proteins **(Figure 4-2A)**. Two proteins were used for this co-immuprecipitation analysis, Dcp1a and LSm1, which are both localized in P-bodies **(Figure 4-5A)** and shown to play a role in mRNA degradation (Jakymiw et al., 2007). We transiently expressed Flag-mCherry-tagged Dcp1a or LSm1 in 293T cells, and proteins were immunoprecipitated with beads conjugated with mouse anti-Flag antibodies; cells transfected with an empty vector expressing Flag-mCherry was used as

the control for non-specific binding to beads. Immunoprecipitated endogenous proteins were detected by western blot with specific antibodies as indicated. To test whether the interaction of RNA binding protein and P-body proteins is RNA-dependent, a portion of the cell lysate was treated with S7 nuclease to eliminate endogenous RNAs. Total RNA was extracted from all the samples and resolved in an RNA gel to examine the efficiency of RNA degradation. As shown in **Figure 4-7**, both Flag-mCherry-tagged LSm1 and Dcp1a co-precipitated hnRNP-Q1, ZBP1, FMRP and also mRNA cap-binding protein eIF4E; no signal was detected in Flag-mCherry immunoprecipitation pellets. Notably, ZBP1, FMRP and eIF4E were co-immunoprecipitated with a higher efficiency than hnRNP-Q1. S7 nuclease treatment efficiently eliminated RNAs **(Supplemental Figure 4-2B)**, yet had no effect on the co-immunoprecipitation of RNA binding proteins **(Figure 4-7)**. The level of co-immunoprecipitated eIF4E was slightly reduced after S7 nuclease treatment, but not as pronounced as the RNA-dependent interaction shown in **Figure 4-2A**. Results were similar with EGFP-tagged proteins **(Supplemental Figure 4-7)**. In these experiments, EGFP-tagged hnRNP-Q1, Zbp1, HuD, FMRP and Pumilio2 were co-immunoprecipitated with Flag-Dcp1a in an RNA-independent manner. Interestingly, we found that PABP, which is excluded from P-bodies **(Figure 4-6G)**, was also present in Flag-mCherry- Dcp1a and LSm1 pellets and this association was S7-treatment insensitive **(Figure 4-7)**. The co-immunoprecipitation of RNA binding proteins, particularly PABP, with LSm1 and Dcp1a indicates that the association of RNA binding proteins with P-body components may not be limited to P-bodies. In fact, a recent study in neuronal cells suggests that LSm1 is a component of transport mRNA granules and possibly involved in translational regulation (di Penta et al., 2009).

Discussion

hnRNP-Qs and hnRNP-R have been suggested as components of mRNP granules implicated in multiple aspects of RNA regulation, such as pre-mRNA splicing, RNA editing, mRNA localization and translational regulation (Blanc et al., 2001; Cho et al., 2007; Kanai et al., 2004; Kim et al., 2007; Mourelatos et al., 2001). To further analyze the molecular functions of these ubiquitous RNA-binding proteins, we examined the subcellular distribution of endogenous hnRNP-Q isoforms and hnRNP-R, as well as their association with several well-characterized RNA-binding proteins. Consistent with the previous overexpression study, we found that endogenous hnRNP-Q1 is mainly localized to the cytoplasm, whereas hnRNP-Q3 and hnRNP-R are predominantly localized to the nucleus. We also characterized the nature of hnRNP-Q1-containing mRNP granules. Our results showed that EGFP-hnRNP-Q1 was actively transported in neuronal processes at a velocity similar to microtubule-dependent transport vesicles. Consistent with this finding, hnRNP-Q1 together with some other RNA binding proteins and translation factors was co-purified with the KIF5 kinesin cargo-binding domain as a component of transporting mRNP granules in a previous study (Kanai et al., 2004). mRNAs within transporting granules are generally believed to be translationally silenced during transport to ensure appropriate translation of mRNAs in restricted subcellular compartments (Martin and Ephrussi, 2009). The observation that hnRNP-Q1 is a component of transport mRNP granules suggests two potential functions of hnRNP-Q1: (1) as an adaptor between mRNAs and molecular motors to facilitate mRNA transport working in a similar fashion to FMRP (Dictenberg et al., 2008) and (2) as a factor involved in translational regulation possibly as a translational repressor, which is in concert with our previous observation

hnRNP-Q1 negatively regulates RhoA mRNA translation **(see Chapter III)**. In favor of the second hypothesis, we also observed hnRNP-Q1 in stress granules and P-bodies, both of which are mRNP granules containing translationally silenced mRNAs (Franks and Lykke-Andersen, 2008; Kedersha and Anderson, 2007). Stress granules are large transient mRNP aggregates composed of poly(A) mRNAs and their binding proteins released from polysomes during stress (Anderson and Kedersha, 2009b). They serve as temporary storage for non-translating mRNAs which can be recycled for active translation as the relief of stress. P-bodies are cytoplasmic foci containing mRNA degradation machineries and proteins functioning in miRNA-mediated translational repression (Franks and Lykke-Andersen, 2008; Kedersha and Anderson, 2007). Since stress granules and P-bodies are dynamically associated cellular structures, mRNAs in stress granules may also be redirected to P-bodies for degradation. Our results show that hnRNP-Q1 is not essential for the formation of stress granules or P-bodies, as knockdown of hnRNP-Q1 does not affect the formation and/or the interaction of these granules **(Supplemental Figure 4-5** and **Figure 4-6)**. The localization of hnRNP-Q1 to these functionally different mRNP granules suggests a possible role of hnRNP-Q1 in regulating mRNA dynamics among these granules under normal or stress condition. The localization of hnRNP-Q1 to P-bodies may be accompanied by mRNA degradation or translational silencing. This function of hnRNP-Q1 may require both, the three RRMs and the RGG domain since all these RNA binding domains are essential for its recruitment to mRNPs, as well as its mRNA binding specificity **(Figure 4-2B)**. In addition, our results show that the targeting of hnRNP-Q1 to P-bodies is mediated through its RGG domain. Similar function of an RGG domain was also observed in

RAP55, a RNA binding protein localized to both stress granules and P-bodies (Yang et al., 2006).

hnRNP-Qs and hnRNP-R have been shown to directly interact with SMN (Mourelatos et al., 2001; Rossoll et al., 2002), the loss of which leads to SMA, an inherited motor neuron degenerative disease (Lefebvre et al., 1995). The interaction of hnRNP-Qs/R and SMN is abolished by missense mutations of SMN found in SMA patients (Mourelatos et al., 2001; Rossoll et al., 2002). SMN has been suggested to regulate the cytoplasmic localization of hnRNP-R (Rossoll et al., 2003). Therefore we examined the effect of SMN overexpression on the subcellular distribution of this family of hnRNPs in Neuro2a cells. We found that overexpression of SMN failed to retain hnRNP-Q3 and hnRNP-R in the cytoplasm. This inconsistency to the previous report may be caused by cell type differences (Neuro2a in this study versus PC12 cells) or variant differentiation stages of these cells. It should also be noted that in mouse motor neurons and rat retina bipolar cells, hnRNP-R has been shown to be localized in the cytoplasm and axon terminals (Peng et al., 2009; Rossoll et al., 2003). Our results also show that SMN and hnRNP-Q1 are colocalized in stress granules but not in P-bodies. SMN is a core protein of snRNP assembly machineries which facilitate the specific and efficient association of snRNAs with Sm proteins (Kolb et al., 2007). The interaction of SMN with mRNA binding proteins and its localization to stress granules suggest a potential function of SMN in mRNA regulation other than pre-mRNA splicing. Since SMN is not a component of P-bodies, we postulate that SMN may regulate the shuttling of its interacting RNA binding proteins from stress granules to P-bodies and the loss of SMN may lead to defective mRNA remodeling upon stress, a deregulation which may

contribute to the pathogenesis of SMA. This hypothesis might be tested in SMN-deficient cells by analyzing the possible defective mRNA and RNA binding protein dynamics among different mRNP granules.

Similar to hnRNP-Q1 and RAP55 mentioned above, some RNA binding proteins including CREB, FMRP, TTP and BRF1 are also simultaneously localized to both stress granules and P-bodies (Cougot et al., 2008; Franks and Lykke-Andersen, 2007; Kedersha et al., 2005; Mazroui et al., 2002; Wilczynska et al., 2005). RNA binding proteins are dynamic components of these mRNP granules and shuttle between them. Recent studies reveal that the localization of TTP and BRF1 to P-bodies facilitates the decay of their associated ARE-containing mRNAs (Franks and Lykke-Andersen, 2007). Besides hnRNP-Q1 and FMRP, our results also show that Zbp1, HuD, hnRNP-R and Pumilio2 are localized to stress granules and P-bodies, whereas PABP is only detected in stress granules. Interestingly, after arsenite treatment, FMRP and Pumilio2 are delocalized from P-bodies. These observations suggest a functional difference of these RNA binding proteins in mRNA regulation under normal or stress condition. RNA binding proteins in stress granules may retain their associated mRNAs in stress granules and protect them from mRNA degradation enzymes, whereas when localized to P-bodies, RNA binding proteins may route their associated mRNAs for rapid degradation. The latter hypothesis is supported by mechanistic studies of TTP and BRF1 in mRNA degradation, both of which are well-established mRNA destabilizing trans-acting factors (Franks and Lykke-Andersen, 2007). However, recent studies are more supportive for an mRNA stabilizing function of both hnRNP-Q1 and Zbp1 (Grosset et al., 2000; Stohr et al., 2006; Weidensdorfer et al., 2009), which are inconsistent with our proposed model for a role of

hnRNP-Q1 in P-body-mediated mRNA degradation. Overexpression of hnRNP-Q1 stabilizes both CRD and ARE-containing mRNAs (Grosset et al., 2000) and knockdown of Zbp1 leads to enhanced degradation of its associated mRNAs under normal conditions as well as upon stress (Stohr et al., 2006). One explanation for this apparent contradiction could be that the targeting of mRNAs to P-bodies for degradation or retention in stress granules is highly selective. Only a subgroup of hnRNP-Q1 or Zbp1 associated mRNAs might be targeted to P-bodies and possibly additional factors are involved in this process. Our co-immunoprecipitation studies therefore most likely represent a mixture of different hnRNP-Q1-containing granules. Apart from hnRNP-Q1 and Zbp1, many other RNA binding proteins may associate with these analyzed mRNAs. It is therefore possible that hnRNP-Q1 and Zbp1 may have no direct role in the regulation of mRNA degradation efficiency. Their localization to P-bodies may be a consequence of targeted sorting of mRNAs selected for rapid degradation by RNA destabilizing factors such as TTP and BRF1 (Franks and Lykke-Andersen, 2007).

This differential localization of hnRNP Qs/R may be caused by the presence of a putative bipartite NLS in the C-termini of hnRNP-Q3 and R and the lack of this sequence in hnRNP-Q1 (**Supplemental Figure 4-1**). The distinct subcellular distribution of hnRNP-Q1, Q3 and R suggests that these hnRNPs are functionally different. hnRNP-Q1 may be the main player regulating cytoplasmic events such as mRNA transport, stability and/or translation whereas hnRNP-Q3 and R may be important for some nuclear activities such as pre-mRNA splicing, mRNA quality control and/or mRNA export from the nucleus. Since hnRNP-Q isoforms contain the same mRNA binding domains and hnRNP-R is highly homologous to hnRNP-Q, possibly these proteins share the same

mRNA targets. Therefore, these proteins may play similar functions in a sequential way. In this scenario, hnRNP-Q3 or R may first bind their target mRNAs in the nucleus and following the export of mRNAs into the cytoplasm, hnRNP-Q1 is recruited in replacement of hnRNP-Q3 or R to execute cytoplasmic mRNA regulation. A similar RNA binding protein "handover" model has been proposed for the function of zipcode binding proteins in β-actin mRNA localization (Pan et al., 2007). In contrast to hnRNP-Q1 and hnRNP-Q3 which are encoded by the same gene, Zbp1 and Zbp2 are two distinct proteins from two genes, both of which can bind to the zipcode sequence of β-actin mRNA (Gu et al., 2002; Ross et al., 1997). Similar to hnRNP-Q1, Zbp1 is a nuclear-cytoplasmic shuttling protein mainly localized to the cytoplasm of chicken forebrain neurons and fibroblast cells (Oleynikov and Singer, 2003), whereas Zbp2 (also known as KSRP) is mainly detected in the nucleus and only a small fraction of Zbp2 can be detected in neuronal growth cones in colocalization with β-actin mRNA (Gu et al., 2002). Pan et al. have revealed that Zbp2 binds to the zipcode sequence preceding the recruitment of Zbp1; additionally, this study shows that Zbp2 and Zbp1 are not simultaneously present in the same β-actin mRNP complexes (Pan et al., 2007). The initial binding of Zbp2 to the zipcode sequence during β-actin transcription is required for the efficient recruitment of Zbp1 which further regulates β-actin mRNA localization and translation (Pan et al., 2007). It is likely that the mRNA binding protein "handover" may happen in both the nucleus and cytoplasm. The initial recruitment of a nuclear RNA binding protein to its target mRNAs may serve as a mechanism to ensure proper mRNP formation by reserving specific binding sites for a mainly cytoplasm-localized protein

which is going to be recruited subsequently. hnRNP-Q1 and hnRNP-Q3/R may function in a similar fashion.

In this study, we uncovered a series of RNA-dependent and independent interaction proteins of hnRNP-Q1. Our results show that the association of hnRNP-Q1 with RNA binding proteins identified as components of transport mRNP granules is RNA-dependent, whereas the interaction of hnRNP-Q1 with P-body proteins, Dcp1a and LSm1, is RNA-independent. In addition, the interaction of P-body proteins with ZBP1, FMRP and Cap-binding proteins (eIF4E) is also RNA-independent. Surprisingly, we found that PABP which is not localized to P-bodies **(Figure 4-6)** was also co-precipitated with Dcp1a and LSm1 in an RNA-independent manner. This observation suggests that the association of Dcp1a and LSm1 with RNA binding proteins may not be limited within P-bodies, indicating a novel function of Dcp1a and LSm1-containing protein complexes. For this function, Dcp1a and LSm1 may interact with RNA binding proteins in transport mRNP granules to regulate mRNA transport or translation. In fact, although enriched in several cytoplasmic foci, endogenous Dcp1a is detected throughout the cytoplasm mainly in small granules distinct from P-bodies **(Supplemental Figure 4-5)**. In neuronal cells, Dcp1a and LSm1 are also localized to distal axons and dendrites (di Penta et al., 2009; Zeitelhofer et al., 2008), two highly polarized subcellular compartments extending from cell bodies. A recent study reveals that LSm1 is associated with transport mRNP granules localized to mature dendrites and possibly regulates mRNA translation locally (di Penta et al., 2009). The association of PABP and other RNA binding proteins with Dcp1a and LSm1 observed in this study provides additional support for this hypothesis. Due to the same binding property of Dcp1a and LSm1, we assume that Dcp1a is also a part of LSm1

protein complexes associated with transport mRNP granules. Although di Penta et al. presented data showing that Dcp1a and LSm1 are not colocalized in distal neuronal processes (di Penta et al., 2009), our unpublished data support an opposite conclusion that Dcp1a and LSm1 are colocalized in neuronal growth cones (data not shown). P-body components have been implicated in general translational regulation (Parker and Sheth, 2007). Besides proteins involved in mRNA degradation, such as decapping proteins, Xrn1 and LSm1-7 ring complex, general translational repressors such as RAP55 (Tanaka et al., 2006), Rck/p54 (Minshall et al., 2009) and YB-1 (Nekrasov et al., 2003), are also localized to and most importantly not limited to P-bodies (Minshall et al., 2009; Yang and Bloch, 2007; Yang et al., 2006), suggesting that they may play the same role in other forms of mRNP granules. Dcp1a and LSm1-containing complexes may recruit these translational repressors to mRNAs which will be subsequently arrested at various translational stages. In addition, decapping proteins may inhibit cap-dependent translation by eliminating 5'-cap structures. In yeast cells lacking decapping proteins, general translation repression upon glucose or amino acid deprivation is defective (Coller and Parker, 2005; Holmes et al., 2004). We postulate that Dcp1a and LSm1, and possibly other P-body resident proteins, may also interfere with translation initiation by blocking the interaction of eIF4E and eIF4G in a way similar to eIF4E-BPs (Nakamura et al., 2004; Napoli et al., 2008; Nelson et al., 2004) since Dcp1a and LSm1 physically associate with eIF4E. The eIF4E-4G complex formation is a prerequisite for cap-dependent translation initiation. The specific binding of RNA binding proteins to mRNAs and the further recruitment of other factors, such as protein complexes containing Dcp1a and LSm1, may regulate the proportion of mRNAs assembled into polysomes and non-

translating mRNP granules and therefore affect protein output and mRNA transport and localization. The interaction of hnRNP-Q1 with Dcp1a and LSm1 may contribute to the function of hnRNP-Q1 in regulating RhoA mRNA translation.

Figures and Legends
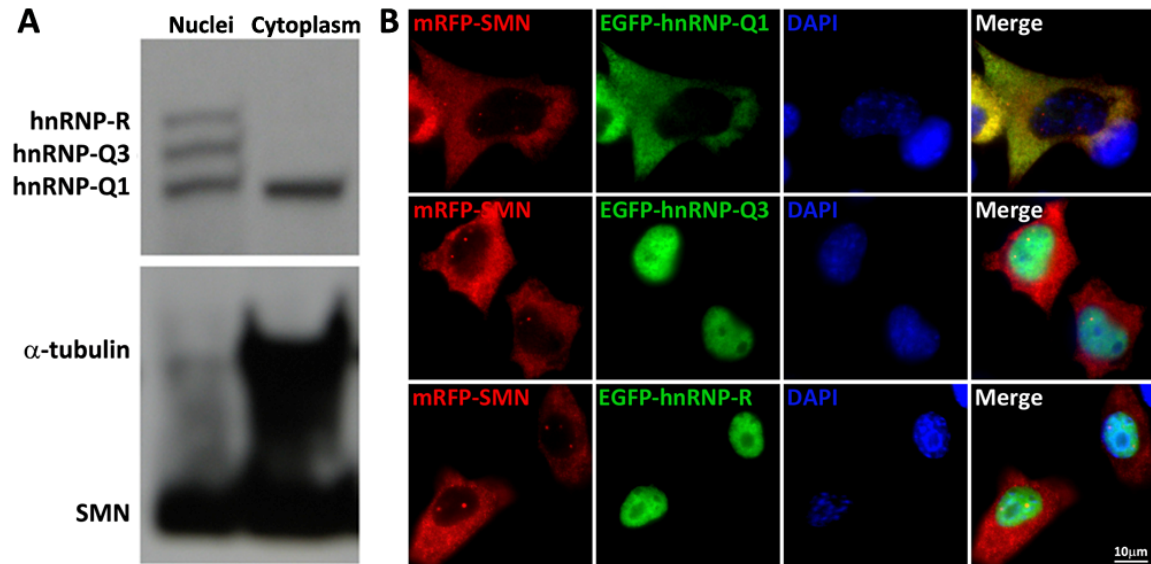
Figure 4-1. Subcellular distribution of hnRNP-Q1, hnRNP-Q3 and hnRNP-R. **(A)** Western blot analysis of cytoplasm and nuclei extracts of Neuro2a cells. hnRNP-Qs and hnRNP-R were detected with pan-hnRNP-Qs/R antibodies. **(B)** Subcellular localization of EGFP-tagged hnRNP-Q1, hnRNP-Q3 and hnRNP-R and mRFP-SMN in Neuro2a cells. Nuclei were stained with DAPI.
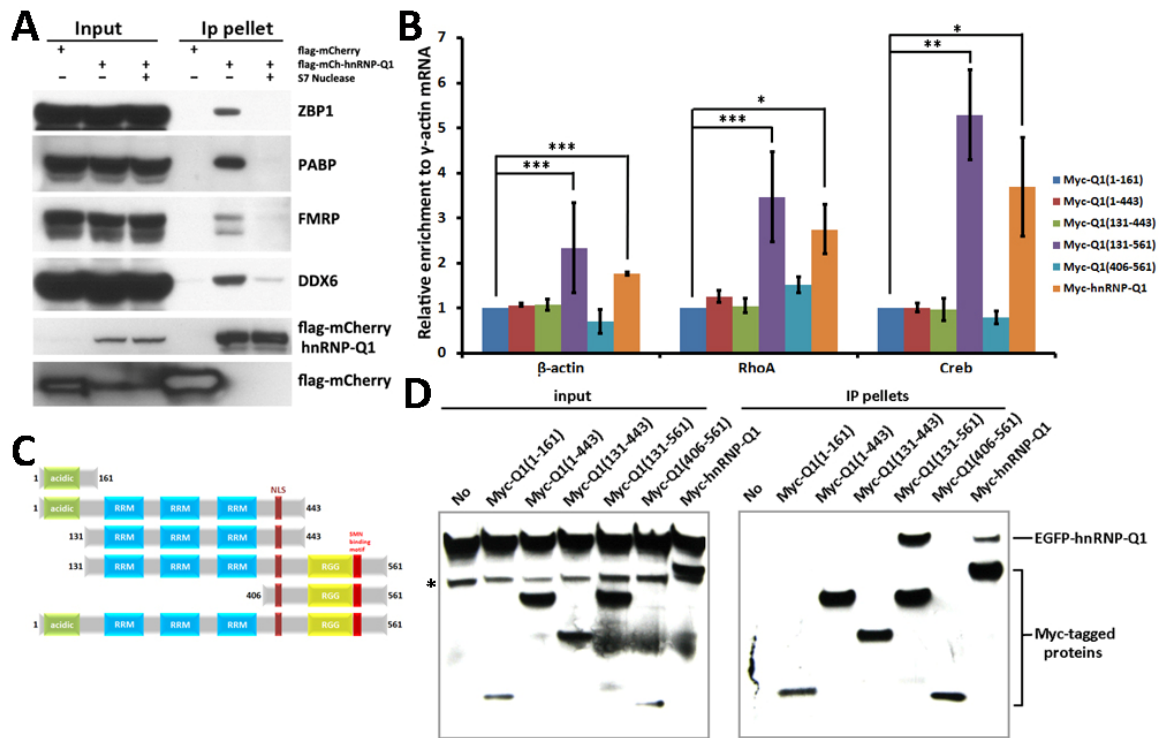
Figure 4-2. Association of hnRNP-Q1 with mRNP components. **(A)** hnRNP-Q1 associates with mRNP components in an RNA-dependent manner. Cell lysates were incubated in parallel with or without S7 nuclease. Flag-mCherry-tagged proteins were immunoprecipitated and endogenous proteins associated with hnRNP-Q1 were detected by specific antibodies for indicated proteins. **(B)** Association of mRNAs with hnRNP-Q1 RNA binding domains quantified by qRT-PCR. β-actin, RhoA and Creb mRNA levels in each sample were first normalized to Myc-Q1(1-161) precipitates and then normalized to γ-actin mRNA levels to show relative enrichment of each mRNA. **(C)** Domain structures of truncated hnRNP-Q1 constructs. **(D)** Co-immunoprecipitation analysis of EGFP-hnRNP-Q1 and Myc-tagged hnRNP-Q1 deletion constructs. *, non-specific bands recognized by the mouse anti-Myc antibody.
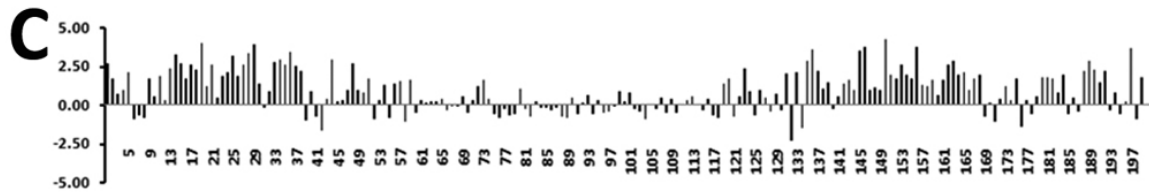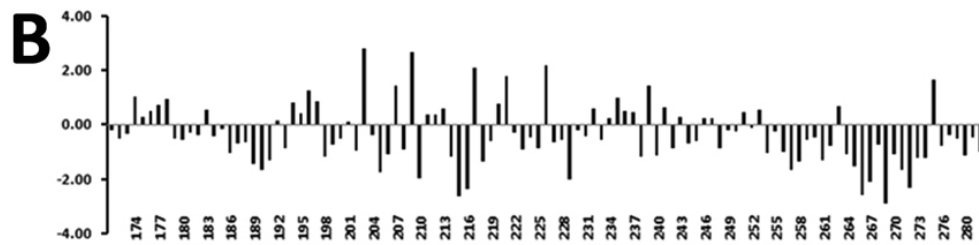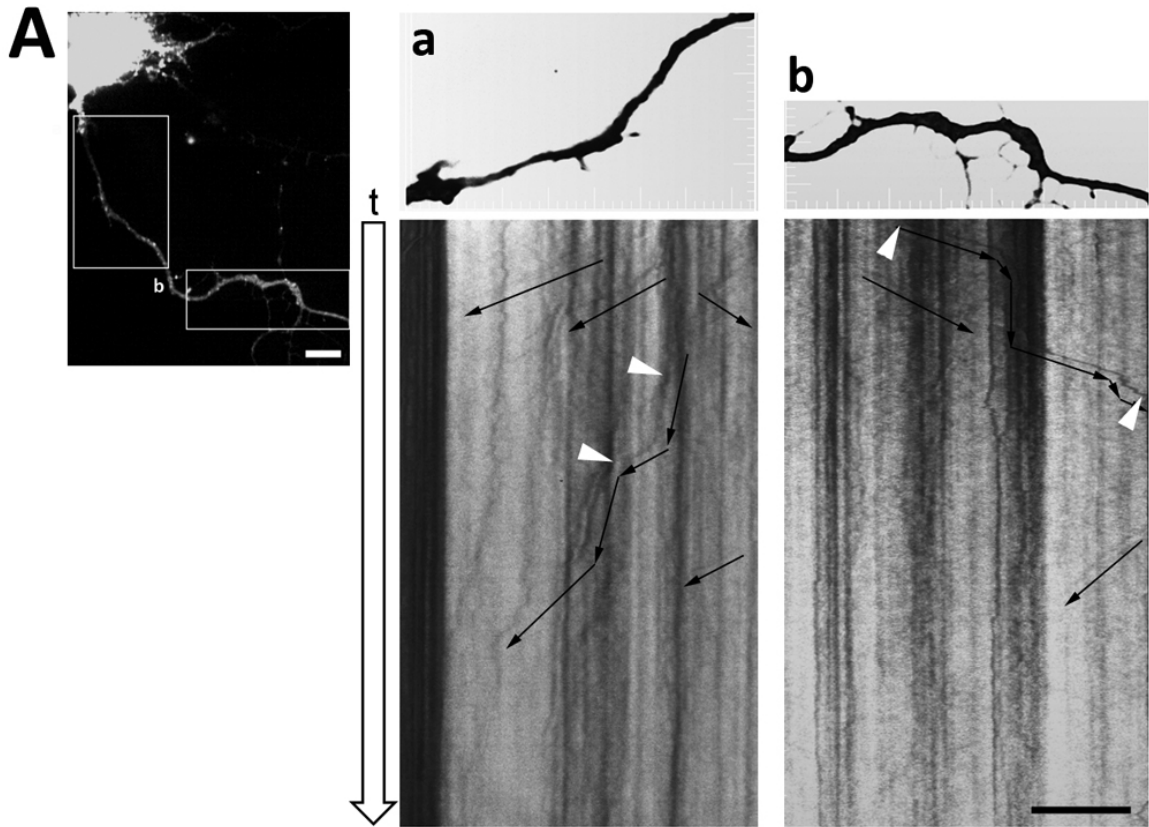
Figure 4-3. Active transport of EGFP-hnRNP-Q1 in neuronal processes. Mouse hippocampal neurons were transfected with a plasmid encoding EGFP-hnRNP-Q1. **(A)** An EGFP-hnRNP-Q1 positive neuron was imaged with a Nikon Swept Field Confocal Microscope at 170ms per frame. EGFP-hnRNP-Q1 is localized in granules within neuronal processes, many of which are actively trafficking along neurites as seen in kymographs **(a, b) re-**constructed from boxed areas using Imaris 6.2.0 software (Bitplane). Moving granules were highlighted with arrows indicating transport directions. **(B, C)** Quantitative analysis of granules exhibiting retrograde **(B)** or anterograde **(C)** movement (using Imaris 6.2.0, Bitplane) (*y, µm/s; x, frame number*). Granules and tracking time courses are marked by arrows in **(a)** and **(b)**. Scale bar, 10µm. (Partially contributed by Andrew Swanson)
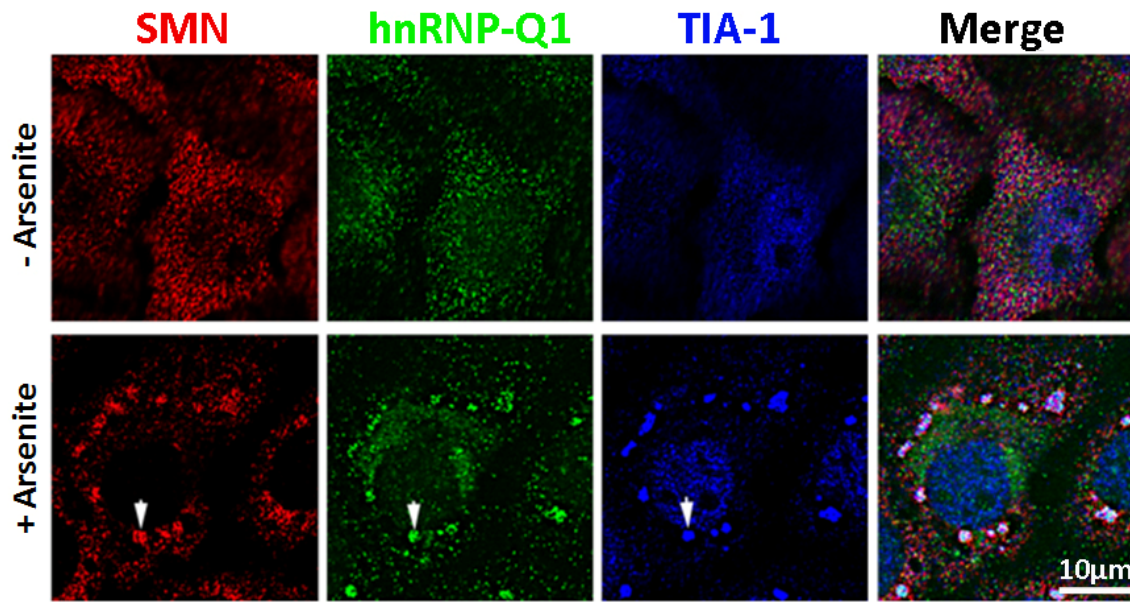
Figure 4-4. Localization of hnRNP-Q1 and SMN to arsenite-induced stress granules. Stress granules were induced by treating 293T cells with 5μM sodium arsenate for 30 minutes. Endogenous hnRNP-Q1 and SMN were detected by immunofluorescence staining. Large discrete TIA-1 positive stress granules (examples are indicated by arrows) were detected only in arsenite-treated cells (lower panel). In non-treated cells, hnRNP-Q1 and SMN exist as small granules (upper panel).
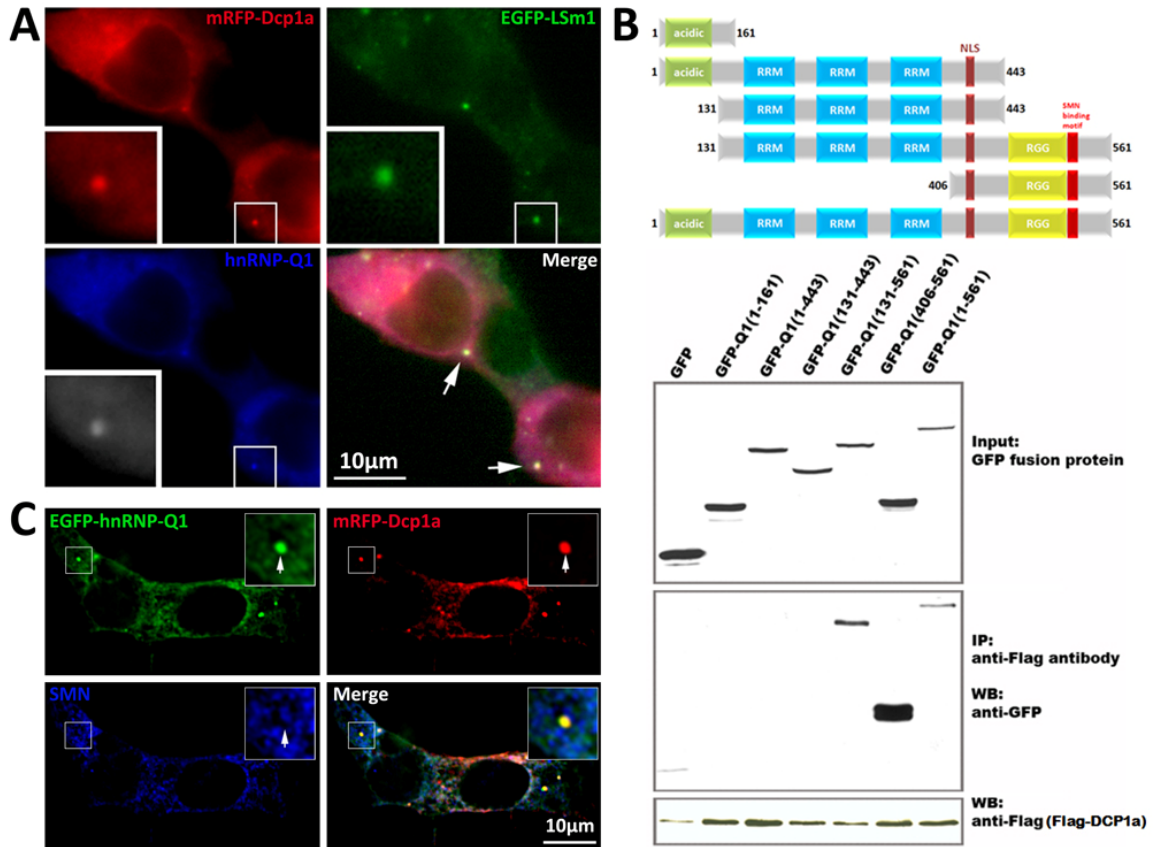
Figure 4-5. Localization of hnRNP-Q1 to P-bodies. **(A)** Enrichment of endogenous hnRNP-Q1 in P-bodies shown as EGFP-LSm1 and mRFP-Dcp1a positive granules. Endogenous hnRNP-Q1 was detected by immunofluorescence staining. **(C)** Localization of EGFP-hnRNP-Q1 to P-bodies, in which SMN was not detected. **(B)** Co-immunoprecipitation of RGG domain-containing truncated hnRNP-Q1 with Flag-Dcp1a. 293 cells were co-transfected with plasmids encoding Flag-tagged Dcp1a and EGFP tagged truncated hnRNP-Q1 constructs as illustrated in the upper panel. Flag-Dcp1a was immunoprecipitated and EGFP-tagged proteins were detected by western blot with a mouse anti-GFP antibody.

10μm
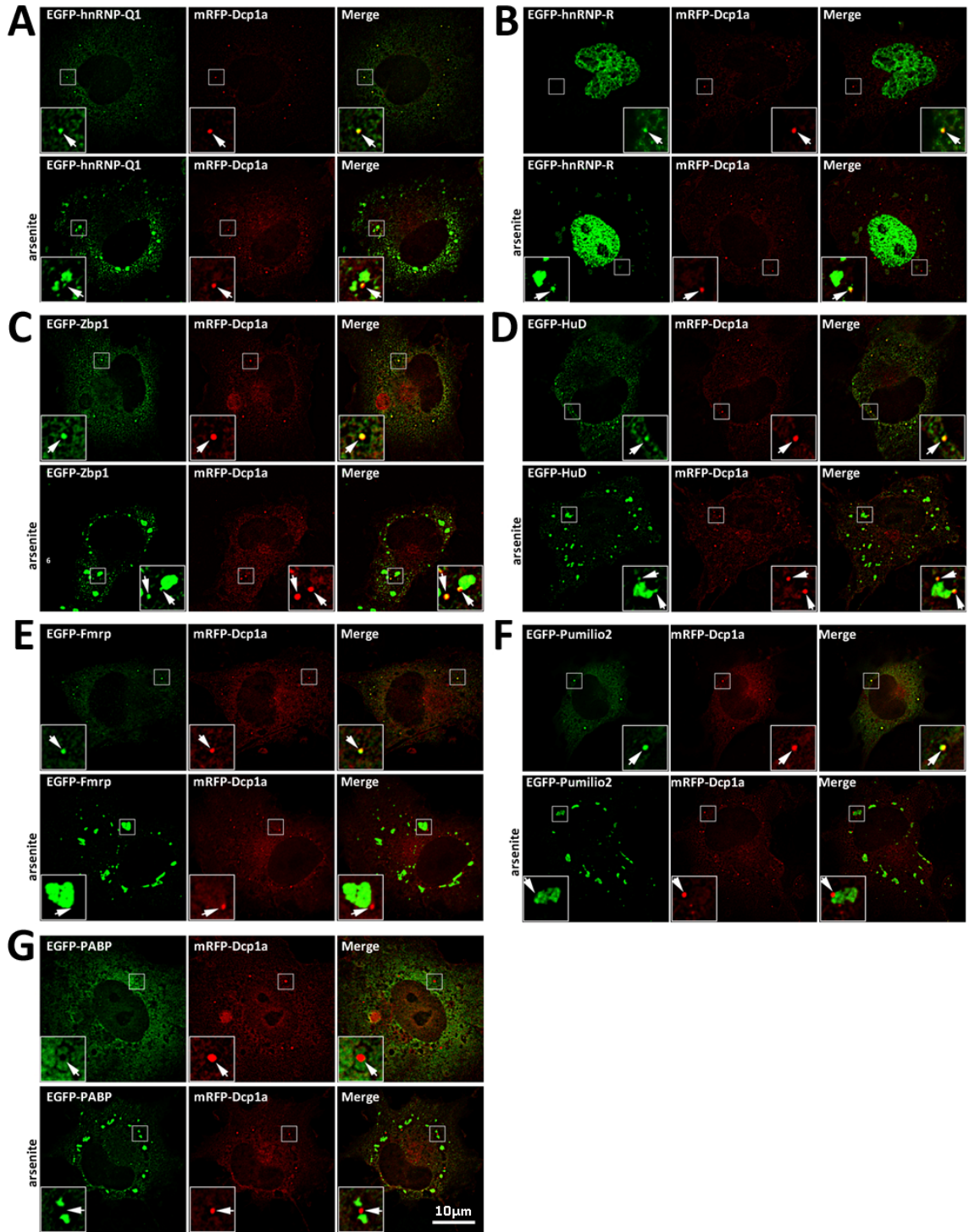
Figure 4-6. Differential localization of RNA binding proteins to P-bodies. COS7 cells were cotransfected with plasmids encoding EGFP-tagged RNA binding proteins, including hnRNP-Q1 **(A)**, hnRNP-R **(B)**, Zbp1 **(C)**, HuD **(D)**, Fmrp **(E)**, Pumilio2 **(F)** and PABPC1 **(G)**, and mRFP-Dcp1a as a marker for P-bodies. All RNA binding proteins were enriched in P-bodies in normal culture conditions except EGFP-PABP **(G, upper panels)**. Arsenite treatment abolished the localization of EGFP-Fmrp and Pumilio2 to P-bodies; however, had no effect on other proteins (lower panels). Examples of P-bodies and arsenite-induced stress are shown as enlarged insets, in which P-bodies are indicated by arrows.
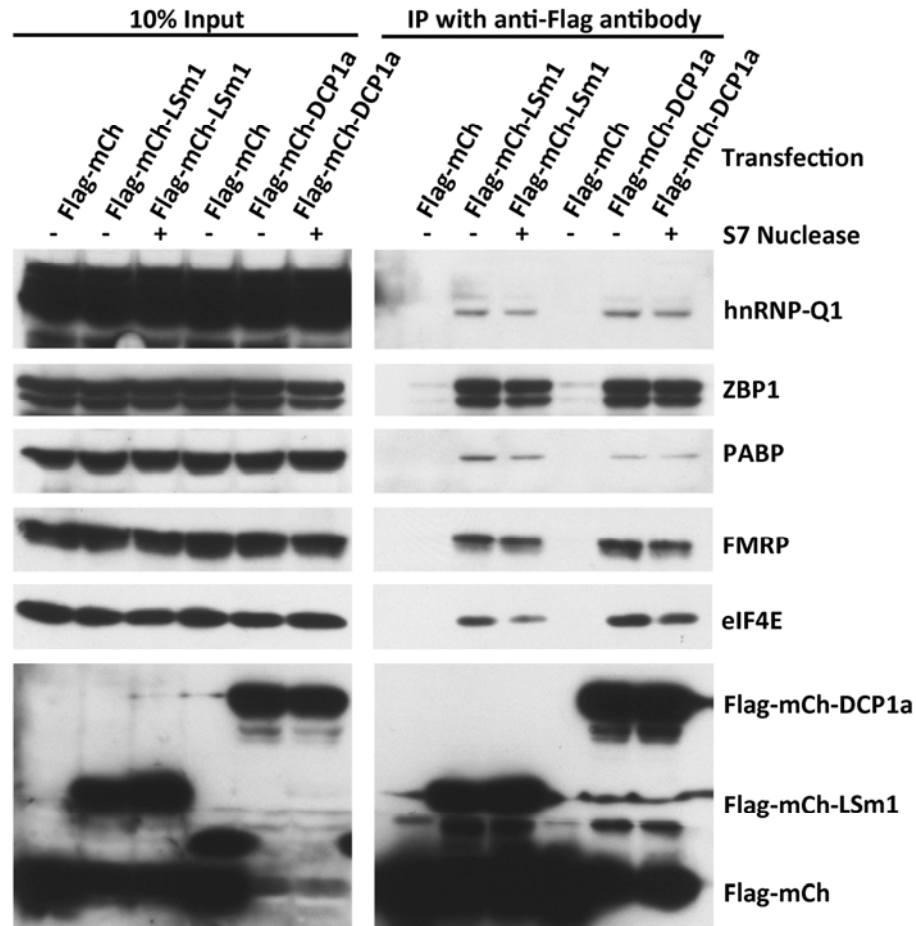
Figure 4-7. Co-immonuprecipitation analysis of indicated RNA binding proteins with Dcp1a and LSm1. 293T cells were transfected with Flag-mCherry tagged Dcp1a and LSm1 or Flag-mCherry as a control. Overexpressed Flag-tagged proteins were immunoprecipitated with agarose beads conjugated with mouse anti-Flag antibodies. Indicated endogenous RNA binding proteins were detected by western blot. To examine the function of RNA in these interactions, a portion of the proteins samples were treated with S7 nucleases prior to immunoprecipitation.

Supplemental Figures

A

hnRNP-Q1

1 — acidic — RRM — RRM — RRM — NLS — RGG — SMN binding motif — Sequence used for antibody production — 561

hnRNP-Q3

1 — acidic — RRM — RRM — RRM — NLS — RGG — Putative NLS — 623

hnRNP-R

1 — acidic — RRM — RRM — RRM — NLS — RGG — Putative NLS — 633

B

```
hnRNP-Q1  MATEHVNGNGT-----EEPMDTTSAVIHSENFQTLLDAGLPQKVAEKLDEIYVAGLVAHS  55
hnRNP-Q3  MATEHVNGNGT-----EEPMDTTSAVIHSENFQTLLDAGLPQKVAEKLDEIYVAGLVAHS  55
hnRNP-Q2  MATEHVNGNGT-----EEPMDTTSAVIHSENFQTLLDAGLPQKVAEKLDEIYVAGLVAHS  55
hnRNP-R   -MANQVNGNAVQLKEEEEPMDT-SSVTHTEHYKTLIEAGLPQKVAERLDEIFQTGLVAYV  58
           :::****..       ****** *:* *:*::::**::*********:****: :****:
hnRNP-Q1  DLDERAIEALKEFNEDGALAVLQQFKDSDLSHVQNKSAFLCGVMKTYRQREKQGTKVADS  115
hnRNP-Q3  DLDERAIEALKEFNEDGALAVLQQFKDSDLSHVQNKSAFLCGVMKTYRQREKQGTKVADS  115
hnRNP-Q2  DLDERAIEALKEFNEDGALAVLQQFKDSDLSHVQNKSAFLCGVMKTYRQREKQGTKVADS  115
hnRNP-R   DLDERAIDALREFNEEGALSVLQQFKESDLSHVQNKSAFLCGVMKTYRQREKQGSKVQES  118
           *******:**:****:***:******:*************************:** :*
hnRNP-Q1  SKGPDEAKIKALLERTGYTLDVTTGQRKYGGPPPDSVYSGQQPSVGTEIFVGKIPRDLFE  175
hnRNP-Q3  SKGPDEAKIKALLERTGYTLDVTTGQRKYGGPPPDSVYSGQQPSVGTEIFVGKIPRDLFE  175
hnRNP-Q2  SKGPDEAKIKALLERTGYTLDVTTGQRKYGGPPPDSVYSGQQPSVGTEIFVGKIPRDLFE  175
hnRNP-R   TKGPDEAKIKALLERTGYTLDVTTGQRKYGGPPPDSVYSGVQPGIGTEVFVGKIPRDLYE  178
           :*************************************** **.:***.*********:*
hnRNP-Q1  DELVPLFEKAGPIWDLRLMMDPLTGLNRGYAFVTFCTKEAAQEAVKLYNNHEIRSGKHIG  235
hnRNP-Q3  DELVPLFEKAGPIWDLRLMMDPLTGLNRGYAFVTFCTKEAAQEAVKLYNNHEIRSGKHIG  235
hnRNP-Q2  DELVPLFEKAGPIWDLRLMMDPLTGLNRGYAFVTFCTKEAAQEAVKLYNNHEIRSGKHIG  235
hnRNP-R   DELVPLFEKAGPIWDLRLMMDPLSGQNRGYAFITFCGKEAAQEAVKLCDSYEIRPGKHLG  238
           ***********************:* ******:*** ********** ::.:***.***:*
hnRNP-Q1  VCISVANNRLFVGSIPKSKTKEQILEEFSKVT---EGLTDVILYHQPDDKKKNRSFCFLE  292
hnRNP-Q3  VCISVANNRLFVGSIPKSKTKEQILEEFSKVT---EGLTDVILYHQPDDKKKNRSFCFLE  292
hnRNP-Q2  VCISVANNRLFVGSIPKSKTKEQILEEFSKVT---EGLTDVILYHQPDDKKKNRSFCFLE  292
hnRNP-R   VCISVANNRLFVGSIPKNKTKENILEEFSKVTGLTEGLVDVILYHQPDDKKKNRGFCFLE  298
           *****************.****:*********    ***.*************.*****
hnRNP-Q1  YEDHKTAAQARRRLMSGKVKVWGNVGTVEWADPIEDPDPEVMAKVKVLFVRNLANTVTEE  352
hnRNP-Q3  YEDHKTAAQARRRLMSGKVKVWGNVGTVEWADPIEDPDPEVMAKVKVLFVRNLANTVTEE  352
hnRNP-Q2  YEDHKTAAQ-------------------------------VKVLFVRNLANTVTEE  317
hnRNP-R   YEDHKSAAQARRRLMSGKVKVWGNVVTVEWADPVEEPDPEVMAKVKVLFVRNLATTVTEE  358
           *****:***                                **********.*.*****
hnRNP-Q1  ILEKAFSQFGKLERVKKLKDYAFIHFDERDGAVKAMEEMNGKDLEGENIEIVFAKPPDQK  412
hnRNP-Q3  ILEKAFSQFGKLERVKKLKDYAFIHFDERDGAVKAMEEMNGKDLEGENIEIVFAKPPDQK  412
hnRNP-Q2  ILEKAFSQFGKLERVKKLKDYAFIHFDERDGAVKAMEEMNGKDLEGENIEIVFAKPPDQK  377
hnRNP-R   ILEKSFSEFGKLERVKKLKDYAFVHFEDRGAAVKAMDEMNGKEIEGEEIEIVLAKPPDKK  418
           ****:**:*******************:**::*...*****:****.*:***:****.*:*
hnRNP-Q1  RKERKAQRQAAKNQMYDDYYYYGPPHMPPPTRGRGRGG-RGGYGYPPDYYGYEDYYD-YY  470
hnRNP-Q3  RKERKAQRQAAKNQMYDDYYYYGPPHMPPPTRGRGRGG-RGGYGYPPDYYGYEDYYD-YY  470
hnRNP-Q2  RKERKAQRQAAKNQMYDDYYYYGPPHMPPPTRGRGRGG-RGGYGYPPDYYGYEDYYD-YY  435
hnRNP-R   RKERQAARQASRSTAYEDYYYHPPPRMPPPIRGRGRGGGRGGYGYPPDYYGYEDYYDDYY  478
           ****:* ***::.  *:****: **:**** ******* ****************** **
hnRNP-Q1  GYDYHNYRGGYEDPYYGYED-FQVGARGRGGRGARGAAPS-RGRGAAPPRGRAGYSQRGG  528
hnRNP-Q3  GYDYHNYRGGYEDPYYGYED-FQVGARGRGGRGARGAAPS-RGRGAAPPRGRAGYSQRGG  528
hnRNP-Q2  GYDYHNYRGGYEDPYYGYED-FQVGARGRGGRGARGAAPS-RGRGAAPPRGRAGYSQRGG  493
hnRNP-R   GYDYHDYRGGYEDPYYGYDDGYAVRGRG-GGRGGRGAPPPPRGRGAPPPRGRAGYSQRGA  537
           *****:************:*  : * .** ****.***.*. ***** .************
hnRNP-Q1  P-GSARGVRGARGG-AQQQRGRGVKGVEAG----------------PDLLQ--------  561
hnRNP-Q3  P-GSARGVRGARGG-AQQQRGRGVRGARGGRGGNVGGKRKADGYNQPDSKRRQTNNQ-NW  585
hnRNP-Q2  P-GSARGVRGARGG-AQQQRGRGVRGARGGRGGNVGGKRKADGYNQPDSKRRQTNNQ-NW  550
hnRNP-R   PLGPPRGSRGGRGGPAQQQRGRGSRGSRGNRGGNVGGKRKADGYNQPDSKRRQTNNQQNW  597
           * *..** **.*** ******* :*  ...                  **  :
hnRNP-Q1  ------------------------------------
hnRNP-Q3  GSQPIAQQPLQ-GGDHSGNYGYKSENQEFYQDTFGQQWK  623
hnRNP-Q2  GSQPIAQQPLQ-GGDHSGNYGYKSENQEFYQDTFGQQWK  588
hnRNP-R   GSQPIAQQPLQQGGDYSGNYGYNNDNQEFYQDTYGQQWK  636
```

Supplemental Figure 4-1. Domain structures and sequences of hnRNP-Qs and hnRNP-R. **(A)** hnRNP-Q1, Q3 and R all contain three RRM motifs **(red in B)** and one RGG domain **(green in B)** for RNA and/or protein interaction. A major difference between hnRNP-Q1 and hnRNP-Q3/ R is that hnRNP-Q1 lacks a putative NLS found in the C-termimi of hnRNP-Q3 and hnRNP-R. **(B)** Isoforms of human hnRNP-Qs and hnRNP-R share over 80% similarity in their amino acid sequences.
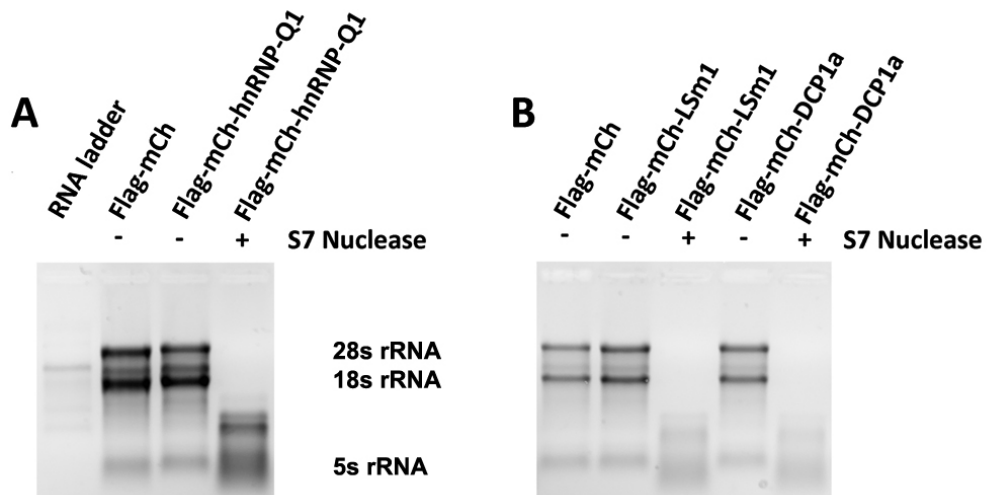
Supplemental Figure 4-2. Efficient elimination of endogenous RNAs by S7 nuclease treatment. **(A)**, for Flag-mCherry-hnRNP-Q1 immunoprecipitation and **(B)**, for Flag-mCherry-Dcp1a and LSm1 immunoprecipitations.
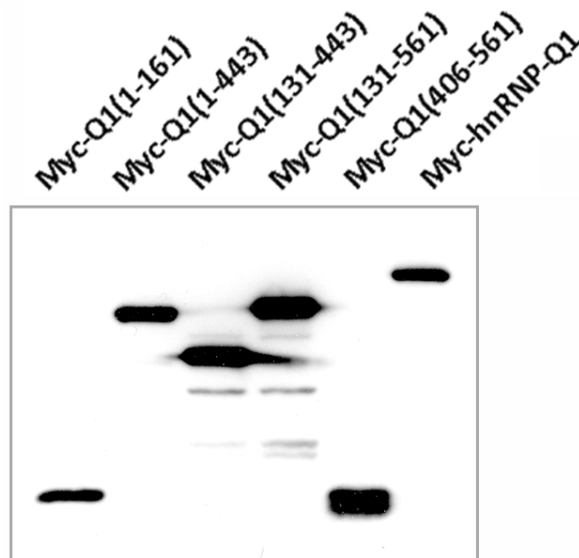
Supplemental Figure 4-3. Western blot analysis of immuprocipitated Myc-tagged proteins for mRNA quantification.
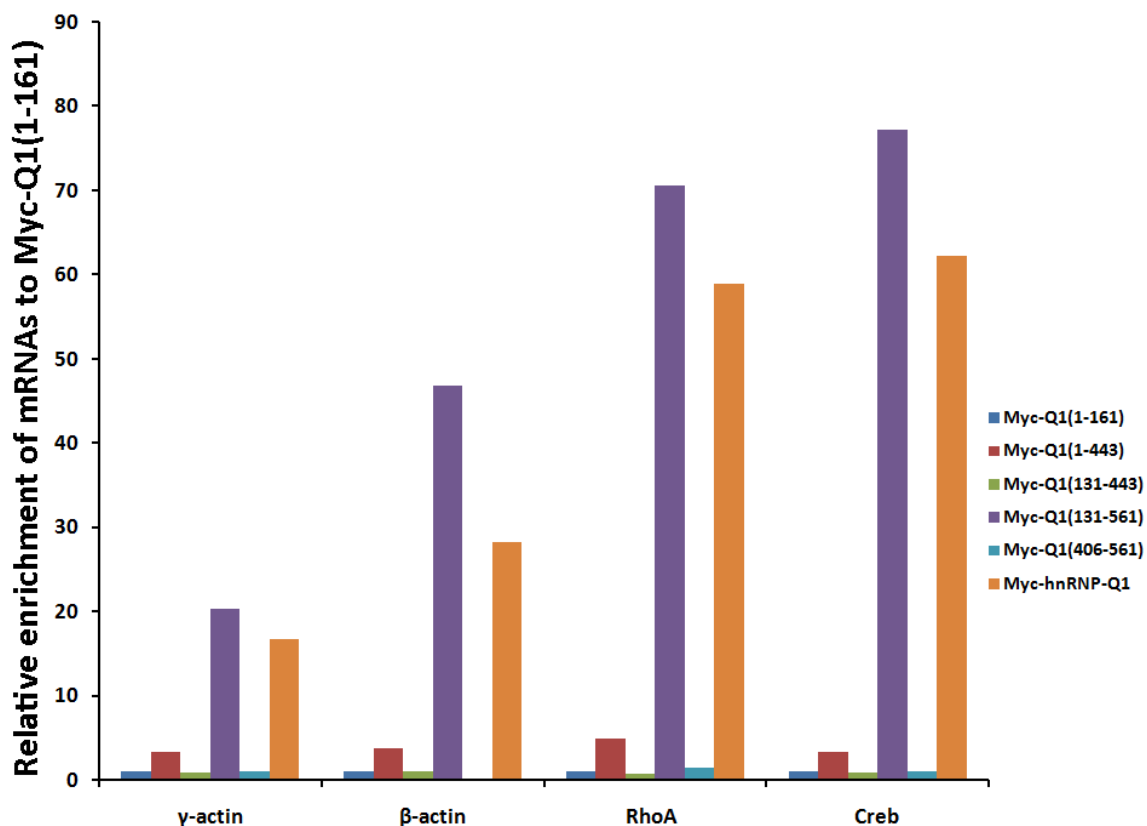
Supplemental Figure 4-4. Relative enrichment of mRNAs normalized to Myc-Q1(1-161) immuprecipitation pellet. Myc-Q1(131-561) and Myc-hnRNP-Q1(full-length) exhibited high (15 to 75 times enrichment) affinity to mRNAs analyzed, whereas Myc-Q1(1-443) exhibited low (3 to 5 times enrichment) mRNA affinity. No obvious mRNA enrichment was observed in Myc-Q1(131-443) and Myc-Q1(406-561) pellets.
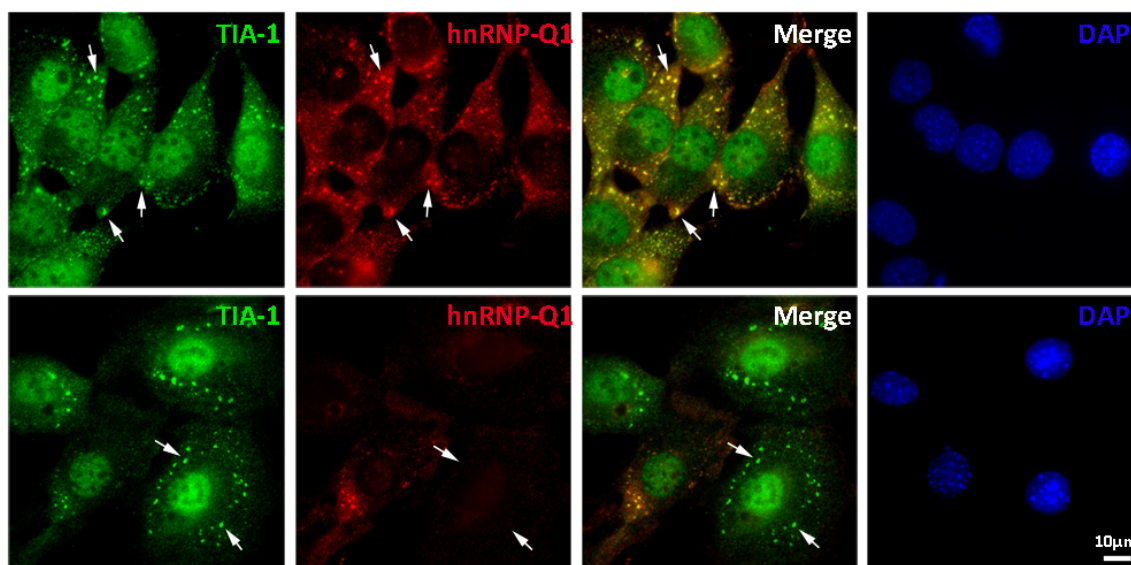
Supplemental Figure 4-5. Knockdown of hnRNP-Q1 did not affect the formation of arsenite-induced stress granules. Due to the availability of mouse-specific hnRNP-Q1 siRNA we performed this experiment on mouse myoblast C2C12 cells. C2C12 cells transfected with control siRNA (upper panel) or hnRNP-Q1 siRNA (lower panel) were treated with 5μM arsenite for 30 minutes to induce stress granules. TIA-1 and hnRNP-Q1 were detected by immunofluorescence staining.
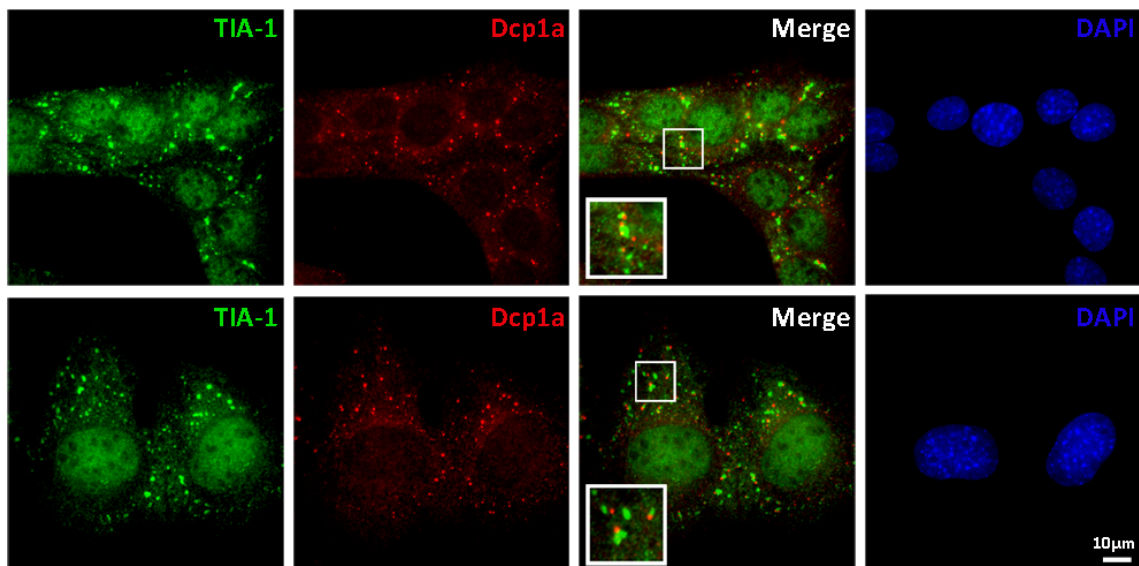
Supplemental Figure 4-6. Knockdown of hnRNP-Q1 did not affect P-body formation. C2C12 cells transfected with control siRNA (upper panel) or hnRNP-Q1 siRNA (lower panel) were treated with 5µM arsenite for 30 minutes before fixation for immunofluorescence staining. TIA-1 and Dcp1a were detected with a goat anti-TIA-1 and rabbit anti-Dcp1a. Since our hnRNP-Q1-specific antibody is also from rabbit, we did not perform co-immunostaining of Dcp1a and hnRNP-Q1. As seen in **Supplemental Figure 4-4**, we achieved efficient hnRNP-Q1 knockdown in C2C12 cells. We did not observe any effect of hnRNP-Q1 knockdown on the number of P-bodies nor the association of P-bodies with stress granules. Example images from both groups were shown here.
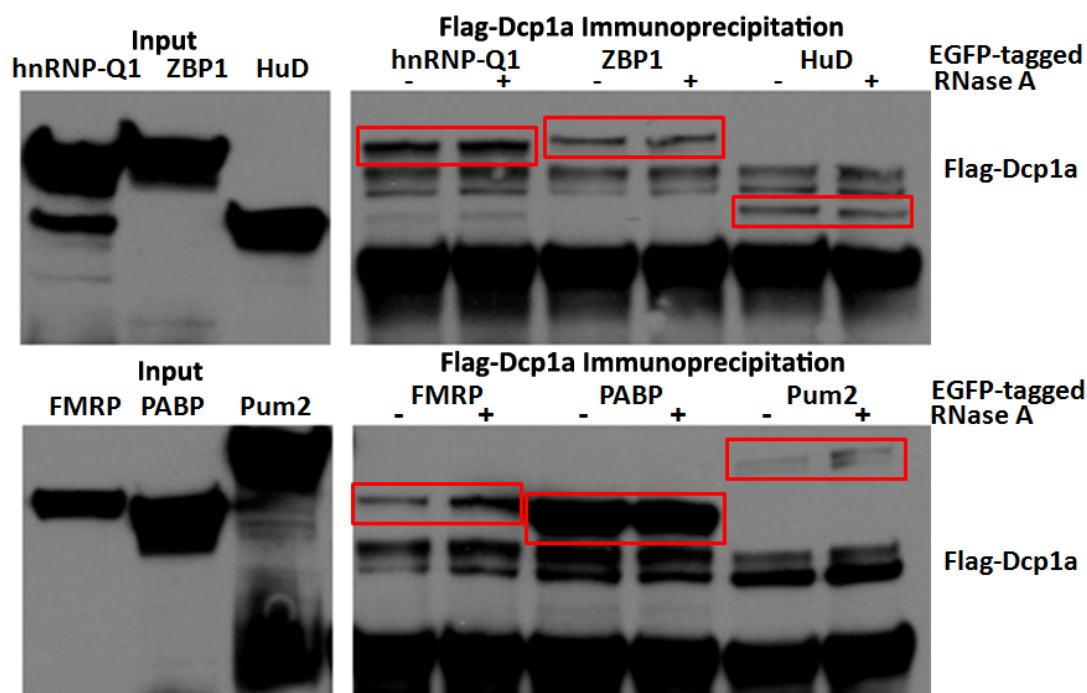
Supplemental Figure 4-7. Co-immonuprecipitation of EGFP-tagged hnRNP-Q1, Zbp1, HuD, FMRP, PABPC1 and Pumilio2 (Pum2) with Dcp1a. 293T cells were transfected with indicated plasmids expressing EGFP-tagged proteins and Flag-Dcp1a. Flag-tagged proteins were immunoprecipitated and EGFP and Flag-tagged proteins were detected by western blot with anti-GFP or Flag antibodies. To test whether the protein interaction is RNA-dependent or not, protein samples were treated in parallel with or without RNaseA prior to immunoprecipitation.

Chapter V

Summary and Future Directions

Summary

The thesis objectives were to investigate the localization, functions and mechanisms of SMN and hnRNQ-1. An overall hypothesis guiding this work is that diverse types of messenger ribonucleoprotein (mRNP) complexes exist in the cytoplasm as RNA granules to enable the compartmentalization and regulation of mRNA expression. Here we describe the presence of RNA granules containing SMN and hnRNP-Q1 in axons, which support a non-canonical role of SMN in axonal mRNA regulation. SMN has been proposed to play diverse roles in the posttranscriptional regulation of gene expression, including mRNA localization and translational regulation, the loss of which may at least in part contribute to the pathogenesis of SMA. This hypothesis is derived from several observations: (1) SMN is localized to growth cones and actively transported within neuronal processes, indicating its possible function in axonal mRNA transport (Zhang et al., 2003); (2) SMN is colocalized with ribosomal RNA and poly(A) mRNAs indicating a possible role of SMN in translational regulation (Zhang et al., 2007; Zhang et al., 2003); (3) SMN interacts with a number of mRNA binding proteins, such as hnRNP-Qs/R, KSRP and FMRP, suggesting the involvement of SMN in mRNA regulation through RNA binding proteins (Mourelatos et al., 2001; Piazzon et al., 2008; Rossoll et al., 2002; Tadesse et al., 2008); (4) the loss of SMN in motor neurons leads to defects in growth cone localization of β-actin mRNA and loss of β-actin enrichment in growth cones (Rossoll et al., 2003) and (5) the developmental defects in axon guidance observed in zebrafish SMA model are snRNP assembly-independent (Carrel et al., 2006). An early objective of my thesis studies was to further test this hypothesis, and ultimately to provide sufficient experimental evidence for a

molecular mechanism underlying the role of SMN in mRNA localization and/or translation.

Initially, my thesis studies were focused on the characterization of the SMN protein complex, which may be involved in the proposed function of SMN in mRNA regulation. We hypothesized that the well-characterized SMN-Gemin complex is also localized to neuronal processes, where SMN may plays its role in regulating mRNA transport and/or translation. To test this hypothesis, we first focused on the characterization of the composition of SMN-containing granules in growth cones and distal axons (Zhang et al., 2006). Using quantitative fluorescent microscopy, we observed partial but non-random colocalization of SMN with Gemin2 and Gemin3 in neuronal growth cones using quantitative colocalization analysis in deconvolved 3D reconstructions, suggesting the existence of other SMN complexes within axons that do not contain Gemin proteins **(Chapter II, Figure 2-1, 2-2 and 2-3)**. Using live cell imaging experiments, we observed that fluorescent protein-tagged SMN and Gemin2 were colocalized and cotransported in neuronal processes **(Chapter II, Figure 2-5)**. Overexpressed SMN and Gemin2 were physically associated as tested by FRET analysis **(Chapter II, Figure 2-6)**. In addition, we showed that SMN granules in motor neuron axons were free of spliceosomal Sm proteins, further suggesting an additional function of SMN in axons other than snRNP assembly (Zhang et al, 2006) **(Chapter II, Figure 2-4)**.

SMN has been shown to associate with a number of RNA binding proteins known to be involved in posttranscriptional regulation of mRNAs, including hnRNP-Qs/R, FMRP, KSRP (Zbp2), TIA-1, Zbp1 and HuD (Hua and Zhou, 2004; Mourelatos et al., 2001; Piazzon et al., 2008; Rossoll et al., 2002; Tadesse et al., 2008). Among these

proteins, hnRNP-Qs/R directly interact with SMN (Mourelatos et al., 2001; Rossoll et al., 2002) and are implicated in mRNA localization in the central nervous system (Kanai et al., 2004; Mourelatos et al., 2001; Rossoll et al., 2002). We hypothesized that SMN may act as a chaperone to facilitate the assembly of specific mRNA binding proteins i.e. hnRNP-Qs onto their target mRNAs, which could be essential for the assembly of RNA transport granules. Therefore we first investigated whether SMN granules associate with hnRNP-Qs in neuronal processes. The possible association of SMN with any mRNA binding proteins in neuronal processes had not been studied yet. Our results showed that SMN was partially colocalized with hnRNP-Qs in neuronal processes **(Chapter II, Figure 2-9A)**. Live cell imaging analysis showed that mRNP-SMN and EGFP-hnRNP-Q1 were colocalized in neuritic granules and cotransported in neuronal processes **(Chapter II, Figure 2-10)**. We also confirm the biochemical interaction of SMN with hnRNP-Q1 **(Chapter II, Figure 2-9B)**.

Previous studies have proposed that hnRNP-Qs are functional components for several aspects of mRNA regulation, such as RNA editing, mRNA transport, decay and translational regulation (Blanc et al., 2001; Cho et al., 2007; Kanai et al., 2004; Kim et al., 2007; Mourelatos et al., 2001); however, such functions of hnRNP-Qs have not been studied in detail. In the second part of my thesis study, we mainly focused on the functional analysis of hnRNP-Qs and expected that results from this study might set up a platform for future SMN studies, particularly to examine the effects of loss of SMN on the function of hnRNP-Qs.

We could show that hnRNP-Q1, but not hnRNP-Q2/3 or hnRNP-R, was present in purified axonal fractions and synaptoneurosomes **(Chapter III, Figure 3-1).** This

observation indicates that hnRNP-Q1 is the functional isoform of hnRNP-Qs in the cytoplasm. We generated an hnRNP-Q1-specific antibody and could show by fluorescent immunostaining that hnRNP-Q1 was localized in granules in both axons and dendrites and was associated with microtubules **(Chapter III, Figure 3-2)**. Additionally, we characterized the localization of hnRNP-Q1 in different mRNP granules. Our results show that hnRNP-Q1 is a component of transport mRNP granules, stress granules and P-bodies **(Chapter IV, Figure 4-3, 4-4, 4-5 and 4-6A)**, suggesting a potential function of hnRNP-Q1 in regulating mRNA dynamics among these mRNP granules. Our results show that hnRNP-Q1 physically associates with P-body protein Dcp1a and LSm1 in an RNA-independent manner **(Chapter IV, Figure 4-5 and 4-7)**, whereas the interaction with RNA binding proteins is RNA dependent **(Chapter IV, Figure 4-2A)**. This work suggests that hnRNP-Q1 may not simply shuttle mRNAs into P-bodies in a passive manner, but may have direct interactions with P-body enzymes involved in mRNA decay within this structure. This study provides additional information that may be helpful for the understanding of the biological functions of hnRNP-Q1.

The function of hnRNP-Q1 was analyzed by hnRNP-Q1 knockdown in both mature neurons and myoblastoma C2C12 cells. Mature neurons transfected with hnRNP-Q1 siRNA exhibited a reduced density of dendritic spines. In C2C12 cells, enhanced cell spreading and focal adhesion formation were observed after hnRNP-Q1 knockdown **(Chapter III, Figure 3-3, 3-5 and 3-8)**. The observed defects in cell morphology after hnRNP-Q1 knockdown in mature neurons and C2C12 cells mimic structural changes induced by small GTPase-RhoA activation. In support of a possible role of the RhoA/ROCK pathway for cell-morphological phenotypes after hnRNPQ1 knockdown,

we could rescue the spine defect in neurons with a ROCK inhibitor, Y-27632 **(Chapter III, Figure 3-3)**. Biochemical analyses showed that RhoA mRNA is selectively enriched in immunoprecipitated hnRNP-Q1 complexes **(Chapter III, Figure 3-3)**, and that hnRNP-Q1 functions as a translation repressor in regulating RhoA mRNA translation. Knockdown of hnRNP-Q1 in C2C12 cells leads to enhanced RhoA mRNA translation and upregulated RhoA expression **(Chapter III, Figure 3-9 and 3-11)**. In addition, the degradation of RhoA mRNA is facilitated in C2C12 cells after hnRNP-Q1 depletion **(Chapter III, Figure 3-10)**. Further analyses suggested that the increased decay rate of RhoA in hnRNP-Q1-deficient C2C12 cells is a consequence of enhanced translation, since it was abolished by the treatment with the translation inhibitor, anisomycin. This finding suggest a use-dependent decay mechanism involved in hnRNP-Q1 mediated regulation of RhoA mRNA, which has been described for other mRNAs. With this study, we provide the first evidence for the physiological function of hnRNP-Q1 in the regulation of cell morphogenesis and cell motility **(Figure 5-1)**. In addition, our results demonstrate a novel regulatory mechanism for RhoA, which is mediated through hnRNP-Q1 by repressing RhoA mRNA translation and modulating RhoA protein levels **(Figure 5-1)**.

In summary, my thesis research supports our hypothesis the SMN plays a role in mRNA regulation, particularly in axonal mRNA transport and local translation. In addition, our results suggest a molecular basis for this SMN function. Our results suggest that SMN may facilitate the assembly of hnRNP-Q1 mRNP granules and regulate the dynamic shuttling of hnRNP-Q1 and its associate mRNAs between specific mRNP granules and thus modulating mRNA metabolism. Second, my studies provided the first

evidence for the function of hnRNP-Q1 in cellular morphogenesis. We propose that future work may show that SMN is a contributor functions mediated by hnRNP-Q1. Additionally, my studies revealed a novel mechanism for the regulation of RhoA. The role of hnRNP-Q1 in repressing RhoA mRNA translation constitutes a key component for this regulatory pathway (see model in **Figure 5-1**).

Future directions

The results presented in my dissertation provide new insights into the biological functions of SMN and hnRNP-Q1. Our findings therefore represent a basis for future studies to advance the knowledge about the underlying mechanisms.

Biochemical characterization of axonal SMN granules

The composition of SMN-containing granules has been characterized in Hela cells (Gubitz et al., 2004). Through these studies, a number of proteins including Gemin proteins (Gemin2-8) and Unrip have been shown to directly interact with SMN or indirectly associate with SMN through one of these proteins (Gubitz et al., 2004; Kolb et al., 2007). This SMN-Gemin complex is essential for the efficient assembly of spliceosomes in the cytoplasm and subsequent translocation into the nucleus (Kolb et al., 2007). In addition to its somatic and nuclear localization, SMN in granules can also be detected in axons and growth cones in primary neurons (Tadesse et al., 2008; Zhang et al., 2006; Zhang et al., 2003). In the current study, we investigated the composition of axonal SMN granules with high resolution microscopy and found that Gemin2 and Gemin3 are absent from a subfamily of SMN granules in growth cones **(Chapter II, Figure 2-1 and 2-2)**, suggesting the presence of an additional type of SMN complexes free of Gemin

proteins, which may possibly have non-canonical functions. One shortcoming of conventional microscopic studies is that only proteins which have been previously identified as SMN interacting partners can be analyzed and results provide only limited implications. Thus, a proteomic characterization of axonal SMN granules would be of great importance for the understanding of SMN functions in axons, particularly its potential role in axonal mRNA transport and local translation. Such analyses could address several questions of interest, e.g. whether axonal SMN granules contain unique components, which are not present in somatic and nuclear granules and thus might be essential for their localization and functions in axons. A major challenge for this study has been that insufficient amounts of experimental material could be obtained with adequate purity. During my thesis study, we have established a novel cell culture system that allows the large scale isolation of axonal compartments free of contaminants from cell bodies and dendrites. These axonal fractions have been used to test the axonal localization of hnRNP-Q isoforms by western blot analysis **(Chapter III, Figure 3-1)**. SMN complexes can be specifically enriched by immunoprecipitation from axonal fractions with anti-SMN antibodies and resolved by SDS-PAGE for proteomic analysis to identify protein factors. We expect such further studies would reveal the identity of axonal SMN granules and provide further insight into its functions in axons, which have been suggested to be involved in the pathogenesis of SMA.

Functional analysis of the possible role SMN in mRNA regulation

Besides of its function in spliceosome assembly, SMN has been proposed to play a role in mRNA regulation which might be mediated by the interaction of SMN with RNA binding proteins (Rossoll and Bassell, 2009). hnRNP-Q1 is one of these proteins

which have been shown to directly interact with SMN (Mourelatos et al., 2001; Rossoll et al., 2002). However, the studies of this novel function of SMN have been progressing slowly, mainly due to the unavailability of a functional test to analyze the role of SMN in mRNA granule assembly, translation, stability and/or transport. Thus, we focused to identify a novel function of the SMN binding protein and granule partner, hnRNP-Q1. Here, we identify RhoA mRNA as a novel target of hnRNP-Q1 and find that hnRNP-Q1 negatively regulates RhoA translation (**Chapter III, Figure 3-9 and 3-11**). Thus, we can now test the possible involvement of SMN in this regulatory event by examining the effect of loss of SMN on the specific association of hnRNP-Q1 with RhoA mRNA and the inhibitory function of hnRNP-Q1 on RhoA translation in neurons cultured from SMA and wild type mice. In fact, a recent study shows that SMN depletion in PC12 cells leads to an upregulation of RhoA protein which causes defective neuritogenesis, suggesting a role of SMN in the regulation of RhoA expression (Bowerman et al., 2007). Studies conducted in a type of SMA mice by the same group have shown that RhoA activity was elevated in spinal cords compared with wild-type spinal cords at the stage when SMA phenotypes start to appear (Bowerman et al., 2010). Administration of ROCK inhibitor Y-27632 dramatically increased the survival rate of SMA mice. Such RhoA/ROCK signaling blockage partially rescued defective neuromuscular junction maturation of SMA mice, suggesting that the elevated RhoA/ROCK signaling contribute to the pathogenesis of SMA. However, the underlying mechanism of increased RhoA activity found in SMA spinal cords is still not understood. Our proposed experiments might provide further mechanistic understanding for this SMN function.

Identification of additional mRNA targets of hnRNP-Q1

We have shown that mRNAs encoding RhoA, Creb and Gap43 are enriched in hnRNP-Q1 immuprecipitation pellets, but not mRNAs for γ-actin, Gapdh and β-tubulin **(Chapter III, Figure 3-3)**, suggesting that a group of mRNAs are selectively associated with hnRNP-Q1. Although we observed that knockdown of hnRNP-Q1 leads to the upregulated RhoA protein expression **(Chapter III, Figure 9A)** which contributes to the reduced spine density in mature neurons, as well as enhanced cell spreading and focal adhesion formation in C2C12 cells, we cannot exclude the possibility that the deregulation of other mRNAs may also contribute to these observed defects or to some other as yet uncharacterized phenotypes. Furthermore, our results showing that hnRNP-Q1 is localized to P-bodies **(Chapter IV, Figure 4-5)** suggest additional functions of hnRNP-Q1 apart from translational regulation. The localization of RNA binding proteins to P-bodies has been proposed as a mechanism for RNA binding protein-mediated mRNA decay, particularly through several mRNA destabilizing factors, such as TTP and BRF1, by which mRNAs are routed to P-bodies for rapid degradation (Franks and Lykke-Andersen, 2007). Although current studies suggest a role of hnRNP-Q1 in RNA stabilization (Grosset et al., 2000; Weidensdorfer et al., 2009), our results imply that the degradation of a subset of hnRNP-Q1 binding mRNAs might be facilitated by the localization of hnRNP-Q1 to P-bodies. Thus, a genome-wide identification of hnRNP-Q1 mRNA targets paired with functional studies will be necessary for the comprehensive understanding of the role of hnRNP-Q1 in mRNA regulation. A cDNA microarray analysis following hnRNP-Q1 immunoprecipitation might be used for this analysis; the same method has been employed for the identification of FMRP binding mRNAs (Brown et al., 2001). One limitation of this technique is that mRNAs indirectly associated with

hnRNP-Q1 may also be co-precipitated, thus leading to a high signal/noise ratio. The ultraviolet cross-linking and immunoprecipitation (CLIP) experiment may help to overcome this flaw of the conventional immunoprecipitation-microarray system. The CLIP method has been used to identified mRNA targets and binding sites for the RNA binding proteins Nova and Argonaute (Chi et al., 2009; Ule et al., 2003). This method advances the identification of mRNAs associated with specific RNA binding proteins in a couple of ways. First, by UV cross-linking, the *in vivo* interactions of mRNAs and RNA binding proteins are preserved which avoids artifacts incurred by mRNPs reorganization in cell lysates. Second, in addition to the identification of mRNA targets, CLIP allows a direct identification of binding motifs for a RNA binding protein. After UV cross-linking, cell lysates are treated with a small amount of RNase to reduce the length of mRNA fragments, which are co-immunoprecipitated with the respective RNA binding protein. Subsequent sequencing reveals the sequence information of immunoprecipitated mRNA fragments containing binding motifs for the RNA binding protein of interest. With either of these two methods, we can identify novel mRNA targets of hnRNP-Q1 and might also be able to resolve the molecular bases for their interactions. Results from such studies will be beneficial for the understanding of the functions of hnRNP-Q1 in mRNA regulation and the underlying mechanisms for phenotypes caused by hnRNP-Q1 or SMN depletion.

Functions of hnRNP-Q1 in mRNA transport and local translational regulation

As mentioned previously, a function of hnRNP-Q1 in axonal mRNA localization has been suggested by several lines of evidence. Firstly, hnRNP-Q1 is a component of neuronal transport mRNP granules (Kanai et al., 2004) and overexpressed fluorescent

protein-tagged hnRNP-Q1 exhibits active bidirectional movement in neuronal processes **(Chapter IV, Figure 4-3)** (Bannai et al., 2004). Secondly, we observed that mRNAs encoding RhoA, Creb and Gap43 are selectively enriched in hnRNP-Q1 immunoprecipitation pellets **(Chapter III, Figure 3-3)**. These mRNAs have been shown to be localized to growth cones of neurons and locally translated, suggesting that hnRNP-Q1 may also associate with these mRNAs in axons. Thirdly, our results in the current study show that hnRNP-Q1 negatively regulates RhoA mRNA translation **(Chapter III, Figure 3-9 and 3-11)**. A translationally dormant status has been demonstrated to be prerequisite for efficient mRNA transport in several studies (Chekulaeva et al., 2006; Nakamura et al., 2004). The inhibitory function of hnRNP-Q1 may be removed by phosphorylation on several sites of hnRNP-Q1. In fact, hnRNP-Q1 is highly tyrosine-phosphorylated in adipocytes when treated with insulin (Hresko and Mueckler, 2002). One possible consequence is that hnRNP-Q1 phosphorylation may abolish its ability for mRNA binding and thus relief the inhibitory effects. A similar model has been suggested for the function of Src tyrosine kinase and Zbp1 in regulating β-acin mRNA localization and local translation (Huttelmaier et al., 2005). This possible function of hnRNP-Q1 in mRNA localization can be investigated in neurons after hnRNP-Q1 depletion. The levels of mRNAs in growth cones can be examined by fluorescent in situ hybridization in neurons or qRT-PCR analysis with purified axonal fractions. Together with the identification of hnRNP-Q1 targets and binding motifs, this study might provide important mechanistic insights into the axonal localization of RhoA, Creb, Gap43, and possibly some other novel hnRNP-Q1 binding mRNAs.

Mechanisms underlying the hnRNP-Q1 function in regulating of RhoA mRNA translation

Several mechanisms have been suggested for the function of RNA binding proteins in translation inhibition, such as by interacting with eIF4E binding proteins (Nakamura et al., 2004; Napoli et al., 2008; Nelson et al., 2004), interfering with the recruitment of 60s ribosomes (Deng et al., 2008; Huttelmaier et al., 2005) and recruiting non-coding small RNAs (Kim et al., 2009). In addition to these known mechanisms, we propose that the interaction of hnRNP-Q1 with P-body proteins (Dcp1a and LSm1) may play a role for the function of hnRNP-Q1 in regulating translation (**Chapter IV, Discussion**). To test this hypothesis, we will examine effects of the disruption of hnRNP-Q1/P-body protein interactions, for example by overexpressing the RGG domain of hnRNP-Q1 in cells. We have shown that the RGG domain is essential for the interaction of hnRNP-Q1 with Dcp1a and the RGG domain alone exhibits no obvious RNA binding ability (**Chapter IV, Figure 4-5, 4-2B and Supplemental Figure 4-3**). Thus, overexpression of the RGG domain will not interfere with the association of hnRNP-Q1 with mRNAs but possibly abolish the interaction with Dcp1a. However, to fully understand the mechanisms for the function of hnRNP-Q1 in translation regulation, it will be necessary to identify other possible binding partners of hnRNP-Q1, such as factors involved in translation initiation and/or miRNAs.

Lastly, future studies will be to general animal models deficient in hnRNP-Q1. We anticipate that an animal model will be critical for continued studies on the molecular mechanisms of hnRNP-Q1 in mRNA granule regulation in vivo. This thesis research using in vitro models predicts that there may be serious developmental defects in vivo. If

a knockout is lethal, we would examine phenotypes in heterozygous mice, or make inducible and conditional loss of function mutants using Cre mediated recombination and appropriate drivers. It will be interesting to look for defects in the development and plasticity of the nervous system, including analysis of dendritic spine development and axonal guidance. In addition, we might predict some phenotypes in axon regeneration, where Rho signaling is essential. These continued studies on hnRNP-Q1 mediated regulation of mRNA expression have broader implications to the study to numerous other mRNA binding proteins which function in cellular morphogenesis and are affected in human disease.

A WT cells
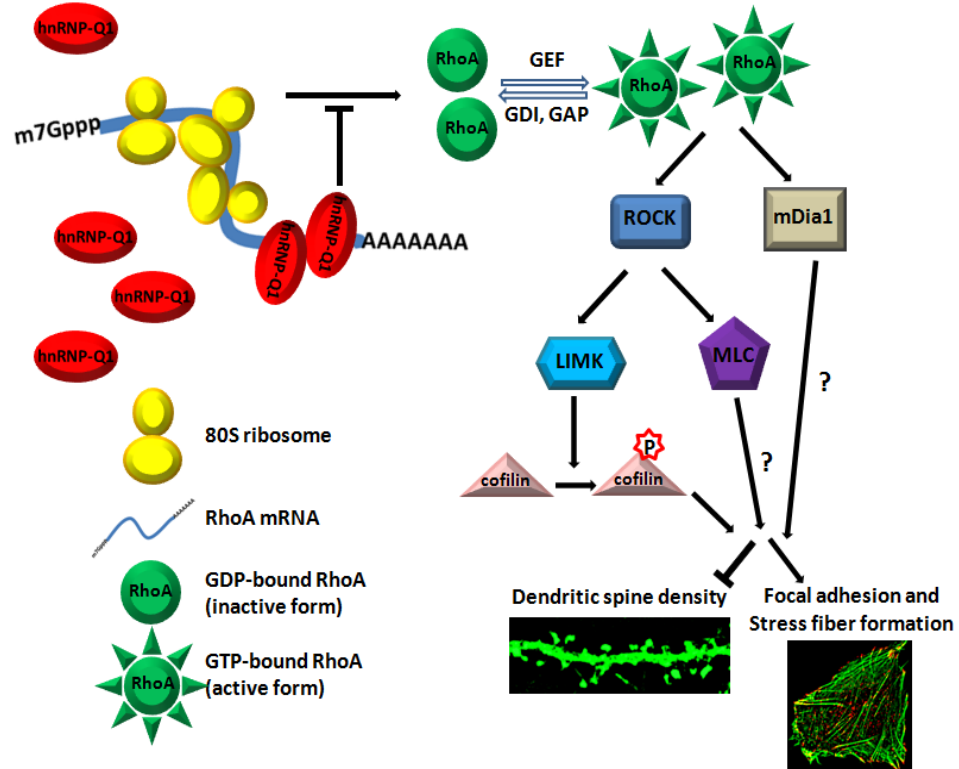
B hnRNP-Q1 depleted cells

80S ribosome

RhoA mRNA

GDP-bound RhoA (inactive form)

GTP-bound RhoA (active form)

GEF

GDI, GAP

RhoA

ROCK

mDia1

LIMK

MLC

cofilin

cofilin

Dendritic spine density

Focal adhesion and Stress fiber formation

(Reduced) Dendritic spine density

(Enhanced) Focal adhesion and Stress fiber formation

m7Gppp

AAAAAAA
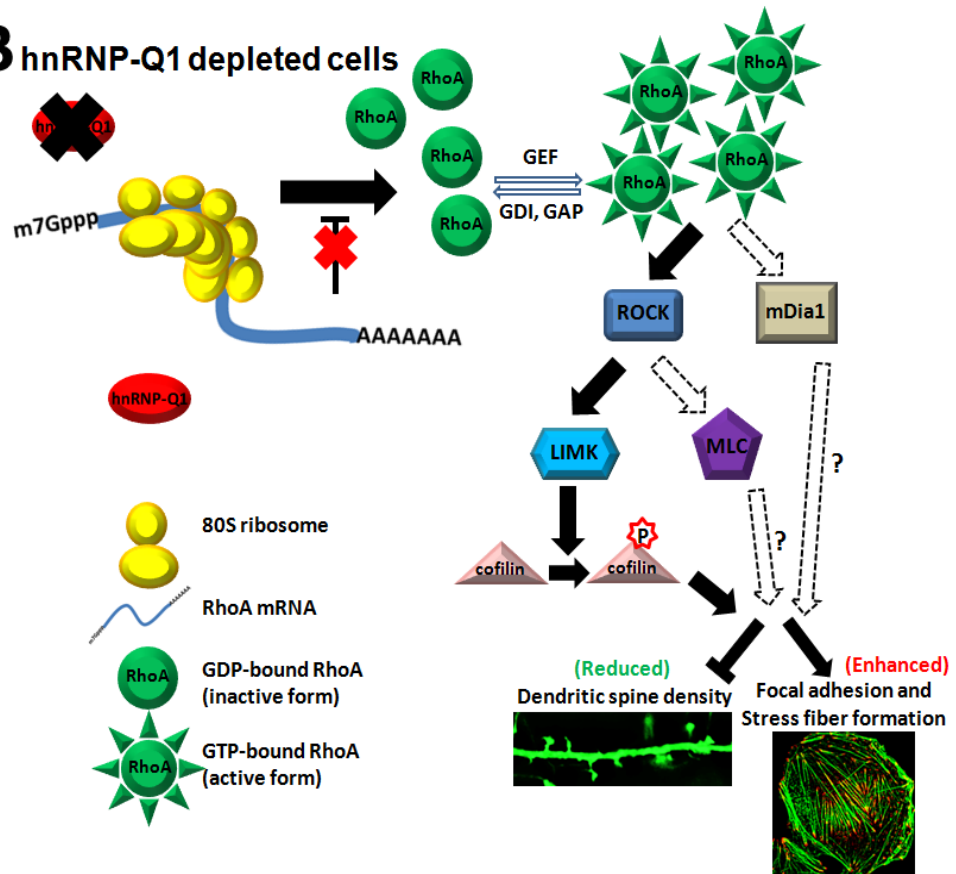
hnRNP-Q1

Figure 5-1. The role of hnRNP-Q1 in regulating the RhoA/ROCK signaling pathway. hnRNP-Q1 functions as a translation repressor for RhoA mRNA, thus modulates RhoA protein expression levels. (A) In normal cells, the expression of RhoA is tightly controlled by hnRNP-Q1 through translation repression and translation dependent mRNA decay. The activity of RhoA is balanced by the presence of RhoA regulators, such as GEF which activates RhoA, and GDI and GAP which inactivates RhoA (Sinha and Yang, 2008). This well-balanced RhoA activity is essential for proper cellular morphogenesis, such as (inhbiting) dendritic spine genesis and (promoting) stress fiber and focal adhesion formation (Govek et al., 2005; Hall, 1998). Such a function of RhoA is mediated through ROCK/LIMK/Cofilin; possibly MLC and mDia1 pathways are also involved (Govek et al., 2005; Narumiya et al., 2009). (B) In cells with hnRNP-Q1 depletion, the inhibition on RhoA mRNA translation is relieved, thus leading to upregulated RhoA expression and RhoA activity. In my dissertation studies, we observed that knockdown of hnRNP-Q1 incurs an upregulated activation of the RhoA/ROCK signaling pathway and thus leads to a reduced spine density in mature neurons and enhance stress fiber and focal adhesion formation in C2C12 cells. I predict that MLC and mDia1 pathways might also be unregulated in these cells.

Chapter VI

References

Amano, T., Tanabe, K., Eto, T., Narumiya, S., and Mizuno, K. (2001). LIM-kinase 2 induces formation of stress fibres, focal adhesions and membrane blebs, dependent on its activation by Rho-associated kinase-catalysed phosphorylation at threonine-505. Biochem J *354*, 149-159.

Anastasiadis, P.Z., Moon, S.Y., Thoreson, M.A., Mariner, D.J., Crawford, H.C., Zheng, Y., and Reynolds, A.B. (2000). Inhibition of RhoA by p120 catenin. Nat Cell Biol *2*, 637-644.

Anderson, P. (2008). Post-transcriptional control of cytokine production. Nat Immunol *9*, 353-359.

Anderson, P., and Kedersha, N. (2008). Stress granules: the Tao of RNA triage. Trends Biochem Sci *33*, 141-150.

Anderson, P., and Kedersha, N. (2009a). RNA granules: post-transcriptional and epigenetic modulators of gene expression. Nat Rev Mol Cell Biol *10*, 430-436.

Anderson, P., and Kedersha, N. (2009b). Stress granules. Curr Biol *19*, R397-398.

Antar, L.N., Afroz, R., Dictenberg, J.B., Carroll, R.C., and Bassell, G.J. (2004). Metabotropic glutamate receptor activation regulates fragile x mental retardation protein and FMR1 mRNA localization differentially in dendrites and at synapses. J Neurosci *24*, 2648-2655.

Antar, L.N., Li, C., Zhang, H., Carroll, R.C., and Bassell, G.J. (2006). Local functions for FMRP in axon growth cone motility and activity-dependent regulation of filopodia and spine synapses. Mol Cell Neurosci *32*, 37-48.

Arce, V., Garces, A., de Bovis, B., Filippi, P., Henderson, C., Pettmann, B., and deLapeyriere, O. (1999). Cardiotrophin-1 requires LIFRbeta to promote survival of mouse motoneurons purified by a novel technique. J Neurosci Res *55*, 119-126.

Arthur, W.T., and Burridge, K. (2001). RhoA inactivation by p190RhoGAP regulates cell spreading and migration by promoting membrane protrusion and polarity. Mol Biol Cell *12*, 2711-2720.

Bakheet, T., Williams, B.R., and Khabar, K.S. (2003). ARED 2.0: an update of AU-rich element mRNA database. Nucleic Acids Res *31*, 421-423.

Bakheet, T., Williams, B.R., and Khabar, K.S. (2006). ARED 3.0: the large and diverse AU-rich transcriptome. Nucleic Acids Res *34*, D111-114.

Balagopal, V., and Parker, R. (2009). Polysomes, P bodies and stress granules: states and fates of eukaryotic mRNAs. Curr Opin Cell Biol *21*, 403-408.

Bannai, H., Fukatsu, K., Mizutani, A., Natsume, T., Iemura, S., Ikegami, T., Inoue, T., and Mikoshiba, K. (2004). An RNA-interacting protein, SYNCRIP (heterogeneous nuclear ribonuclear protein Q1/NSAP1) is a component of mRNA granule transported with inositol 1,4,5-trisphosphate receptor type 1 mRNA in neuronal dendrites. J Biol Chem *279*, 53427-53434.

Barnard, D.C., Ryan, K., Manley, J.L., and Richter, J.D. (2004). Symplekin and xGLD-2 are required for CPEB-mediated cytoplasmic polyadenylation. Cell *119*, 641-651.

Barreau, C., Paillard, L., and Osborne, H.B. (2005). AU-rich elements and associated factors: are there unifying principles? Nucleic Acids Res *33*, 7138-7150.

Bashkirov, V.I., Scherthan, H., Solinger, J.A., Buerstedde, J.M., and Heyer, W.D. (1997). A mouse cytoplasmic exoribonuclease (mXRN1p) with preference for G4 tetraplex substrates. J Cell Biol *136*, 761-773.

Bassell, G.J., and Warren, S.T. (2008). Fragile X syndrome: loss of local mRNA regulation alters synaptic development and function. Neuron *60*, 201-214.

Bassell, G.J., Zhang, H., Byrd, A.L., Femino, A.M., Singer, R.H., Taneja, K.L., Lifshitz, L.M., Herman, I.M., and Kosik, K.S. (1998a). Sorting of beta-actin mRNA and protein to neurites and growth cones in culture. J Neurosci *18*, 251-265.

Bassell, G.J., Zhang, H.L., Byrd, A.L., Femino, A.M., Singer, R.H., Taneja, K.L., Lifshitz, L.M., Herman, I.M., and Koisk, K.S. (1998b). Sorting of beta actin mRNA and protein to neurites and growth cones in culture. Journal of Neuroscience *18*, 251-265.

Battaglia, G., Princivalle, A., Forti, F., Lizier, C., and Zeviani, M. (1997). Expression of the SMN gene, the spinal muscular atrophy determining gene, in the mammalian central nervous system. Hum Mol Genet *6*, 1961-1971.

Battle, D.J., Kasim, M., Yong, J., Lotti, F., Lau, C.K., Mouaikel, J., Zhang, Z., Han, K., Wan, L., and Dreyfuss, G. (2006a). The SMN complex: an assembly machine for RNPs. Cold Spring Harb Symp Quant Biol *71*, 313-320.

Battle, D.J., Lau, C.K., Wan, L., Deng, H., Lotti, F., and Dreyfuss, G. (2006b). The Gemin5 protein of the SMN complex identifies snRNAs. Mol Cell *23*, 273-279.

Bechade, C., Rostaing, P., Cisterni, C., Kalisch, R., La Bella, V., Pettmann, B., and Triller, A. (1999). Subcellular distribution of survival motor neuron (SMN) protein:

possible involvement in nucleocytoplasmic and dendritic transport. Eur J Neurosci *11*, 293-304.

Bechara, E.G., Didiot, M.C., Melko, M., Davidovic, L., Bensaid, M., Martin, P., Castets, M., Pognonec, P., Khandjian, E.W., Moine, H*., et al.* (2009). A novel function for fragile X mental retardation protein in translational activation. PLoS Biol *7*, e16.

Berleth, T., Burri, M., Thoma, G., Bopp, D., Richstein, S., Frigerio, G., Noll, M., and Nusslein-Volhard, C. (1988). The role of localization of bicoid RNA in organizing the anterior pattern of the Drosophila embryo. Embo J *7*, 1749-1756.

Bernstein, P.L., Herrick, D.J., Prokipcak, R.D., and Ross, J. (1992). Control of c-myc mRNA half-life in vitro by a protein capable of binding to a coding region stability determinant. Genes Dev *6*, 642-654.

Bertrand, E., Chartrand, P., Schaefer, M., Shenoy, S.M., Singer, R.H., and Long, R.M. (1998). Localization of ASH1 mRNA particles in living yeast. Mol Cell *2*, 437-445.

Besse, F., and Ephrussi, A. (2008). Translational control of localized mRNAs: restricting protein synthesis in space and time. Nat Rev Mol Cell Biol *9*, 971-980.

Besson, A., Gurian-West, M., Schmidt, A., Hall, A., and Roberts, J.M. (2004). p27Kip1 modulates cell migration through the regulation of RhoA activation. Genes Dev *18*, 862-876.

Billuart, P., Bienvenu, T., Ronce, N., des Portes, V., Vinet, M.C., Zemni, R., Roest Crollius, H., Carrie, A., Fauchereau, F., Cherry, M*., et al.* (1998). Oligophrenin-1 encodes a rhoGAP protein involved in X-linked mental retardation. Nature *392*, 923-926.

Blanc, V., Navaratnam, N., Henderson, J.O., Anant, S., Kennedy, S., Jarmuz, A., Scott, J., and Davidson, N.O. (2001). Identification of GRY-RBP as an apolipoprotein B RNA-binding protein that interacts with both apobec-1 and apobec-1 complementation factor to modulate C to U editing. J Biol Chem *276*, 10272-10283.

Bowerman, M., Beauvais, A., Anderson, C.L., and Kothary, R. (2010). Rho-kinase inactivation prolongs survival of an intermediate SMA mouse model. Hum Mol Genet.

Bowerman, M., Shafey, D., and Kothary, R. (2007). Smn depletion alters profilin II expression and leads to upregulation of the RhoA/ROCK pathway and defects in neuronal integrity. J Mol Neurosci *32*, 120-131.

Bramham, C.R. (2008). Local protein synthesis, actin dynamics, and LTP consolidation. Curr Opin Neurobiol *18*, 524-531.

Brengues, M., Teixeira, D., and Parker, R. (2005). Movement of eukaryotic mRNAs between polysomes and cytoplasmic processing bodies. Science *310*, 486-489.

Briese, M., Esmaeili, B., and Sattelle, D.B. (2005). Is spinal muscular atrophy the result of defects in motor neuron processes? Bioessays *27*, 946-957.

Brown, V., Jin, P., Ceman, S., Darnell, J.C., ODonnell, W.T., Tenenbaum, S.A., Jin, X., Feng, Y., Wilkinson, K.D., Keene, J.D*., et al.* (2001). Microarray identification of FMRP associated brain mRNAs and altered mRNA translational profiles in Fargile X Syndrome. Cell *107*, 477-487.

Bullock, S.L. (2007). Translocation of mRNAs by molecular motors: think complex? Semin Cell Dev Biol *18*, 194-201.

Burghes, A.H., and Beattie, C.E. (2009). Spinal muscular atrophy: why do low levels of survival motor neuron protein make motor neurons sick? Nat Rev Neurosci *10*, 597-609.

Burry, R.W., and Smith, C.L. (2006). HuD distribution changes in response to heat shock but not neurotrophic stimulation. J Histochem Cytochem *54*, 1129-1138.

Calabrese, B., Wilson, M.S., and Halpain, S. (2006). Development and regulation of dendritic spine synapses. Physiology (Bethesda) *21*, 38-47.

Campbell, D.S., and Holt, C.E. (2001). Chemotropic responses of retinal growth cones mediated by rapid local protein synthesis and degradation. Neuron *32*, 1013-1026.

Cao, Q., and Richter, J.D. (2002). Dissolution of the maskin-eIF4E complex by cytoplasmic polyadenylation and poly(A)-binding protein controls cyclin B1 mRNA translation and oocyte maturation. Embo J *21*, 3852-3862.

Carrel, T.L., McWhorter, M.L., Workman, E., Zhang, H., Wolstencroft, E.C., Lorson, C., Bassell, G.J., Burghes, A.H., and Beattie, C.E. (2006). Survival motor neuron function in motor axons is independent of functions required for small nuclear ribonucleoprotein biogenesis. J Neurosci *26*, 11014-11022.

Carvalho, T., Almeida, F., Calapez, A., Lafarga, M., Berciano, M.T., and Carmo-Fonseca, M. (1999). The spinal muscular atrophy disease gene product, SMN: A link between snRNP biogenesis and the Cajal (coiled) body. J Cell Biol *147*, 715-728.

Castano, J., Solanas, G., Casagolda, D., Raurell, I., Villagrasa, P., Bustelo, X.R., Garcia de Herreros, A., and Dunach, M. (2007). Specific phosphorylation of p120-catenin regulatory domain differently modulates its binding to RhoA. Mol Cell Biol *27*, 1745-1757.

Chartrand, P., Meng, X.H., Singer, R.H., and Long, R.M. (1999). Structural elements required for the localization of ASH1 mRNA and of a green fluorescent protein reporter particle in vivo. *Current Bio.*, 333-336.

Chekulaeva, M., Hentze, M.W., and Ephrussi, A. (2006). Bruno acts as a dual repressor of oskar translation, promoting mRNA oligomerization and formation of silencing particles. Cell *124*, 521-533.

Chen, H.H., Chang, J.G., Lu, R.M., Peng, T.Y., and Tarn, W.Y. (2008). The RNA binding protein hnRNP Q modulates the utilization of exon 7 in the survival motor neuron 2 (SMN2) gene. Mol Cell Biol *28*, 6929-6938.

Chi, S.W., Zang, J.B., Mele, A., and Darnell, R.B. (2009). Argonaute HITS-CLIP decodes microRNA-mRNA interaction maps. Nature *460*, 479-486.

Cho, S., Park, S.M., Kim, T.D., Kim, J.H., Kim, K.T., and Jang, S.K. (2007). BiP internal ribosomal entry site activity is controlled by heat-induced interaction of NSAP1. Mol Cell Biol *27*, 368-383.

Chou, C.F., Mulky, A., Maitra, S., Lin, W.J., Gherzi, R., Kappes, J., and Chen, C.Y. (2006). Tethering KSRP, a decay-promoting AU-rich element-binding protein, to mRNAs elicits mRNA decay. Mol Cell Biol *26*, 3695-3706.

Coller, J., and Parker, R. (2005). General translational repression by activators of mRNA decapping. Cell *122*, 875-886.

Cosson, B., Berkova, N., Couturier, A., Chabelskaya, S., Philippe, M., and Zhouravleva, G. (2002). Poly(A)-binding protein and eRF3 are associated in vivo in human and Xenopus cells. Biol Cell *94*, 205-216.

Cougot, N., Babajko, S., and Seraphin, B. (2004). Cytoplasmic foci are sites of mRNA decay in human cells. J Cell Biol *165*, 31-40.

Cougot, N., Bhattacharyya, S.N., Tapia-Arancibia, L., Bordonne, R., Filipowicz, W., Bertrand, E., and Rage, F. (2008). Dendrites of mammalian neurons contain specialized P-body-like structures that respond to neuronal activation. J Neurosci *28*, 13793-13804.

Cox, L.J., Hengst, U., Gurskaya, N.G., Lukyanov, K.A., and Jaffrey, S.R. (2008). Intra-axonal translation and retrograde trafficking of CREB promotes neuronal survival. Nat Cell Biol *10*, 149-159.

Darnell, J.C., Jensen, K.B., Jin, P., Brown, V., Warren, S.T., and Darnell, R.B. (2001). Fragile X Mental Retardation Protein targets G Quartet mRNAs important for neuronal function. Cell *107*, 489-499.

Dean, J.L., Wait, R., Mahtani, K.R., Sully, G., Clark, A.R., and Saklatvala, J. (2001). The 3' untranslated region of tumor necrosis factor alpha mRNA is a target of the mRNA-stabilizing factor HuR. Mol Cell Biol *21*, 721-730.

Decker, C.J., Teixeira, D., and Parker, R. (2007). Edc3p and a glutamine/asparagine-rich domain of Lsm4p function in processing body assembly in Saccharomyces cerevisiae. J Cell Biol *179*, 437-449.

Deng, Y., Singer, R.H., and Gu, W. (2008). Translation of ASH1 mRNA is repressed by Puf6p-Fun12p/eIF5B interaction and released by CK2 phosphorylation. Genes Dev *22*, 1037-1050.

Deshler, D.O., Highett, M.I., and Schnapp, B.J. (1997). Localization of Xenopus Vg1 mRNA by Vera protein and the endoplasmic reticulum. Science *276*, 1128-1130.

di Penta, A., Mercaldo, V., Florenzano, F., Munck, S., Ciotti, M.T., Zalfa, F., Mercanti, D., Molinari, M., Bagni, C., and Achsel, T. (2009). Dendritic LSm1/CBP80-mRNPs mark the early steps of transport commitment and translational control. J Cell Biol *184*, 423-435.

Dictenberg, J.B., Swanger, S.A., Antar, L.N., Singer, R.H., and Bassell, G.J. (2008). A direct role for FMRP in activity-dependent dendritic mRNA transport links filopodial-spine morphogenesis to fragile X syndrome. Dev Cell *14*, 926-939.

Dundr, M., Hebert, M.D., Karpova, T.S., Stanek, D., Xu, H., Shpargel, K.B., Meier, U.T., Neugebauer, K.M., Matera, A.G., and Misteli, T. (2004). In vivo kinetics of Cajal body components. J Cell Biol *164*, 831-842.

Echaniz-Laguna, A., Miniou, P., Bartholdi, D., and Melki, J. (1999). The promoters of the survival motor neuron gene (SMN) and its copy (SMNc) share common regulatory elements. Am J Hum Genet *64*, 1365-1370.

Elia, L.P., Yamamoto, M., Zang, K., and Reichardt, L.F. (2006). p120 catenin regulates dendritic spine and synapse development through Rho-family GTPases and cadherins. Neuron *51*, 43-56.

Elvira, G., Wasiak, S., Blandford, V., Tong, X.K., Serrano, A., Fan, X., del Rayo Sanchez-Carbente, M., Servant, F., Bell, A.W., Boismenu, D*., et al.* (2006). Characterization of an RNA granule from developing brain. Mol Cell Proteomics *5*, 635-651.

Eom, T., Antar, L.N., Singer, R.H., and Bassell, G.J. (2003). Localization of a beta-actin messenger ribonucleoprotein complex with zipcode-binding protein modulates the density of dendritic filopodia and filopodial synapses. J Neurosci *23*, 10433-10444.

Ephrussi, A., and Lehman, R. (1992). Induction of germ cell formation by oskar. Nature *358*, 387-392.

Eulalio, A., Helms, S., Fritzsch, C., Fauser, M., and Izaurralde, E. (2009). A C-terminal silencing domain in GW182 is essential for miRNA function. RNA *15*, 1067-1077.

Eulalio, A., Huntzinger, E., and Izaurralde, E. (2008). GW182 interaction with Argonaute is essential for miRNA-mediated translational repression and mRNA decay. Nat Struct Mol Biol *15*, 346-353.

Eurwilaichitr, L., Graves, F.M., Stansfield, I., and Tuite, M.F. (1999). The C-terminus of eRF1 defines a functionally important domain for translation termination in Saccharomyces cerevisiae. Mol Microbiol *32*, 485-496.

Eystathioy, T., Jakymiw, A., Chan, E.K., Seraphin, B., Cougot, N., and Fritzler, M.J. (2003). The GW182 protein colocalizes with mRNA degradation associated proteins hDcp1 and hLSm4 in cytoplasmic GW bodies. RNA *9*, 1171-1173.

Fahling, M., Mrowka, R., Steege, A., Kirschner, K.M., Benko, E., Forstera, B., Persson, P.B., Thiele, B.J., Meier, J.C., and Scholz, H. (2009). Translational regulation of the human achaete-scute homologue-1 by fragile X mental retardation protein. J Biol Chem *284*, 4255-4266.

Feng, Y., Gutekunst, C.A., Eberhart, D.E., Yi, H., and Warren, S.T. (1997). FMRP: Nucleocytoplasmic shuttling and association with somatodendritic polyribosomes. J Neurosci *17*, 1539-1547.

Ferrandon, D., Koch, I., Westhof, E., and Nusslein-Volhard, C. (1997). RNA-RNA interaction is required for the formation of specific bicoid mRNA 3' UTR-STAUFEN ribonucleoprotein particles. Embo J *16*, 1751-1758.

Fischer, U., Liu, Q., and Dreyfuss, G. (1997). The SMN-SIP1 complex has an essential role in spliceosomal snRNP biogenesis. Cell *90*, 1023-1029.

Forrest, K.M., and Gavis, E.R. (2003). Live imaging of endogenous RNA reveals a diffusion and entrapment mechanism for nanos mRNA localization in Drosophila. Curr Biol *13*, 1159-1168.

Frank-Kamenetsky, M., Zhang, X.M., Bottega, S., Guicherit, O., Wichterle, H., Dudek, H., Bumcrot, D., Wang, F.Y., Jones, S., Shulok, J.*, et al.* (2002). Small-molecule modulators of Hedgehog signaling: identification and characterization of Smoothened agonists and antagonists. J Biol *1*, 10.

Franks, T.M., and Lykke-Andersen, J. (2007). TTP and BRF proteins nucleate processing body formation to silence mRNAs with AU-rich elements. Genes Dev *21*, 719-735.

Franks, T.M., and Lykke-Andersen, J. (2008). The control of mRNA decapping and P-body formation. Mol Cell *32*, 605-615.

Friesen, W.J., and Dreyfuss, G. (2000). Specific sequences of the Sm and Sm-like (Lsm) proteins mediate their interaction with the spinal muscular atrophy disease gene product (SMN). J Biol Chem *275*, 26370-26375.

Frugier, T., Nicole, S., Cifuentes-Diaz, C., and Melki, J. (2002). The molecular bases of spinal muscular atrophy. Curr Opin Genet Dev *12*, 294-298.

Funakoshi, Y., Doi, Y., Hosoda, N., Uchida, N., Osawa, M., Shimada, I., Tsujimoto, M., Suzuki, T., Katada, T., and Hoshino, S. (2007). Mechanism of mRNA deadenylation: evidence for a molecular interplay between translation termination factor eRF3 and mRNA deadenylases. Genes Dev *21*, 3135-3148.

Gabanella, F., Butchbach, M.E., Saieva, L., Carissimi, C., Burghes, A.H., and Pellizzoni, L. (2007). Ribonucleoprotein assembly defects correlate with spinal muscular atrophy severity and preferentially affect a subset of spliceosomal snRNPs. PLoS One *2*, e921.

Garner, C.C., Tucker, R.P., and Matus, A. (1988). Selective localization of mRNA for cytoskeletal protein MAP2 in dendrites. Nature *336*, 674-679.

Gavis, E.R., Curtis, D., and Lehmann, R. (1996). Identification of cis-acting sequences that control nanos RNA localization. Dev Biol *176*, 36-50.

Gherzi, R., Lee, K.Y., Briata, P., Wegmuller, D., Moroni, C., Karin, M., and Chen, C.Y. (2004). A KH domain RNA binding protein, KSRP, promotes ARE-directed mRNA turnover by recruiting the degradation machinery. Mol Cell *14*, 571-583.

Gherzi, R., Trabucchi, M., Ponassi, M., Ruggiero, T., Corte, G., Moroni, C., Chen, C.Y., Khabar, K.S., Andersen, J.S., and Briata, P. (2006). The RNA-binding protein KSRP promotes decay of beta-catenin mRNA and is inactivated by PI3K-AKT signaling. PLoS Biol *5*, e5.

Gilks, N., Kedersha, N., Ayodele, M., Shen, L., Stoecklin, G., Dember, L.M., and Anderson, P. (2004). Stress granule assembly is mediated by prion-like aggregation of TIA-1. Mol Biol Cell *15*, 5383-5398.

Gordon, G.W., Berry, G., Liang, X.H., Levine, B., and Herman, B. (1998). Quantitative fluorescence resonance energy transfer measurements using fluorescence microscopy. Biophys J *74*, 2702-2713.

Govek, E.E., Newey, S.E., Akerman, C.J., Cross, J.R., Van der Veken, L., and Van Aelst, L. (2004). The X-linked mental retardation protein oligophrenin-1 is required for dendritic spine morphogenesis. Nat Neurosci *7*, 364-372.

Govek, E.E., Newey, S.E., and Van Aelst, L. (2005). The role of the Rho GTPases in neuronal development. Genes Dev *19*, 1-49.

Gross, R.E., Mei, Q., Gutekunst, C.A., and Torre, E. (2007). The pivotal role of RhoA GTPase in the molecular signaling of axon growth inhibition after CNS injury and targeted therapeutic strategies. Cell Transplant *16*, 245-262.

Grosset, C., Chen, C.Y., Xu, N., Sonenberg, N., Jacquemin-Sablon, H., and Shyu, A.B. (2000). A mechanism for translationally coupled mRNA turnover: interaction between the poly(A) tail and a c-fos RNA coding determinant via a protein complex. Cell *103*, 29-40.

Gu, W., Pan, F., Zhang, H., Bassell, G.J., and Singer, R.H. (2002). A predominantly nuclear protein affecting cytoplasmic localization of beta-actin mRNA in fibroblasts and neurons. J Cell Biol *156*, 41-51.

Gubitz, A.K., Feng, W., and Dreyfuss, G. (2004). The SMN complex. Exp Cell Res *296*, 51-56.

Hachet, O., and Ephrussi, A. (2004). Splicing of oskar RNA in the nucleus is coupled to its cytoplasmic localization. Nature *428*, 959-963.

Hall, A. (1998). Rho GTPases and the actin cytoskeleton. Science *279*, 509-514.

Harris, C.E., Boden, R.A., and Astell, C.R. (1999). A novel heterogeneous nuclear ribonucleoprotein-like protein interacts with NS1 of the minute virus of mice. J Virol *73*, 72-80.

Hengst, U., Deglincerti, A., Kim, H.J., Jeon, N.L., and Jaffrey, S.R. (2009). Axonal elongation triggered by stimulus-induced local translation of a polarity complex protein. Nat Cell Biol *11*, 1024-1030.

Hoek, K.S., Kidd, G.J., Carson, J.H., and Smith, R. (1998). hnRNPA2 selectively binds the cytoplasmic transport sequence of MBP mRNA. Biochem *37*, 7021-7029.

Holmes, L.E., Campbell, S.G., De Long, S.K., Sachs, A.B., and Ashe, M.P. (2004). Loss of translational control in yeast compromised for the major mRNA decay pathway. Mol Cell Biol *24*, 2998-3010.

Holt, C.E., and Bullock, S.L. (2009). Subcellular mRNA localization in animal cells and why it matters. Science *326*, 1212-1216.

Hosoda, N., Kobayashi, T., Uchida, N., Funakoshi, Y., Kikuchi, Y., Hoshino, S., and Katada, T. (2003). Translation termination factor eRF3 mediates mRNA decay through the regulation of deadenylation. J Biol Chem *278*, 38287-38291.

Hresko, R.C., and Mueckler, M. (2002). Identification of pp68 as the Tyrosine-phosphorylated Form of SYNCRIP/NSAP1. A cytoplasmic RNA-binding protein. J Biol Chem *277*, 25233-25238.

Hua, Y., and Zhou, J. (2004). Survival motor neuron protein facilitates assembly of stress granules. FEBS Lett *572*, 69-74.

Huang, Y.S., Jung, M.Y., Sarkissian, M., and Richter, J.D. (2002). N-methyl-D-aspartate receptor signaling results in Aurora kinase-catalyzed CPEB phosphorylation and alpha CaMKII mRNA polyadenylation at synapses. Embo J *21*, 2139-2148.

Huber, K.M., Gallagher, S.M., Warren, S.T., and Bear, M.F. (2002). Altered synaptic plasticity in a mouse model of fragile x mental retardation. PNAS *99*, 7746-7750.

Huttelmaier, S., Zenklusen, D., Lederer, M., Dictenberg, J., Lorenz, M., Meng, X., Bassell, G.J., Condeelis, J., and Singer, R.H. (2005). Spatial regulation of beta-actin translation by Src-dependent phosphorylation of ZBP1. Nature *438*, 512-515.

Ioannidis, P., Mahaira, L., Papadopoulou, A., Teixeira, M.R., Heim, S., Andersen, J.A., Evangelou, E., Dafni, U., Pandis, N., and Trangas, T. (2003a). 8q24 Copy number gains and expression of the c-myc mRNA stabilizing protein CRD-BP in primary breast carcinomas. Int J Cancer *104*, 54-59.

Ioannidis, P., Mahaira, L., Papadopoulou, A., Teixeira, M.R., Heim, S., Andersen, J.A., Evangelou, E., Dafni, U., Pandis, N., and Trangas, T. (2003b). CRD-BP: a c-Myc mRNA stabilizing protein with an oncofetal pattern of expression. Anticancer Res *23*, 2179-2183.

Ioannidis, P., Trangas, T., Dimitriadis, E., Samiotaki, M., Kyriazoglou, I., Tsiapalis, C.M., Kittas, C., Agnantis, N., Nielsen, F.C., Nielsen, J*., et al.* (2001). C-MYC and IGF-II mRNA-binding protein (CRD-BP/IMP-1) in benign and malignant mesenchymal tumors. Int J Cancer *94*, 480-484.

Jablonka, S., Bandilla, M., Wiese, S., Buhler, D., Wirth, B., Sendtner, M., and Fischer, U. (2001). Co-regulation of survival of motor neuron (SMN) protein and its interactor SIP1 during development and in spinal muscular atrophy. Hum Mol Genet *10*, 497-505.

Jablonka, S., Holtmann, B., Meister, G., Bandilla, M., Rossoll, W., Fischer, U., and Sendtner, M. (2002). Gene targeting of Gemin2 in mice reveals a correlation between defects in the biogenesis of U snRNPs and motoneuron cell death. Proc Natl Acad Sci U S A *28*, 28.

Jakymiw, A., Pauley, K.M., Li, S., Ikeda, K., Lian, S., Eystathioy, T., Satoh, M., Fritzler, M.J., and Chan, E.K. (2007). The role of GW/P-bodies in RNA processing and silencing. J Cell Sci *120*, 1317-1323.

Jobin, C.M., Chen, H., Lin, A.J., Yacono, P.W., Igarashi, J., Michel, T., and Golan, D.E. (2003). Receptor-regulated dynamic interaction between endothelial nitric oxide synthase and calmodulin revealed by fluorescence resonance energy transfer in living cells. Biochemistry *42*, 11716-11725.

Johnstone, O., and Lasko, P. (2001). Translational regulation and RNA localization in Drosophila oocytes and embryos. Annu Rev Genet *35*, 365-406.

Jonson, L., Vikesaa, J., Krogh, A., Nielsen, L.K., Hansen, T., Borup, R., Johnsen, A.H., Christiansen, J., and Nielsen, F.C. (2007). Molecular composition of IMP1 ribonucleoprotein granules. Mol Cell Proteomics *6*, 798-811.

Kanai, Y., Dohmae, N., and Hirokawa, N. (2004). Kinesin transports RNA: isolation and characterization of an RNA-transporting granule. Neuron *43*, 513-525.

Kedersha, N., and Anderson, P. (2002). Stress granules: sites of mRNA triage that regulate mRNA stability and translatability. Biochem Soc Trans *30*, 963-969.

Kedersha, N., and Anderson, P. (2007). Mammalian stress granules and processing bodies. Methods Enzymol *431*, 61-81.

Kedersha, N., Chen, S., Gilks, N., Li, W., Miller, I.J., Stahl, J., and Anderson, P. (2002). Evidence that ternary complex (eIF2-GTP-tRNA(i)(Met))-deficient preinitiation complexes are core constituents of mammalian stress granules. Mol Biol Cell *13*, 195-210.

Kedersha, N., Stoecklin, G., Ayodele, M., Yacono, P., Lykke-Andersen, J., Fritzler, M.J., Scheuner, D., Kaufman, R.J., Golan, D.E., and Anderson, P. (2005). Stress granules and processing bodies are dynamically linked sites of mRNP remodeling. J Cell Biol *169*, 871-884.

Kedersha, N.L., Gupta, M., Li, W., Miller, I., and Anderson, P. (1999). RNA-binding proteins TIA-1 and TIAR link the phosphorylation of eIF-2 alpha to the assembly of mammalian stress granules. J Cell Biol *147*, 1431-1442.

Kiebler, M.A., and Bassell, G.J. (2006). Neuronal RNA granules: movers and makers. Neuron *51*, 685-690.

Kim, H.H., Kuwano, Y., Srikantan, S., Lee, E.K., Martindale, J.L., and Gorospe, M. (2009). HuR recruits let-7/RISC to repress c-Myc expression. Genes Dev *23*, 1743-1748.

Kim, T.D., Woo, K.C., Cho, S., Ha, D.C., Jang, S.K., and Kim, K.T. (2007). Rhythmic control of AANAT translation by hnRNP Q in circadian melatonin production. Genes Dev *21*, 797-810.

Kim, Y.K., Back, S.H., Rho, J., Lee, S.H., and Jang, S.K. (2001). La autoantigen enhances translation of BiP mRNA. Nucleic Acids Res *29*, 5009-5016.

Kislauskis, E.H., Li, Z., Singer, R.H., and Taneja, K.L. (1993). Isoform-specific 3'-untranslated sequences sort alpha-cardiac and beta-cytoplasmic actin messenger RNAs to different cytoplasmic compartments. J Cell Biol *123*, 165-172.

Kislauskis, E.H., Zhu, X., and Singer, R.H. (1994). Sequences responsible for intracellular localization of beta-actin messenger RNA also affect cell phenotype. J Cell Biol *127*, 441-451.

Knowles, R.B., Sabry, J.H., Martone, M.E., Deerinck, T.J., Ellisman, M.H., Bassell, G.J., and Kosik, K.S. (1996). Translocation of RNA granules in living neurons. Journal of Neuroscience *16*, 7812-7820.

Kobayashi, T., Funakoshi, Y., Hoshino, S., and Katada, T. (2004). The GTP-binding release factor eRF3 as a key mediator coupling translation termination to mRNA decay. J Biol Chem *279*, 45693-45700.

Kohrman, M., Lui, M., Kaether, C., DesGroseillers, L., Dotti, C.G., and Kiebler, M.A. (1999). Microtubule dependent recruitment of Staufen-GFP into large RNA containing

granules and dendritic transport in living hippocampal neurons. Mol Bio Cell *10*, 2945-2953.

Kohrmann, M., Luo, M., Kaether, C., DesGroseillers, L., Dotti, C.G., and Kiebler, M.A. (1999). Microtubule-dependent recruitment of Staufen-green fluorescent protein into large RNA-containing granules and subsequent dendritic transport in living hippocampal neurons. Mol Biol Cell *10*, 2945-2953.

Kolb, S.J., Battle, D.J., and Dreyfuss, G. (2007). Molecular functions of the SMN complex. J Child Neurol *22*, 990-994.

Kononenko, A.V., Mitkevich, V.A., Atkinson, G.C., Tenson, T., Dubovaya, V.I., Frolova, L.Y., Makarov, A.A., and Hauryliuk, V. (2009). GTP-dependent structural rearrangement of the eRF1:eRF3 complex and eRF3 sequence motifs essential for PABP binding. Nucleic Acids Res.

Kononenko, A.V., Mitkevich, V.A., Dubovaya, V.I., Kolosov, P.M., Makarov, A.A., and Kisselev, L.L. (2008). Role of the individual domains of translation termination factor eRF1 in GTP binding to eRF3. Proteins *70*, 388-393.

Kugler, J.M., and Lasko, P. (2009). Localization, anchoring and translational control of oskar, gurken, bicoid and nanos mRNA during Drosophila oogenesis. Fly (Austin) *3*, 15-28.

Lasko, P. (2003). Cup-ling oskar RNA localization and translational control. J Cell Biol *163*, 1189-1191.

Lawrence, J.B., and Singer, R.H. (1986). Intracellular localizationof messenger RNAs for cytoskeletal proteins. Cell *45*, 407-415.

Lecuyer, E., Yoshida, H., Parthasarathy, N., Alm, C., Babak, T., Cerovina, T., Hughes, T.R., Tomancak, P., and Krause, H.M. (2007). Global analysis of mRNA localization reveals a prominent role in organizing cellular architecture and function. Cell *131*, 174-187.

Lefebvre, S., Burglen, L., Reboullet, S., Munnich, A., and Melki, J. (1995). Identification and characterization of a spinal muscular atrophy determining gene. Cell *80*, 155-165.

Lemm, I., and Ross, J. (2002). Regulation of c-myc mRNA decay by translational pausing in a coding region instability determinant. Mol Cell Biol *22*, 3959-3969.

Leung, T., Chen, X.Q., Manser, E., and Lim, L. (1996). The p160 RhoA-binding kinase ROK alpha is a member of a kinase family and is involved in the reorganization of the cytoskeleton. Mol Cell Biol *16*, 5313-5327.

Li, C., Sasaki, Y., Takei, K., Yamamoto, H., Shouji, M., Sugiyama, Y., Kawakami, T., Nakamura, F., Yagi, T., Ohshima, T.*, et al.* (2004). Correlation between semaphorin3A-induced facilitation of axonal transport and local activation of a translation initiation factor eukaryotic translation initiation factor 4E. J Neurosci *24*, 6161-6170.

Li, Z., Zhang, Y., Ku, L., Wilkinson, K.D., Warren, S.T., and Feng, Y. (2001). The Fragile X Mental Retardation Protein inhibits translation via interacting with mRNA. Nucleic Acid Research *29*, 2276-2283.

Lian, S., Jakymiw, A., Eystathioy, T., Hamel, J.C., Fritzler, M.J., and Chan, E.K. (2006). GW bodies, microRNAs and the cell cycle. Cell Cycle *5*, 242-245.

Lin, A.C., and Holt, C.E. (2008). Function and regulation of local axonal translation. Curr Opin Neurobiol *18*, 60-68.

Lin, D., Pestova, T.V., Hellen, C.U., and Tiedge, H. (2008). Translational control by a small RNA: dendritic BC1 RNA targets the eukaryotic initiation factor 4A helicase mechanism. Mol Cell Biol *28*, 3008-3019.

Litman, P., Barg, J., Rindzoonski, L., and Ginzburg, I. (1993). Subcellular localization of tau mRNA in differentiating neuronal cell culture : Implications for neuronal polarity. Neuron *10*, 627-638.

Liu, J., Valencia-Sanchez, M.A., Hannon, G.J., and Parker, R. (2005). MicroRNA-dependent localization of targeted mRNAs to mammalian P-bodies. Nat Cell Biol *7*, 719-723.

Liu, Q., and Dreyfuss, G. (1996). A novel nuclear structure containing the survival of motor neurons protein. Embo J *15*, 3555-3565.

Liu, Q., Fischer, U., Wang, F., and Dreyfuss, G. (1997). The spinal muscular atrophy disease gene product, SMN, and its associated protein SIP1 are in a complex with spliceosomal snRNP proteins. Cell *90*, 1013-1021.

Long, R.M., Gu, W., Lorimer, E., Singer, R.H., and Chartrand, P. (2000). She2p is a novel RNA-binding protein that recruits the Myo4p-She3p complex to ASH1 mRNA. EMBO J *19*, 6592-6601.

Long, R.M., Singer, R.H., Meng, X., Gonzalez, I., Nasmyth, K., and Jansen, R.P. (1997). Mating type switching in yeast controlled by asymmetric localization of ASH1 mRNA. Science *277*, 383-387.

Lorson, C.L., and Androphy, E.J. (2000). An exonic enhancer is required for inclusion of an essential exon in the SMA-determining gene SMN. Hum Mol Genet *9*, 259-265.

Lorson, C.L., Hahnen, E., Androphy, E.J., and Wirth, B. (1999). A single nucleotide in the SMN gene regulates splicing and is responsible for spinal muscular atrophy. Proc Natl Acad Sci U S A *96*, 6307-6311.

Lykke-Andersen, J., and Wagner, E. (2005). Recruitment and activation of mRNA decay enzymes by two ARE-mediated decay activation domains in the proteins TTP and BRF-1. Genes Dev *19*, 351-361.

Macdonald, P.M., Kerr, K., Smith, J.L., and Leask, A. (1993). RNA regulatory element Ble1 directs the early step on bicoid RNA localization. Development *118*, 1233-1243.

Macdonald, P.M., and Struhl, G. (1988). Cis-acting sequences responsible for anterior localization of bicoid mRNA in Drosophila embryos. Nature *336*, 595-598.

Maekawa, M., Ishizaki, T., Boku, S., Watanabe, N., Fujita, A., Iwamatsu, A., Obinata, T., Ohashi, K., Mizuno, K., and Narumiya, S. (1999). Signaling from Rho to the actin cytoskeleton through protein kinases ROCK and LIM-kinase. Science *285*, 895-898.

Mallardo, M., Deitinghoff, A., Muller, J., Goetze, B., Macchi, P., Peters, C., and Kiebler, M.A. (2003). Isolation and characterization of Staufen-containing ribonucleoprotein particles from rat brain. Proc Natl Acad Sci U S A *100*, 2100-2105.

Martin, K.C. (2004). Local protein synthesis during axon guidance and synaptic plasticity. Curr Opin Neurobiol *14*, 305-310.

Martin, K.C., Barad, M., and Kandel, E.R. (2000). Local protein synthesis and its role in synapse-specific plasticity. Curr Opin Neurobiol *10*, 587-592.

Martin, K.C., and Ephrussi, A. (2009). mRNA localization: gene expression in the spatial dimension. Cell *136*, 719-730.

Marx, R., Henderson, J., Wang, J., and Baraban, J.M. (2005). Tech: a RhoA GEF selectively expressed in hippocampal and cortical neurons. J Neurochem *92*, 850-858.

Mazroui, R., Huot, M.E., Tremblay, S., Filion, C., Labelle, Y., and Khandjian, E.W. (2002). Trapping of messenger RNA by Fragile X Mental Retardation protein into cytoplasmic granules induces translation repression. Hum Mol Genet *11*, 3007-3017.

McWhorter, M.L., Monani, U.R., Burghes, A.H., and Beattie, C.E. (2003). Knockdown of the survival motor neuron (Smn) protein in zebrafish causes defects in motor axon outgrowth and pathfinding. J Cell Biol *162*, 919-931.

Meister, G., Landthaler, M., Peters, L., Chen, P.Y., Urlaub, H., Luhrmann, R., and Tuschl, T. (2005). Identification of novel argonaute-associated proteins. Curr Biol *15*, 2149-2155.

Merkulova, T.I., Frolova, L.Y., Lazar, M., Camonis, J., and Kisselev, L.L. (1999). C-terminal domains of human translation termination factors eRF1 and eRF3 mediate their in vivo interaction. FEBS Lett *443*, 41-47.

Minshall, N., Kress, M., Weil, D., and Standart, N. (2009). Role of p54 RNA helicase activity and its C-terminal domain in translational repression, P-body localization and assembly. Mol Biol Cell *20*, 2464-2472.

Mizutani, A., Fukuda, M., Ibata, K., Shiraishi, Y., and Mikoshiba, K. (2000). SYNCRIP, a cytoplasmic counterpart of heterogeneous nuclear ribonucleoprotein R, interacts with ubiquitous synaptotagmin isoforms. J Biol Chem *275*, 9823-9831.

Mohseni, M., and Chishti, A.H. (2008). The headpiece domain of dematin regulates cell shape, motility, and wound healing by modulating RhoA activation. Mol Cell Biol *28*, 4712-4718.

Mollet, S., Cougot, N., Wilczynska, A., Dautry, F., Kress, M., Bertrand, E., and Weil, D. (2008). Translationally repressed mRNA transiently cycles through stress granules during stress. Mol Biol Cell *19*, 4469-4479.

Monani, U.R. (2005). Spinal muscular atrophy: a deficiency in a ubiquitous protein; a motor neuron-specific disease. Neuron *48*, 885-896.

Monani, U.R., Sendtner, M., Coovert, D.D., Parsons, D.W., Andreassi, C., Le, T.T., Jablonka, S., Schrank, B., Rossol, W., Prior, T.W.*, et al.* (2000a). The human centromeric survival motor neuron gene (SMN2) rescues embryonic lethality in Smn(-/-) mice and results in a mouse with spinal muscular atrophy. Hum Mol Genet *9*, 333-339.

Monani, U.R., Sendtner, M., Coovert, D.D., Rossol, W., Morris, G.E., and Burghes, A.H. (2000b). The human SMN2 gene rescues embryonic lethality in SMN -/- mice and results in a mouse with SMA. Human Mol Genetics *9*, 333-339.

Moon, S.Y., Zang, H., and Zheng, Y. (2003). Characterization of a brain-specific Rho GTPase-activating protein, p200RhoGAP. J Biol Chem *278*, 4151-4159.

Moser, J.J., Eystathioy, T., Chan, E.K., and Fritzler, M.J. (2007). Markers of mRNA stabilization and degradation, and RNAi within astrocytoma GW bodies. J Neurosci Res *85*, 3619-3631.

Mourelatos, Z., Abel, L., Yong, J., Kataoka, N., and Dreyfuss, G. (2001). SMN interacts with a novel family of hnRNP and spliceosomal proteins. EMBO J *20*, 5443-5452.

Muddashetty, R.S., Kelic, S., Gross, C., Xu, M., and Bassell, G.J. (2007). Dysregulated metabotropic glutamate receptor-dependent translation of AMPA receptor and postsynaptic density-95 mRNAs at synapses in a mouse model of fragile X syndrome. J Neurosci *27*, 5338-5348.

Nabors, L.B., Gillespie, G.Y., Harkins, L., and King, P.H. (2001). HuR, a RNA stability factor, is expressed in malignant brain tumors and binds to adenine- and uridine-rich elements within the 3' untranslated regions of cytokine and angiogenic factor mRNAs. Cancer Res *61*, 2154-2161.

Nabors, L.B., Suswam, E., Huang, Y., Yang, X., Johnson, M.J., and King, P.H. (2003). Tumor necrosis factor alpha induces angiogenic factor up-regulation in malignant glioma cells: a role for RNA stabilization and HuR. Cancer Res *63*, 4181-4187.

Nakamura, A., Sato, K., and Hanyu-Nakamura, K. (2004). Drosophila cup is an eIF4E binding protein that associates with Bruno and regulates oskar mRNA translation in oogenesis. Dev Cell *6*, 69-78.

Napoli, I., Mercaldo, V., Boyl, P.P., Eleuteri, B., Zalfa, F., De Rubeis, S., Di Marino, D., Mohr, E., Massimi, M., Falconi, M.*, et al.* (2008). The fragile X syndrome protein represses activity-dependent translation through CYFIP1, a new 4E-BP. Cell *134*, 1042-1054.

Narumiya, S., Tanji, M., and Ishizaki, T. (2009). Rho signaling, ROCK and mDia1, in transformation, metastasis and invasion. Cancer Metastasis Rev *28*, 65-76.

Nekrasov, M.P., Ivshina, M.P., Chernov, K.G., Kovrigina, E.A., Evdokimova, V.M., Thomas, A.A., Hershey, J.W., and Ovchinnikov, L.P. (2003). The mRNA-binding protein

YB-1 (p50) prevents association of the eukaryotic initiation factor eIF4G with mRNA and inhibits protein synthesis at the initiation stage. J Biol Chem *278*, 13936-13943.

Nelson, M.R., Leidal, A.M., and Smibert, C.A. (2004). Drosophila Cup is an eIF4E-binding protein that functions in Smaug-mediated translational repression. EMBO J *23*, 150-159.

Nielsen, J., Kristensen, M.A., Willemoes, M., Nielsen, F.C., and Christiansen, J. (2004). Sequential dimerization of human zipcode-binding protein IMP1 on RNA: a cooperative mechanism providing RNP stability. Nucleic Acids Res *32*, 4368-4376.

Niessing, D., Huttelmaier, S., Zenklusen, D., Singer, R.H., and Burley, S.K. (2004). She2p is a novel RNA binding protein with a basic helical hairpin motif. Cell *119*, 491-502.

Nobes, C.D., and Hall, A. (1995). Rho, rac, and cdc42 GTPases regulate the assembly of multimolecular focal complexes associated with actin stress fibers, lamellipodia, and filopodia. Cell *81*, 53-62.

Oleynikov, Y., and Singer, R.H. (2003). Real-time visualization of ZBP1 association with beta-actin mRNA during transcription and localization. Curr Biol *13*, 199-207.

Ortega, A.D., Sala, S., Espinosa, E., Gonzalez-Baron, M., and Cuezva, J.M. (2008). HuR and the bioenergetic signature of breast cancer: a low tumor expression of the RNA-binding protein predicts a higher risk of disease recurrence. Carcinogenesis *29*, 2053-2061.

Ozawa, T., Araki, N., Yunoue, S., Tokuo, H., Feng, L., Patrakitkomjorn, S., Hara, T., Ichikawa, Y., Matsumoto, K., Fujii, K.*, et al.* (2005). The neurofibromatosis type 1 gene

product neurofibromin enhances cell motility by regulating actin filament dynamics via the Rho-ROCK-LIMK2-cofilin pathway. J Biol Chem *280*, 39524-39533.

Paek, K.Y., Kim, C.S., Park, S.M., Kim, J.H., and Jang, S.K. (2008). RNA-binding protein hnRNP D modulates internal ribosome entry site-dependent translation of hepatitis C virus RNA. J Virol *82*, 12082-12093.

Pagliardini, S., Giavazzi, A., Setola, V., Lizier, C., Di Luca, M., DeBiasi, S., and Battaglia, G. (2000). Subcellular localization and axonal transport of the survival motor neuron (SMN) protein in the developing rat spinal cord. Hum Mol Genet *9*, 47-56.

Pan, F., Huttelmaier, S., Singer, R.H., and Gu, W. (2007). ZBP2 facilitates binding of ZBP1 to beta-actin mRNA during transcription. Mol Cell Biol *27*, 8340-8351.

Paquin, N., and Chartrand, P. (2008). Local regulation of mRNA translation: new insights from the bud. Trends Cell Biol *18*, 105-111.

Paquin, N., Menade, M., Poirier, G., Donato, D., Drouet, E., and Chartrand, P. (2007). Local activation of yeast ASH1 mRNA translation through phosphorylation of Khd1p by the casein kinase Yck1p. Mol Cell *26*, 795-809.

Paradies, M.A., and Steward, O. (1997). Multiple subcellular mRNA distribution patterns in neurons: a nonisotopic in situ hybridization analysis. J Neurobiol *33*, 473-493.

Parker, R., and Sheth, U. (2007). P bodies and the control of mRNA translation and degradation. Mol Cell *25*, 635-646.

Paushkin, S., Gubitz, A.K., Massenet, S., and Dreyfuss, G. (2002). The SMN complex, an assemblyosome of ribonucleoproteins. Curr Opin Cell Biol *14*, 305-312.

Pellizzoni, L. (2007). Chaperoning ribonucleoprotein biogenesis in health and disease. EMBO Rep *8*, 340-345.

Pellizzoni, L., Yong, J., and Dreyfuss, G. (2002). Essential role for the SMN complex in the specificity of snRNP assembly. Science *298*, 1775-1779.

Peng, Z.Y., Huang, J., Lee, S.C., Shi, Y.L., Chen, X.H., and Xu, P. (2009). The expression pattern of heterogeneous nuclear ribonucleoprotein R in rat retina. Neurochem Res *34*, 1083-1088.

Piazzon, N., Rage, F., Schlotter, F., Moine, H., Branlant, C., and Massenet, S. (2008). In vitro and in cellulo evidences for association of the survival of motor neuron complex with the fragile X mental retardation protein. J Biol Chem *283*, 5598-5610.

Pietrobono, R., Tabolacci, E., Zalfa, F., Zito, I., Terracciano, A., Moscato, U., Bagni, C., Oostra, B., Chiurazzi, P., and Neri, G. (2005). Molecular dissection of the events leading to inactivation of the FMR1 gene. Hum Mol Genet *14*, 267-277.

Reijns, M.A., Alexander, R.D., Spiller, M.P., and Beggs, J.D. (2008). A role for Q/N-rich aggregation-prone regions in P-body localization. J Cell Sci *121*, 2463-2472.

Ren, Y., Li, R., Zheng, Y., and Busch, H. (1998). Cloning and characterization of GEF-H1, a microtubule-associated guanine nucleotide exchange factor for Rac and Rho GTPases. J Biol Chem *273*, 34954-34960.

Ridley, A.J., and Hall, A. (1992). The small GTP-binding protein rho regulates the assembly of focal adhesions and actin stress fibers in response to growth factors. Cell *70*, 389-399.

Roegiers, F., and Jan, Y.N. (2000). Staufen: a common component of mRNA transport in oocytes and neurons? Trends Cell Biol *10*, 220-224.

Rongo, C., Gavis, E.R., and Lehmann, R. (1995). Localization of oskar RNA regulates oskar translation and requires oskar protein. Development *121*, 2737-2746.

Ross, A.F., Oleynikov, Y., Kislauskis, E.H., Taneja, K.L., and Singer, R.H. (1997). Characterization of a beta-actin mRNA zipcode-binding protein. Mol Cell Biol *17*, 2158-2165.

Ross, J., Lemm, I., and Berberet, B. (2001). Overexpression of an mRNA-binding protein in human colorectal cancer. Oncogene *20*, 6544-6550.

Rossoll, W., and Bassell, G.J. (2009). Spinal muscular atrophy and a model for survival of motor neuron protein function in axonal ribonucleoprotein complexes. Results Probl Cell Differ *48*, 289-326.

Rossoll, W., Jablonka, S., Andreassi, C., Kroning, A.K., Karle, K., Monani, U.R., and Sendtner, M. (2003). Smn, the spinal muscular atrophy-determining gene product, modulates axon growth and localization of beta-actin mRNA in growth cones of motoneurons. J Cell Biol *163*, 801-812.

Rossoll, W., Kroning, A.K., Ohndorf, U.M., Steegborn, C., Jablonka, S., and Sendtner, M. (2002). Specific interaction of Smn, the spinal muscular atrophy determining gene product, with hnRNP-R and gry-rbp/hnRNP-Q: a role for Smn in RNA processing in motor axons? Hum Mol Genet *11*, 93-105.

Ruggiero, T., Trabucchi, M., Ponassi, M., Corte, G., Chen, C.Y., al-Haj, L., Khabar, K.S., Briata, P., and Gherzi, R. (2007). Identification of a set of KSRP target transcripts upregulated by PI3K-AKT signaling. BMC Mol Biol *8*, 28.

Sawada, N., Itoh, H., Miyashita, K., Tsujimoto, H., Sone, M., Yamahara, K., Arany, Z.P., Hofmann, F., and Nakao, K. (2009). Cyclic GMP kinase and RhoA Ser188 phosphorylation integrate pro- and antifibrotic signals in blood vessels. Mol Cell Biol *29*, 6018-6032.

Schiavi, S.C., Wellington, C.L., Shyu, A.B., Chen, C.Y., Greenberg, M.E., and Belasco, J.G. (1994). Multiple elements in the c-fos protein-coding region facilitate mRNA deadenylation and decay by a mechanism coupled to translation. J Biol Chem *269*, 3441-3448.

Schrank, B., Gotz, R., Gunnersen, J.M., Ure, J.M., Toyka, K.V., Smith, A.G., and Sendtner, M. (1997). Inactivation of the survival motor neuron gene, a candidate gene for human spinal muscular atrophy, leads to massive cell death in early mouse embryos. Proc Natl Acad Sci U S A *94*, 9920-9925.

Sharma, A., Lambrechts, A., Hao le, T., Le, T.T., Sewry, C.A., Ampe, C., Burghes, A.H., and Morris, G.E. (2005). A role for complexes of survival of motor neurons (SMN) protein with gemins and profilin in neurite-like cytoplasmic extensions of cultured nerve cells. Exp Cell Res *309*, 185-197.

Shestakova, E.A., Singer, R.H., and Condeelis, J. (2001). The physiological significance of beta -actin mRNA localization in determining cell polarity and directional motility. Proc Natl Acad Sci U S A *98*, 7045-7050.

Sheth, U., and Parker, R. (2006). Targeting of aberrant mRNAs to cytoplasmic processing bodies. Cell *125*, 1095-1109.

Singer, R.H. (2008). Highways for mRNA transport. Cell *134*, 722-723.

Sinha, S., and Yang, W. (2008). Cellular signaling for activation of Rho GTPase Cdc42. Cell Signal *20*, 1927-1934.

Smith, C.L., Afroz, R., Bassell, G.J., Furneaux, H.M., Perrone-Bizzozero, N.I., and Burry, R.W. (2004). GAP-43 mRNA in growth cones is associated with HuD and ribosomes. J Neurobiol *61*, 222-235.

Smith, J.L., Wilson, J.E., and Macdonald, P.M. (1992). Overexpression of oskar directs ectopic activation of nanos and presumptive pole cell formation in Drosophila embryos. Cell *70*, 849-859.

Sparanese, D., and Lee, C.H. (2007). CRD-BP shields c-myc and MDR-1 RNA from endonucleolytic attack by a mammalian endoribonuclease. Nucleic Acids Res *35*, 1209-1221.

Stohr, N., Lederer, M., Reinke, C., Meyer, S., Hatzfeld, M., Singer, R.H., and Huttelmaier, S. (2006). ZBP1 regulates mRNA stability during cellular stress. J Cell Biol *175*, 527-534.

Sumi, T., Matsumoto, K., and Nakamura, T. (2001a). Specific activation of LIM kinase 2 via phosphorylation of threonine 505 by ROCK, a Rho-dependent protein kinase. J Biol Chem *276*, 670-676.

Sumi, T., Matsumoto, K., Shibuya, A., and Nakamura, T. (2001b). Activation of LIM kinases by myotonic dystrophy kinase-related Cdc42-binding kinase alpha. J Biol Chem *276*, 23092-23096.

Sumi, T., Matsumoto, K., Takai, Y., and Nakamura, T. (1999). Cofilin phosphorylation and actin cytoskeletal dynamics regulated by rho- and Cdc42-activated LIM-kinase 2. J Cell Biol *147*, 1519-1532.

Suswam, E.A., Nabors, L.B., Huang, Y., Yang, X., and King, P.H. (2005). IL-1beta induces stabilization of IL-8 mRNA in malignant breast cancer cells via the 3' untranslated region: Involvement of divergent RNA-binding factors HuR, KSRP and TIAR. Int J Cancer *113*, 911-919.

Tadesse, H., Deschenes-Furry, J., Boisvenue, S., and Cote, J. (2008). KH-type splicing regulatory protein interacts with survival motor neuron protein and is misregulated in spinal muscular atrophy. Hum Mol Genet *17*, 506-524.

Tanaka, K.J., Ogawa, K., Takagi, M., Imamoto, N., Matsumoto, K., and Tsujimoto, M. (2006). RAP55, a cytoplasmic mRNP component, represses translation in Xenopus oocytes. J Biol Chem *281*, 40096-40106.

Tashiro, A., and Yuste, R. (2008). Role of Rho GTPases in the morphogenesis and motility of dendritic spines. Methods Enzymol *439*, 285-302.

Taylor, A.M., Berchtold, N.C., Perreau, V.M., Tu, C.H., Li Jeon, N., and Cotman, C.W. (2009). Axonal mRNA in uninjured and regenerating cortical mammalian axons. J Neurosci *29*, 4697-4707.

Teixeira, D., Sheth, U., Valencia-Sanchez, M.A., Brengues, M., and Parker, R. (2005). Processing bodies require RNA for assembly and contain nontranslating mRNAs. RNA *11*, 371-382.

Tessier, C.R., Doyle, G.A., Clark, B.A., Pitot, H.C., and Ross, J. (2004). Mammary tumor induction in transgenic mice expressing an RNA-binding protein. Cancer Res *64*, 209-214.

Tharun, S., and Parker, R. (2001). Targeting an mRNA for decapping: displacement of translation factors and association of the Lsm1p-7p complex on deadenylated yeast mRNAs. Mol Cell *8*, 1075-1083.

Tiedge, H., Fremeau, R.T., Jr., Weinstock, P.H., Arancio, O., and Brosius, J. (1991). Dendritic location of neural BC1 RNA. Proc Natl Acad Sci U S A *88*, 2093-2097.

Tiruchinapalli, D.M., Oleynikov, Y., Kelic, S., Shenoy, S.M., Hartley, A., Stanton, P.K., Singer, R.H., and Bassell, G.J. (2003). Activity-dependent trafficking and dynamic localization of zipcode binding protein 1 and beta-actin mRNA in dendrites and spines of hippocampal neurons. J Neurosci *23*, 3251-3261.

Uchida, N., Hoshino, S., Imataka, H., Sonenberg, N., and Katada, T. (2002). A novel role of the mammalian GSPT/eRF3 associating with poly(A)-binding protein in Cap/Poly(A)-dependent translation. J Biol Chem *277*, 50286-50292.

Uchida, N., Hoshino, S., and Katada, T. (2004). Identification of a human cytoplasmic poly(A) nuclease complex stimulated by poly(A)-binding protein. J Biol Chem *279*, 1383-1391.

Ule, J., Jensen, K.B., Ruggiu, M., Mele, A., Ule, A., and Darnell, R.B. (2003). CLIP identifies Nova-regulated RNA networks in the brain. Science *302*, 1212-1215.

Vainer, G., Vainer-Mosse, E., Pikarsky, A., Shenoy, S.M., Oberman, F., Yeffet, A., Singer, R.H., Pikarsky, E., and Yisraeli, J.K. (2008). A role for VICKZ proteins in the progression of colorectal carcinomas: regulating lamellipodia formation. J Pathol *215*, 445-456.

Vessey, J.P., Vaccani, A., Xie, Y., Dahm, R., Karra, D., Kiebler, M.A., and Macchi, P. (2006). Dendritic localization of the translational repressor Pumilio 2 and its contribution to dendritic stress granules. J Neurosci *26*, 6496-6508.

Vogelaar, C.F., Gervasi, N.M., Gumy, L.F., Story, D.J., Raha-Chowdhury, R., Leung, K.M., Holt, C.E., and Fawcett, J.W. (2009). Axonal mRNAs: characterisation and role in the growth and regeneration of dorsal root ganglion axons and growth cones. Mol Cell Neurosci *42*, 102-115.

Wang, J., and Dreyfuss, G. (2001a). A cell system with targeted disruption of the SMN gene: functional conservation of the SMN protein and dependence of Gemin2 on SMN. J Biol Chem *276*, 9599-9605.

Wang, J., and Dreyfuss, G. (2001b). Characterization of functional domains of the SMN protein in vivo. J Biol Chem *276*, 45387-45393.

Wang, W., Caldwell, M.C., Lin, S., Furneaux, H., and Gorospe, M. (2000). HuR regulates cyclin A and cyclin B1 mRNA stability during cell proliferation. EMBO J *19*, 2340-2350.

Wang, W., Chai, B.F., Heckmann, K., and Liang, A.H. (2004). Cloning, characterization and expression of the polypeptide release factor gene, eRF1, of Blepharisma japonicum. Biotechnol Lett *26*, 959-963.

Weidensdorfer, D., Stohr, N., Baude, A., Lederer, M., Kohn, M., Schierhorn, A., Buchmeier, S., Wahle, E., and Huttelmaier, S. (2009). Control of c-myc mRNA stability by IGF2BP1-associated cytoplasmic RNPs. RNA *15*, 104-115.

Wichterle, H., Lieberam, I., Porter, J.A., and Jessell, T.M. (2002). Directed differentiation of embryonic stem cells into motor neurons. Cell *110*, 385-397.

Wilczynska, A., Aigueperse, C., Kress, M., Dautry, F., and Weil, D. (2005). The translational regulator CPEB1 provides a link between dcp1 bodies and stress granules. J Cell Sci *118*, 981-992.

Willis, D.E., van Niekerk, E.A., Sasaki, Y., Mesngon, M., Merianda, T.T., Williams, G.G., Kendall, M., Smith, D.S., Bassell, G.J., and Twiss, J.L. (2007). Extracellular stimuli specifically regulate localized levels of individual neuronal mRNAs. J Cell Biol *178*, 965-980.

Wu, K.Y., Hengst, U., Cox, L.J., Macosko, E.Z., Jeromin, A., Urquhart, E.R., and Jaffrey, S.R. (2005). Local translation of RhoA regulates growth cone collapse. Nature *436*, 1020-1024.

Wu, X.Q., Xu, L., and Hecht, N.B. (1998). Dimerization of the testis brain RNA-binding protein (translin) is mediated through its C-terminus and is required for DNA- and RNA-binding. Nucleic Acids Res *26*, 1675-1680.

Yang, W.H., and Bloch, D.B. (2007). Probing the mRNA processing body using protein macroarrays and "autoantigenomics". RNA *13*, 704-712.

Yang, W.H., Yu, J.H., Gulick, T., Bloch, K.D., and Bloch, D.B. (2006). RNA-associated protein 55 (RAP55) localizes to mRNA processing bodies and stress granules. RNA *12*, 547-554.

Yao, J., Sasaki, Y., Wen, Z., Bassell, G.J., and Zheng, J.Q. (2006). An essential role for beta-actin mRNA localization and translation in Ca(2+)-dependent growth cone guidance. Nat Neurosci *9*, 1265-1273.

Yisraeli, J., and Melton, D. (1988). The maternal mRNA Vg1 is correctly localized following injection. Nature *336*, 592-595.

Ymlahi-Ouazzani, Q., O, J.B., Paillard, E., Ballagny, C., Chesneau, A., Jadaud, A., Mazabraud, A., and Pollet, N. (2009). Reduced levels of survival motor neuron protein leads to aberrant motoneuron growth in a Xenopus model of muscular atrophy. Neurogenetics.

Yong, J., Wan, L., and Dreyfuss, G. (2004). Why do cells need an assembly machine for RNA-protein complexes? Trends Cell Biol *14*, 226-232.

Yoo, S., van Niekerk, E.A., Merianda, T.T., and Twiss, J.L. (2009). Dynamics of axonal mRNA transport and implications for peripheral nerve regeneration. Exp Neurol.

Yoshihara, Y., De Roo, M., and Muller, D. (2009). Dendritic spine formation and stabilization. Curr Opin Neurobiol *19*, 146-153.

Young, P.J., Le, T.T., Nguyen, T.M., Burghes, A.H., and Morris, G.E. (2000). The relationship between SMN, the spinal muscular atrophy protein, and nuclear colied bodies in differentiated tissues and cultured cells. Exp Cell Res *256*, 365-374.

Zalfa, F., Giorgi, M., Primerano, B., Moro, A., Di Penta, A., Reis, S., Oostra, B., and Bagni, C. (2003). The fragile X syndrome protein FMRP associates with BC1 RNA and regulates the translation of specific mRNAs at synapses. Cell *112*, 317-327.

Zeitelhofer, M., Karra, D., Macchi, P., Tolino, M., Thomas, S., Schwarz, M., Kiebler, M., and Dahm, R. (2008). Dynamic interaction between P-bodies and transport ribonucleoprotein particles in dendrites of mature hippocampal neurons. J Neurosci *28*, 7555-7562.

Zhang, H., and Macara, I.G. (2008). The PAR-6 polarity protein regulates dendritic spine morphogenesis through p190 RhoGAP and the Rho GTPase. Dev Cell *14*, 216-226.

Zhang, H., Xing, L., Rossoll, W., Wichterle, H., Singer, R.H., and Bassell, G.J. (2006). Multiprotein complexes of the survival of motor neuron protein SMN with Gemins traffic to neuronal processes and growth cones of motor neurons. J Neurosci *26*, 8622-8632.

Zhang, H., Xing, L., Singer, R.H., and Bassell, G.J. (2007). QNQKE targeting motif for the SMN-Gemin multiprotein complexin neurons. J Neurosci Res *85*, 2657-2667.

Zhang, H.L., Eom, T., Oleynikov, Y., Shenoy, S.M., Liebelt, D.A., Dictenberg, J.B., Singer, R.H., and Bassell, G.J. (2001). Neurotrophin-induced transport of a beta-actin mRNP complex increases beta-actin levels and stimulates growth cone motility. Neuron *31*, 261-275.

Zhang, H.L., Pan, F., Hong, D., Shenoy, S.M., Singer, R.H., and Bassell, G.J. (2003). Active transport of the survival motor neuron protein and the role of exon-7 in cytoplasmic localization. J Neurosci *23*, 6627-6637.

Zhang, H.L., Singer, R.H., and Bassell, G.J. (1999). Neurotrophin regulation of beta-actin mRNA and protein localization within growth cones. Journal of Cell Biology *147*, 59-70.

Zhang, Z., Lotti, F., Dittmar, K., Younis, I., Wan, L., Kasim, M., and Dreyfuss, G. (2008). SMN deficiency causes tissue-specific perturbations in the repertoire of snRNAs and widespread defects in splicing. Cell *133*, 585-600.

Zhou, Y., and King, M.L. (2004). Sending RNAs into the future: RNA localization and germ cell fate. IUBMB Life *56*, 19-27.

Zhouravleva, G., Frolova, L., Le Goff, X., Le Guellec, R., Inge-Vechtomov, S., Kisselev, L., and Philippe, M. (1995). Termination of translation in eukaryotes is governed by two interacting polypeptide chain release factors, eRF1 and eRF3. EMBO J *14*, 4065-4072.